

**Studies on the molecular
mechanism of function and genetic
regulation of truncated hemoglobin of
*Mycobacterium tuberculosis***



THESIS
SUBMITTED FOR THE DEGREE OF
DOCTOR OF PHILOSOPHY
IN THE FACULTY OF SCIENCE
TO
JAWAHARLAL NEHRU UNIVERSITY
NEW DELHI



IMTECH

Sandeep Kumar Singh
INSTITUTE OF MICROBIAL TECHNOLOGY
CHANDIGARH
March 2013



इमटेक
IMTECH

सूक्ष्मजीव प्रौद्योगिकी संस्थान
सैक्टर 39-ए, चण्डीगढ़ 160 036 (भारत)
INSTITUTE OF MICROBIAL TECHNOLOGY
(A CONSTITUENT ESTABLISHMENT OF CSIR)
Sector 39-A, Chandigarh-160 036 (INDIA)

CERTIFICATE

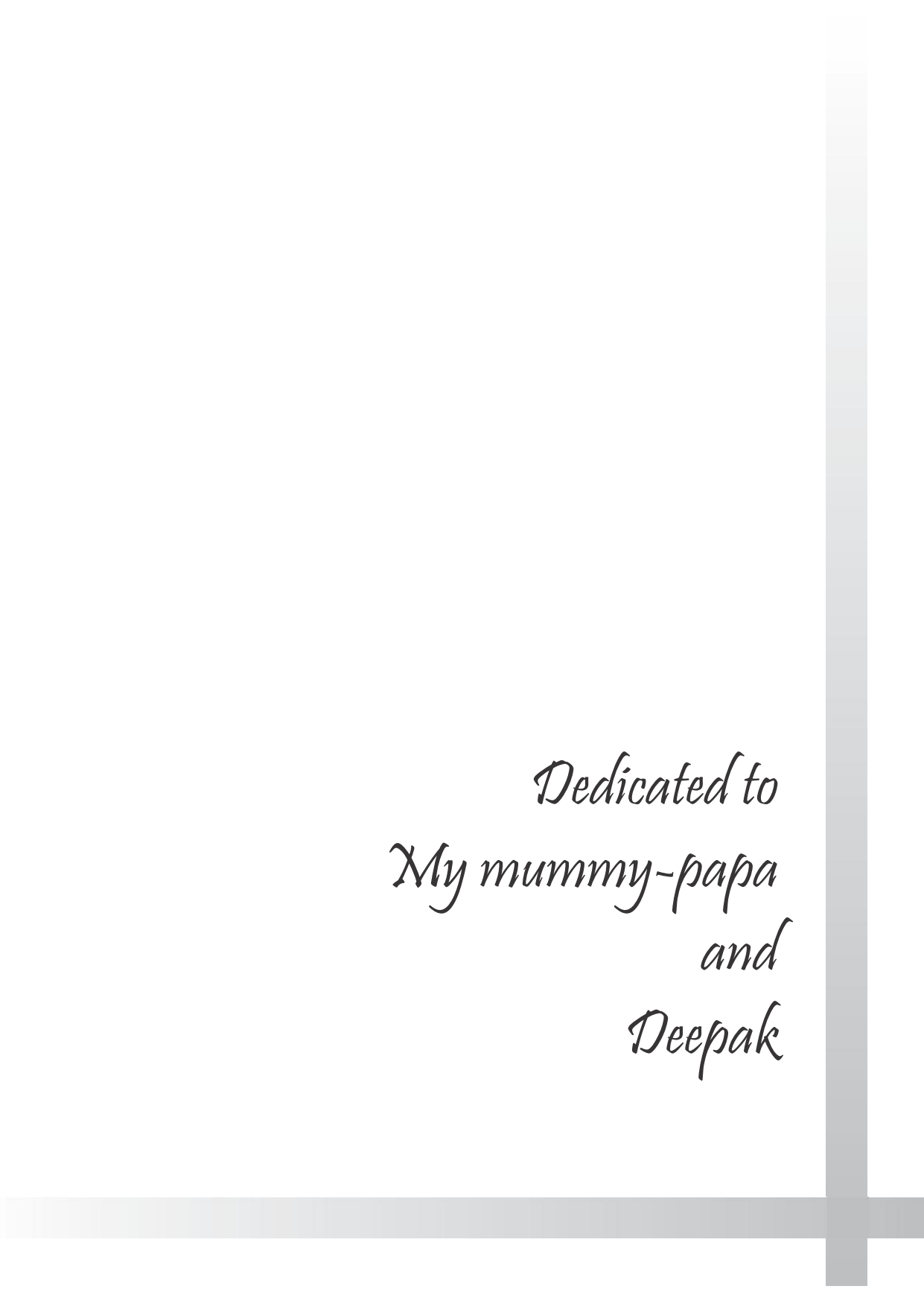
The research work entitled “**Studies on the Molecular Mechanism of Function and Genetic Regulation of Truncated Hemoglobin of *Mycobacterium tuberculosis***” in this thesis has been carried out at the Institute of Microbial Technology, Chandigarh, India. This thesis is an original work and has not been submitted, in the whole or in part, for a degree at this or any other university. The thesis also does not contain, to the best of our knowledge and belief, any material published or written by another person, except as acknowledged in the text

Dr. Kanak L. Dikshit

Supervisor

Sandeep Kumar Singh

*Dedicated to
My mummy-papa
and
Deepak*



Acknowledgements

“Learn from yesterday, live for today, hope for tomorrow.

The important thing is to not stop questioning. “

Albert Einstein

It is rightly said that life is a constant learning process and the quest for knowledge is never ending process, as it is fuelled by its own curiosity. The learning process that I have begun long back is continued throughout my PhD tenure and towards the end this course I utilize this opportunity to thank everyone who have assisted me in slightest of manner.

Foremost, I would like to extend my deepest gratitude to Dr Kanak .L.Dikshit, who has contributed enormously to the genesis of this thesis both in terms of intellectual input and encouragement. Her extraordinary scientific acumen has chiselled me as a budding researcher. She has always acted like a bridge, whenever I have faced the abyss of problems. This dissertation would not have been possible without her constant support and expert guidance. She has effortlessly played the role of a mentor and guided me in all possible ways, in every possible aspects of this dissertation. I am indebted to her for her contribution in my life.

I duely acknowledge Dr. Girish Sahni, director, IMTECH, Chandigarh, for providing excellent research facilities. He has made profound difference to the spirit and facilities of the institute and I take this opportunity to thank him for being so approachable, considerate and student oriented nature.

I would also like to thank Professor Dario and Professor Xavier for performing simulation related studies which has helped me in painting the complete picture of my research assignment. Biophysical studies of the proteins would not have been possible without the assistance of Dr. Suman Kundu. I thank him for allowing me to use his lab space and conducting crucial experiments. I am also grateful to Dr. Pradeep sen for helping me in molecular biology studies, related to the DNA-protein interaction. His precious suggestions were quite useful to me. During the fag end of my thesis, significant contribution of Dr. Raman Parkeshi in the docking realted studies, is duly acknowledged

Many people of the faculty and staff have assisted and encouraged me in various ways during the course of my study. I owe a great deal of gratitude to Dr.Pradip Chakraborty and Mrs. Sashi Batra for their effort to administer necessary formalities during my PhD tenure, including submission of my thesis and arrangement of fellowship. It was a great pleasure to have light conversations with Dr,Rajamohan, Dr Vijaya and Dr. Saumaya Ray Choudhary. I am also thankful to Dr.Pradeep Sen and Dr. Debyendu Sarkar for timely distribution of radioactivity. I thank Dr. Alok Mondol and Mr Deepak Bhatt for his DNA sequencing works, Mrs. Paramjeet Kaur for protein sequencing and Mrs. Sharanjeet Kaur CD data acquisition. I take this occasion to thank staff of administration, accounts, bioinformatics and library. Constant support of entire instrumentation staff, especially of Mr Ashok Rana is highly commendable.

I am deeply grateful to my seniors Amrita, Sudesh ,Arvind , Satish and Muthu with whom I have began my journey of PhD. They were very helpful and taught me the initial experiments in the lab. Their lovable nature never let me feel the pressure of science. My journey was continued to be pleasant with the arrival of friendly and mirthful juniors Preeti, Simar, Neeru, Auro, Narender, Mangesh, Timsy, Naveen, Deepti and Chaahat. The timely help extended by Mangesh and Naveen to me is duely acknowledged.

I have been extremely lucky to join the lab during the tenure of Arvind, Satish and Preeti. They became very close to my heart. Apart from helping me in mind boggling research, they have always accompanied me in the extralab affairs. We have visited many places, organised parties and lived together many memorable moments. I could not have earned for better friend than Preeti. The small fights that we picked up with each other, were the best part of my PhD. I will ever cherish all the fond memories of the time that we have enjoyed together. Those moments were my stress busters.

In Imtech, I was fortunate to came across many good friends. Some were seniors while some were juniors, but all of them helped me to become a better person. Special thanks to Chetna , Santa, Payal, Sanjay, Sandeep and Ranjana for being such a special friend to me. It was a proud feeling to be a close friend of fanatastic four Chinu, Deepti, Bhawna and Aman. Today I also remember my seniors who were very special to me Netrapal sir, Gowthman, Shweta Jain, Eshu, Gautam, Balveer, Pankaj Chauhan, Anuj, Satyaparakash, Kishore, Neeraj, Prakash, Mahesh etc. I also

happened to meet some extraordinary friends Rajesh, Aslum, Sakshi, Neelam, Gunjan, Rajni, Jesse, Nisha, Surender, Vaibhav, Harinder, Ali, Ranjeet, Neeraj Maurya, Sahil, Pradeep-2, Vikas, Sudheer, Ravi, Richa, Vasanth, Neeraj, Suneet, Neha, Ghanshyam, Mary, Nargis, Amer, Ashish, Kalpana, Shikha, Nagesh, Gaurav-2, Wesley, Kit, Anubhav, Rehan, Abhishek, Ravi, Shailesh-2, Vinay etc . My party fellow Pankaj and Abhijeet will always be missed. Special thanks to Ravinder for helping me in experiments. Small mischief with Kanchan ji was very special and zillions of thanks to mess worker for providing me with excellent food.

I was very fortunate to have special batchmates Vinod, Arijit, Jagpreet, Anil, Rahman, Ravi, Poonam, Leena, Harsimran, Tikam, Ram Babu and Fatima. They were few, but each one of them was of a unique personality, that made them a bundle of joy. I will ever cherish the frivolous moments that I spent with them during my stay. Group events such as freshers, hostel night, new year celebrations were incomplete without them.

My family is my perpetual source of inspiration and driving force. I am blessed to have such a loving, caring and farsighted mummy in my life. Her insatiable desire to seek knowledge through hard work and perseverance is worth learning. My parents were my first teacher to teach me the most important thing in my life i.e. the importance of knowledge. Today whatever I am is only because of their sacrifice and dream. My younger brother Deepak has been loving, caring and mischievous. I also extend my utmost love to my best friend Vinoy for being like my own brother. He is the only person in my life who knows everything about me and cares about me, even more than me. He has always stood by my side during all the ups and downs of my life. I thank for the love and affection that I received from Mamta didi, Jijaji, Subhi, Shashank, Vivek bhaiya, Uncle, Aunty, Dheeraj, Nayana, Sonal, Pinki, Rohit, Rinku, Anurag, Nanhi, Sonu, Ekta, Shweta, Honey, Anil and Dilip chacha, Fu, Mamaji and my both the chachi. Encouragement and support from my Ganesh mausaji, Kamal mausaji, Bebi mausi and Geeta mausi have made me a better person.

The financial assistance provided by Department of Biotechnology is duly acknowledged.

Above all I thank Mata a zillions of times for blessing me with loved ones and loving ones and this opportunity to thank them all. Mata please keep showering your kindness on us and give us strength to live through tough times

JAI MATA DI

SANDEEP

Contents

Chapter-1	Introduction and review	1-24
Chapter-2	Material and methods	25-45
Chapter-3	Role of structural elements on NO-dioxygenation function of HbN	46-63
Chapter-4	Protein-protein interaction of HbN with redox partners and its implications on NO-dioxygenase function	64-81
Chapter -5	Genetic regulation of <i>glbN</i> gene in <i>Mycobacterium tuberculosis</i>	82-94
	Overview	95-103
	Bibliography	104-117

Abbreviations

Weight and Measures

%	Percent
°C	Degree centigrade
bp	Base pairs
cm, mm, nm	Centimeter, millimeter, nanometer
Da, kDa	Dalton, kilodalton
hr, min, sec	Hour, minute, second
kb	Kilobases
M, mM, μ M, nM	Molar, millimolar, micromolar, nanomolar
mA	Milliampere
mg, μ g, ng	Milligram, microgram, nanogram
ml, μ l	Milliliter, microliter
OD	Optical density
V, mV	Volt, millivolt

Symbols

α	Alpha
β	Beta
γ	Gamma
π	Pi
ϵ	Epsilon
Å	Angstrom
~	Approximately
=	Equal to

Chemicals

TEMED	N,N,N',N'-tetramethylethylenediamine
X-gal	5-bromo-4-chloro-3-indolyl β D-galactopyranoside
β -ME	β -mercaptoethanol
Amp	Ampicillin
Kan	Kanamycin

APS	Ammonium persulfate
ATP	Adenosine triphosphate
BSA	Bovine serum albumin
DTT	Dithiothreitol
EDTA	Ethylene diamine tetraacetic acid
IPTG	Isopropyl β D-thiogalactopyranoside
SDS	Sodium dodecyl sulphate
SP-Sepharose	Sulphopropyl-Sepharose
NADH	Reduced Nicotinamide Adenine Dinucleotide
FAD	Flavin adenine dinucleotide

Amino acids

Gln	Glutamine
Glu	Glutamate
Gly	Glycine
His	Histidine
Leu	Leucine
Phe	Phenylalanine
Pro	Proline
Tyr	Tyrosine
Val	Valine
Thr	Threonine
Ser	Serine
Met	Methionine
Arg	Arginine
Lys	Lysine
Asp	Aspartate

Miscellaneous

FNR	Ferredoxin NADP reductase
HbN	Truncated hemoglobin N
HbO	Truncated hemoglobin O

PCR	Polymerase chain reaction
PAGE	Polyacrylamide gel electrophoresis
CD	Circular dichroism
CO	Carbon monoxide
CO ₂	Carbon dioxide
NO	Nitric oxide
DNA	Deoxyribonucleic acid
Pg	Plasminogen
BCA	Bicinchoninic acid
SPR	Surface plasmon resonance
PDB	Protein data bank
P <i>glbN</i>	Promoter of <i>glbN</i>



Introduction

1. Introduction.....	1-2
1.1 Vertebrate globins.....	2-5
1.1.1 Function of Hemoglobin and Myoglobin.....	3
1.1.2 Neuroglobin and Cytochrome b.....	3-4
1.1.2.1 Functions of NgB and Cyb.....	4-5
1.2 Non-vertebrate globins.....	5-6
1.2.1 Function of Non-vertebrate haemoglobin.....	6
1.3 Hemoglobins from Single celled Organisms.....	6-18
1.3.1 Bacterial Hemoglobin.....	6-8
1.3.1.1 Single domain hemoglobins.....	7-8
1.3.1.1.1 Function of Single domain haemoglobin.....	8
1.3.2 Two domain hemoglobins.....	8-11
1.3.2.1 Flavohemoglobin.....	9
1.3.2.1.1 Functions of Flavohemoglobin.....	10
1.3.2.2 Heme based sensors(HBSs).....	10-11
1.3.2.2.1 Functions of Heme Based Sensors.....	11
1.3.3 Truncated haemoglobins.....	11-18
1.3.3.1 Functions of truncated haemoglobin.....	12-13
1.3.3.1.1 Role of haemoglobin in bacterial pathogenesis.....	13-14
1.3.3.2 Truncated haemoglobins of <i>Mycobacterium tuberculosis</i> ...	14
1.3.3.2.1 Structural features of HbN and HbO of <i>Mycobacterium tuberculosis</i>	14-18
1.4 Interaction Nitric Oxide with haemoglobin.....	18-19
1.5 Scope of the present study.....	20-24

1. Introduction

During the pre-historic times atmosphere was very inhospitable (Figure 1.1). It was highly reducing because of the absence of free oxygen. Thus, the early life forms were anaerobic in nature and dependent on the non equilibrium cycles of the electron transfers between five initial elements N, C, H, S and O. The energy yield per reaction was quite low because the electron acceptors were CO₂ and to a lesser extent SO₄ apart from the alternative electron acceptor N₂. The biggest electron donor pool i.e. H₂O was inaccessible to the biological machinery. The onset of oxygen on the planet was a blessing in disguise. Initially the free oxygen, which was a metabolic waste, was extremely beneficial as an electron acceptor but it created havoc to the intricate metabolic pathways that had evolved over billions of years. By experiencing the benefits of the potentially dangerous molecule, living organisms gradually evolved a molecular cage called porphyrin ring, which has the ability to bind oxygen and tear away the electrons for the metabolic pathways. Porphyrin rings are heterocyclic, macro cycles, composed of four modified pyrrole subunits, interconnected at their carbon atoms via methane bridges. Four nitrogen atoms were present in the pyrrole ring and a metal atom is at the centre of the ring cluster. The four nitrogen atoms provided an ideal environment for the insertion of the metal ion, such as iron or magnesium, which is extremely useful for reaction with diatomic gaseous ligands. As the complexity raised during the course of evolution, these porphyrin rings got embedded inside large organic compounds called proteins. The descendents of these compounds include chlorophyll and heme. Porphyrins that contain iron are called as haemoglobin whereas magnesium containing are called chlorophyll.

Depending upon the metal centre and the arrangement of protein around it, it has got a gamut of functions and properties, making it indispensable for the life processes. The Primary function of the heme protein was to quench the toxic effect of oxygen, but, later it started participating in various oxygen based metabolism and some novel functions, such as electron transfer reaction.

According to Nick Lane, the Last Universal Common Ancestor or LUCA, the precursor of all lives on earth, most likely to have made use of a Hb-like protein to manage O₂ homeostasis. Such protoglobins, which are considered to be the source of all Hbs, have been explored in *Archea* (Freitas *et al.*, 2004), *Aeropyrum pernix* and

Methanosarcina acetivorans, and as predicted for LUCA, they were found to be O₂ sensitive. In the present O₂ rich environment, Hbs are ubiquitous in the biosphere and found in all phyla of living organisms, including prokaryotes, fungi, plants and animals. The common characteristic of all Hbs is their ability to reversibly bind oxygen and presence of classical globin fold, containing the heme moiety and surrounded by hydrophobic residues. Hemoglobins are classified into vertebrate and non vertebrate classes.



Figure 1.1: Depiction of early earth's condition, millions of year ago, when life was originating. (courtesy: Stephen Mojzsis)

1.1 Vertebrate globins

Vertebrate hemoglobins include haemoglobin, myoglobin and newly discovered cytoglobin as well as neuroglobin. Due to its predominance haemoglobin (Hb) and myoglobin (Mb) were the first O₂ binding proteins to be discovered, characterised and structurally elucidated (Gray, 1983; Hardison, 1996, 2001) (Figure 1.2). They were later served as models for a variety of biochemical phenomenon, such as co-operativity in ligand binding and modulation of biochemical properties by allosteric regulators (Perutz, 1978, 1989a). The most common haemoglobin is type A haemoglobin which exist in the red blood cells. It is a non-covalently bound hetrotetramer of ~64kDa, consisting of two α - and two β -subunits, each made up of 141 and 146 amino acids residues respectively (Perutz, 1978). On the other hand myoglobin is a monomeric globular protein of 153 amino acids, which is found in muscles tissue such as cardiac and striated tissues where

high aerobic activity occurs (Wittenberg, 1992; Wittenberg and Wittenberg, 1990, 2003). All the hemoglobins fold spontaneously into a 3 dimensional, three-over-three helical sandwich motif known as “globin fold”, that holds Fe-protoporphyrin IX by which they can bind gaseous ligands such as O₂, CO and NO. The signature residues in all hemoglobins are the PheCD1 and His F8. The heme iron is linked to globin through His F8 (proximal) amino acid that acts as an electron donor in its reaction with O₂. His E7 stabilizes bound O₂ by hydrogen bonding.

1.1.1 Function of Hemoglobin and Myoglobin

Haemoglobin (Hb) acts as an oxygen carrier in blood. While, the primary function of myoglobin (Mb) is to supply oxygen to the muscular tissue. Unlike haemoglobin, myoglobin does not show co-operative binding. Myoglobin facilitates diffusion of O₂ to mitochondria (Wittenberg, 1992; Wittenberg and Wittenberg, 1990, 2003). It also possesses dioxygenase function (Flogel *et al.*, 2001) which is not seen in haemoglobin.

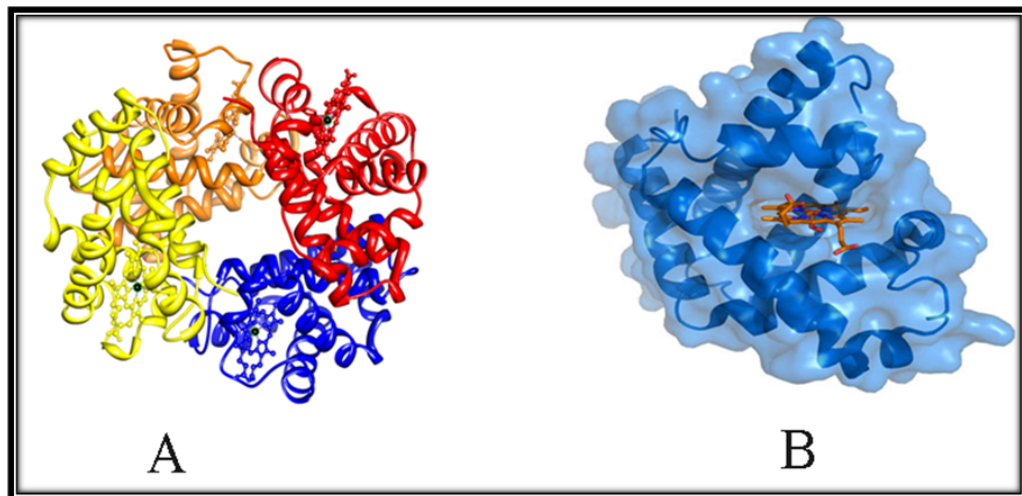


Figure 1.2: Ribbon representation of (A) haemoglobin structure and (B) myoglobin structure, heme group is shown in ball and stick model.

1.1.2 Neuroglobin and Cytoglobin

Recently two more members have been added to the vertebrate globin family, namely Neuroglobin (Ngb) and Cytoglobin (Cygb) (Burmester *et al.*, 2002; Burmester *et al.*, 2000; Pesce *et al.*, 2002; Trent and Hargrove, 2002). Neuroglobin (Ngb) is mainly expressed in neuronal (brain and retina) and some endocrine tissue, whereas, cytoglobin (cygb), also called as histoglobins is present in nucleus and cytoplasm of many tissues

(Burmester *et al.*, 2002; Geuens *et al.*, 2003; Reuss *et al.*, 2002; Trent and Hargrove, 2002). They are monomeric in nature, consisting of 151 and 190 amino acid residues, respectively (Figure 1.3). They have very little identity to vertebrate Hb and Mb (20-25%) (Pesce *et al.*, 2002). They are well conserved among species. For eg. human and mouse Ngbs are 94% similar. Ngbs and Cygbs play role in O₂ metabolism by facilitating its diffusion to the mitochondria.

The crystal structure of Ngb (Pesce *et al.*, 2003) displays unusual cavities, whereas, Cygb revealed the presence of apolar tunnel which may facilitates, ligand tunnelling pathways (de Sanctis *et al.*, 2004a, b). Neuroglobins and cytoglobins are hexa-coordinated. EPR (Electronic Paramagnetic Resonance) and the kinetic studies have revealed that the binding affinity of the reactive nitric oxide (NO) to Ngb-Fe²⁺ is relatively low in comparison to penta-coordinated Hb and Mb, however, Ngb-Fe²⁺-NO may readily form and scavenge peroxynitrite (Herold *et al.*, 2004) (Figure 1.4).

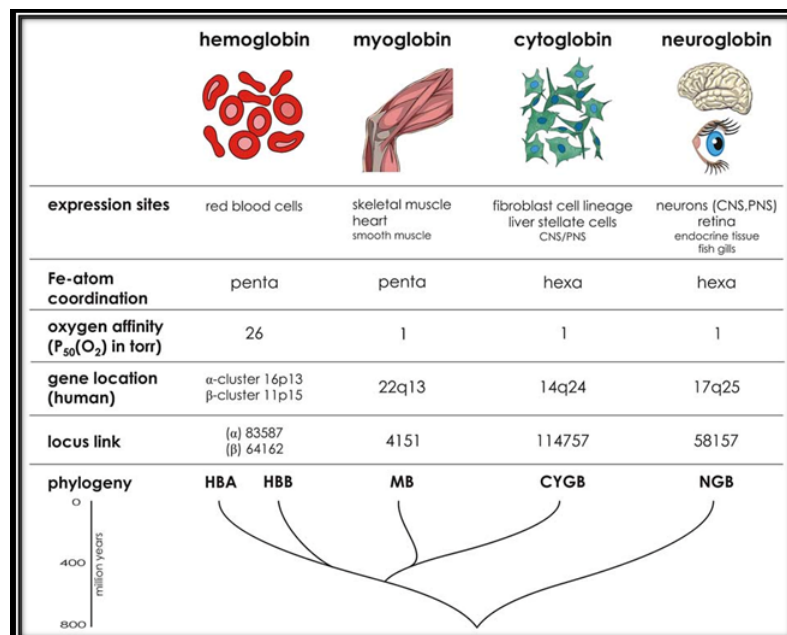


Figure 1.3: Characteristics of vertebrate globins. The graphic summarizes selected expressional, biochemical and phylogenetic features of vertebrate globin types.(Hanklen *et. al.*)

1.1.2.1 Functions of Ngb and CygB

Their function is debatable and further investigations are required to assign the exact functions. Ngb was observed to be upregulated during hypoxic condition in cultured rat cortical neurons. CygB may have substantial biomedical impact due to its involvement in organ fibrosis and in the production of extracellular matrix collagens du-

ring the normal tissue generation and fibrotic pathogenesis (Hankeln *et al.*, 2005).

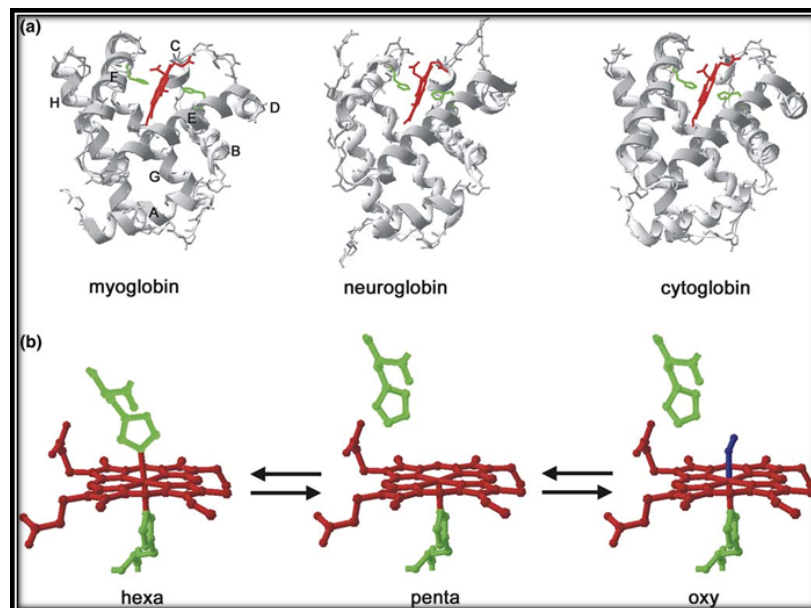


Figure 1.4: 3-D protein structure of human Mb (PDB: 2MM1), Ngb (1OJ6) and Cygb (1UMO). In Mb, the eight alpha-helices are designated A through H. Note that the globin fold is conserved in all three proteins. (b) Schematic scheme of globin hexa-coordination. The equilibrium of the hexa- and penta-coordinated form is the rate limiting step in ligand binding for Ngb and Cygb. Colors: red, heme group; green, interacting histidines; blue, oxygen ligand. (Hanklen *et.al.*)

1.2 Non-vertebrate globins

Non vertebrate globins are widely present in different anatomical structures, such as cytoplasm of specific tissues or freely dissolved in various body fluids, from monomeric to multisubunit structure, in manifold variations. These Hbs occur widely but sporadically in phyla Platyhelminthes, Netmetoda, Annelida, Mollusca, Echinodermata etc. Many single chain globins are found in nonleguminous plants, algae and number of prokaryotes, ranging from bacteria to cyanobacteria. Although non-vertebrates are phylogenetically more primitive than vertebrates, the high variability encountered in their Hbs reflects specializations and adaption to a greater range of operating conditions (Weber and Pauptit, 1972). Non-vertebrate globins can be divided into several distinct groups (1) single-chain globins, containing one heme binding domain; (2) truncated, single chain, globins; (3) chimeric, two domain globins and (4) chimeric, multi-domain globins.

Single chain, single domain globins are comparable in size to the vertebrate globins and exhibit the widest distribution: intracellular Hbs include *Glycera*, *Urechis*, *Scapharca*, etc; extracellular Hbs include the Hbs of *Chironomus*, *Caenorhabditis*, etc;

cytoplasmic Hbs include Mbs of *Aplysia*, *Bursatella* etc.

1.2.1 Function of Non-vertebrate hemoglobin

Apart from oxygen transport and storage these invertebrate hemoglobins perform other functions such as control of NO level in nematodes, protection against sulphide, scavenging of O₂ in symbiotic leguminous plants, carbon fixing in bacteria and archaeobacteria and regulation of buoyancy of aquatic backswimmer insects (Edmond *et al.*, 1982; Truchot, 1976).

1.3 Hemoglobins from Single celled Organisms

Although Hb is a special molecule in the physiology of vertebrates, its origin is supposed to have occurred in the earlier life forms such as bacteria. A new chapter in the field of oxygen binding proteins was added with the discovery of haemoglobin in a prokaryote, a gram negative bacterium, *Vitreoscilla*, which otherwise was thought to be present in eukaryotes only (Wakabayashi *et al.*, 1986). This discovery started the chain reaction and many Hb-like proteins have been reported in various microbial systems ranging from prokaryotes to unicellular protozoans, alga etc. Recently there has been an upsurge in the identification of the Hb like proteins in the microbial system and more than 90% bacteria have been reported to carry this protein. What is more surprising is that a single organism harbours hemoglobins of different types, emphasizing upon the divergent role of these hemoglobins apart from the well established oxygen binding and transportation property. Bacteria living in diverse habitats have been found to carry this protein.

1.3.1 Bacterial Hemoglobin

Amongst archaea, only *Halobacterium salinarum* is reported to have globin like protein, which acts as an aerotactic transducer (Hou *et al.*, 2000). Haemoglobin of cyanobacteria *Nostoc commune* is homologous to that found in protozoans. These results demonstrate that haemoglobin or heme domains from eukaryotic (protozoa and fungi) are similar to the hemoglobins of bacterial origin than that of other eukaryotic globins, thus increasing our understanding of the evolutionary and functional relationship within globins. VHb like classical globin fold is reported in Hb of *Clostridium perferingens*, an anaerobe and *Campylobacter jejuni*, a microaerobe. Truncated haemoglobin type protein

is found in thermophilic bacterium, *Geobacillus stearothermophilus* (Ilari *et al.*, 2007) and other in a psychrophilic bacterium, *Pseudoalteromonas haploplanktis* TAC125 (Giordano *et al.*, 2007). It is also found in the gram negative soil bacterium, *Ralstonia eutrophus*, formerly called *Alkaligenes eutrophus*. Other bacterial species that contains globin like proteins are *Vibrio*, *Erwinia*, *Bradyrhizobium*, and *Chromatium*. Vasudevan *et al.* unexpectedly came across the Hb like protein while identifying the genes encoding dihydropteridine reductase activity (Vasudevan *et al.*, 1991). Later it was found to be a two domain flavohemoglobin with the ability to catalyse redox reactions and also possessing NOD function (Vasudevan *et al.*, 1991). Afterwards flavohemoglobin has been reported in *Pseudomonas aeruginosa*, *Klebsiella pneumonia* and *Deinococcus radiodurans* and have been shown to enhance cell growth and productivity in *E.coli* in microaerobic conditions (Vinogradov *et al.*, 2006). These bacterial globins have been further subdivided into 3 categories:

- 1) Single domain hemoglobins: classical “three-over-three” α -helical globin domain
- 2) Two domain hemoglobins: classical “three-over-three” α -helical globin domain coupled to a redox active domain at its C-terminus
- 3) Truncated hemoglobins: mini hemoglobins with “two-over-two” α -helical globin domain

1.3.1.1 Single domain hemoglobins

VHb was the first single domain haemoglobin to be discovered from a gram negative bacterium, *Vitreoscilla stercoraria*. Later 2 more members were added to this group, one from *Clostridium perfringens* (Shimizu *et al.*, 2002), an anaerobe and other from *Campylobacter jejuni*, a microaerobe (Elvers *et al.*, 2004). VHb is a 15.7 kDa homodimeric protein (Orii and Webster, 1986; Webster, 1988). The crystal structure of VHb revealed the retention of classical 3 over 3 fold (Tarricone *et al.*, 1997), which is very rare in bacteria, along with the conserved heme binding residues (Phe CD1, His F8). Its structure is very similar to the globin domains of FHbs from *E.coli* (Ilari *et al.*, 2002) and *Ralstonia eutropha* (Ermler *et al.*, 1995). A few structural deviations from the eukaryotic haemoglobins include the region between C and E helices and presence of Fe-HisF8-tyrG5-GluH23 hydrogen binding network in the proximal site. *Campylobacter jejuni* expresses a homologue of VHb called Cgb. It is a monomeric structure having classical 3 over 3 globin fold. The C and D region of the Cgb adopts 3_{10} - and α -helical

conformation respectively. This is similar to the sperm whale myoglobin, although D-helix in Cgb is closer to heme binding cleft of sperm whale myoglobin.

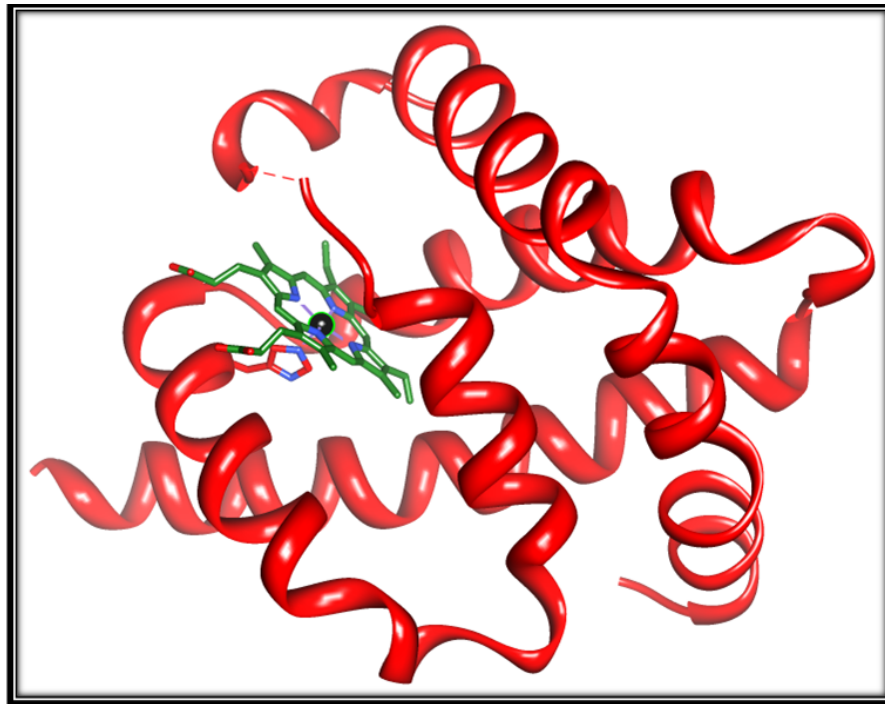


Figure 1.5: Structure of *Vitrescilla* (VHb) [PDB:1VHB]. The 3-over-3 globin fold is shown in red and heme cofactor is shown in green (Tarricone *et al.*, 1997).

1.3.1.1.1 Function of Single domain hemoglobin

VHb binds oxygen at low levels and delivers it to the terminal respiratory oxidase. Due to its high oxygen affinity it acts as a terminal respiratory oxidase (Park *et al.*, 2002; Ramandeep *et al.*, 2001) and enhances oxidative phosphorylation under hypoxic condition. VHb may also play role in increasing the biodegradation of aromatic compounds by providing oxygen to the oxygenases, which incorporates the oxygen atom into the compound being oxidised (Stark *et al.*, 2011). VHb expressing cells showed increased production of antibiotics and biopolymers (Horng *et al.*, 2010; Priscila *et al.*, 2008; Stark *et al.*, 2011). Vgb also has the ability to relieve the cells from nitrosative stress (Frey and Kallio, 2005; Kaur *et al.*, 2002). Cgb is known to be up regulated by transcription factor NssR during nitrosative stress and detoxify NO.

1.3.2 Two domain hemoglobins

These two domain hemoglobins are also called as chimeric hemoglobins because they have N-terminal globin domain and a C-terminal variable domain. It is divided into

two main categories: Flavohemoglobins and Heme based sensors.

1.3.2.1 Flavohemoglobin

Flavohemoproteins are chimeric hemoglobins which are divided into two distinct domains: the N-terminal classical globin domain, which is homologous to single domain Hb and covalently attached C-terminal reductase or a kinase domain. The reductase domain is variable and structurally similar to the ferredoxin-NADP⁺ reductase family in yeast and *E.coli* and to the cytochrome reductase in *Ralstonia eutropha* (Karplus *et al.*, 1991). It was 1st discovered in *E.coli* as a 44kDa protein (Vasudevan *et al.*, 1991). The crystal structure from *Alcaligenes eutrophus* (Ermler *et al.*, 1995) and from *E.coli* (Ilari *et al.*, 2002) revealed that the N-terminal globin adopt the classical “three-over-three” α -helical fold with a characteristic Phe CD1 and His F8 residue (Figure 1.6). The reductase domain can be subdivided into two structurally and functionally different independent domains: a FAD binding domains and an NAD(P)H-binding domain.

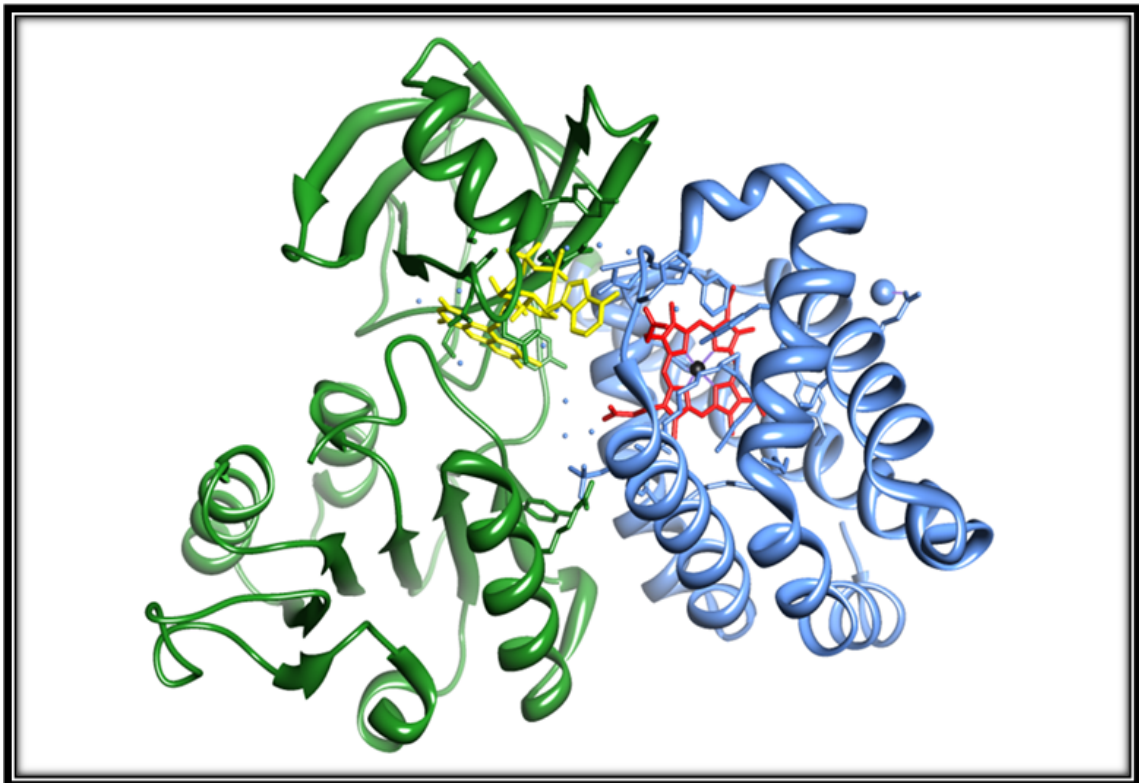


Figure 1.6: Structure of *Ralstonia* flavoHb (FHB)[PDB 1CQX]. The globin domain is shown in blue, attached to the reductase domain shown in green. FAD (yellow) and heme cofactor is shown in red (Ermler *et al.*, 1995).

1.3.2.1.1 Functions of Flavohemoglobin

Besides oxygen binding and transport, flavohemoglobins are involved in myriad of functions. Hmp plays important role in providing resistance to bacteria during nitrosative stress by playing as a NO oxygenase in the presence of oxygen, as a denitrosylase or by performing NO dioxygenase activity (Gardner et al., 1998b; Hausladen et al., 2001; Hausladen et al., 1998). It is able to show alkylhydroperoxidase activity, in which it is able to reduce O_2 to O_2^{2-} as well as H_2O_2 to H_2O . Recently it is also shown to perform D lactate dehydrogenase (D-LDH) function (Gupta *et al.*, 2012).

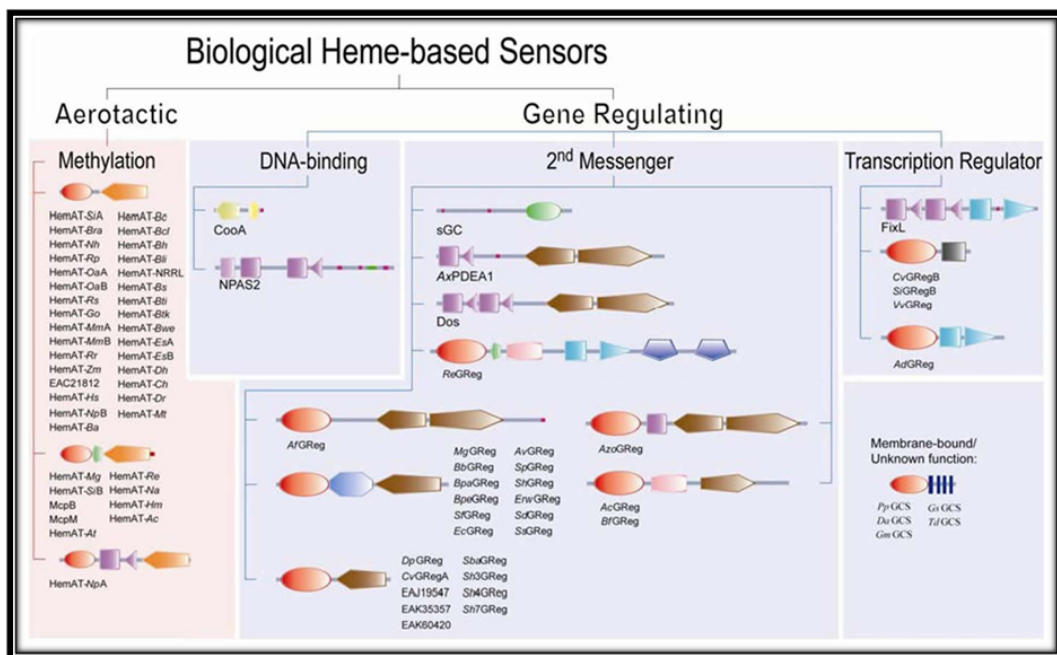


Figure 1.7 Classification of the globin-coupled sensors in relation to other biological heme-based sensors (Freitas *et al.*, 2005).

1.3.2.2 Heme based sensors (HBSs)

Heme based sensor is a regulatory heme binding domain or subunit that controls a neighbouring transmitter region of the same protein (Gilles-Gonzalez and Gonzalez, 2005). These are mediators of cellular responses to metabolic and environmental stimuli such as NO, CO and O_2 (Chan, 2001) (Figure 1.7). For example, histidine protein kinase, nucleotide cyclase, DNA binding transcription activities etc. On the basis of heme binding domains heme based sensors are divided into four different families:

- a) **Heme PAS** - These are ubiquitous and found in all kingdoms of life. They get activated specifically by oxygen and carbon monoxide and bring about changes in

adaptive responses (Taylor and Zhulin, 1999; Zhulin *et al.*, 1997).

- b) **CooA** - It is a CO sensing transcription factor found in purple non sulphur bacterium *R. rubrum* that regulate the oxidation of CO to CO₂ (Aono *et al.*, 1997; Roberts *et al.*, 2001).
- c) **Globin coupled sensors** - With the discovery of two aerotaxis transducers in *H. salinarum* and *Bacillus subtilis* by Alam and colleagues, the role of globin like fold was confirmed in regulation also (Hou *et al.*, 2000). The N-terminal sequence of the proteins are weakly homologous to sperm whale myoglobin, whereas C-terminal end is about 30% identical to the cytoplasmic-binding domain of the *E.coli* methyl accepting chemotaxis protein called Tsr.
- d) **Heme nitric oxide binding domain (HNOB)** - Except the archeal genome, many bacterial genome were found to encode a region homologous to N-terminal domain of sGC (soluble guanylyl cyclase) subunit (~185 residues). Although it is absent in lower eukaryotes, in higher eukaryotes it is coupled to guanylyl cyclase like region (Iyer *et al.*, 2003). Two novel classes of HNOB have been discovered heme nitric oxide /oxygen sensors(H-NOX) and sensors of nitric oxide (SONO) because of their ability to bind oxygen and nitric oxide, respectively, with high affinity (Karow *et al.*, 2004; Pellicena *et al.*, 2004).

1.3.2.2.1 Functions of Heme Based Sensors

Heme-Pas domain containing FixL enables the symbiotic *Rhizobia* to survive O₂ starvation (Gong *et al.*, 1998). The phosphodiesterase 1 of *Acetobacter xylinum* regulates cellulose excretion: an aerobic, irreversible and metabolically expensive process. Globin coupled sensors containing proteins such as HemAT-B have been demonstrated to show aerophilic response in *Bacillus subtilis* and aerophobic response in *H. salinarum* (Boudko *et al.*, 2003).

1.3.3 Truncated haemoglobins

Truncated hemoglobins are small heme proteins present in bacteria, plants and unicellular eukaryotes (Vuletich and Lecomte, 2006; Wittenberg *et al.*, 2002). They are 20-40 residues shorter than vertebrate haemoglobin and are distantly related to it. Sequence alignment with vertebrate haemoglobins showed substantial deletion at either

N- or C- termini and in the CD-D region of the non-vertebrate globins back bone. They share <15% sequence similarity with vertebrate and non-vertebrate hemoglobins. In a major contrast to classical vertebrate partner, which is 3 over 3 α helical fold, it is having 2-on-2 α helical fold. The truncated hemoglobins have been so far characterised in ciliated protozoa *Paramecium caudatum*, unicellular alga *Chlamydomonas eugametos*, eubacteria *Nostoc commune*, *Mycobacterium tuberculosis*, *Mycobacterium smegmatis*, *Mycobacterium leprae* etc (Couture et al., 1994; Fabozzi et al., 2006a; Iwaasa et al., 1989; Lama et al., 2006; Thorsteinsson et al., 1999; Tsubamoto et al., 1990; Visca et al., 2002). Truncated hemoglobins are generally characterised as a single domain proteins, however Hb identified in *Streptomyces avermitilis* and *Frankia* sp are found to be dual domain and are called as Sa-ktrHb and Fa-ktrHb, respectively. Here the globin domain is fused to a domain assigned to the “antibiotic biosynthesis monooxygenase” (ABM) (Bonamore et al., 2007).

Phylogenetically, truncated haemoglobins are branched out into 3 distinct categories i.e. group I (trHbN), Group II (TrHbO) and group III (TrHbP) (Wittenberg et al., 2002). Between these groups, the sequence similarity is as low as 18%, whereas orthologous sequences show high similarity of upto 84%. As in the case of TrHbO of *M. tuberculosis* and *M. avium*, the similarity is 84% and *M. leprae* is 83% (Vuletich and Lecomte, 2006).

Opportunistic pathogen *M. marinum* contains one trHbn from each group of the family, trHbP (group III), trHbO (group II) and trHbN (group I). The facultative intracellular pathogen *M.tuberculosis* contains two trHbN and trHbO and obligate pathogen *M.leprae* retain only HbO during the course of evolution (Wittenberg et al., 2002).

1.3.3.1 Functions of truncated hemoglobin

In contrast to vertebrate and other non-vertebrate hemoglobins, trHbs are characterised by the nature of residues on the active site, especially on the distal site of the heme pocket (Wittenberg et al., 2002). This may be related to diverse physiological roles proposed. Group I trHbN from unicellular alga, *Chlamydomonas eugametos*, has been ascribed the role of photosynthesis. It is mainly present in the chloroplast thylakoid membrane and protects photosynthesis from reactive oxygen species (Couture et al., 1994; Das et al., 1999). Group I trHb of the photoautotrophic cyanobacterium,

Nostoc commune, is localized on the cytoplasmic face of the cell membrane, being expressed only in the conditions that favors nitrogen fixation (Potts *et al.*, 1992). Group I Hb in *M. tuberculosis* and *M. bovis* perform efficient nitrogen dioxygenase function. It has been proposed that *Campylobacter jejuni* trHbP may plays a role in cell respiration (Wainwright *et al.*, 2005; Wainwright *et al.*, 2006). In *Streptomyces avermitilis* and *Frankia* sp trHbs are fused with “antibiotic biosynthesis monooxygenase domain” (ABM) and act as oxygen radical scavenging partner for the monooxygenation reaction (Bonamore *et al.*, 2007). HbP of *Campylobacter jejuni* is seen to possess high reactivity for cyanide, suggesting that this haemoglobin may plays a role in cyanide poisoning (Bolli *et al.*, 2008).

There is no single function assigned to the trHb group but definitely they play a vital role in metabolism and survival of the host. The array of functions is increasing with the increase in the discovery of trHbs from organisms present in diverse locations like hot springs e.g. *Geobacillus stearothermophilus* (Ilari *et al.*, 2007) and Antarctica e.g. *Pseudomonas haloplanktis* (Giordano *et al.*, 2007).

1.3.3.1.1 Role of haemoglobin in bacterial pathogenesis.

The ability of flavohemoglobin to detoxify NO anaerobically (Hausladen *et al.*, 1998) and aerobically (Gardner *et al.*, 1998b; Hausladen *et al.*, 1998) led to the revelation of unified enzymatic mechanism. Later series of pathogenic bacteria were found to contain hemoglobin like protein with NOD as one of their function. The FHB deficient *Salmonella typhimurium* was impaired in NO consumption and showed defective virulence in mice. The virulence was fully restored in iNOS mutant mice (Bang *et al.*, 2006). FlavoHb from *Pseudomonas aeruginosa*, *Salmonella typhimurium*, *Klebsiella pneumonia* and *Dinococcus radiodurans* (Bollinger *et al.*, 2001), *Bacillus subtilis* also contains flavohemoglobin, strongly induced under anaerobic condition (LaCelle *et al.*, 1996). *Campylobacter jejuni*, a predominant pathogenic agent in bacterial gastrointestinal disease, suffers from restricted growth under aerobic condition when its trHbP is defective. In *M. bovis* BCG, and *M. tuberculosis*, group I trHbN catalyses efficient NOD reaction and protect the pathogens against nitrosative stress. HbN also rescued its surrogate host *E. coli* and salmonella from NO toxicity (Pathania *et al.*, 2002a; Pawaria *et al.*, 2007). Similarly HbO, the only truncated haemoglobin present in *M. leprae*, is endowed with O₂ uptake or delivery properties during its hypoxia.

TrHbO also protects *M. leprae* from nitrosative stress by scavenging peroxynitrite (Fabozzi et al., 2006b).

1.3.3.2 Truncated haemoglobins of *Mycobacterium tuberculosis*

When the complete genome sequence of *Mycobacterium tuberculosis* was first published, bioinformatics analysis suggested the presence of two putative haemoglobin genes, namely glbN and glbO (Cole et al., 1998). They were found to be expressed at different stages of growth, suggesting different functional attributes for these oxygen binding proteins. Careful observation of the sequence of other pathogenic species of mycobacterium revealed a unique retrogression in the expression profile of truncated hemoglobins, which otherwise is evolutionary progressive. The genome of opportunistic pathogen, *M. avium* contains one trHb from each of the three trHb groups: HbP, HbO and HbN. The facultative intracellular pathogen, *M. tuberculosis* has two types of trHbN, namely HbN and HbO and the obligate intracellular pathogen, *M. leprae*, has retained only HbO (Vuletic and Lecomte, 2006; Wittenberg et al., 2002). This reduction reflects the adaptation of organism from saprophytic to pathogenic life style and clearly hints towards the crucial role played by trHb in the physiology of the organism.

The extent of amino acids identity between HbN and HbO is only 18%. HbN is expressed during the stationary phase, whereas, HbO is expressed throughout the growth phase of the *M. tuberculosis* (Mukai et al., 2002; Pathania et al., 2002b). HbN binds oxygen co-operatively with high affinity ($P_{50} \sim 0.013\text{mM Hg}$) (Couture et al., 1999), while HbO binds O_2 with moderate affinity ($P_{50} \sim 0.5\text{mM Hg}$). Structure-based fingerprints for trHbs, including the presence of three glycine motifs and the occupancy of the B9 and E14 positions by two Phe residues (Pesce et al., 2000), are present in both HbN and HbO. In HbN, proximal ligand to the heme is His and the distal residues at the E7 and B10 positions, which stabilize heme-bound ligands in other hemoglobins, (Couture et al., 1999; Olson et al., 1988; Yang et al., 1995) are Leu and Tyr, respectively. More interestingly, the highly conserved CD1 residue, which is phenylalanine in all Hbs studied to date, is Tyr in HbO.

1.3.3.2.1 Structural features of HbN and HbO of *Mycobacterium tuberculosis*

The three dimensional structures of HbN and HbO were determined by Milani et al., in 2001 and 2003, respectively (Milani et al., 2001; Milani et al., 2003). According

to the conservation of sequence-specific motifs, both the trHbs display the “2-over-2” fold. The trHbO crystal shows aggregation of the protein in a compact dodecameric assembly (Figure 1.8). The compact dodecamer can be visualised as a stack of equilateral triangles, which is defined by the vertex-subunits A, B, C and D, E, F in the upper and lower layers, respectively. Local two-fold axes, hosted between the two triangular protein layers, relate pairs of HbO subunits (A/D, B/E, C/F and G/K, H/L, I/J).

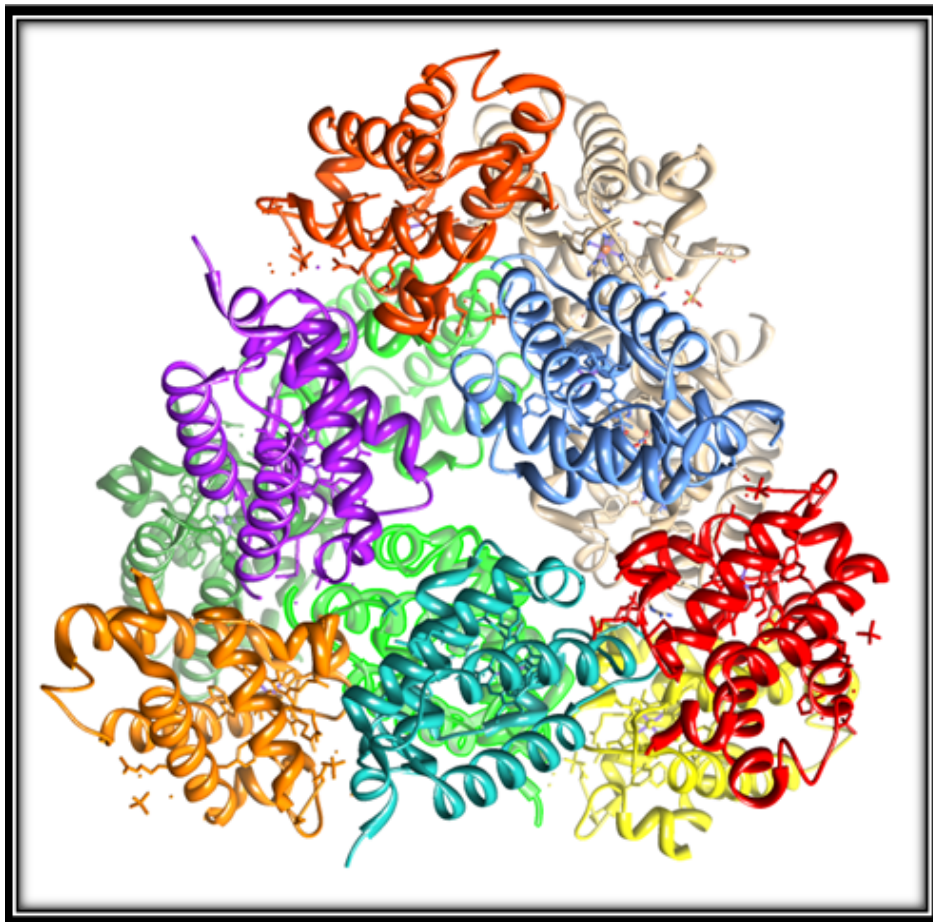


Figure 1.8: Structure of truncated haemoglobin HbO (PDB: 1NGK), showing its dodecameric alignment.

There's a clear structural conservation of the main protein regions held to be crucial for stabilization of the trHb fold in both the mycobacterial Hbs. Among these are a one turn A-helix, tying the N-terminal region to protein core, the short (3_{10}) C-helix, supporting PheCD1 in HbN and TyrCD1 in HbO, the E-helix hosting residues LeuE7, the three Gly-based motifs at the AB, E-pre-F and Pre-F-F secondary structure transition regions and the trHb invariant PheE14. In case of HbN, 11 residues extended

polypeptide segment (pre-F) on the heme proximal side is followed by a one turn F-helix, supporting HisF8. In contrast to this in trHbO the Pre-F hosts 15 residues as a result of two residues insertions characteristic of group II Hbs. The first insertion (residues 64-66 in HbO) is reflected by the presence of a novel six-residue α -helix (the ϕ -helix), involved in the interaction with heme propionates D. The segment following the ϕ -helix (the “ ϕ F-loop”) contains the group II conserved sequence motifs Gly-His-Pro-X (where X indicated group II specific second insertion), which adopts an irregular extended conformation and precedes the one turn F-helix.

HbN has a unique 12 amino acids, highly polar extended portion called as pre-A region in the N-terminus, protruding from compact globin fold (Figure 1.9). This additional structure is absent in its homologous C-trHbN and P-trHbN and HbO as well. It is composed of a short Pre-A helix [Gly(2)-Lys(9)] and an extended tetrapeptide [Arg(10)-Ile(13)]. The Highly polar sequence motif: Arg-Leu-Arg-Lys-Arg in the 6-10 pre-A region may be responsible for the breakdown of the elongated α -helix expected here for a conventionally folded Hb. Moreover an intra-molecular hydrogen bonded salt bridge between residues Arg (6) and Asp (17) and crystal packing contacts to G-helix and the pre-F loop, may support the orientation of the pre-F segment.

The most extraordinary feature of the trHbN is the presence of two continuous tunnels orthogonal to each other. They connect the outer surface of the protein to inner distal heme pocket (DHP). One entry point is the AB and GH hing region and another is marked by the residues of G and H helix e.g. Ala69, Leu G12 (98) and Ile H 11(119). Length of the long tunnel is ~ 20 Å and of the short tunnel is ~ 8 Å. Inner lining of the tunnel is apolar in nature, as it is composed of [Ile A15(19), AlaB1(24), IleB2(25), Val B5(28), Val B6(29), Phe B9(32), Phe E15(62), Ala E16(63), Leu 19(66), Leu 12(98), Leu 16(102) and Ala G19(105) on the main tunnel branch; Ala G9(95), Leu H8 (116) and Ile H11(119) on the short tunnel branch]. The heme bound oxygen falls at the intersection of the two tunnel branches where the distal residues TyrB10 and GlyE11 are located. In fact, due to the orientation of the E-helix being close to the heme distal side and to the location of the side chains of ThrCD4, ArgE6, LeuE7 and Lys10, solvent access to the distal site cavity through the classical E7 path is completely impaired (Bolognesi *et al.*, 1982; Perutz, 1989b; Scott *et al.*, 2002). Considering this fact, HbN’s tunnel may provide an efficient diffusion path for O₂ and other small ligands. Phe E15(62) present at the end of the long tunnel inside the protein, is seen in dual

conformation, differing by 63° by rotation around the C_α - C_β bond in subunit A. This tunnel system helps in efficient diffusion of gaseous ligand to the DHP and E7 gate is inaccessible to the ligand. Further the presence of Phe E15 in two different conformations hint at the gating mechanism for modulating the ligand diffusion.

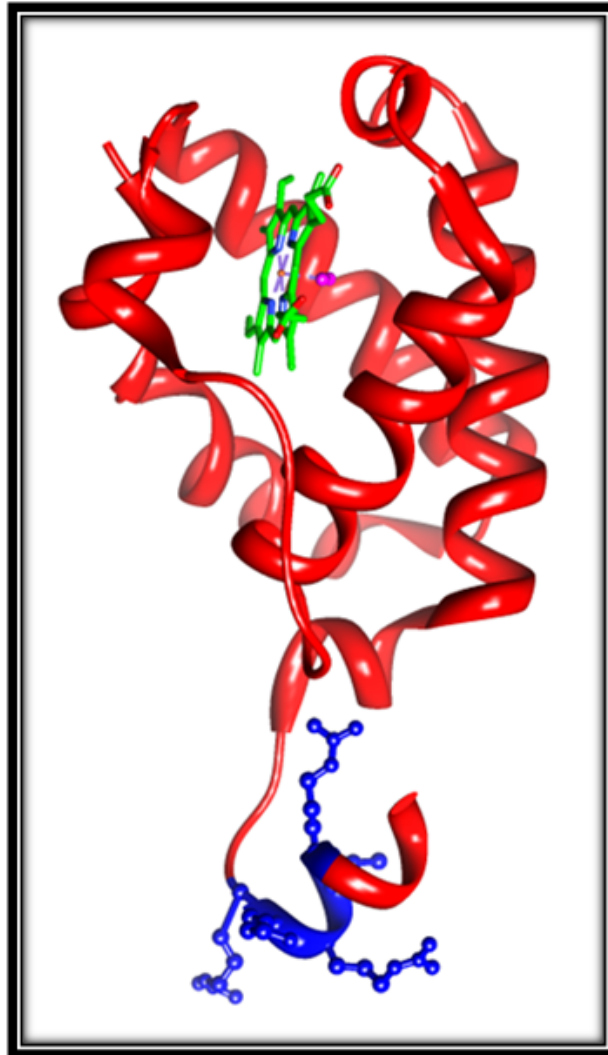


Figure 1.9: Structure of truncated haemoglobin HbN (PDB:1IDR). The 2-over-2 globin fold of HbN is depicted in red, heme in green and the charged residues of the pre-A region are highlighted in magenta colour.

The crystal structure of HbO (Milani *et al.*, 2003) showed that the protein matrix tunnel observed in HbN, dramatically restricted in HbO, where different relative orientations of G- and H- helices and an increased volume of side chains at topological positions, (AlaB13Thr, ValB53Ile, ValG83Trp, AlaG93Leu, LeuG123Met, and AlaH123Glu), partly fill the protein matrix tunnel space. Thus, the long tunnel branch retains only two cavities in HbO, both fully shielded from solvent contact. The highly

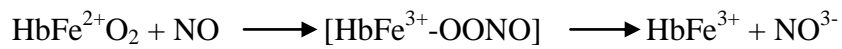
restricted protein matrix tunnel seems to be mirrored by the general presence of a small distal site E7 residue in group II HbO (Vuletic and Lecomte, 2006), contrary to what is observed in group I, where a Gln/Leu residue is highly conserved at position E7. Therefore, accessibility of diatomic ligands (such as O₂, CO, and NO) to the HbO heme distal site is favoured by a small apolar E7 residue, which does not obstruct entrance to the heme distal cavity and which may support an E7 route entry system. Nevertheless, the two cavities present in the protein, indicate that they may be required as ligand docking stations. Another intriguing structural feature found in trHbO (Milani *et al.*, 2003) is the presence of a shallow a depression that (lined by conserved hydrophobic residues), which provides partial solvent access to heme C-pyrrole, and may serve as docking a site for the reductase partner, thus possibly having functional significance in heme redox chemistry.

In the crystal structure of oxygenated *M. tuberculosis* HbN, the heme-bound oxygen is stabilised by network of hydrogen bonds, which include TyrB10 and GlnE11. As a result, the dioxygen is tightly buried in the distal site, and may be polarized to a partial superoxide character. In HbO specific residue mutations remarkably modify the distal distal site environment and size. On one hand, the CD1 site is occupied by Tyr residue, whose phenolic hydroxyl (OH) group protrudes well into the heme distal pocket. On the other hand, the side chain of TrpG8 (the G8 residue in group I trHbs is generally valine) is large enough to reach the heme ligand binding site, filling a significant fraction of heme crevices.

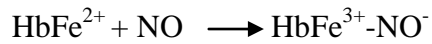
1.4 Interaction of Nitric Oxide with hemoglobin

With the accreditation of new functions to NO as a vascular relaxing factor and as an immune cell-derived antibiotic and anti-tumour agent, new avenues in the NO binding proteins were opened. The basic chemistry of heme group is promiscuous in nature, which allows it to bind to different gaseous ligands with variable efficiency and purpose. Later significant amount of studies were conducted to measure the reactivity of NO with the conventional and other newly discovered haemoglobins. Various life forms have developed different ways to quench the poisonous effects of NO. NO is mainly detoxified by three ways

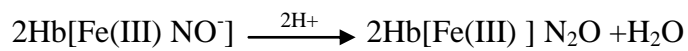
a) Nitric Oxide Dioxygenase (NOD) activity in which the oxy-haemoglobin rapidly reacts with NO to form ferric-Hb and nitrate. This activity is shown by flavohemoglobins, *vitreoscilla* Hb, GlnN etc.



b) Oxygen nitroxylase activity in which the oxygen binding to heme is preceded by NO-heme complex formation.



c) Oxygen independent NO reductases (NORs). In which NO is converted to nitrous oxide.



In addition, a novel catalytic role for NO in detoxifying O₂ was identified with *Ascaris* Hb (Minning *et al.*, 1999). In mammals (presumably in birds) S-nitrosylation/ denitrosylation of Hb subserves RBC mediated hypoxic vasodilation that matches blood flow to metabolic demand (Singel and Stamler, 2005; Sonveaux *et al.*, 2007).

1.5 Scope of the present study

Complete genome of the *Mycobacterium tuberculosis* unveiled the presence of 2 distinct truncated hemoglobin encoding genes namely, *glbN* and *glbO*. Based on their structural organisation they were categorised into two separate groups, i.e. group I and group II, respectively (Wittenberg *et al.*, 2002). Subsequent analysis of microbial genome indicated that Group I trHbs (HbN) are present in restricted group of microorganisms unlike group II trHbs (HbO), that are widely distributed among microbes and plants. Type I Hbs have been found to exhibit an array of functions in different hosts, such as photosynthesis in *Chlamydomonas eugamatos* (Couture *et al.*, 1994), O₂ supply to mitochondria in *Paramecium caudatum* (Wittenberg *et al.*, 2002), as a part of electron transfer system in *Nostoc commune* etc (Potts *et al.*, 1992). The occurrence of HbN in pathogenic species makes it even more special, as it may be playing some crucial physiological functions that may assist the pathogen in its survival and pathogenicity. In *M.bovis* and *M.tuberculosis*, expression of HbN occurs during stationary phase when levels of nutrients and oxygen drop significantly (Couture *et al.*, 1999; Pathania *et al.*, 2002a). Additionally, transcriptional regulation activities of *glbN* gene increases under hypoxic and nitrosative stress conditions *in vitro* grown cells and *in vivo* during macrophage infection (Ouellet *et al.*, 2003; Ouellet *et al.*, 2002) (Pawaria *et al.*, 2007). Available experimental studies thus indicate its pivotal role under these conditions.

HbN deviates from the orthodox functions of haemoglobin, i.e. as an oxygen storehouse and transporter. This can be attributed to its unique structural features which were revealed by its X-ray structure. HbN of *M.tuberculosis* is a single domain molecule with 2-over-2 globin fold instead of classical 3-over-3 globin fold of haemoglobin and myoglobin. HbN contains two distinguished features: the presence of a highly flexible, polar, 12 amino acids extended pre-A region and the presence of two orthogonal tunnels connecting the outer surface of the protein to the distal heme pocket (DHP) (Milani *et al.*, 2001). They are known as long and short tunnel because of their sizes. These two tunnels intersect at the Distal Heme Pocket (DHP). At the end of the long tunnel, inside the cavity, there is a presence of Phe62 amino acid residue that acts as a tunnel gate. Phe62 is supposed to modulate the opening and closing of the long tunnel and facilitates the ligand entry and diffusion to the active site. Several residues such as PheE14(61) along with Tyr72 provide efficient closure of lower part of the heme pocket. Similarly

residues of the pre-F helix and E helix form extensive hydrogen bonds and around 51 van der Waals bonds to completely hinder the solvent access to the heme distal site. These arrays of bonds render the tunnels to be the only route available for ligand access to the porphyrin ring. Interestingly Raman spectra of O₂, CO and OH recommend that the HbN's heme-Fe coordination is highly favourable for O₂/NO chemistry (Yeh *et al.*, 2000). All the above mentioned structural aspects synergistically drive HbN to perform oxygen mediated NO detoxification.

The proposition that HbN actively participates in the NO related chemistry has been substantiated through rounds of experiments. This was proved by the ability of HbN to rescue its native as well as surrogate hosts such as *E.coli* and *Salmonella* from the toxicity of NO and nitrosative stress (Ouellet *et al.*, 2002; Pawaria *et al.*, 2007). Similar effect was observed in the Δ HbN strain of *M.bovis* which was growth compromised during NO stress as compared to its wild type strain (Ouellet *et al.*, 2002). HbN of the pathogenic strain *M.tuberculosis* (H37Rv), is known to perform O₂ mediated NO detoxification activity, several folds higher than its homologous HbN of non pathogenic strain *M.smegmatis* despite having 80% similarity (Lama *et al.*, 2006). This suggests that the HbN of *M.tuberculosis* is far more evolved to resist NO toxicity and nitrosative stress than its close relative, HbN of *M.smegmatis*.

Subsequently, Lama *et al* came up with a crucial finding that the difference in the NOD activity between HbN of *M.tuberculosis* and *M.smegmatis* mainly depends on the presence or absence of additional 12 amino acids residues, constituting the pre-A region (Lama *et al.*, 2009). Surprisingly, this pre-A motif is absent in fast growing non pathogenic strain such as *Mycobacterium sp.* KMS, *Mycobacterium sp.* JLS, *M. flavescens*, *M. vanbaalenii* is present in many slow growing pathogenic species of mycobacterium such as *M. bovis*, *Mycobacterium avium*, *Mycobacterium microti*, *Mycobacterium marinum*. Their findings were further substantiated by demonstrating the increase in the NOD activity of *M.smegmatis* HbN with the fusion of pre-A region from *M.tuberculosis* HbN, thereby proving that the pre-A region is indispensable for *M.tuberculosis* HbN to be functionally active during NOD reaction. What is fascinating is the unknown mechanism by which an extended, 12 amino acids pre-A portion is controlling the compact protein's backbone. Some insight has been provided by the Molecular dynamics (MD) simulation studies and homology modelling (Lama *et al.*, 2009).

Homology modelling of *M.smegmatis* HbN, based on the *M.tuberculosis* HbN's crystal structure (pdb:1IDR), depicted the well preservation of the globin fold, specially the tunnels and the phe62 molecular switch formed by the pair of Tyr(B10)-Gln(E11). Molecular Dynamics simulations, based on the homology model, demonstrate that the overall globin fold of HbN of *M.tuberculosis* and *M.smegmatis* remained constant, however high R.M.S.D value or flexibility were seen in the pre-A and F helix. Phe62 was observed to be trapped in the close confirmation in pre-A deleted HbN mutant and *M.smegmatis* HbN, resulting in the closure of the long tunnel, thus jeopardizing the NO access to the heme (Lama *et al.*, 2009). In the simulation studies, pre-A segment was seen to form four major representative confirmations during the 100ns trajectory. Arg6 in the pre-A was involved in salt bridge formation with Asp17 residue. However, how these intra-molecular interactions between pre-A and protein's core modulate NOD function of HbN is not known. The intriguing functional correlation between its unique structural elements, such as pre-A motif and tunnels, are yet to be elucidated. Another crucial structural element of HbN is the presence of hydrophobic tunnels within the protein matrix. From the simulation studies it could be hypothesized that the entry of O₂ molecule through the short tunnel may bring about some conformational change in the protein leading to opening of the long tunnel for the entry of the NO through it. These ligands access pathways need to be validated. The role of Phe62 as a gatekeeper amino acid also needs to be experimentally corroborated to demonstrate the importance of tunnels in ligands migration. Clear understanding of the exact role played by each component will help us to solve the intricate mechanism of HbN function and its role in modulating the pathogenicity of tubercule bacillus.

It is quite surprising that inspite of evolving as a single domain protein, HbN possess an efficient NOD activity ($k_{\text{NOD}} \sim 745 \mu\text{M}$ at 23 °C) second only to flavohemoglobin which has a reductase domain attached to its C-terminal region (Pathania *et al.*, 2002a). The fact that a reductase is required for recycling of HbN post NOD or NO denitroxylase activities, makes it even more indispensable for efficient NOD function. In the absence of a cognate reductase partner it was hypothesized that it might interact with some reductase protein to bring about the change in its oxidation state. Earlier over expression studies of HbN in surrogate hosts have revealed that it is capable of performing its NOD function with the same vigour. This suggests that it has the ability to interact with the substitute reductase partners existing in the range of hosts.

HbN encounters array of reductases in its milieu at a particular moment, so the factors involved for the selection of appropriate partner need to be looked into. To best of our knowledge there is no information available regarding the HbN-reductase interaction, therefore, studying this will not only expand our insight on importance of HbN in intracellular survival of *M.tuberculosis* but also on the *modus operandi* of it within the macrophagic environment.

Ability to swiftly adapt to the external stimuli is the key to success of *Mycobacterium tuberculosis*. To counteract the lethal responses of host, *Mtb* has large repertoire of effector molecules that has to be expressed under the strict supervision of transcriptional factors. Previously, the transcriptional fusion studies on HbN with the green fluorescent protein have established the substantial upregulation of *glbN* promoter during stationary phase. It showed approximately 2 fold increase in the promoter activity during nitrosative stress (Pawaria *et al.*, 2008). Thus it is quite reasonable to look into the stringent genetic regulation of HbN which otherwise has been overlooked till now. To obtain the holistic view on the role of HbN in cellular metabolism and pathogenicity of *M.tuberculosis*, it is important to identify factor(s) regulating HbN expression. The fact that it is expressed during the latency, demand for the detailed study of the promoter region, that will provide clue about the transcriptional factors responsible for its survival within the macrophage.

The present study has been undertaken to understand the molecular mechanism of HbN function in *M.tuberculosis* and identify structural and genetic factors that are vital for regulating the functional characteristic of this trHb. Detailed biochemical and biophysical studies were conducted to gain insight about the role(s) of two unusual structural features, pre-A and tunnels, of HbN. Site directed mutagenesis studies on pre-A region of HbN have provided novel information on involvement of pre-A residues in regulating intramolecular interaction with protein core that may be vital for the optimal NO dioxygenation by HbN and interaction with redox partner. Biochemical studies have also been done to decipher the relative efficiency of electron transfer between HbN and different reductases. Protein protein docking studies have been performed to deduce the probable path attained by the electrons for transfer. Attempts have also been made to determine the transcriptional regulator for *glbN* gene through *in vitro* binding studies. All these studies will give novel integrated knowledge about the NOD mechanism behaviour and regulation of HbN, which in the greater picture will be a step closure

towards understanding the biology of this pathogen. Finally, this study has unfolded some putative vulnerable portions in the HbN, which if targeted with some drug, can abrogate its NOD function.



Chapter2

Material and Methods

2.1.1 Bacterial Strains.....	25
2.1.2 Plasmids	25-26
2.1.3 Oligonucleotides.....	26-28
2.1.4 Reagents.....	28
2.1.5 Media used.....	28-30
2.1.6 Preparation of antibiotics	30
2.1.7 Preparation of organic reagents.....	30
2.1.8 Preparation of commonly used stock solutions.....	30-33
2.1.9 Buffers for plasmid DNA preparation.....	33
2.1.10 Electrophoresis buffers.....	33-35
2.1.11 Solutions for Western blotting.....	35
2.2 Methods.....	35-45
2.2.1 Sequence retrieval and analysis.....	35-36
2.2.2 Growth studies.....	36
2.2.3 Determination of NO consumption activity	36
2.2.4 Determination of cell respiration in the presence of NO.....	36
2.2.5 Heme Assay.....	37
2.2.6 Estimation of hemoglobin content.....	37
2.2.7 Isolation of plasmid DNA.....	37-38
2.2.8 Polymerase chain reaction (PCR).....	38
2.2.9 Agarose gel electrophoresis.....	38
2.2.10 Restriction endonuclease digestion.....	38-39

2.2.11 Purification of DNA fragment from agarose gel.....	39
2.2.12 Ligation.....	39
2.2.13 DNA sequencing.....	39-40
2.2.14 Preparation of competent cells and transformation in <i>E. coli</i>	40-41
2.2.14.1 Calcium chloride method.....	40
2.2.14.2 Electrotransformation.....	40-41
2.2.15 Purification of 6X His-tag proteins.....	41
2.2.16 Purification of HbN and HbN-reductase proteins.....	41-42
2.2.17 Protein estimation.....	42
2.2.18 Sodium Dodecyl Sulphate-Polyacrylamide Gel Electrophoresis (SDS-PAGE)	
2.2.19 Coomassie Blue staining.....	42-43
2.2.20 Silver Staining	43
2.2.21 Western Blotting and Immunoassay.....	43-44
2.2.21.1 By DAB.....	44
2.2.21.2 By Chemiluminescence.....	44
2.2.22 Growth curves in the presence of sodium nitrite.....	44
2.2.23 Electrophoretic mobility shift assay.....	44-45
2.2.24 Enzymatic reduction of HbN by individual reductase proteins.....	45
2.2.25 Dnase I Footprinting analysis of the promoter.....	45

2. Materials and Methods

2.1 Materials used in the present study

2.1.1 Bacterial Strains

All the bacterial strains used in this study are listed in Table 2.1 *Escherichia coli* were maintained on LB agar plates, with 30 µg/ml kanamycin and 100µg/ml ampicillin in case of *E. coli* NC4112. *M.tuberculosis* H37Ra were grown in Middlebrook 7H9 medium or on 7H10 agar plates (Difco) supplemented with 0.05% Tween-80, 0.2% glycerol and OADC (10% bovine serum albumin fraction V, dextrose, catalase and oleic acid) enrichment for *M.tuberculosis*. For short-term storage of weeks to a month, the strains were maintained on their respective agar plates, supplemented with appropriate antibiotics whenever required, at 4 °C. For long-term storage of months to years, the cultures were maintained in 15% glycerol at -70 °C.

Table 2.1: Host strains used in the present study

Strains	Relevant Characteristics	Source
<i>E. coli</i> JM109	Rec A1, hsd R17 Δ(lac-pro AB) [F ⁺ tra D36 pro AB lacI ^q Z ΔM15]	Promega
<i>M.tuberculosis</i> H37Ra	Slow growing (doubling time), attenuated derivative of H37Rv	--
<i>E. coli</i> BL21(DE3)	F ⁻ , ompT, r _B -m _B -prophage carrying T7 RNA polymerase. Has lacUV5 promoter inducible by IPTG	Novagen

2.1.2 Plasmids

The following vectors and pre-constructs were used in this study:

pBluescript KS⁺ (pBS KS⁺): A pUC19 derived phagemid (2.9kb) carrying ColE1 origin of replication, Amp^r, an extensive polylinker cloning site and a β-galactosidase with first 14 amino acids deleted. In JM series of *E. coli* strains, α-complementation of the deleted amino acids takes place resulting in a functional β-galactosidase. Thus, in the presence of IPTG (inducer) and X-gal (substrate), cells containing pBS KS⁺ show up as blue colonies. Recombinant colonies can be easily screened on the plate as white colonies due to insertional inactivation; obtained from Stratagene.

pET9b: This is a low copy number expression vector (Studier *et al.*, 1990), which is derivative of pBR322 and carries Kan^r and a strong T7 promoter which is inducible by IPTG; obtained from Novagen, USA.

pET28c: This is a low copy number expression vector which is a derivative of pBR322 and carries Kan^r and a strong T7 promoter which is inducible by IPTG. These series of vectors are designed for generating target proteins fused with cleavable His-tag or T7-tag sequences with the option to include a C-terminal His-tag sequence; obtained from Novagen, USA.

2.1.3 Oligonucleotides

Oligonucleotides were obtained from commercial sources *e.g.* BioBasic Inc., Canada or Integrated DNA Technologies Inc., USA.

HbNNde: This is the N-terminus primer used along with C-terminus primer GlnNCT to amplify *glbN* gene of *M.tuberculosis* and clone in *E.coli*. The primer incorporates *NdeI* site (shaded) in the gene to facilitate its subcloning in the expression vector pET9b or pET28c under T7 promoter.

5'-GATCACATATGGGACTACTGTACGCTTGCGCAAAC-3' (38 mer)

GlnNCT : This is the C-terminus primer used along with N-terminus primer HbNNde to amplify *glbN* gene of *M.tuberculosis* and clone in *E.coli*. The primer incorporates *BamHI* site (shaded) in the gene to facilitate its subcloning in the expression vector pET9b or pET28c under T7 promoter.

5'-GATCAGGATCCTCAGACTGGTGCCGTGGTGCTCTCGCCC-3'

Nter1: This primer binds to the N-terminus of *glbN* of *M.tuberculosis* and was used along with GlnNCT to change 4 positively charged residues (R6, R8, K9 and R10) of HbN N-terminus to alanine. The resulting PCR was used as a template for primer pair Nter2 and GlnNCT.

5'-GCCTTAGCCGAGCCGATCAGCATCTACGACAAGA-3'

Nter2: This is the N-terminus primer used along GlnNCT to amplify the *glbN* gene of *M.tuberculosis*. It used to change R8 (the 2nd positively charged residue) of trHbN N-terminus to alanine.

5'-ACGCTTAGCCAAACGTGAGCCGATCA-3'

Nter3: This is the N-terminus primer used along GlnNCT to amplify the *glnN* gene of *M.tuberculosis*. It used to change K9 (the 3rd positively charged residue) of trHbN N-terminus to alanine.

5'-AGCTTGCGCGCACGTGAGCCGATCAGC-3'

Nter4: This is the N-terminus primer used along GlnNCT to amplify the *glnN* gene of *M.tuberculosis*. It used to change R10 (the 4th positively charged residue) of trHbN N-terminus to alanine.

5'ATAGGCATATGATGGGACTACTGTCACGATTACGCAAAGCTGAGCCGATC-3'

Nterall: This primer binds to the N-terminus of *glnN* of *M.tuberculosis* and was used along with GlnNCT to change 4 positively charged residues (R6, R8, K9 and R10) of HbN N-terminus to alanine.

5'-ATAGGCATATGATGGGACTACTGTCCGCCTTGGCCGCAGCTGAACCGATC-3'

Rv3133cNT: This is the N-terminus primer used along with C-terminus primer 3133cCT to amplify *devR* gene of *M.tuberculosis* and clone in *E.coli*. The primer incorporates *NdeI* site (shaded) in the gene to facilitate its subcloning in the expression vector pET9b or pET28c under T7 promoter.

5'-TACGGTCATATGGTGGTAAAGGTCTTCTTGGTC-3'

Rv3133cCT: This is the N-terminus primer used along with C-terminus primer 3133cNT to amplify *devR* gene of *M.tuberculosis* and clone in *E.coli*. The primer incorporates *NdeI* site (shaded) in the gene to facilitate its subcloning in the expression vector pET9b or pET28c under T7 promoter.

5'-CATTGGGATCCTCATGGTCCATCACCGGG-3'

WhiB1NT: This is the N-terminus primer used along with C-terminus primer WhiB1CT to amplify *whiB1* gene of *M.tuberculosis* and clone in *E.coli*. The primer incorporates *NdeI* site (shaded) in the gene to facilitate its subcloning in the expression vector pET28c under T7 promoter.

5'-ATATCACATATGGATTGGCGCC-3'

WhiB1CT: This is the C-terminus primer used along with N-terminus primer WhiB1NT to amplify *whiB1* gene of *M.tuberculosis* and clone in *E.coli*. The primer incorporates *NdeI* site (shaded) in the gene to facilitate its subcloning in the expression vector pET28c under T7 promoter.

5'-ATACTAGGATCCTCAGACCCCGGTACG-3'

5' Promoter HI: This is the N-terminus primer used along with C-terminus primer K6 CT to amplify promoter region of *glbN* gene of *M.tuberculosis*.

5'-GATCATTGGATCCCTCCTGATGGC GG-3'

3' Promoter Hind III: This is the C-terminus primer used along with N-terminus primer Promoter HI to amplify promoter region of *glbN* gene of *M.tuberculosis*.

5'-AGTCTGAAGCTTGCGTGACAGTAGTCCCAT-3'

2.1.4 Reagents

All reagents used in this study were of analytical grade. Various fine chemicals were procured from the sources listed below:

- ✿ Antibiotics – Amersham Biosciences, Roche, Sigma Chemical Co.
- ✿ Restriction endonucleases, T4 DNA ligase, Poly Nucleotide Kinase, Klenow Fragment – Promega, New England Biolabs (NEB).
- ✿ Urea, Acrylamide, Bis-Acrylamide, APS, DAB, TEMED, Ethidium Bromide, DTT USB.
- ✿ X-ray films, Developer, Fixer- Indu, Hindustan photo films manufacturing Co. Ltd., Madras, India.
- ✿ Deep Vent Polymerase – New England Biolabs, USA.
- ✿ Tryptone, Yeast Extract, Agar – HiMedia, India.
- ✿ IPTG, Lysozyme, Protein molecular weight markers, X-gal, Imidazole, BSA and Bromo Phenol Blue– Sigma Chemical Co.
- ✿ Sequencing kit and Miniprep kit – ABI PRISM, Amersham Biosciences.
- ✿ Glassware, Plasticware, Microfuge tubes, Tips etc. – Tarson, India.

2.1.5 Media used

LB medium (Luria Bertani medium)

Tryptone	10 g
Yeast extract	5 g
NaCl	10 g

The contents were dissolved in 900 ml of deionized water and pH was adjusted to 7.4 with 10 N NaOH. Final volume was made to 1 L with deionized water. Sterilized by aut-

oclaving for 15 min at 15 lb/in² in liquid cycle.

LB agar

15 g/L agar was added to the LB medium and sterilized by autoclaving for 15 min at 15 lb/in² in liquid cycle. Plates were stored at 4 °C for a period of 15-20 days.

LB agar with antibiotics

The autoclaved LB medium was allowed to cool to 45 °C before adding the antibiotics.

Super Broth

Tryptone	32 g
Yeast extract	20 g
NaCl	5 g

The above contents were dissolved in 900 ml of deionized water and pH was adjusted to 7.4 with 10 N NaOH. Final volume was made to 1 L with deionized water and was sterilized by autoclaving for 15 min at 15 lb/in² in liquid cycle.

Terrific Broth

Tryptone	12 g
Yeast extract	24 g
Glycerol	4 ml

The solutes were dissolved in 700 ml of deionized water and final volume was made to 900 ml with deionized water. Sterilized by autoclaving for 15 min at 15 lb/in² in liquid cycle. The buffer solution was prepared separately by dissolving 2.31 g of KH₂PO₄ and 12.54 g of K₂HPO₄ in 100 ml of deionized water and autoclaving under similar conditions. The two solutions were mixed under aseptic conditions before use.

X-gal indicator plates

X-gal indicator plates were made (Sambrook *et al.*, 1989) to screen the recombinant clones by blue-white screening. 40µl of X-gal (40 mg/ml in dimethyl formamide) and 70 µl of IPTG (0.1 M in water, filter sterilized) were spread on agar

plates before plating the cells.

2.1.6 Preparation of antibiotics

Ampicillin

A 100 mg/ml stock solution of the sodium salt of ampicillin (USB) in water was made and filter sterilized using 0.22 µm Millipore filter. Aliquots were stored at -20 °C. A working solution of 100 µg/ml ampicillin was used for *E. coli*.

Kanamycin

A 30 mg/ml stock solution of the kanamycin (USB) was prepared and filter sterilized using 0.22 µm Millipore filter. Aliquots were stored at -20 °C. The working solution of 30 µg/ml was used for *E. coli*.

2.1.7 Preparation of organic reagents

Phenol

Tris-saturated phenol (pH 7.5-8.0) was obtained from Bangalore Genei, India.

Phenol : Chloroform

A mixture consisting of equal parts of equilibrated phenol and chloroform was used throughout the study to remove proteins from preparation of nucleic acids. Equal volume of phenol and chloroform was stored in 100 mM Tris.HCl, pH 8.0 in a light-tight bottle.

2.1.8 Preparation of commonly used stock solutions

30% Acrylamide

Acrylamide	29.2 g
N-N ³ -methylene-bis-acrylamide	0.8 g

The above ingredients were first dissolved in 60 ml of double distilled water by stirring on a magnetic stirrer. The final volume was then adjusted to 100 ml with double distilled water. The solution was kept in a brown container and stored at room temperature.

100 mM ATP

60 mg ATP (Sigma) was dissolved in 0.8 ml of autoclaved water. The pH was then adjusted to 7.0 with 0.1 N NaOH. The volume was finally adjusted to 1 ml with autoclaved water and stored at -20°C .

1 M CaCl₂

21.90 g of CaCl₂.6H₂O (Sigma) was dissolved in 100 ml water and filter sterilized using 0.22 μm Millipore filter.

0.5 M EDTA

18.61 g of ethylenediamine-tetra-acetic acid disodium salt (Qualigens, India) was added to 80 ml of double distilled water and pH was raised to 8.0 using NaOH pellets. EDTA usually gets dissolved at pH 8.0. The volume was adjusted to 100 ml, sterilized by autoclaving and kept at room temperature.

10 mg/ml Ethidium bromide

1 g of ethidium bromide (Sigma) was added to 100 ml distilled water and dissolved properly by stirring for 2 hr. The solution was stored in a dark bottle at room temperature.

IPTG (Isopropyl-thio- β -D-galactoside)

0.2 g of IPTG was dissolved in 0.8 ml of double distilled water. Final volume was adjusted to 1 ml and filter sterilized using 0.22 μm Millipore filter. The solution was stored at -20°C .

X-Gal (5-Bromo-4-chloro-3-indolyl- β -D-galactopyranoside)

40 mg/ml stock solution of X-gal was prepared in dimethyl formamide. Stock was stored in a microcentrifuge tube wrapped in aluminum foil at -20°C .

3 M Sodium acetate

40.81 g of sodium acetate, was dissolved in 80 ml of distilled water. The pH was either adjusted to 5.2 with glacial acetic acid or adjusted to 7.0 using dilute acetic acid.

Final volume was adjusted to 100 ml with distilled water and autoclaved.

10% SDS

10 g of SDS (Sigma) was dissolved in 90 ml of distilled water. It was dissolved by heating at 65 °C. Final volume was adjusted to 100 ml and stored at room temperature.

1 M Tris

121.1 g of Tris-base (Sigma) was dissolved in 80 ml of distilled water and pH was adjusted to 8.0 by adding 4.2 ml of concentrated HCl. Final volume was made to 1 L by using distilled water. Sterilized by autoclaving and stored at room temperature.

10% Glycerol

100 ml of glycerol was mixed with 900 ml of water and sterilized by autoclaving.

50% Glycerol

50 ml of glycerol was mixed with 50 ml of water and sterilized by autoclaving.

0.5 M SNP (Sodium nitroprusside)

Sodium nitroprusside was prepared freshly when required and was not sterilized.

1 M NaNO₂

0.69 g of sodium nitrite (HiMedia) was dissolved in 10 ml of autoclaved distilled water and used immediately without sterilizing.

1 M Potassium phosphate buffer, pH 7.0

615 ml of 1 M K₂HPO₄ was combined with 385 ml of 1 M KH₂PO₄. Solution was sterilized by autoclaving.

TE (pH 8.0)

Tris.HCl (pH 8.0)

10 mM

EDTA (pH 8.0)	1 mM
---------------	------

2.1.9 Buffers for plasmid DNA preparation

Solution I

Glucose	50 mM
Tris.HCl (pH 8.0)	25 mM
EDTA	10 mM
RNase	100 µg/ml

Each component (except RNase) was autoclaved separately and the final solution was reconstituted in an autoclaved container using autoclaved double distilled water. Stored at 4°C.

Solution II

NaOH	0.2 N
SDS	1.0%

Freshly prepared and kept at room temperature.

Solution III

5M Potassium acetate (autoclaved)	60.0 ml
Glacial acetic acid	11.5 ml
Distilled water (autoclaved)	28.5 ml

Stored at 4°C.

2.1.10 Electrophoresis buffers

50X TAE buffer

Tris.HCl	242 g
Glacial acetic acid	57.1 ml
0.5M EDTA (pH 8.0)	100 ml

Volume was made to 1 L with double distilled water.

6X DNA Gel loading buffer

Bromophenol blue	0.25%
Glycerol	30.0%

5X Protein sample buffer

Tris.HCl (pH 6.8)	125 mM
SDS	4%
Glycerol	20%
β -mercaptoethanol	10%
Bromophenol blue	0.006%

Laemmli buffer (Polyacrylamide gel electrophoresis)

Tris.HCl	3 g
Glycine	14.4 g
SDS	1 g

The volume was adjusted to 1 L with deionized water.

Lower Tris (pH 8.8)

Tris.HCl	18.17 g
----------	---------

Volume made to 100 ml with deionized water after adjusting pH 8.8 with 6 N HCl and the solution was then autoclaved.

Upper Tris (pH 6.8)

Tris.HCl	6.06 g
----------	--------

Volume made to 100 ml with deionized water after adjusting pH to 6.8 with 6 N HCl and the solution was then autoclaved.

Gel staining solution

Acetic acid	10%
Methanol	40%
Coomassie brilliant blue R250	0.25%

Made in deionized water.

Gel destaining solution

Acetic acid 10%

Methanol 40%

Made in deionized water

2.1.11 Solutions for Western blotting

Transfer buffer

Glycine 11.25 g

Tris.HCl 2.34 g

Dissolved the components in 600 ml of deionized water. pH was adjusted to 8.3 and volume was made up to 800 ml. 200 ml of methanol was then added.

10X Phosphate buffered saline (10X PBS, pH 7.4)

NaCl 80 g

KCl 2 g

Na₂HPO₄ 14.4 g

KH₂PO₄ 2.4 g

Volume was made to 1 L with deionized water after adjusting the pH to 7.4.

1X PBST

0.1% Tween-20 in 1X PBS.

Blocking agent

5% Skimmed milk in 1X PBST.

2.2 Methods

2.2.1 Sequence retrieval and analysis

The amino acid sequences for various hemoglobins was fished out of the various

genome projects of microbes from TIGR (www.tigr.org) after performing a Comprehensive Microbial Resource CMR-BLAST (<http://tigrblast.tigr.org/cmrbblast/>) search in various complete and incomplete genome databases. The sequences so retrieved were then aligned using CLUSTAL-W online sequence alignment facility at European Bioinformatics Institute (EBI) (<http://www.ebi.ac.uk/clustalw/index.html>). The alignments were then checked manually for any discrepancies and were corrected accordingly. The percentage identity was directly retrieved from CLUSTAL-W output and computed onto Excel worksheet.

2.2.2 Growth studies

The overnight culture grown in rich media was inoculated into fresh medium at an optical density at 600 nm (OD_{600nm}) of 0.05. For adjusting the oxygen level for aerobic growth, the flasks were filled to one-fifth of their volume with medium and shaken at 180 rpm (pO_2 of 21%). OD_{600nm} was checked after every 2 hr on Cary-100 spectrophotometer.

2.2.3 Determination of NO consumption activity

A Clark type NO electrode (World Precision Instruments), immersed in a stirred glass vial, was used to measure NO uptake by bacteria or cell extract. A saturated solution of NO was prepared in a vessel thoroughly flushed with nitrogen gas according to the procedure described previously (Kaur *et al.*, 2002). The concentration of saturated solution of NO at room temperature was taken as 1.8 mM. The NO uptake activity in HbN and cells were measured in 2 ml of 50 mM potassium phosphate buffer (pH 7.2) containing 1 μ M NO and 100 μ M NADH as described earlier (Pathania *et al.*, 2002a).

2.2.4 Determination of cell respiration in the presence of NO

Oxygen consumption by cells or cell extract was measured polarographically using a Yellow Spring Instrument Model oxygen monitor at 37 °C in 3 ml of air saturated 0.1 M potassium phosphate buffer (pH 7.2). The electrode was calibrated with air-saturated water and upon adding sodium dithionite anoxia was achieved. Then, 1 ml of cell culture was concentrated by centrifugation at 14,000 rpm (the number of cells/milliliter was calculated simultaneously by plating on LB medium) and washed

twice with 0.1 M potassium phosphate buffer (pH 7.2) and the resulting pellet was added quantitatively to 3 ml air saturated buffer. The change in the oxygen concentration of the buffer containing cells was monitored for 5 min. NO was injected with a Hamilton syringe in the test sample to observe the effect of NO on cell respiration

2.2.5 Heme Assay

Total cellular heme was determined as described by Appleby (Appleby *et al.*, 1978). Briefly, cells were washed by centrifugation with minimal salt medium (60 mM K_2HPO_4 , 33 mM KH_2PO_4 , 7.6 mM $(NH_4)_2SO_4$ and 1.7 mM sodium citrate) containing 10 mM glucose and 200 μ g/ml chloramphenicol. Approximately 3×10^9 cells were resuspended with 0.6 ml of alkaline pyridine reagent containing 2.2 M pyridine and 0.1 M sodium hydroxide and lysed with 30 sec of sonic burst. The resulting lysate was clarified by centrifugation and supernatant was then used to calculate heme concentration from the absorption difference at 556 nm and 539 nm for the dithionite-reduced and ferricyanide-oxidized samples.

2.2.6 Estimation of hemoglobin content

CO-difference spectra of the whole cells or purified protein was recorded at RT with a Perkin Elmer spectrophotometer and heme content was calculated using $\epsilon_{419nm-436nm} = 274 \text{ mM}^{-1} \text{ cm}^{-1}$ for the CO-difference spectrum.

2.2.7 Isolation of plasmid DNA

The rapid alkaline lysis method of plasmid isolation described by Sambrook *et al.* (Sambrook *et al.*, 1989) was followed. For small-scale preparation of plasmid DNA, 1.5 ml of overnight culture was pelleted and suspended in 0.1 ml of ice-cold Solution I by vigorous vortexing. The cells were lysed by the addition of 0.2 ml of freshly prepared Solution II. The contents of the tube were mixed gently and stored at room temperature till the lysis was complete. After lysis, 0.15 ml of ice-cold Solution III was added; contents were mixed by inverting the tube gently. The tube was kept on ice for 10 min after which it was centrifuged at 10,000 rpm for 10 min at RT. The supernatant was transferred to a fresh tube and extracted with equal volume of chloroform:isoamyl alcohol (24:1). The plasmid DNA was precipitated by adding 2 volumes of ice-cold ethanol and the tube was kept on ice for 15 min. The plasmid was recovered by

centrifugation at 12,000 rpm for 15 min at RT and washed with 70% ethanol. The pellet was dried and dissolved in appropriate volume of TE (pH 8.0). The DNA was stored at -20 °C until used.

For large-scale plasmid DNA preparation, plasmid miniprep method was scaled up accordingly, except that after suspending the cell pellet in Solution I, the cells were treated with lysozyme (10 mg/ml) for 15 min at 37 °C.

2.2.8 Polymerase chain reaction (PCR)

This technique was utilized to clone different cDNAs and to carry out site-directed mutagenesis. Appropriate oligonucleotides were used as listed in materials. PCR was performed according to the method developed by Mullis (Mullis and Faloona, 1987). For normal reaction, 20 pmol of primers and nearly 50 ng of template DNA (genomic or plasmid), 500 µM of each dNTP, 1X Thermopol buffer (NEB, UK) and two units of Deep Vent Polymerase (NEB, UK) were added. The final volume of the reaction mix was made to 100 µl with autoclaved double distilled water and the contents were mixed gently. The PCR cycle consisted of: Denaturation at 95 °C for 1 min, annealing at 45 °C to 50 °C for 1 min depending on T_m of the primer used, followed by extension at 72 °C for 1 min or more depending on the size of the DNA fragment being amplified. These reaction conditions were repeated for 30 cycles followed by a final extension at 72 °C for 10 min. Amplification was verified by agarose gel electrophoresis.

2.2.9 Agarose gel electrophoresis

DNA fragments were fractionated on 0.8% (w/v) agarose gels as a routine. 1% - 2% gels were run for analyzing very small fragments (<500bp). 6X gel loading buffer was added to DNA samples at a final concentration of 1X prior to loading onto the gel. Electrophoresis was carried out in 1X TAE buffer at 10 V/cm for the resolution of restricted plasmid DNA or at 3-5 V/cm for chromosomal DNA. Ethidium bromide (0.5 mg/ml) was supplemented in the agarose gel for visualizing DNA on a UV transilluminator (Spectroline, USA).

2.2.10 Restriction endonuclease digestion

The restriction enzyme digestion of DNA samples (4-6 µg) was carried out according to the manufacturer's instructions (NEB, UK). After incubation at appropriate

temperature, the reaction mixture was heated at 75 °C for 10 min to inactivate the enzyme and was then immediately quenched on ice. The digested DNA was mixed with DNA gel loading buffer and fractionated on agarose slab gel electrophoresis. Lambda DNA fragments generated by *Hind*III digestion, 100bp DNA ladder and 1kb DNA ladder were used as molecular size markers for calculating the size of unknown DNA fragments from their relative mobility.

2.2.11 Purification of DNA fragment from agarose gel

After electrophoresis, DNA was visualized using a UV transilluminator, the fragment(s) of interest was located and cut out from gel and purified using GFX PCR DNA and Gel Band Purification *Kit from Amersham Biosciences, UK*. The purified DNA was used for further applications.

2.2.12 Ligation

The vector and insert DNA were mixed in an equimolar ends ratio in a total volume of 20 µl at a final concentration of approximately 250 µg/ml DNA. Blunt end ligation was carried out at 18 °C by adding 2 µl of 10X T4 DNA ligase buffer, 1 µl of (1-2 Weiss units) of T4 DNA ligase (NEB, UK). In case of sticky ends, 2 µl of 10 mM ATP was also included and the reaction was incubated at 16 °C for 16-18 hr.

2.2.13 DNA sequencing

Sequencing grade DNA was prepared using ABI PRISM miniprep kit. Briefly, the cell pellet was treated with alkaline lysis solutions. The contents were centrifuged and the supernatant obtained, was mixed with binding buffer. The entire solution was poured onto a miniprep column, the resin of which preferentially binds supercoiled plasmid DNA. The resin was washed with wash buffer and the DNA was finally eluted in TE (pH 8.0). Both commercially available as well as custom synthesized primers (3.2 pmol) were used in PCR reactions. 200-500 ng of template DNA was taken for sequencing PCR in a total volume of 10 µl. The following PCR steps were used:

1. 96 °C, 5 min
2. 96 °C, 30 sec
3. 50 °C, 15 sec
4. 60 °C, 4 min

5. Go to step 2, 23 cycles
6. 4 °C hold

The PCR samples were further processed for sequencing. DNA was precipitated by adding 2 µl of 125 mM EDTA, pH 8.0 and 50 µl of absolute ethanol. The contents were mixed and incubated at RT for 15 min. The tubes were centrifuged at 13,000 rpm for 20 min and the pellet was washed twice with 70% ethanol and air-dried. Just prior to submission of samples for sequencing, the DNA pellet was resuspended in 12 µl of HiDi formamide and heated at 95 °C for 3 min. The samples were immediately chilled on ice. Sequencing was carried out on an automated sequencer (ABI PRISM 377 DNA Sequencer, Perkin Elmer Applied Biosystems).

2.2.14 Preparation of competent cells and transformation in *E. coli*

Single colony of *E. coli* was inoculated in 10 ml of LB or superbroth medium and grown to saturation. The culture was re-inoculated in fresh medium at a dilution of 1:100 and grown to mid log phase (OD_{600nm} of 0.3-0.5) at 37 °C with shaking. The cells were harvested by centrifugation at 5,000 rpm at 4 °C and processed further for the preparation of competent cells and transformation by any of the following methods.

2.2.14.1 Calcium chloride method

CaCl₂ competent *E. coli* cells were prepared by the method of Cohen *et al.* (Cohen *et al.*, 1972). The harvested cells were resuspended in 0.1 volume of ice-cold 0.1 M CaCl₂ and incubated on ice for 30 min. Following centrifugation, the pellet was resuspended in 0.02 volumes of the buffer containing 0.1 M CaCl₂ and 15% glycerol. The aliquots of 200 µl were made on ice and stored at -70 °C for later use. For transformation, ligation mix (10 µl containing ~100 ng of DNA) or plasmid DNA (100 ng) was added to an aliquot and incubated on ice for 30 min. Following heat shock treatment at 42 °C for 90 sec, the cells were kept on ice for 5 min. The transformed cells were incubated at 37 °C for 1 hr after the addition of 800 µl of LB broth to allow the expression of antibiotic marker. Cells were then plated on LB agar plates supplemented with appropriate antibiotic. For blue-white screening, 40 µl of X-gal (20 mg/ml) and 70 µl of IPTG (0.1 M) were spread on the plates prior to plating the cells.

2.2.14.2 Electrotransformation

Electrocompetent *E. coli* cells were prepared according to the method of Dower

et al. (Dower *et al.*, 1988) whenever high frequency of transformation was required. The cells were first washed with equal volume and then with half the volume of ice-cold 1 mM HEPES buffer (pH 7.0). The cells were then washed with 0.04 volumes of ice-cold 10% glycerol. Finally, these were suspended in 0.002 volume of ice-cold 10% glycerol and 50 μ l aliquots were made on ice that were stored in -70 °C for later use. For electroporation, ligation mix (1 μ l containing ~20 ng DNA) or 50 ng of plasmid DNA was added to an aliquot and put in a 0.2 cm cuvettes (Bio Rad, USA). Care was taken to avoid formation of air bubbles. The cuvette was placed in the cuvette holder and electric pulse was given using a Bio-Rad Gene Pulser at a setting of 2.5 kV, 25 μ F and 100 Ω . Immediately, 1 ml LB broth was added to the transformed cells and properly mixed. The contents of the cuvette were transferred to fresh tube and incubated at 37 °C for 1 hr. Cells (50-100 μ l) were plated on LB agar plates supplemented with appropriate antibiotics. X-gal and IPTG were included at this step whenever blue-white selection was required.

2.2.15 Purification of 6X His-tag proteins

Ni²⁺-NTA affinity chromatography was used to purify His-tagged proteins. Briefly, the culture of *E. coli* cells expressing the protein was harvested by centrifugation at 5,000 rpm for 10 min at 4 °C and resuspended in lysis buffer (50 mM NaH₂PO₄, 300 mM NaCl and 10 mM imidazole, pH 8.0). The cells were sonicated for about half an hour with 30 sec pulse on and 20 sec pulse off and then subjected to ultracentrifugation (45,000 rpm, 4 °C, 1 hr). The clear supernatant thus obtained, was loaded on Ni²⁺-NTA column pre-equilibrated with lysis buffer (pH 8.0) and kept at 4 °C for an hour with gentle rocking. After that, the flow through was collected and the column was washed with 8 volumes of wash buffer (50 mM NaH₂PO₄, 300 mM NaCl and 20 mM imidazole, pH 8.0). The protein was eluted with 2 volumes of elution buffer (50 mM NaH₂PO₄, 300 mM NaCl and 200 mM imidazole, pH 8.0). The eluted protein was analyzed by SDS-PAGE.

2.2.16 Purification of HbN and HbN-reductase proteins

For the protein purification, the culture of *E. coli* cells expressing HbN and HbN-Reductase proteins were harvested by centrifugation at 6,000 g for 10 min at 4 °C and

were resuspended in 10 mM Tris.Cl (pH 8.0) having 10 mM DTT, 1 mM EDTA, 45 µg/ml PMSF, 500 µg/ml RNase and 100 units/ml DNase I. The cells were lysed after passing through French Pressure cell (two cycles) and then subjected to ultracentrifugation (170,000 g, 4 °C, 2 hr). The clear reddish brown supernatant thus obtained, was loaded on an ion-exchange column (DEAE-sepharose CL-6B, Pharmacia), pre-equilibrated with 10 mM Tris.Cl (pH 8.0) and eluted using increasing concentration gradient of NaCl and the protein containing fractions were collected. The eluted proteins were then loaded onto then loaded on to Superdex-75 column (Pharmacia, 30 cm x 10 cm) and eluted in 10 mM Tris.Cl (pH 8.0) at a flow rate of 1ml/min. The protein elution profile was monitored at 280 nm and 412 nm, respectively.

2.2.17 Protein estimation

The protein concentration was estimated according to the Bicinchoninic Acid (BCA) method using BSA as the standard. The protein samples in compatible buffer were made to 25 µl and to this was added 200 µl of BCA reagent (Thermo Scientific, USA) in an Elisa plate. The contents were incubated at 37°C for 30 min and absorbance was monitored at 562 nm in an Elisa plate reader.

2.2.18 Sodium Dodecyl Sulphate-Polyacrylamide Gel Electrophoresis (SDS-PAGE)

SDS-PAGE was carried out essentially according to Laemmli (Laemmli, 1970). Briefly, protein samples were prepared by mixing with 5X sample buffer at a final concentration of 1X. The samples were boiled for 10 min in water bath and centrifuged at 13,000 rpm for 15 min prior to loading onto the gel. The discontinuous gel system was usually used with 10-15% resolving gel (depending on the size of the protein) in 0.375 M Tris.HCl, pH 8.8 and a 4% stacking gel in 0.125 M Tris.HCl, pH 6.8. Electrophoresis was carried out in Laemmli buffer at a constant current of 20 mA till samples entered the resolving gel and then at 30 mA till the completion of gel run. Protein molecular weight markers were also run concurrently on the gels till completion.

2.2.19 Coomassie Blue staining

On completion of electrophoresis, the gel was immersed in 0.25% Coomassie Brilliant Blue R250 (Sigma) in methanol:water:acetic acid (4:5:1) with gentle shaking

and was then destained in destaining solution, methanol: water: acetic acid (4:5:1) till the background was clear.

2.2.20 Silver Staining

In this method, after electrophoresis, the gel was fixed for 20 mins in a mixture of methanol : acetic acid : water (4:1:5) and then washed twice in distilled water for 10 min. The gel was washed in washing solution (methanol : water, 8:1) for 10 mins. Then, the gel was emersed in sensitivity solution (Sodium thiosulphate = 20mg in 100 ml water) for 10 min. The gel was stained in prechilled staining solution (silver nitrate = 0.2g, formaldehyde = 76ul in 100ml water) for 10mins and then developed by developing solution (Sodium thiosulfate = 0.4mg, sodium carbonate = 6g, formaldehyde = 50 μ l). The developing was stopped by adding acetic acid (10ml in 90ml solution).

2.2.21 Western Blotting and Immunoassay

Western blotting of the cell lysate of *E coli* cells expressing recombinant proteins was carried out as described by Towbin *et al.* (Towbin *et al.*, 1979). The cell lysate in 6X sample buffer was resolved on SDS-PAGE gel. The dimensions of the gel were measured and two sheets of Whattman paper and one sheet of nitrocellulose membrane of dimensions equal to that of the gel were cut. The gel along with the electro-blotting pads, Whattman paper and nitrocellulose membrane (USB, UK) was equilibrated with the transfer buffer. In the electro-blotting apparatus (Bio Rad, USA), the gel cassette was arranged on the negative side (black colored) in the following sequence from bottom to top: gel pads, Whattman sheet, gel, nitrocellulose membrane, Whattman sheet and finally gel pad. The cassette was closed and blotting was done electrophoretically onto nitrocellulose membrane at 30 mA for 2 hr. The nitrocellulose membrane (blot) was carefully removed from the cassette and put in blocking solution (5% skimmed milk in 1X PBST) for 12-16 hr at 4 °C. The blot was then washed with 1X PBST and incubated with primary antibodies, raised in rabbit against the recombinant protein blotted, at appropriate dilution in 5% skimmed milk in 1X PBST for 2 hr at RT with gentle shaking. The blot was washed thrice with 1X PBST followed by 3 washings with 1X PBS, each for 15 min. The blot was then incubated with HRP-conjugated goat anti-rabbit antibody (Sigma) at a dilution of 1:6000 in 1X PBST at RT with gentle shaking. It was then washed with 1X PBST three times, each for 15 min.

The blot was now developed by either of the following two methods:

2.2.21.1 by DAB

The color reaction for HRP-linked secondary antibody using DAB was carried out by immersing the blot in 10 ml of reaction buffer solution having 10 mg each of DAB (Diamino benzidine, Sigma) and imidazole (Sigma) and 3 μ l of H₂O₂. The reaction was terminated by washing with distilled water.

2.2.21.2 by Chemiluminescence

The blot was developed using ECL plus Western Blotting Detection System Kit from Amersham Biosciences, UK according to the manufacturer's instructions. Briefly, detection reagents A and B, provided in the kit, were mixed in a ratio of 1:1, respectively and poured as a thin film on the blot. The blot was kept at RT for 5 min and the excess detection reagent was drained off by holding the membrane gently in forceps and touching the edge against tissue. The blot was wrapped in a fresh piece of saran wrap and X-ray film was exposed in dark for 30 sec to 1 min depending on the signal strength. The X-ray film was developed by putting in developer for 4-5 min, washing with water and then putting in fixer for 5 min. The X-ray film was washed under running tap water for 15 min before drying.

2.2.22 Growth curves in the presence of sodium nitrite

E. coli BL21DE3 cells were transformed with recombinant plasmids, HbN, and HbN mutants and a control vector pET28c. Control and recombinant cells carrying hemoglobin genes were grown overnight and inoculated into fresh medium at an OD_{600nm} of 0.05 along with different concentrations of sodium nitrite. The cultures were shaken at 180 rpm for high aeration. OD_{600nm} was checked after every 2 hr on CARY-100 spectrophotometer.

2.2.23 Electrophoretic mobility shift assay

The 250 bp *glbN* promoter fragment (-200 to +50 of *glbN* was end-labeled with γ AT³²P using T4 polynucleotide kinase and 100 ng incubated with 40 to 100ng of purified whiB1 at 20 °C for 20 min in a buffer containing 50 mM Tris-HCl, pH 7.6, 50%

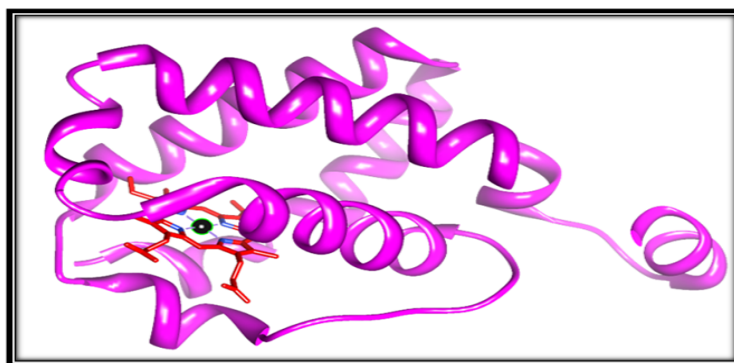
glycerol, 5mM DTT, 0.5M EDTA and 5 $\mu\text{g mL}^{-1}$ herring sperm DNA. Unlabelled *glnB* promoter region was added at 4ng/assay when required for competition experiments. Samples were analyzed for DNA-protein complex formation on 6 % TBE-buffered polyacrylamide gels. After electrophoresis, the gels were transferred to filter paper (3MM, Whatman) and dried for autoradiography.

2.2.24 Enzymatic reduction of HbN by individual reductase proteins

The method used in this study was adapted from one described earlier by Hayashi *et al* (Hayashi *et al.*, 1973) and modified by Hargrove 's group (Smagghe *et al.*, 2008). First a 1 ml cuvette was flushed for 1 min with 1 atm CO. Then 100mM Tris pH 7.0 equilibrated with 1 atm CO was added through a rubber stopper. After addition of 60 mM NADP⁺ (Sigma), 1 mM ferredoxin-NADP reductase (*E. coli*), and 5 mM Hb was added to start the reduction reaction. Absorbance spectra at 420nm were collected over a period of 30 min at room temperature. The difference in absorbance between ferric and CO-bound protein was plotted versus time to calculate the initial velocity of the reaction.

2.2.25 DNase I Footprinting analysis of the promoter

For DNase I footprinting, radiolabelled *PglnB* DNA (~60 ng) was incubated with 80ng of WhiB1 in the presence of 50 mM Tris/HCl, pH 8.0, 100 mM KCl, 12.5 mM MgCl₂, 1mM EDTA, 20% (v/v) glycerol and 1 mM DTT. The complexes were then digested with 1 unit of DNase I for 30–90 s at 25°C. Reactions were stopped by the addition of 200mM NaCl, 30mM EDTA, 100mM SDS, followed by phenol/chloroform extraction. The DNA was ethanol precipitated and resuspended in loading buffer [80% (v/v) formamide, 10% (v/v) glycerol, 8 mM EDTA, 0.1% Bromophenol Blue and 0.1% Xylene Cyanole] for electrophoretic fractionation on 11% polyacrylamide-urea gels and autoradiographic analysis.



Chapter 3

Role of structural elements on NO-dioxygenation function of HbN

3.1 Introduction.....	46
3.2 Results	48
3.2.1 Requirement of charged residues in the pre-A motif for NOD function of HbN.....	48-55
3.2.1.1 Distribution of charged residues within Pre-A motif.....	48
3.2.1.2 Mutating the charged cluster of HbN have no effect on the O ₂ /CO binding.....	50
3.2.1.3 Pre-A mutants of HbN have lower NO oxidation ability.....	50-54
3.2.1.4 Pre-A mutants display lower NO consumption rate.....	54-55
3.2.2 Role of long tunnel of HbN in NOD function: Contribution of Phenylalanine62 as a gatekeeper of long tunnel.....	55-61
3.2.2.1 Construction of Phe62 (E15) gate mutants of HbN.	56
3.2.2.2 Effect of mutations at PheE15 gate of HbN on O ₂ /CO binding.	56-57
3.2.2.3 Mutations at PheE15 gate of HbN alter its NOD activity.....	57-58
3.2.2.4 Oxidation of NO by oxygen adduct of PheE15gate mutants of HbN	58-61
3.3 Discussion.....	62-63

3.1 Introduction

Mycobacterium tuberculosis poses a serious threat to the public health worldwide, infecting nearly one third of the global population. The remarkable adaptability of the tubercle bacillus to cope with hazardous level of reactive nitrogen/oxygen species within the intracellular environment contributes to its pathogenicity. An enhanced levels of nitric oxide (NO) and reactive nitrogen species produced within activated macrophages during infection plays a vital role in host defence, limiting the intracellular survival of *M. tuberculosis*, and contributes in restricting the bacteria to latency. Nevertheless, *M. tuberculosis* has evolved efficient resistance mechanisms by which toxic effects of NO and nitrosative stress can be evaded. One of the unique defence mechanisms by which *M. tuberculosis* protects itself from the toxicity of NO relies on the oxygenated form of truncated hemoglobin N (HbN), which catalyzes the rapid oxidation of NO to harmless nitrate (Couture et al., 1999; Ouellet et al., 2002; Pathania et al., 2002a). Compared to horse heart myoglobin, the nitric oxide dioxygenase (NOD) reaction catalyzed by *M. tuberculosis* HbN is 15-fold faster, suggesting that it may be crucial in relieving nitrosative stress (Pawaria *et al.*, 2008). Despite having single domain architecture, the NO-scavenging ability of *M. tuberculosis* HbN is comparable to flavoHbs that are integrated with a reductase domain and known to have a high NOD activity. It is thus important to understand what structural and dynamical features of HbN contribute to the efficiency of its enhanced NO scavenging function, and therefore ensure survival of the bacillus under nitrosative stress.

X-ray crystallographic studies revealed that *M. tuberculosis* HbN has two unique structural features: presence of a 12 amino acids long, extended pre-A region and a protein matrix tunnel composed by two orthogonal branches (Milani *et al.*, 2001; Milani *et al.*, 2004). MD simulation studies have revealed that *M. tuberculosis* HbN has evolved a novel dual-path mechanism to drive migration of O₂ and NO to the distal heme cavity (Bidon-Chanal *et al.*, 2006; Crespo *et al.*, 2005). According to this mechanism, access of O₂ to the heme cavity primarily involves migration through the tunnel short branch (~10 Å long, shaped by residues in helices G and H). Binding of O₂ to the heme then regulates opening of the tunnel long branch (~20 Å long, mainly defined by helices B and E) through a ligand-induced conformational change of PheE15 (62) residue, which would act as a gate. Recent studies have demonstrated that opening of PheE15 is also regulated by the N-terminal pre-A motif (Lama *et al.*, 2009). This

shows that although both pre-A motif and tunnels are two distinct components of HbN, they are functionally interwoven to each other to bring about NOD activity.

Lama *et al* have clearly shown that in the absence of pre-A region, HbN has one-third of its NOD activity (Lama *et al.*, 2009). When this pre-A motif was added to *M. smegmatis* HbN, which has 80% sequence similarity with *M. tuberculosis* HbN but lacks this extended region, its NOD activity was restored, to confirm its role in NO scavenging. So, how exactly is the presence of an extended region confer NO scavenging activity to HbN, needs to be explored and further it would be interesting to investigate the regulation of signalling to Phe62 amino acid, distantly located to it. Owing to its highly flexible and polar nature, it has the freedom to interact with the surface exposed amino acids present in the main globin fold, which was confirmed with simulation studies where salt bridge formation between Arg6 and Asp17 and between Arg10 and Glu70 were captured. Thus, the charged residues present in the pre-A region may be crucial for sustaining the NOD function of HbN.

Since the NOD function of HbN depends on the diffusion of NO to the O₂-bound heme through the long tunnel branch, the PheE15 gate emerges as a fundamental residue in determining the overall efficiency of NO scavenging. Accordingly, the NOD function of HbN must result from a balanced tuning of the opening/closing of the gate. Moreover, the functional implication of PheE15 in assisting the NOD activity is supported by the preservation of this residue in mycobacterial HbNs, while it is replaced by other residues in truncated hemoglobins, HbO and HbP (Ascenzi *et al.*, 2007; Milani *et al.*, 2005).

To the best of our knowledge, no experimental data have yet been reported to examine the role of charged residues in the pre-A region and gating role of PheE15 and their influence on the NOD activity conducted by *M. tuberculosis* HbN. In this context, this study has been undertaken to probe the role of charged residues in the pre-A motif and PheE15 in context of the NOD function of HbN. To this end, several mutants of the pre-A region, core region and several PheE15 gate mutants have been tested experimentally to delineate their exact role. Attempts have been made to establish the correlation between the two unique structural features, which work synergistically for a common cause. To this end detailed biochemical and biophysical studies have been conducted to elucidate the molecular mechanism of NOD function. This study will further help to gain insight into the molecular dynamics of the tunnel containing proteins.

3.2 Results

To figure out the functional relevance of the charged amino acids of Pre-A motif and Phe62 amino acid, dual approach has been taken. Firstly, the pre-A mutants were characterised to look for their significance and then Phe62 mutants were analysed.

3.2.1 Requirement of charged residues in the pre-A motif for NOD function of HbN

3.2.1.1 Distribution of charged residues within Pre-A motif

Sequence analysis of pre-A region revealed it to be a highly charged structure, comprising of one negatively charged amino acid Glu11 and 4 positively charged amino acids Arg6, Arg8, Lys9 and Arg10 (Figure 3.1). Charged nature along with the flexibility, provides pre-A all the possibility to form salt bridge interactions with counter charged residues present in the core domain by attaining spatial conformation. To verify these interactions, different types of pre-A mutants were generated by site directed mutagenesis to study their role in catalytic activity. The four positively charged amino acids Arg6, Arg8, Lys9 and Arg10 were replaced individually by smaller uncharged amino acid alanine and the mutants were named Nter1, Nter2, Nter3 and Nter4 respectively. One mutant Nter-all was created in which all the positively charged amino

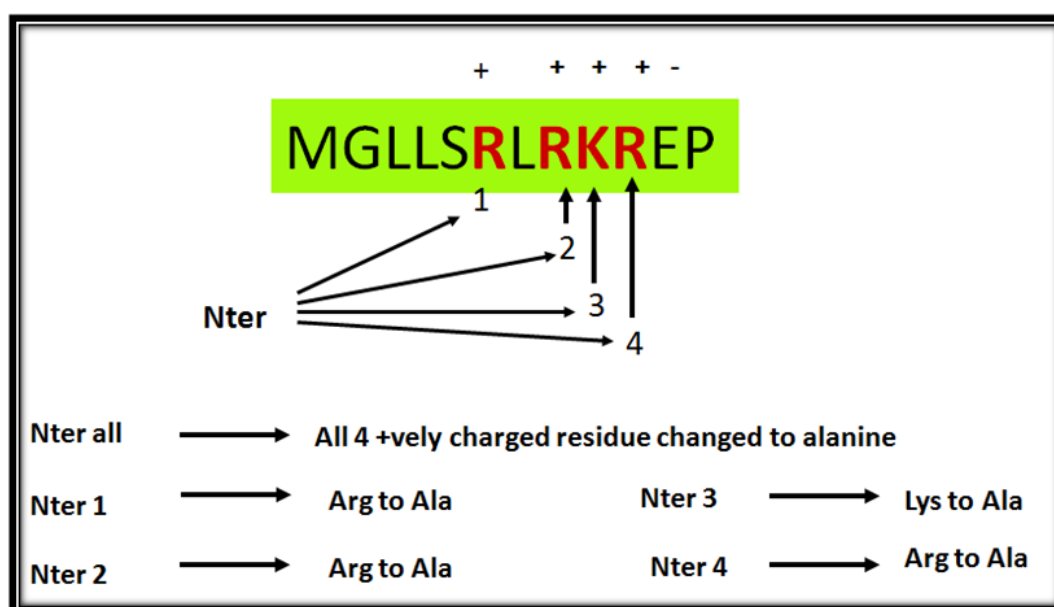


Figure 3.1: Structural organisation of pre-A region. Upper panel is showing the amino acid sequence of the Pre-A region, positively charged amino acids are highlighted in red, whereas, the lower panel is showing the schematic representation of the nomenclature of pre-A mutants.

acids Arg6, Arg8, Lys9 and Arg10 were mutated to alanine. Conversion of positive cha-

rges to alanine will disrupt any putative interaction with oppositely charged amino acid residues. Two pre-A deletion mutants were also created with first 12 amino acids deletion in one mutant (pre-A deleted) and one mutant where first six amino acids were deleted to decipher the role of the length of pre-A region.

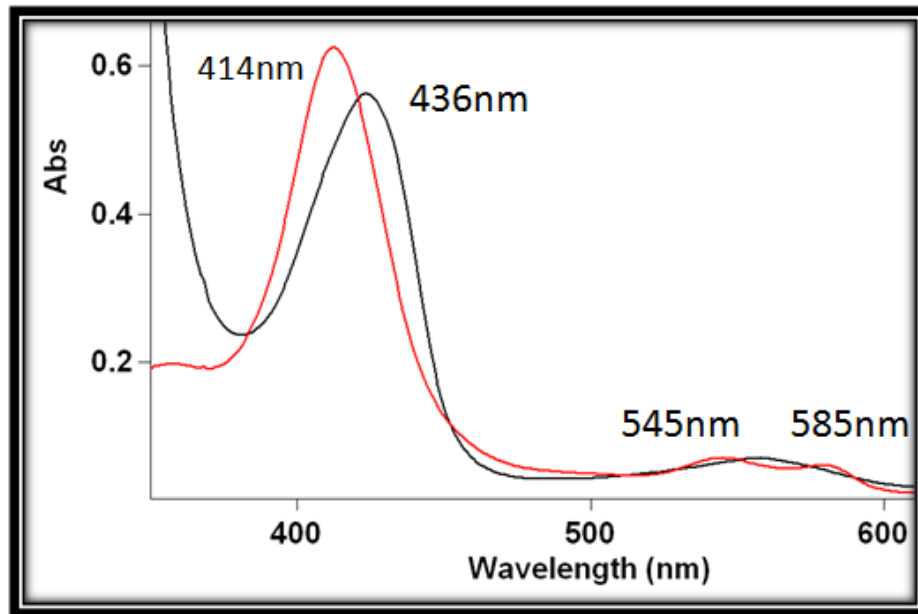


Figure 3.2: Spectral properties of PheE15Ala mutant of HbN. (A) Optical absorption spectra of oxygenated (red line) and sodium dithionite reduced species of mutant HbN, recorded in 50 mM Tris.Cl and pH 7.5 (black line).

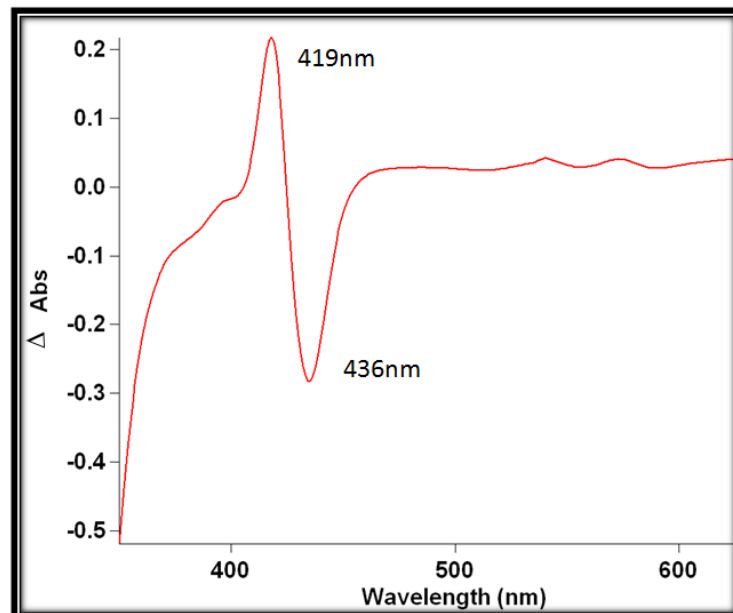


Figure 3.3: CO-difference spectrum of Pre-A mutants of HbN. Spectral profile of other pre-A mutants (Pre-A deleted, Nter-all, Nter1, Nter2, Nter3 and Nter4) appeared similar and matched with the wild type spectrum.

3.2.1.2 Mutating the charged cluster of HbN have no effect on the O₂/CO binding

Site directed alanine mutants of HbN carrying single or multiple mutations displayed spectral properties identical to that of wild type HbN and formed typical oxyform spectra after oxygen binding, indicating that these HbN mutants were able to interact with oxygen and form stable oxyform (Figure 3.2 and 3.3). Characteristics of Pre-A mutants were further checked after studying their O₂/CO binding kinetics. Alanine mutations on the pre-A region did not have any effect on the O₂/CO binding properties of HbN. CO difference spectra and absorption spectra of oxygenated HbN and Pre-A mutants were exactly the same. This was further confirmed by the CO association kinetics were K_{on} value for the wild type HbN and its pre-A mutants were determined. The K_{on} for wild type HbN was found to be 2.5x10⁷ M⁻¹s⁻¹ slightly higher than the value reported by Couture *et al* (0.657x10⁷ M⁻¹s⁻¹) (Couture *et al.*, 1999). Pre-A mutants have K_{on} value comparable to that of wild type suggesting similar behaviour towards CO association (Table 3.1).

Table 3.1: CO association kinetics of Pre-A mutants of HbN of *M. tuberculosis*. Values derived from three independent measurements, each consisting of multiple shots (>50) and averaged out by the program to give the final value. The standard deviation is in the range 0.3–0.5 (x 10⁷).

S.No	Protein	<i>k_{on}</i> (CO) μM ⁻¹ S ⁻¹
1	HbN	2.5 x 10 ⁷
2	Pre-A deleted	2.4 x 10 ⁷
3	Nter-all	2.2x 10 ⁷
4	Nter-1	2.0 x 10 ⁷
5	Nter-2	2.0x 10 ⁷
6	Nter-3	2.3x 10 ⁷
7	Nter-4	2.2x 10 ⁷

3.2.1.3 Pre-A mutants of HbN have lower NO oxidation ability

Oxygenated absorbance spectra of HbN and its mutants were similar having soret peak at around 412-414nm and stable α and β peaks at 545nm and 570nm, indicating proteins to be in similar oxygenated state. Rate of oxidation of NO by oxybound HbN is a measure of NO scavenging ability of the protein and can be easily inferred by the decrease in the rate of α and β peaks upon addition of NO. With the

sequential addition of 2 μ M NO to 50 μ M TrHbN protein, α , β peaks diminished gradually and finally got flattened indicating complete oxidation of HbN. However, with the equivalent amount of addition of NO, all the oxygenated pre-A mutants (Nter1, Nter2, Nter3, Nter4 and Nter-all) showed very slow oxidation rate and α , β peaks did not completely disappear even after 30 mins, indicating that mutants were not been able to completely oxidised with the identical number of NO addition (Figure 3.4, A-E).

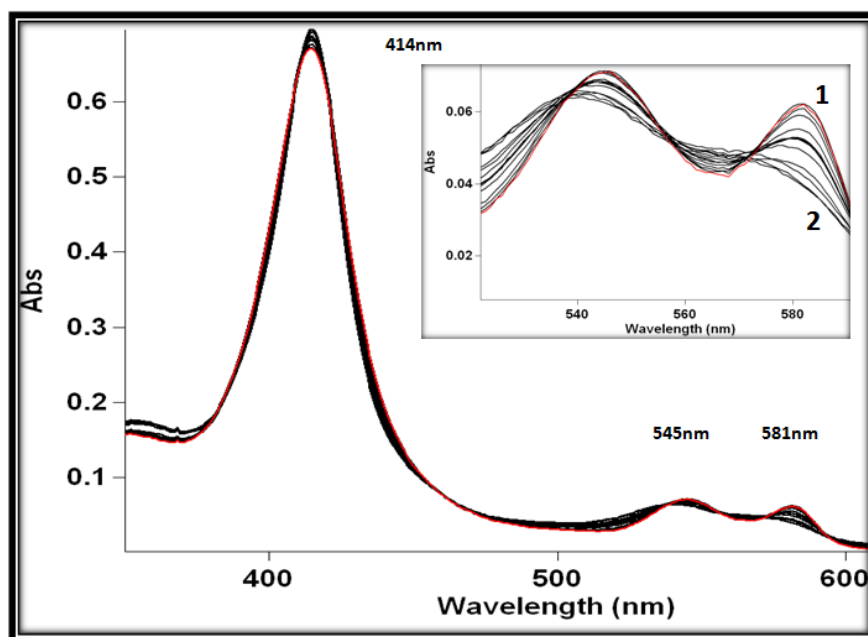


Figure 3.4 A: HbN

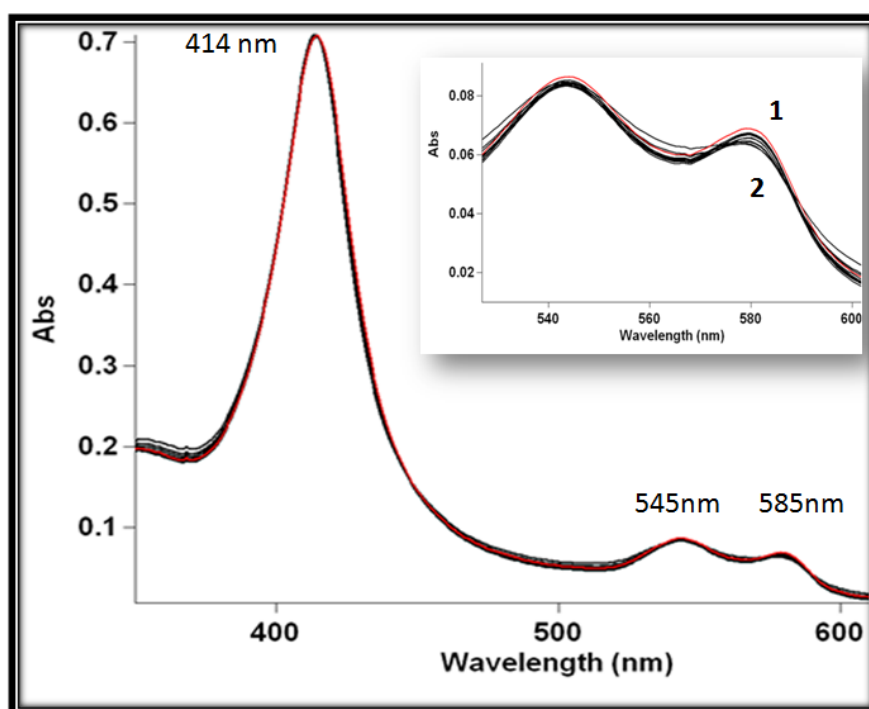


Figure 3.4 B: Pre-A deleted HbN

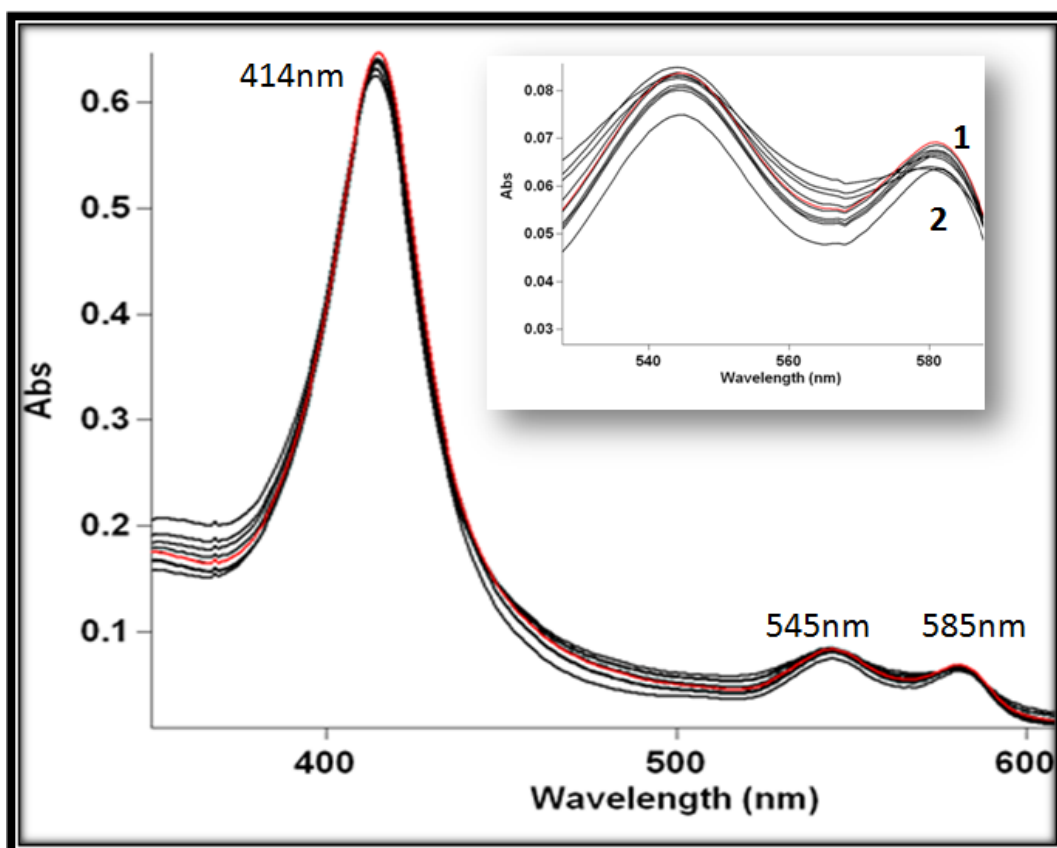


Figure 3.4 C: Nter-all

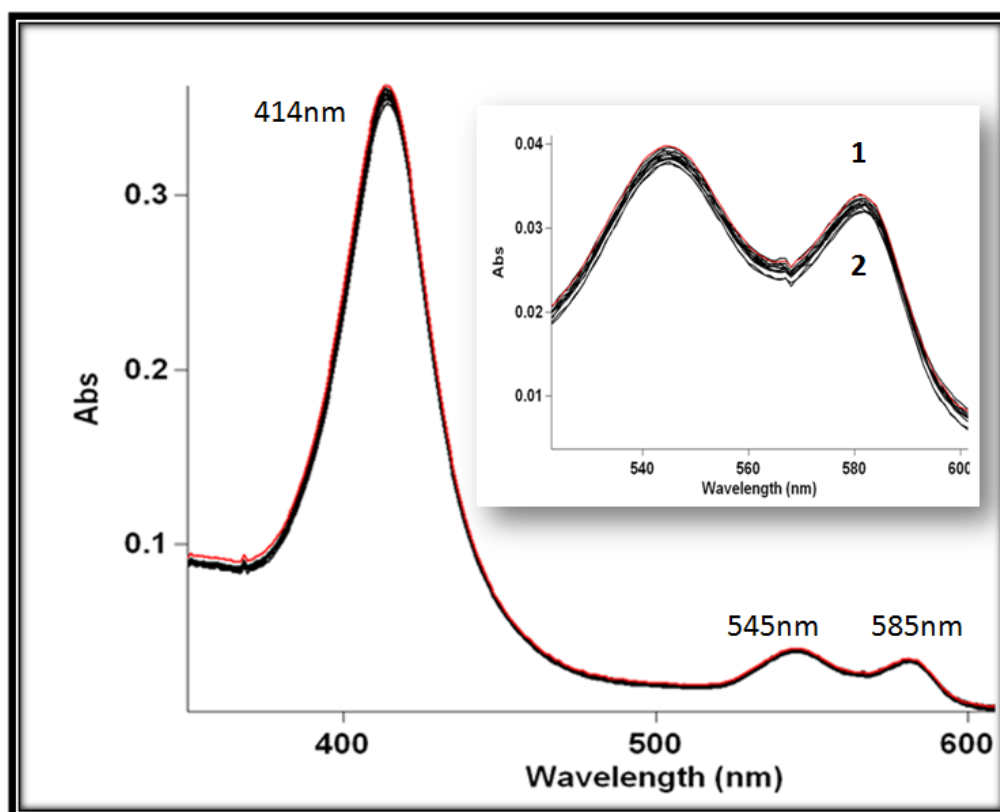


Figure 3.4 D: Nter1

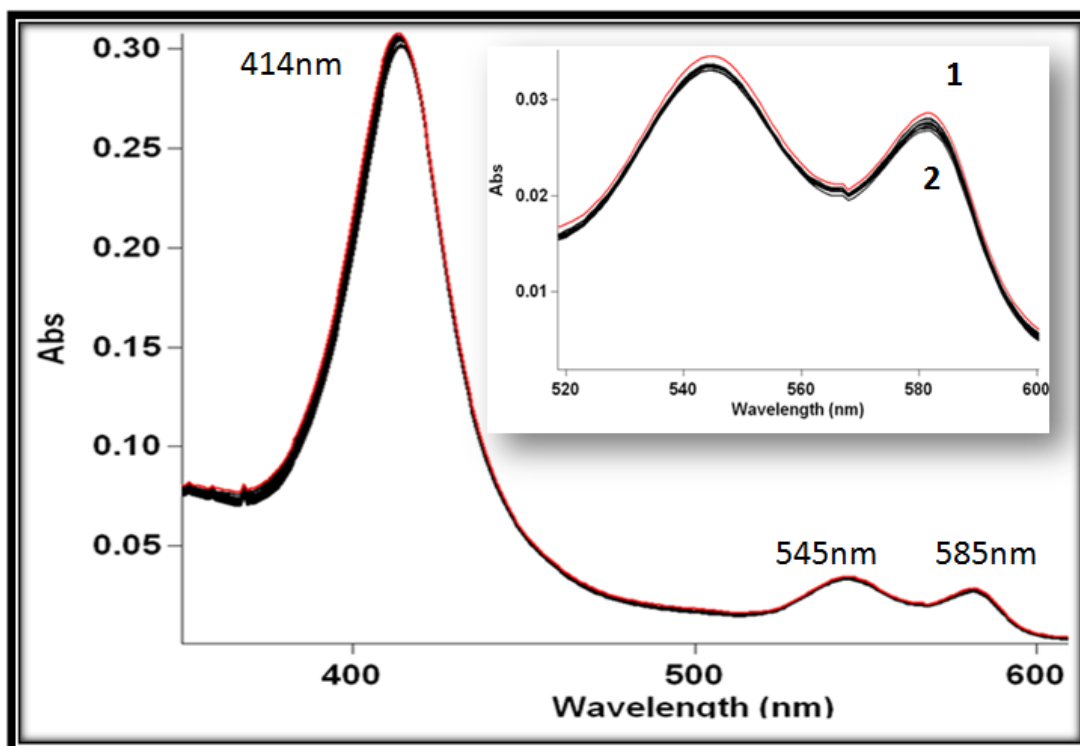


Figure 3.4 E: Nter2

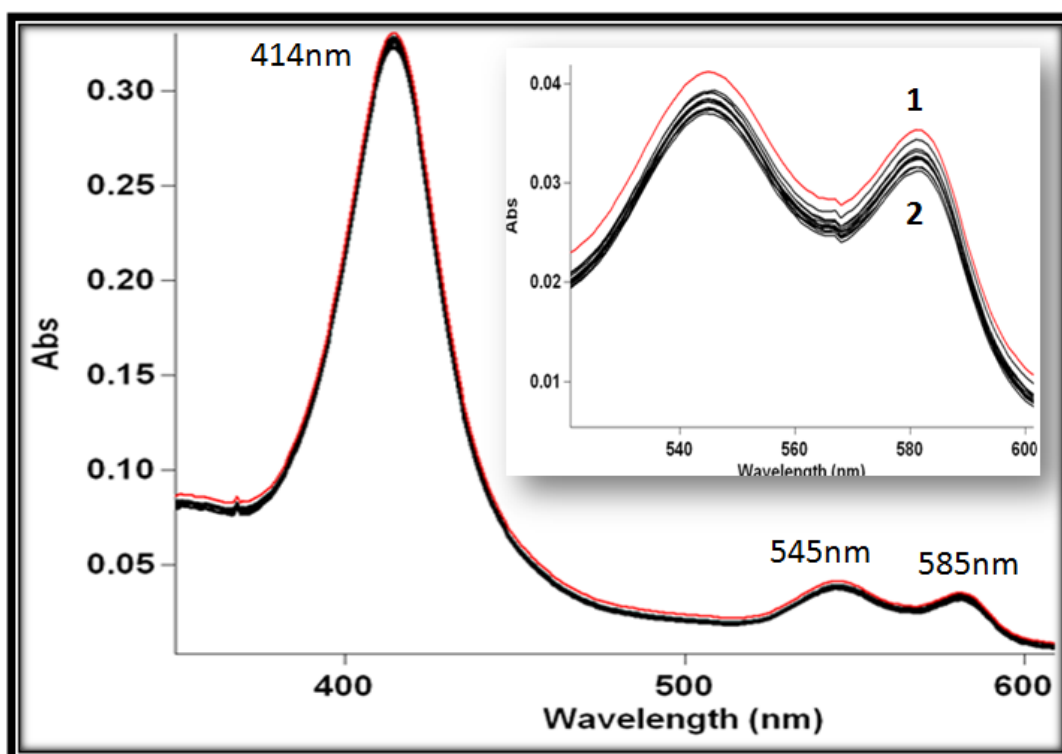


Figure 3.4 F: Nter3

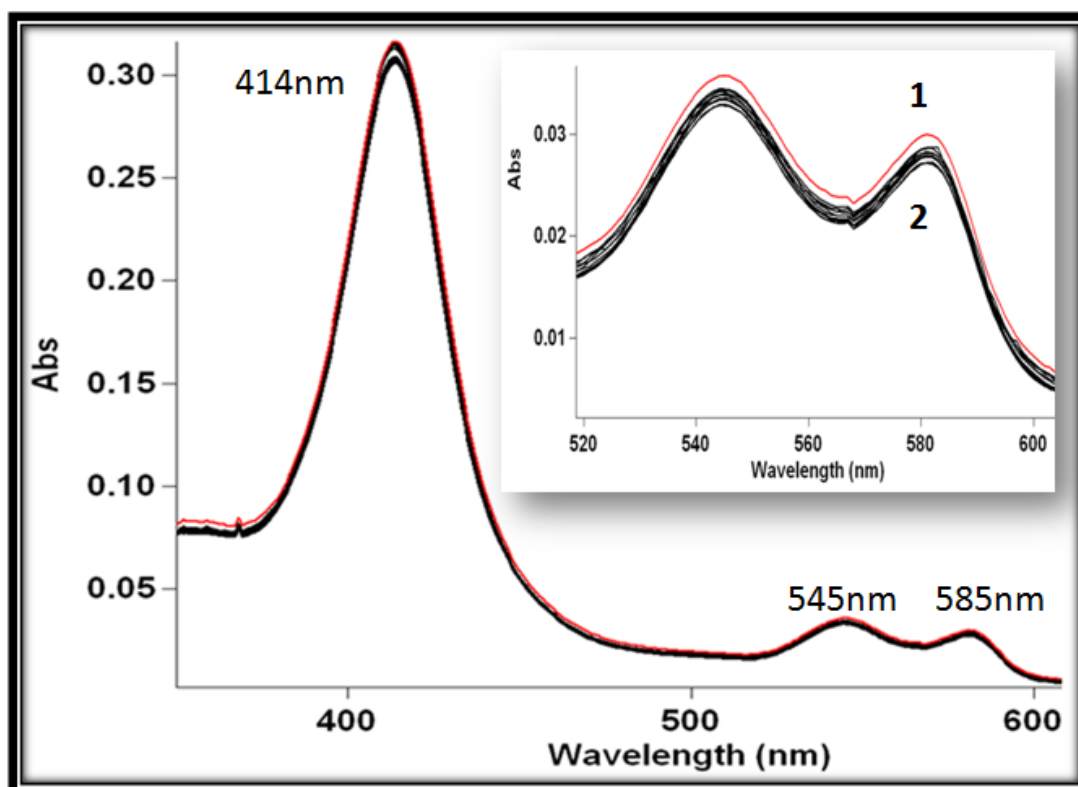


Figure 3.4 G: Nter4

Figure 3.4: NO oxidation profile of Pre-A mutants of HbN. The picture shows the absorption scan of the protein with the inset showing the change in the α and β peaks. Titration of oxygenated HbN protein (20 mM) was done by adding 15 mM NO sequentially and recording spectra after each addition. Wild type HbN displayed fully oxidized spectra after 12 additions (3A), whereas mutants pre-A deleted (B), Nter-all (C), Nter1 (D) and Nter2 (E), Nter3 (F), Nter4 (G) displayed very slow oxidation of the protein and could not be fully oxidized even after 20 additions of NO. The first and last additions are labeled as 1 and 2, respectively.

3.2.1.4 Pre-A mutants display lower NO consumption rate

After qualitatively analysing the effect of alanine mutations on NO oxidation, differences in NO consumption rate were calculated. In the control experiment having only buffer and no proteins, peak of NO decline at a very slower rate and took hours to reach the baseline, whereas in the presence of HbN the peaks declined at a faster rate and touched baseline in 15 mins, implying scavenging of NO by the protein. However, in case of pre-A mutants the peaks decline at much slower rates and peak reached baseline in 40 mins. HbN was found to scavenge NO at a rate of 48.85 ± 2.44 n mole of protein/ min/ mg of protein, which is around 3 fold higher than the pre-A mutants whose rates were found to be 18.43 ± 0.92 n mole of protein/ min/ mg of protein. This result

matches with the NO oxidation results where mutants showed lower oxidation rate (Table 3.2).

Table 3.2: NO-dioxygenase activity of pre-A mutants of HbN. The NOD activity of HbN mutants were determined at fixed concentration of NO (1.8 micromole).

HbN mutants	NO consumption rate (n mole of NO/min/mg of protein)	% NOD activity
HbN	27.8±2.44	100
Pre-A deleted	9.93±0.87	35.71
Nter-all	10.27±0.90	36.94
Nter-1	10.29±0.92	37.0
Nter-2	10.92±0.96	39.28
Nter-3	9.90±0.87	35.61
Nter-4	9.95±0.87	35.79

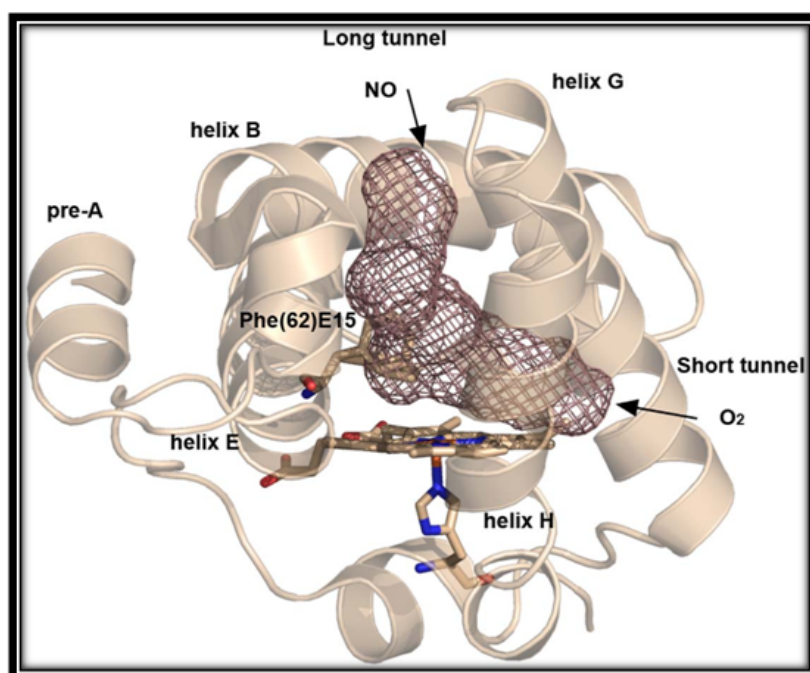


Figure 3.5: Representation of the long and short branches of the tunnel system. The graphical display is based on the X-ray crystallographic structure of Mtb HbN (PDB entry 1IDR), and the access routes of O₂ and NO in the dual-path ligand-modulated mechanism proposed for this protein are indicated. The gating residue PheE15 (residue 62) is shown in the two conformations found in the X-ray structure as sticks.

3.2.2 Role of long tunnel of HbN in NOD function: Contribution of Phenylalanine62 as a gatekeeper of long tunnel

3.2.2.1 Construction of Phe62 (E15) gate mutants of HbN

Four gate mutants, where PheE15 was replaced by Ala (PheE15Ala), Ile (PheE15Ile), Tyr (PheE15Tyr) and Trp (PheE15Trp), were created by site-directed mutagenesis. Mutations were chosen to span a wide range of sizes, varying from the small size of the methyl group in Ala to the large indole ring in Trp, the replacement of the planar benzene by the branched chain of Ile, and even the conservative mutation of PheE15 by Tyr. It can be expected that the distinct chemical nature of the side chains will translate into differences in the ligand migration through the long tunnel branch, which in turn should lead to differences in the NOD activity measured for the mutants. Thus, in the absence of relevant structural alterations in the tunnel due to the changes in the side chain at position E15, which might be particularly relevant for the bulky Trp, it can be expected that replacement of PheE15 to Ala should open permanently the long tunnel, whereas mutation to Trp should occlude the access of ligands. Likewise, the branched side chain of Ile is expected to limit the accessibility of diatomic ligands through the tunnel. Finally, it is reasonable to expect that the PheE15Tyr mutation should a priori have little effect on the migration properties.

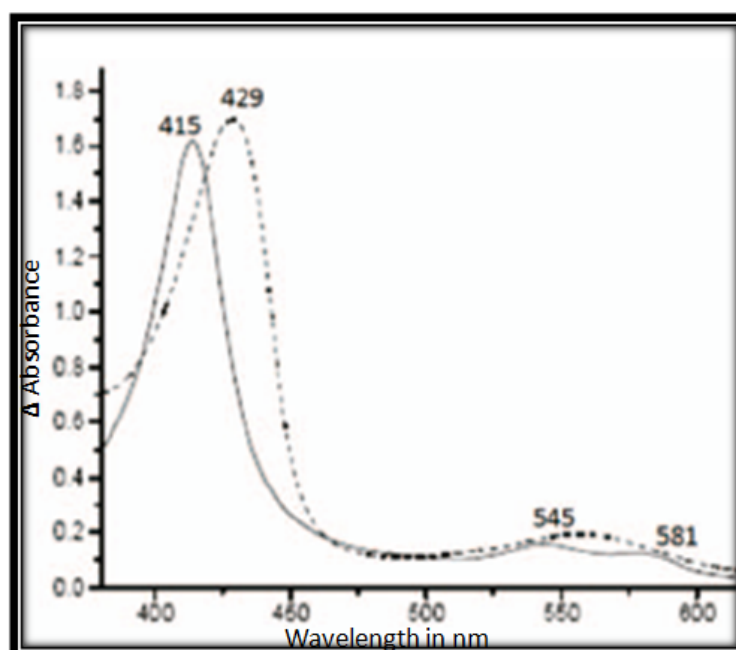


Figure 3.6: Spectral properties of PheE15Ala mutant of HbN. (A) Optical absorption spectra of oxygenated (solid line) and sodium dithionite reduced species of mutant HbN, recorded in 50 mM Tris.Cl and pH 7.5 (dashed lines).

3.2.2.2 Effect of mutations at PheE15 gate of HbN on O₂/CO binding

To check the implications of mutations at the long tunnel gate on protein functi-

on, the PheE15 gate mutants of HbN were cloned, expressed and purified. Absorption spectra of O₂ and CO bound forms of these mutants were indistinguishable from that of wild type HbN, suggesting that all these mutants are able to bind oxygen (Figure 3.6 and 3.7). The ability of the wild type HbN and its mutated variants to bind O₂ was assessed by their p^{50} values. For the wild type protein, the measured value corresponded to 0.019,

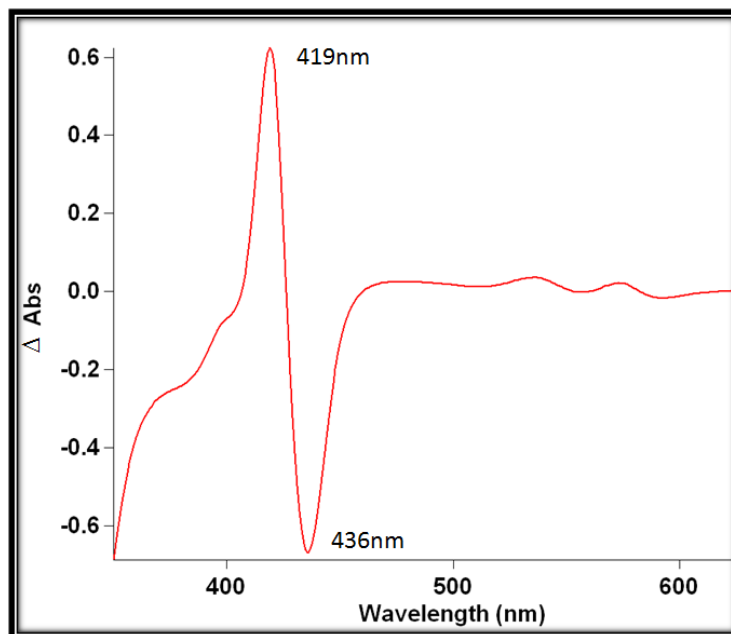


Figure 3.7: CO-difference spectrum of PheE15Ala mutant of HbN. Spectral profile of other PheE15 gate mutants (PheE15Tyr, PheE15Trp and PheE15Trp) appeared similar and matched with the wild type.

which resembles the previously reported data (Couture *et al.*, 1999). When the PheE15 gate mutants were compared with native HbN, no significant difference in their p^{50} profile was observed suggesting that oxygen binding properties of these mutants are not impaired. To substantiate these primary results, we checked the kinetics of ligand association by measuring the rate of CO association by various HbN E15 mutants. The k_{on} value determined for the wild type protein ($2.5 \cdot 10^7 \text{ M}^{-1} \text{ s}^{-1}$) is slightly larger than the value reported by Couture *et al.* ($0.657 \cdot 10^7 \text{ M}^{-1} \text{ s}^{-1}$) (Couture *et al.*, 1999) (Table 3.3). Nevertheless, all the mutants displayed CO association rates comparable to that of wild type HbN, suggesting that mutation at PheE15 long tunnel gate does not affect the O₂/CO binding properties of HbN significantly.

3.2.2.3 Mutations at PheE15 gate of HbN alter its NOD activity

Even though mutants exhibit much similar O₂ binding properties, relevant diff-

erences were observed in their NO metabolizing activities (Table 3.4). The NOD activity of PheE15Ile was reduced to around 55% of the activity measured for the wild type enzyme, whereas a larger reduction (around 70%) in NOD activity was observed for the PheE15Trp mutant. Unexpectedly, mutation of PheE15 to Tyr also yielded a significant reduction (around 65%) in the NOD activity, suggesting that the apparently

Table 3.3: Oxygen binding and CO association kinetics of PheE15 gate mutants of HbN of *M. tuberculosis*. Values derived from three independent measurements, each consisting of multiple shots (>50) and averaged out by the program to give the final value. The standard deviation is in the range 0.3–0.5 ($\times 10^7$).

Protein	P^{50} of O ₂ in mm Hg	k_{on} of CO $\mu\text{M}^{-1}\text{S}^{-1}$
HbN	0.019	2.5×10^7
PheE15Ala	0.021	3.0×10^7
PheE15Ile	0.016	2.3×10^7
PheE15Tyr	0.013	2.0×10^7
PheE15trp	0.023	1.8×10^7

conservative replacement of benzene by phenol has a drastic influence on the ligand migration properties of the mutant. Finally, the PheE15Ala mutant also exhibited a significant reduction (around 49%) in the NOD activity.

Table 3.4: NO-dioxygenase activity of PheE15 gate mutants of HbN. The NOD activity of HbN mutants were determined at fixed concentration of NO (1.8 micromole).

Protein	NO consumption rate (nmole of NO/min/mg of protein)	% NOD activity
HbN	27.8 ± 1.3	100
PheE15Ala	15.9 ± 1.4	51.1
PheE15Ile	12.6 ± 0.6	45.3
PheE15Tyr	9.9 ± 0.6	34.5
PheE15Trp	8.6 ± 0.4	30.2

3.2.2.4 Oxidation of NO by Oxygen Adduct of PheE15 Gate Mutants of HbN

The NO oxidation profile of wt HbN and its mutants was determined by titrating

the oxy forms of protein with NO in a time course manner (Fig. 3.8 A-E). The addition of NO (5 mM) resulted in the appearance of a partially oxidized spectrum of HbN and repeated addition of NO solution to this sample resulted in a fully oxidized spectrum

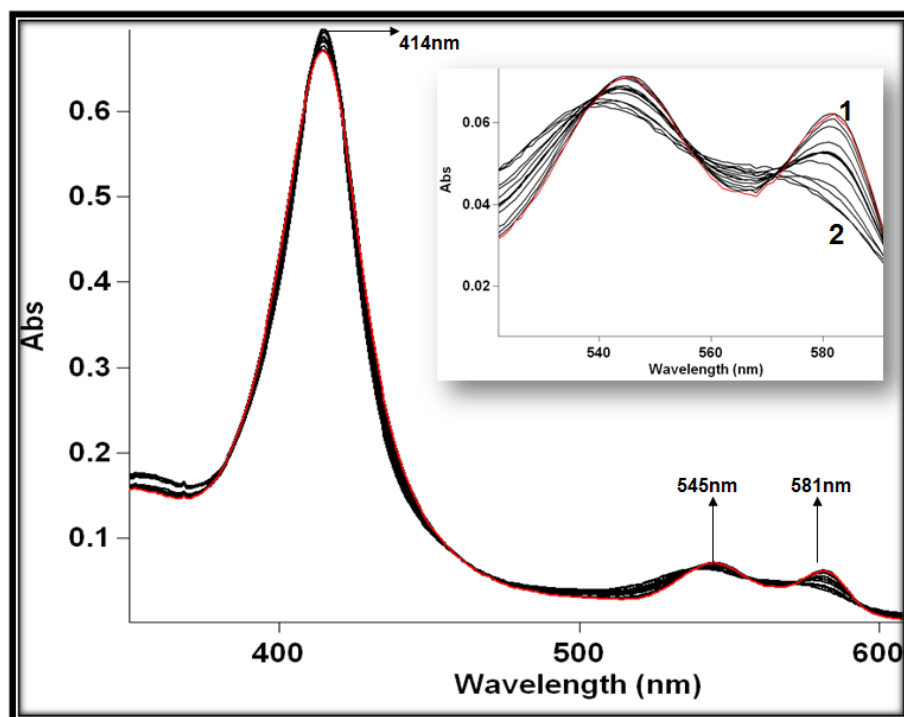


Figure 3.8A: HbN

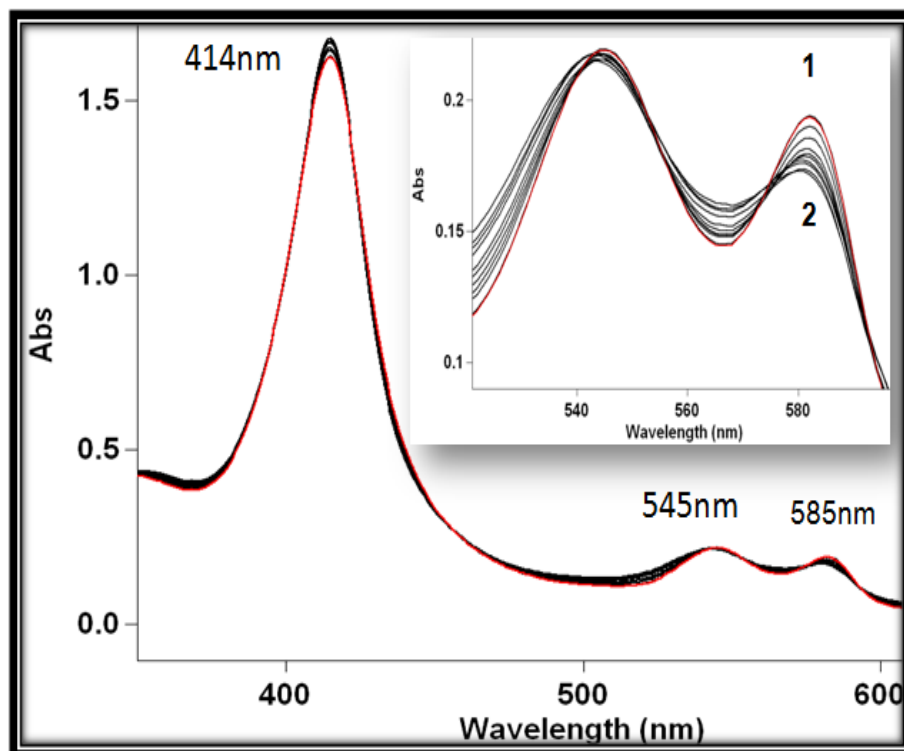


Figure 3.8B: Phe62Tyr

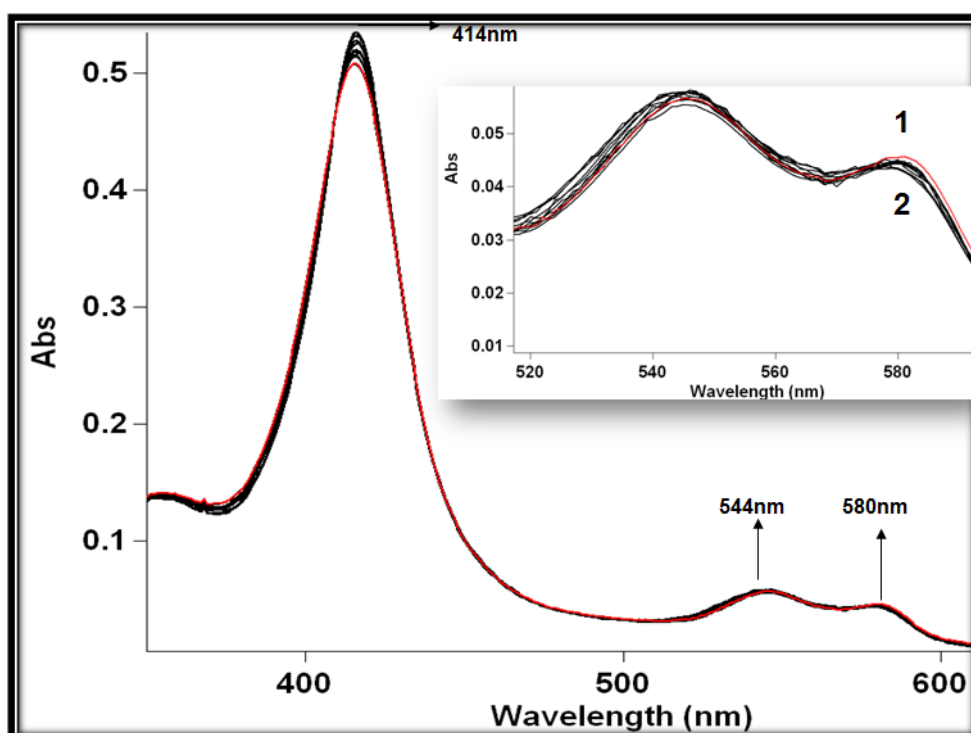


Figure 3.8C: Phe62Ile

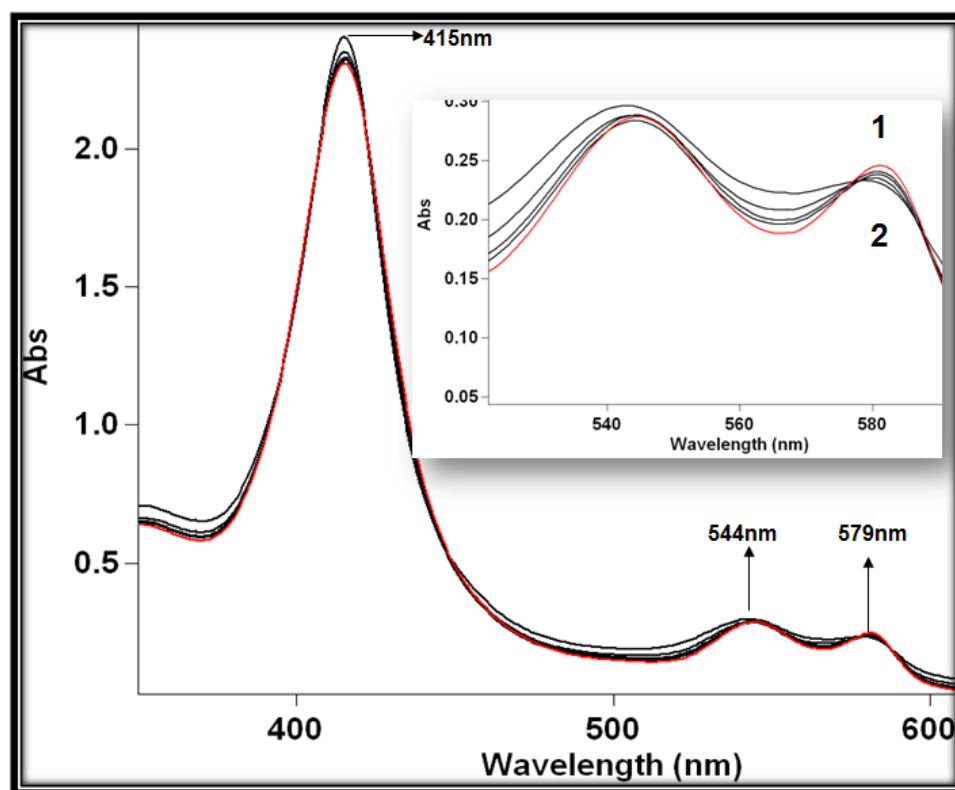


Figure 3.8D: Phe62 Trp

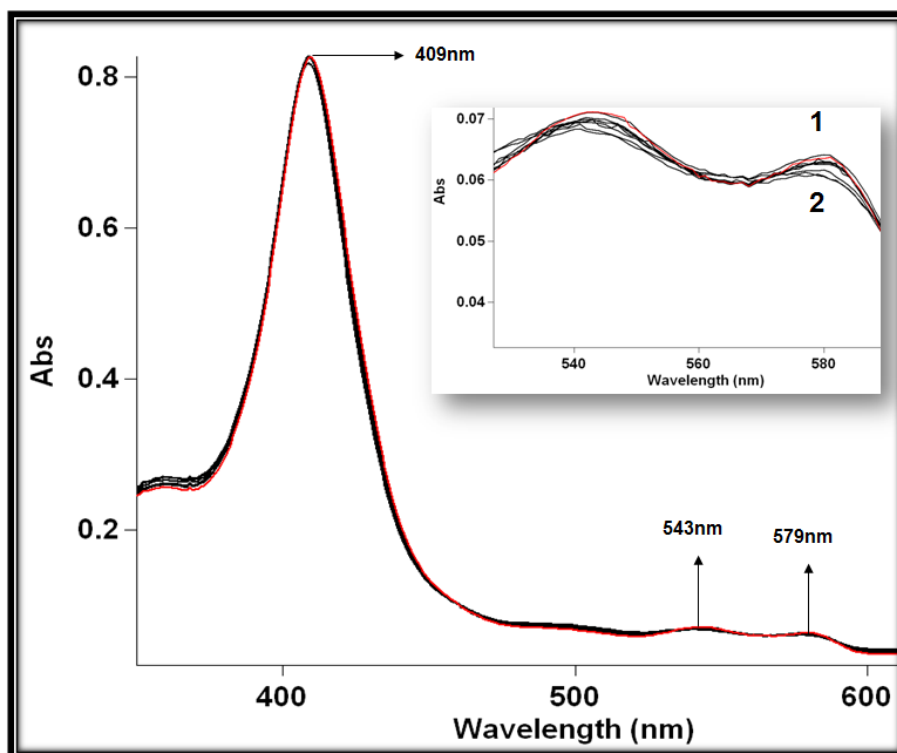


Figure 3.8E: Phe62Ala

Figure 3.8 : NO oxidation profile of PheE15 gate mutants of HbN. The picture shows the absorption scan of the protein with the inset showing the change in the α and β peaks. Titration of oxygenated HbN protein (20 mM) was done by adding 15 mM NO sequentially and recording spectra after each addition. Wild type HbN displayed fully oxidized spectra after 12 additions (A), whereas mutants PheE15Tyr (B), PheE15Ile (C), PheE15Trp (D) and PheE15Ala (E) displayed very slow oxidation of the protein and could not be fully oxidized even after 20 additions of NO. The first and last additions are labelled as 1 and 2, respectively.

shifting the Soret peak of oxyHbN from 415 to 405 nm. In contrast, similar number of additions of NO to the oxygenated form of mutants PheE15Trp, PheE15Ile and PheE15Tyr changed the spectra to the oxidized form slowly after 30–35 min of exposure, thus indicating very slow NO oxidation. Finally, NO oxidation by PheE15Ala mutant displayed a spectral profile similar to PheE15Ile and PheE15Tyr, which is intermediate between those observed for the wt protein and the PheE15Trp mutant.

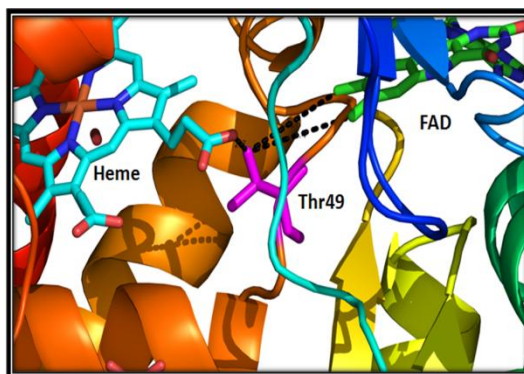
3.3 Discussion

Importance of pre-A portion of HbN came into light with the observation that it is absent in HbN of many fast growing, non pathogenic species of mycobacterium, *e.g. Mycobacterium sp. JLS, Mycobacterium sp KMS, M. flavescens, M. smegmatis* etc (they have very less NOD activity), whereas it is characteristic in HbN of slow growing pathogenic mycobacterium species, known to cause various diseases, *e.g. M. bovis, M. microti, M. avium, M. marinum, etc* (they have high NOD activity). To study how pre-A portion imparts this functional variation, this segment was deleted. Upon deletion, the NOD activity was reduced to one third of its original (Lama *et al.*, 2009). The contribution of this domain to the function of the HbN, is partially answered by this study.

A closer look at the pre-A segment reveals two important facts: firstly, it is composed of four positively charged (Arg6, Arg8, Lys9 and Arg10) and one negatively charged (Glu11) residues and secondly, it is highly flexible in nature. Crystal structure (pdb:1IDR) depicts it to be helical in nature, however recent NMR data solved it as a random coil (Milani *et al.*, 2001; Savard *et al.*, 2011). Random coil imparts much greater degree of freedom to the pre-A motif than the helical nature. These two qualities helps HbN synergistically, because flexible nature allows it to fold on to its core domain and positive charges help it to form salt bridges with counter charged amino acids present on the surface of the protein. Thus when positively charge amino acids were mutated to neutral amino acid alanine, it might have disrupted the crucial linkages with other negatively charged amino acids leading to compromised activity. CO dissociation experiments demonstrated that pre-A mutations have neither affected the ligand (oxygen) migration through the short tunnels, nor the oxygen binding property of the protein. MD simulations experiments have captured the interaction between Arg6 and Asp17 and Arg10 and Glu70. The positive charges on the pre-A motif can easily form a salt bridge with the amino acids such as Asp17 and H22 present along with Glu70. Asp17, H22 and Glu70 form a triad. Normally H22 is seen to be hydrogen bonded to Glu70 amino acid. Therefore there lies a probability that the pre-A region and the triad allow the formation and breakage of non-covalent bonds to modulate the motion of the backbone in an ATP independent manner. This alteration in the backbone helices leads to the opening and closing of the Phe62 amino acid to regulate the diffusion of NO from the long tunnel, ultimately executing the NOD activity.

Further, series of experiments were conducted to validate the importance of Phe62 amino acid. The experimental data collected for the mutants indicate that the PheE15 mutation does not affect the binding of O₂ to the heme, as noted in the similar absorption spectra of O₂ and CO bound forms, as well as in the similar p50 and k_{on} values determined for both wild type and mutated proteins. These findings suggest that the PheE15 mutation has a little impact on the tunnel short branch, which is proposed to be the main pathway for migration of O₂ to the heme cavity. However, since the mutants exhibit a distinctive reduction in the NOD activity, PheE15 residue has to play a key role in mediating the access of NO to the oxygenated protein. In agreement with the dual-path migration mechanism, the main pathway for NO migration is the tunnel long branch. This finding points out the delicate structural balance imposed by the PheE15 gate, which not only regulates ligand migration, but also contributes to avoid the collapse of helices B and E, thus preserving the ligand accessibility along the tunnel long branch. Overall, the results presented herein demonstrate the pivotal role of charged residues in the pre-A region and PheE15 in modulating the NOD function of M. tuberculosis HbN. Experiments on Phe62 amino acids also confirm the suggestion by Milani and coworkers about the gating role of PheE15 in HbN.

Thus, this study elucidates that both the unique structural features: Phe62 gatekeeper amino acid and the charged pre-A segment, are essential for the proper functioning of HbN as a NO scavenging molecule.



Chapter-4

Protein-protein interactions of HbN with redox partners and its implications on NO-dioxygenase function

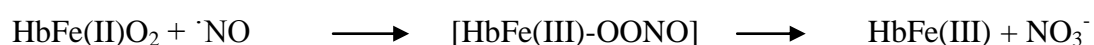
4.1	Introduction	64-66
4.2	Results.....	67-77
4.2.1	Search for the redox partner(s) of HbN: Screening of reductases from native and heterologous host.....	67
4.2.2	Interaction of HbN with reductase protein from native and heterologous host.....	67-69
4.2.3	Highly efficient reductases are favoured over less efficient redox partner for electron transfer.....	69-70
4.2.4	Integration of redox domain with HbN:.....	70-73
4.2.5	Pre-A region of HbN is crucial for efficient electron transfer	73-74
4.2.6	Role of individual charged residues in the Pre-A region for electron transfer.....	75
4.2.6	Docking analysis of HbN with Ferredoxin reductase	75-77
4.3	Discussion.....	78-81

4.1 Introduction

NO is an ubiquitous poisonous compound and many organisms from different strata of life employ different types of haemoglobin as their first line of defence to cope with NO toxicity. It is now evident that majority of haemoglobins, truncated haemoglobins and flavohemoglobins show NO scavenging activity (Gardner et al., 1998b; Hausladen et al., 1998). However, their degrees of efficiency for NO dioxygenation (NOD) depend mainly on their structural organisation and the availability of a cognate reductase partner. This is because while catalyzing the NO to NO_3^- , heme iron gets oxidised from oxygenated active Fe^{2+} form to inactive deoxygenated Fe^{3+} form. This Fe^{3+} form cannot bind oxygen. To regain its functional form for the next round of NOD activity, Fe^{3+} -heme should be reduced back to its Fe^{2+} state with the help of a reductase protein. Thus, the electron transfer process in this reaction, is a rate limiting step in the process of NO dioxygenation (Gardner *et al.*, 2000). During the course of evolution, reductase partner was evolved simultaneously along with the hemoglobins to recycle them into their functional state. Within the red blood cells, NADH dependent cytochrome b5 reductase and cytochrome b5 play an important role in reducing the Hb (Hultquist and Passon, 1971). Similarly, cytochrome b5 also serves as a reductase to myoglobinFe(III) (Liang *et al.*, 2002). Highest NOD value is reported for two domain flavohemoglobin ($k_{\text{NOD}} \sim 2400 \mu\text{M}^{-1}\text{s}^{-1}$) and it is expected, because it has a reductase partner attached to it, which instantly converts Fe^{3+} heme into Fe^{2+} state (Gardner, 2005). Human haemoglobin and sperm whale myoglobin have poor NOD activity of $k_{\text{NOD}} \sim 89 \mu\text{M}^{-1}\text{s}^{-1}$ and $k_{\text{NOD}} \sim 43 \mu\text{M}^{-1}\text{s}^{-1}$, respectively (Doyle and Hoekstra, 1981; Eich *et al.*, 1996). Their minimal activity may be attributed to their structure as well as the absence of attached reductase protein. Truncated haemoglobin, HbN, of *M. tuberculosis* displays a potent O_2 dependent NO dioxygenase activity that protects aerobic respiration of its host from NO toxicity. The catalytic efficiency of HbN for NO oxidation is very similar to that of two domain flavohemoglobins, which carry an integrated redox domain for efficient transfer of electrons to keep the globin in active ferrous state for O_2 binding.

HbN, inspite of being a single domain truncated haemoglobin, possesses a very high NOD activity ($k_{\text{NOD}} \sim 745 \mu\text{M}^{-1}\text{s}^{-1}$) (Ouellet et al., 2002; Pathania et al., 2002a). The high NOD activity of HbN is mainly due to its unique structure that has evolved to carry out NOD function. It has 2-over-2 globin fold instead of 3-over-3 classical globin fold. Within this small protein core, it harbours two hydrophobic tunnels, present orthogonal

to each other, known as long and short tunnel (Milani *et al.*, 2001). These tunnels facilitate efficient ligand migration into and out of the protein. They connect the outer exposed surface to inner distal heme pocket (DHP). The opening and closing of the long tunnel is supposed to be modulated by amino acid Phe62, which in turn is regulated by change in backbone motion, controlled by an extended 12 amino acids, highly flexible, pre-A region (Lama *et al.*, 2009). This regulation allows the entry of diatomic gaseous ligand NO into the distal heme pocket where it combines with iron bound O₂ to form the final product NO₃⁻. This is called Nitric oxide dioxygenase activity and can be explained by the given equation:



However, inspite of being gifted with special structural features, it lacks the benefit of having reductase partner attached to it. Reductase partner is absent in truncated hemoglobins of other organisms also, such as, ciliated protozoa *Paramecium caudatum*, the unicellular alga *Chlamydomonas eugametos* and the eubacteria *Nostoc commune*. Their activities depend upon their transient interaction with the available reductases. Experimental studies have indirectly proved that HbN is able to interact with native as well as heterologous redox partners for electron cycling because it was functionally active in its surrogate hosts such as *E.coli* and *Salmonella typhimurium* and has protected them from nitrosative stress (Ouellet *et al.*, 2002; Pawaria *et al.*, 2007). However, till now no reductase protein has been identified that can recycle the Fe³⁺ HbN to Fe²⁺ state.

There are plethoras of reductases expressed inside the *M. tuberculosis* but the one participating in the reduction of HbN, has not been reported yet. For the efficient electron transfer to hemoglobin, the reductase requires a precise coordination and structural alignment with the globin domain, so that the porphyrin ring and the FAD moiety come in the permissible distance for transfer. Flavohemoglobin from *E. coli* and *Alcaligenes eutrophus* have similar reductase domain, yet they have dissimilar NOD values ($k_{\text{NOD}} \sim 2400 \mu\text{M}^{-1}\text{s}^{-1}$ and $k_{\text{NOD}} \sim 2900 \mu\text{M}^{-1}\text{s}^{-1}$ respectively) (Ermler *et al.*, 1995; Ilari *et al.*, 2002). Their reductase domain belongs to ferredoxin NADP⁺ reductase type of protein family (Karplus *et al.*, 1991), which can be structurally and functionally divided into two independent domains: a FAD binding domain made up of six stranded antiparallel β barrel and a NAD(P)H- binding domain comprising of five stranded parallel β sheet. It has been experimentally seen that slight variation in the amino acid

sequence near the FAD-heme interaction site alters the rate of electron transfer, stressing upon the fact that precise structural orientation and interaction of heme with redox domain is required. Thus, the type of reductase partner is decisive for the optimal NO dioxygenation. Flavohemoglobin gives us a clue that naturally ferredoxin-NADH type reductase is favoured for transfer of electrons to heme iron in the globin fold. Therefore, the proteins belonging to ferredoxin NADP⁺ reductase family could be the most plausible candidate for the reductase partner. It will be interesting to find out the type of reductase that HbN will prefer for its heme iron reduction and the amino acids residues or regions in the proteins that will be essential for the interaction and transfer of electrons. It will also be important to find out the behaviour of HbN, when it comes across reductase of varying efficiency.

Keeping the above mentioned questions in mind, extensive attempts have been made to screen and study the interactions of some native and heterologous redox partners that can bring about state change from Fe³⁺ to Fe²⁺HbN. Detailed spectroscopic studies along with structural analysis have been conducted to accomplish the complete picture of molecular mechanism of NOD function in *M. tuberculosis*, in context of its reaction with a reductase partner. We have also explored the potential of HbN to associate with a reductase protein of a particular family but could be from different hosts, to bring about its conversion. Some experiments also highlight the partner switching behaviour of HbN, where we have shown its ability to form an alliance with other highly efficient partner, in spite of being already in association with a protein. Surprisingly, we have discovered the role of pre-A in reduction process, which otherwise is known to be crucial for the NOD function. Finally, at the end of this study some docking analyses were performed to elucidate the regions of proteins participating in the reaction.

4.2 Results

4.2.1 Search for the redox partner(s) of HbN: Screening of reductases from native and heterologous host

Two domain flavohemoglobin contains ferredoxin-NADP type reductase protein, which are naturally fused to the globin domain. Flavohemoglobins from *Erwinia chrysanthemi*, *Bacillus subtilis*, *Salmonella enterica* serovar typhimurium and *M. tuberculosis* have been isolated and characterized (Bollinger *et al.*, 2001; Favey *et al.*, 1995). They contain a 29kDa, ferredoxin-NADP type reductase domain attached to their C-terminus region. These reductases are best suited for transfer of electrons to heme iron and well distributed in nature. Therefore, it can be anticipated that they can be the most probable candidate for interaction with HbN. At first, the reductase domain from the flavohemoglobin of *E. coli* has been cloned because it is the natural partner of its globin domain and is structurally and functionally adapted to transfer electrons to the porphyrin ring across the globin fold. Basic FAD and NADP binding domains are conserved across different species therefore, ferredoxin reductase (FdR) from *E. coli* was also cloned. Ferredoxin-NADP type reductases come under the family of oxidoreductase, therefore other oxidoreductases such as KshB (Rv3571) and TrxB (Rv3913) were also selected to test their interactions. KshB (Rv3571) is an oxidoreductase, which is also known as 3-ketosteroid-9- α -hydroxylase reductase. It is found to express during nitrosative stress and hypoxia and have critical role in pathogenesis, cholesterol catabolic processes, glycolipid biosynthesis processes, etc. Similarly, trxB is also an oxidoreductase involved in cell redox homeostasis, protein thiol disulphide exchange etc.

4.2.2 Interaction of HbN with reductase protein from native and heterologous host

Different reductases from native as well as heterologous hosts, such as reductase domain of *M. tuberculosis* flavohemoglobin, oxidoreductases such as KshB, trxB and FdR were spectroscopically tested to find out their relative efficiency to reduce Fe^{3+} to Fe^{2+} HbN. This assay was initially developed by Hayashi *et al* (Hayashi *et al.*, 1973). It exploits the ability of HbN to bind CO in its ferrous state only (not in its ferric state) and this CO bound hemeoglobin gives a soret peak at 420nm. It can be differentiated from its Fe^{3+} form, which gives a soret peak at 406nm. So, if the reductase protein is able to make a functional alliance with the HbN than it would be able to convert the oxidised

Fe³⁺ into reduced Fe²⁺ ion. This conversion can be easily monitored by the shift and increase in absorption spectra at 420nm from 406nm, due to the formation of Fe-CO adduct. When 1μM concentration of reductase protein was added to the CO flushed,

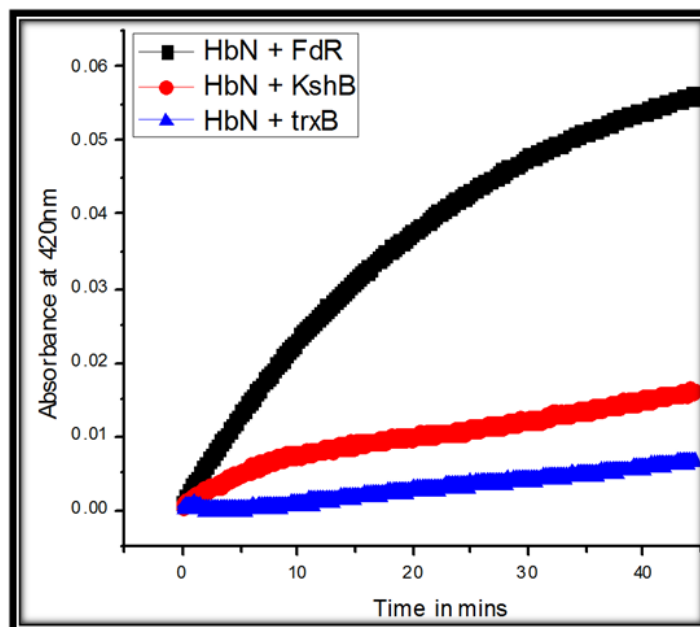


Figure 4.1: Reduction of oxidised HbN by various reductases. Change in the absorbance at the solet peak (CO bound) at 420 nm, resulted by the enzymatic reduction of HbN (8μM) by 1μM of several reductases (FdR, Rv3571 and trxB), in the presence of 250μM NADH and CO.

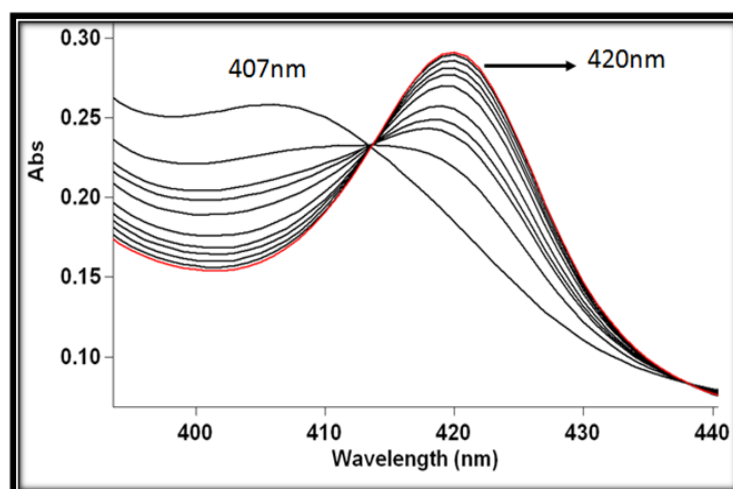


Figure 4.2: Reduction of HbN by *E. coli* ferredoxine reductase. Absorption spectra associated with the reduction of HbN (8μM) by 1μM of FdR in the presence of 250μM NADH and CO.

phosphate buffer, containing oxidised HbN (8μM) and 250μM of NADH, as a cofactor, the solet peak shifted from 407 nm to 420 nm. The relative performance of the various

reductases was then measured by monitoring the relative rates of increase in absorbance at 420nm (Figure 4.1). All the reductases have shown functional participations with HbN, but with varying degree. FdR and reductase protein from Hmp of *E. coli* have shown almost three fold higher activity than KshB and trxB (Figure 4.2). The trxB protein was the least efficient in transfer of electrons, whereas, WhiB1 protein did not show any activity with HbN.

4.2.3 Highly efficient reductases are favoured over less efficient redox partner for electron transfer

CO binding experiments have clearly demonstrated that among the selected reductases, ferredoxin-NADP type reductase was the most efficient one and possessed the highest conversion rate. However, in the real time scenario, HbN comes across numerous reductases but it associates with one of them, for its reduction. So, to mimic

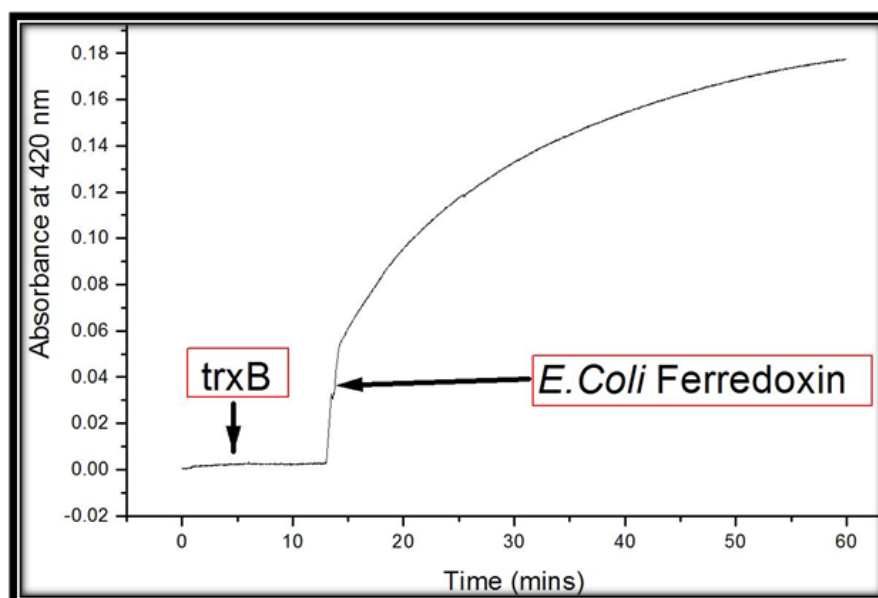


Figure 4.3: Replacement of low efficient reductase with high efficient one. Change in the absorbance at the solet peak (CO bound) at 420 nm, resulted by the enzymatic reduction of HbN (8 μ M) by 1 μ M of trxB, in the presence of 250 μ M NADH and CO, for intial 10 mins and later FdR was added to the same mixture.

the real time scenario HbN encountering with reductases of different efficiency, the following experiment was conducted. 8 μ M of HbN was allowed to pre-react with 1 μ M of less efficient reductase (KshB or trxB) in the presence of 250 μ M of NADH in a CO flushed chamber. Absorption data was collected for Fe-CO adduct formation at 420nm for 10 mins and then midway, in the ongoing reaction, 1 μ M of FdR (more efficient) was

added, and then again rate of Fe-CO complex formation data acquisition was resumed (Figure 4.3). We find that after the addition of highly efficient FdR to the preincubated HbN-low efficient reductase complex, such as HbN-trxB, the absorbance at 420nm increased drastically from near baseline to an O.D of 0.18. This indicates the replacement of pre-existing reductase with the newly added one. Similar reaction happened in case of KshB also (Figure 4.4). This proves that HbN is able to disrupt its interaction with the unfavourable reductase, to form an alliance with other reductase for higher yield.

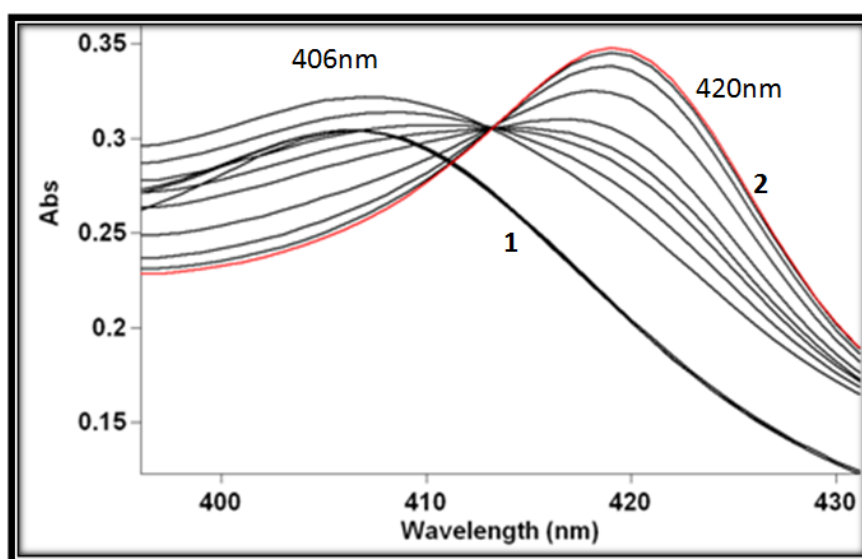


Figure 4.4: HbN prefers high efficiency reductase for its conversion to Fe^{2+} form. Shows the absorption spectra of the reduction of HbN ($8\mu\text{M}$) by $1\mu\text{M}$ of KshB and FdR. (1) represents the reduction of HbN by KshB only, whereas (2) is obtained after adding FdR, 10 mins after the addition of KshB.

4.2.4 Integration of redox domain with HbN

It is now evident that HbN can distinguish the efficiency of reductases for its optimum activity. However, to mimic the condition in two domain flavohemoglobin, where the reductase is naturally attached, Rv3571, *E.coli* ferredoxin reductase and reductase domain of *E.coli* Hmp were fused to the C-terminus of HbN with a linker peptide in between the two domains (Figure 4.5 and 4.6). These chimeras were created with the notion that it will speed up the process of forming close contact between the HbN and reductase in a correct orientation, so that the heme and the FAD moiety comes in the permissible distance of electron transfer. HbN-reductase chimeras were cloned, expressed and purified. The purified proteins were showing the characteristic red colour and the molecular weights of the proteins were found to be ~54kDa and 42kDa for HbN-

Rv3571 and HbN-*E.coli* Hmp reductase chimera, respectively, as seen in SDS page with standard molecular weight marker. Absorption spectra of fusion proteins resembled the oxyform spectra of HbN with soret peak at 414nm and α , β peaks at 540 and 575nm respectively, indicating the protein to be in robust condition.

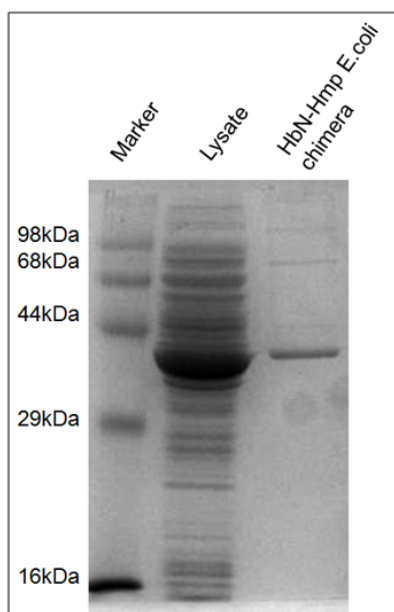


Figure 4.5: Expression of HbN-*E.coli* Hmp reductase chimera in the BL21DE3 strain. Lane1, molecular weight marker; Lane2, cell lysate of BL21DE3 strain containing the overexpressed chimeric protein; Lane3, purified HbN-*E.coli* Hmp reductase protein after Ni-NTA chromatography.

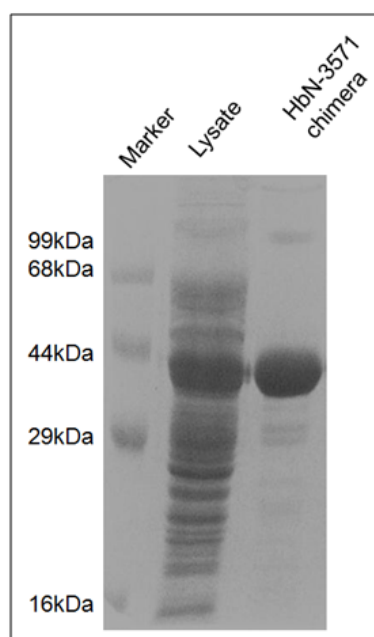


Figure 4.6: Expression of HbN-Rv3571 chimera protein in the BL21DE3 strain. Lane1, molecular weight marker; Lane2, cell lysate of BL21DE3 strain containing the overexpressed chimeric protein; Lane3, purified HbN-Rv3571 chimera protein, after Ni-NTA chromatography.

HbN-CO adduct formation was monitored spectroscopically for these chimera proteins. Interestingly, instead of showing increase in the activity, HbN-Rv3571 chimera showed marked decrease in the activity and no absorption spectra was seen at 420nm (Figure 4.7). In the (Figure 4.8) left hand side graph shows no change in soret peak at 406nm after the addition of Rv3571. This means that Rv3571 was unable to convert the

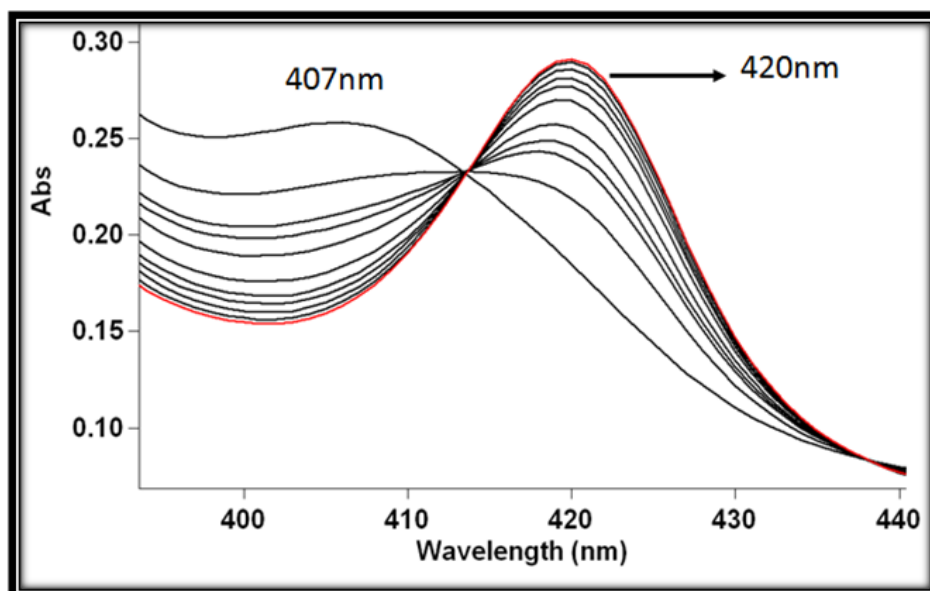


Figure 4.7: HbN-FdR chimera was able to reduce. Absorption spectra associated with the auto reduction of HbN-FdR and HbN-*E.coli* Hmp red chimera (8 μ M), by its own reductase domain, attached its C-terminus, in the presence of 250 μ M NADH and CO.

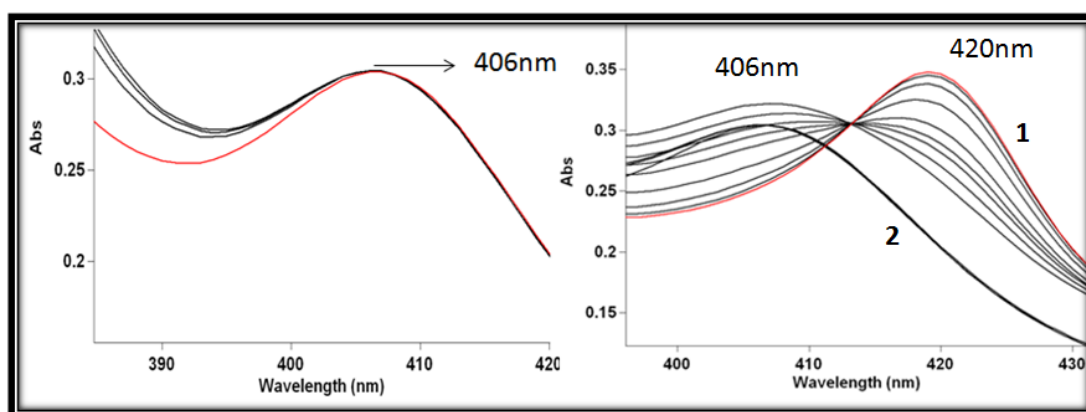


Figure 4.8: HbN-Rv3571 chimera was not functional. The absorption spectra of the autoreduction of the HbN-Rv3571 chimera is shown on the left. Right side figure shows the shift in the soret peak from 406nm to 420nm on the addition of FdR to the HbN-Rv3571 chimera.

heme iron from Fe³⁺ to Fe²⁺ form. However, the reduction of ferric HbN was restored and soret peak shifts to 420nm by the addition of ferredoxin reductase, midway of the reaction (graph on the right hand side in Fig 3a). On the other hand, chimera of HbN and

reductase domain of *E.coli* flavohemoglobin showed excellent activity and the solet peak shifted from 406nm to 420nm, indicating that it was able to convert the Fe^{3+} to Fe^{2+} form (Figure 4.7).

4.2.5 Pre-A region of HbN is crucial for efficient electron transfer

Proper movement of proteins helices is very important for the accurate alignment of HbN and reductase. Pre-A motif, like master regulator, modulate the HbN's backbone to carry out the NOD function whereas, with the deletion of this pre-A motif, HbN's NOD activity was compromised, because of its hindered backbone motion. This hinderance was easily visualised during molecular dynamics (MD) studies. Therefore, to study the effect of compromised backbone's movement on reductase association, we have checked the ability of pre-A deleted HbN to get reduced with ferredoxin reductase. Surprisingly, the pre-A deleted HbN was defective in conversion from Fe^{3+} to Fe^{2+} state, as the solet peak at 406nm shifted very slowly to 420nm (Figure 4.9). To further confirm the importance of pre-A motif, we have also deleted the pre-A region from the HbN-*E. coli* Hmp reductase fusion, which otherwise showed very efficient transfer of electrons, thinking that deletion should hamper the ability of HbN-red chimera to get reduced. The hypothesis proved to be correct because the deletion mutant lost its activity, signifying the necessity of pre-A motif (Figure 4.10).

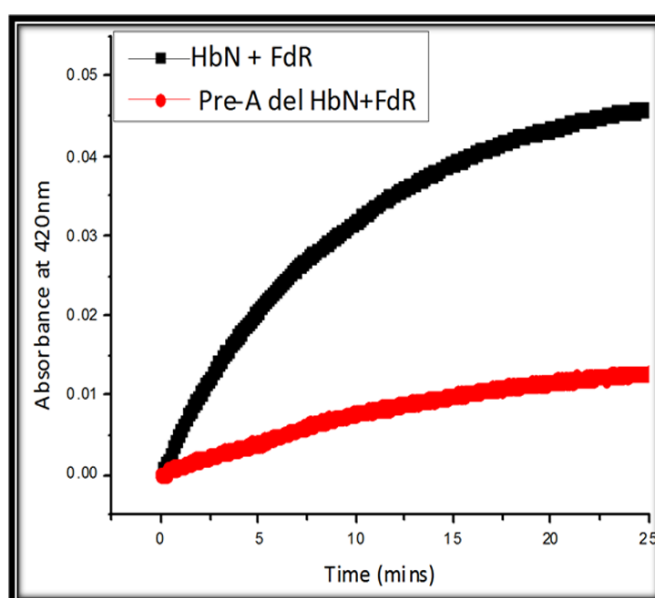


Figure 4.9: Pre-A deleted HbN has compromised reducing ability. The relative rate of enzymatic reduction of HbN(black) and pre-A deleted HbN (red) by $1\mu M$ of FdR, in the presence of $250\mu M$ NADH and CO. The graph depicts the change in the absorbance by the solet peak (CO bound) at 420 nm by the HbN and Pre-A deleted HbN.

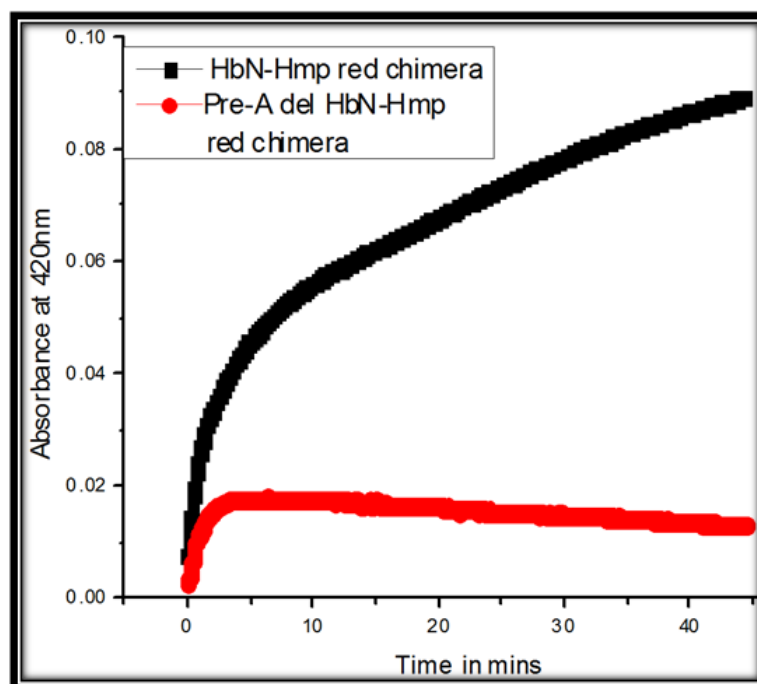


Figure 4.10: Pre-A deletion renders the chimera non functional. Change in the absorbance at 420 nm by the solet peak (CO bound), resulted by the enzymatic reduction of HbN-*E. Coli* Hmp reductase chimera (black) and its pre-A deleted mutant, by 1 μ M of reductase FdR, in the presence of 250 μ M NADH and CO.

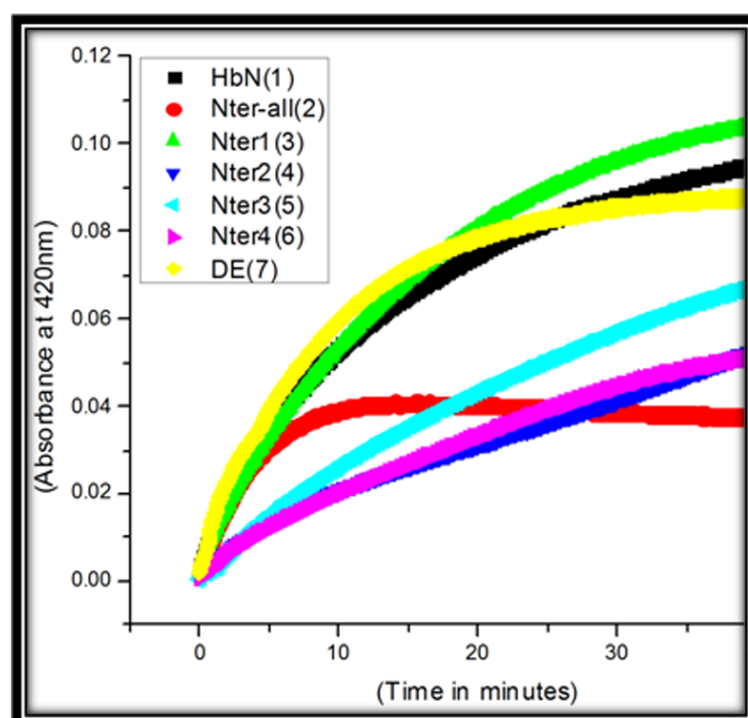


Figure 4.11: Pre-A mutations affects the process of transfer of electrons. The graph represents the comparative efficiency, of enzymatic reduction, between HbN and its pre-A mutants, by FdR. The graph represents the change in the absorption at 420nm, by the solet peak (CO bound), with respect to time.

4.2.6 Role of individual charged residues in the Pre-A region for electron transfer

It has been hypothesised that pre-A region regulates the backbone motion with the help of the charged residues present in it. We have already seen that abrogation of charge from this region resulted in defective NOD activity, which might be accounted for its restricted backbone motion. Therefore, to check the significance of the charged amino acids of pre-A segment on the reduction ability of the HbN, reductase assay was performed. Of all the mutants, Nter-all mutant was least efficient in electron accepting ability. Nter2, Nter3 and Nter4 mutants showed similar activity, as all of them showed very slow increase in the peaks at 420 nm, suggesting slow transfer of electrons. Interestingly, Nter1 and D17E mutants showed no effect of mutation and had activity comparable to that of the wild type (Figure 4.11).

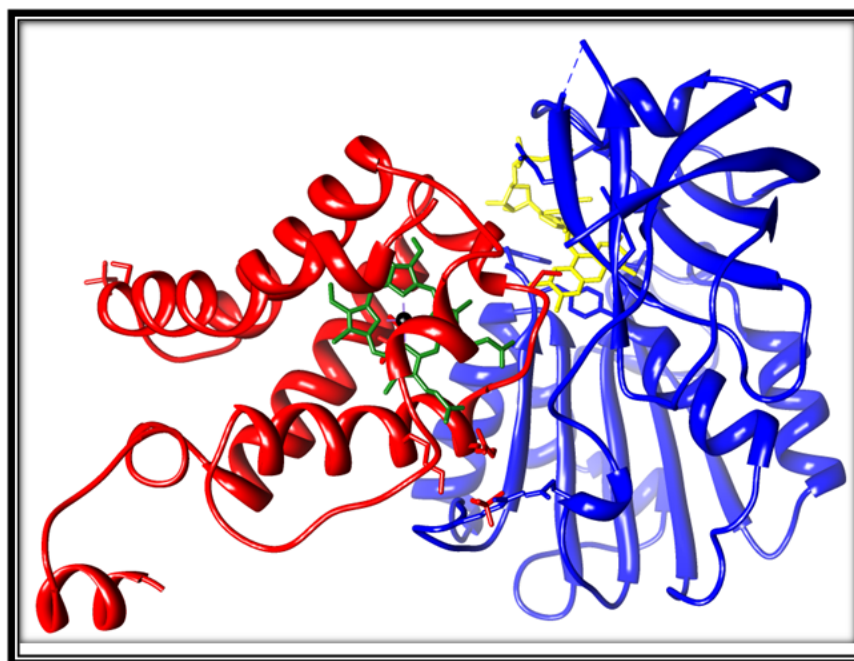


Figure 4.12: The ribbon diagram represents the docked structure of *M.tuberculosis* HbN (pdb: 1IDR) and *E. coli* ferredoxin reductase (FdR) [1FDR]. The cofactors heme (green) and FAD (yellow) are attached to the globin domain (red) and *E. coli* ferredoxin reductase (1FDR) [blue] in colour, respectively.

4.2.7 Docking analysis of HbN with Ferredoxin reductase

In the absence of crystal structure, docking studies were executed to get better insight about the HbN reductase interacting region. For this, ferredoxin reductase (pdb:1FDR) was docked onto HbN crystal structure (pdb:1IDR) using the online GRAMM-X protein-protein online server. Out of various possible structures, the most

probable one was selected on the basis of its resemblance to the crystal structure of flavohemoglobin of *Alcaligenes eutropha*. To further confirm the accuracy of the docked structure, in one mutant Ser46 residue was mutated to Trp and in another mutant Thr49 and Asn50 (TN-WI) was mutated to Trp and Ile, respectively. Reductase assay was done for the two mutants. Ser46Trp mutant showed no effect and behaved like wild type HbN, whereas, TN-WI mutant showed compromised activity (Figure 4.12).

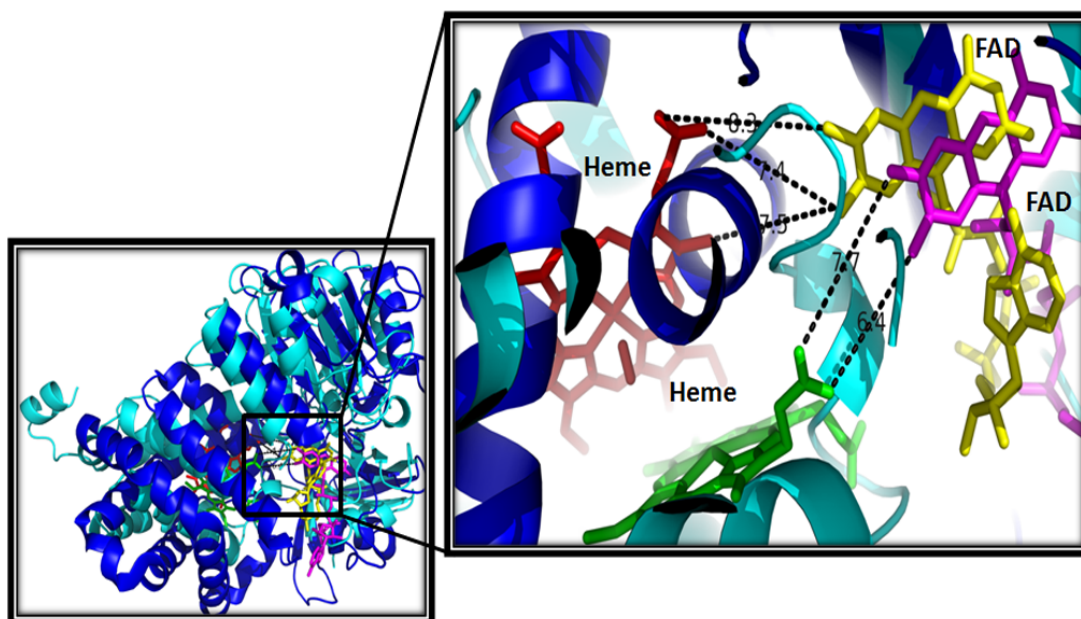


Figure 4.13: Alignment of the crystal structure 1CQX and the docked structure. Panel on the left, represents the overlay of docked structure (HbN and FdR) and crystal structure of flavohemoglobin from *Alcaligenes eutropha* (pdb: 1CQX). Right panel shows the relative distance between the heme and the FAD molecule in the two crystal structures, 1CQX and the docked structure, respectively. The heme in the red and FAD in the yellow colour, represents the cofactors of docked structure, whereas, heme in the green and FAD in the magenta colour, indicates the cofactors of the crystal structure 1CQX. All the measurements are in Å.

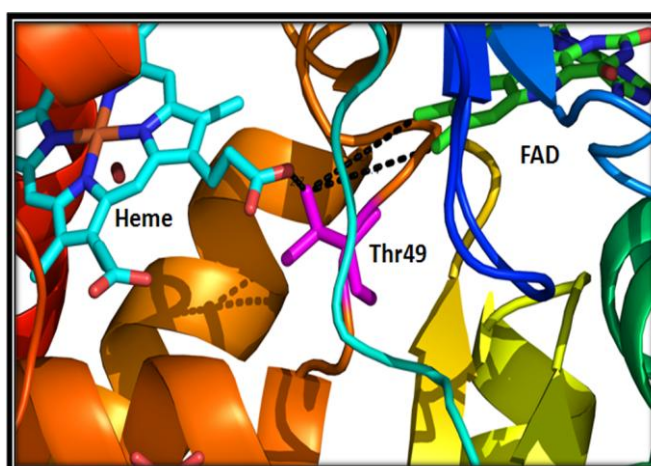


Figure 4.14: Representation of the distances between the cofactors in the docked structure. The graph displays the distance between the heme (blue) and the amino acid Thr49 (2.7Å), in magenta colour, which is turn is ~5Å from FAD moiety.

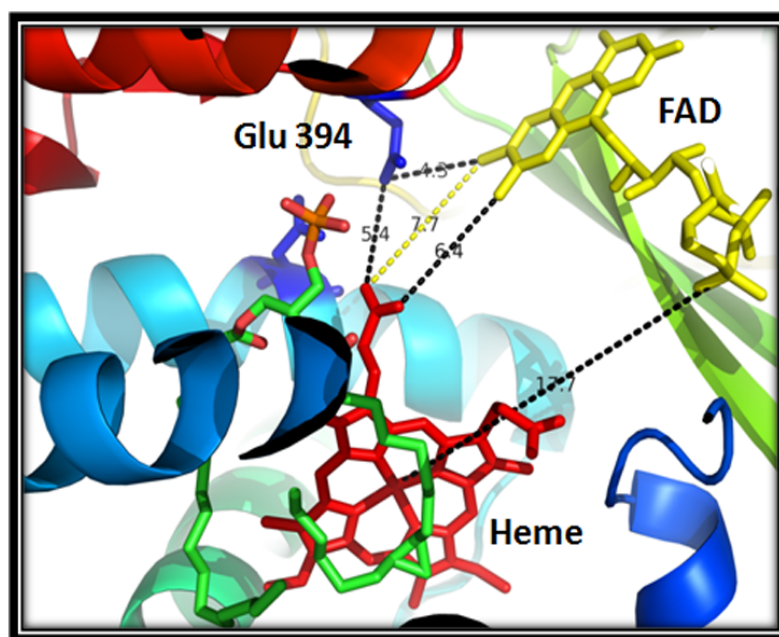


Figure 4.15: Representation of distances between the cofactors, in the flavohemoglobin from *Alcaligenes eutropha* (1CQX). The graph displays heme (red) separated from FAD (yellow) by minimum of 6.4 Å and maximum of 17.7 Å. Both heme and FAD form a triad with Glu394 (magenta).

4.3 Discussion

Literature is flooded with the information about the nitric oxide scavenging property of HbN by the Nitric Oxide Dioxygenase (NOD) mechanism, in which a toxic NO molecule combines with an O₂ molecule to form a harmless nitrate (eqn 1). What is missing is very integral to its uninterrupted activity, that is its association with any reductase to replenish itself for next round of NOD activity. This is because after the release of NO₃⁻ ion, the Fe at the heme centre is left in the Fe³⁺ state which cannot bind O₂. Since, HbN lacks an inherent machinery to reduce itself, like the attached reductase partner in falvohemoglobin, its reduction is only possible by a transient association with a redox protein.

In vivo situation, HbN must be encountering plenty of reductases for electron transfer, which can have different spatial and temporal expression profiles. Therefore, HbN has to be extremely selective in associating with reductases to recycle itself, for its utmost productivity. Our experimental data have clearly suggested that although HbN has 2-over-2 globin fold rather than 3-over-3 fold of two domain flavohemoglobin, it can still form compatible alliance with ferredoxin-NADH type reductase, which is naturally present in flavohemoglobin. Although reductase proteins were from different sources, such as: ferredoxin reductase(fdr) from *E.coli*, reductase domain of *E.coli* flavohemoglobin, KshB and trxB from *M. tuberculosis*, they were able to transfer electrons to HbN with varying efficiency. This can be advantageous to HbN because it is able to functionally attach to any of the available reductases at that particular moment. Truncated hemoglobins are known to participate in various physiological functions. Thus, it will be strategically beneficial to the host, if single protein can switch its function by simply changing its associated partners. KshB and TrxB are expressed during oxidative and nitrosative stress condition, so their association with HbN signifies their active participation during these conditions.

Highest electron transfer rate was noticed with ferredoxin reductase (fdr) and reductase domain of *E. coli* flavohemoglobin. Both are having similar type of structural fold, the ferredoxin-NADP type. Minimal activity was seen with KshB and trxB because although they contain FAD moiety, their alignment with HbN may not be that favourable as compared to fdr. Differential efficiency for catalyzing the electron transfer may be due to their structural differences, as heme and FAD domain should be in precise vicinity to each other for optimal transfer of electrons. WhiB1 protein failed to

reduce HbN, because neither it has FAD molecule nor the ferredoxin type structural fold. KshB whose chimera with HbN was created to mimic the 2 domain flavohemoglobin like complex, did not show any improvement in activity. On the contrary, the chimera was not even functional, as they were, when free in solution. They were fused to increase the probability of interaction between them, but fusion might have locked the two proteins in unfavourable state, leading to the loss in activity. Infact joining the KshB to the C-terminal must have provided some structural hindrance that has completely shut the transfer of electrons. At the same time chimera of HbN with ferredoxin reductase behaved like flavohemoglobin and was able to form Fe-CO complex, proving that the geometry of ferredoxin type reductase has appropriately evolved for smooth transfer of electrons to the heme group.

The preference for the ferredoxin type reductase is so high that it can replace the previously bound less efficient reductase from HbN. That is why the absorbance at 420nm shoots up when the *fdr* was supplemented midway in the reaction between HbN and *kshB* or between HbN and *trxB*. Even HbN-KshB chimera which was not showing activity, showed it, when *fdr* was added to the reaction mix. In addition, association at improper positions, places heme and FAD domain not very close to each other, resulting in slow transfer of electrons. Alternatively, reductases are not occupying the precise position on the HbN during transient interaction and might provide the chance to other reductases to dock optimally, thus increasing the NOD rate. This attribute might help the HbN *in vivo* conditions because under the stress condition it might be able to interact with other low efficient reductases, which it can easily replace with the higher efficient one, when it is available.

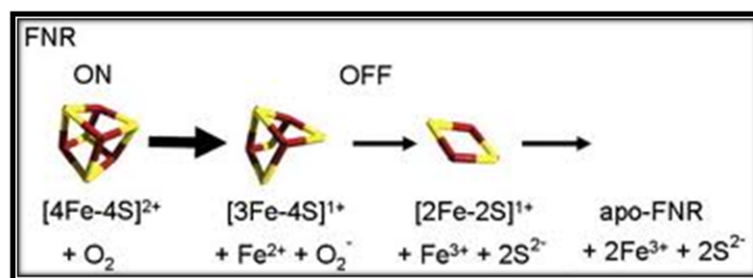
Our experiments have also assigned a novel role to the pre-A motif, which otherwise is known to be essential for NOD activity. The principle for the participation in the dual role by a single structure is the same, i.e. it controls the movement of the protein's helices. The answer is partially provided by the MD simulation studies, which has mapped and compared the movements of helices in HbN and pre-A deleted HbN. It recorded some distinct fluctuations in the B and E helices and EF loop of the oxygenated wild type HbN in comparison to its oxygenated pre-A deleted mutant, ultimately affecting the opening and closing of Phe62 gatekeeper amino residue. Alternatively, pre-A del HbN has got movement in the G and H helices. CD loop region lies in between the B and E helix (Lama *et al.*, 2009). Therefore, when the movement of B and E helix

is harmed, they automatically hamper the motion of CD loop, which then acts as a barrier between the porphyrin ring and the FAD moiety. Overall, the mutant might have restricted movement of helices and this might have abrogated the proper interaction, leading to failure of transfer of electrons. To further investigate the interface region crucial for the HbN and reductase interaction, structural analysis was performed.

In the absence of crystal structure of HbN interacting with reductase, we have theoretically docked the two structures, HbN (pdb:1IDR) and ferredoxin reductase (pdb:1FDR), to gain insight about the residues that might be playing critical role in stabilizing the two structures and helping in the electron transfer. The Docked structure has a great resemblance to the crystal structure of flavohemoglobin (FHP) from *Alcaligenes eutrophus* (1CQX). Reductase was seen to interact with HbN in the CD loop and F-G region. All the crucial distances, such as, the distance between the propionate of heme to the nearest atom in the isoalloxazine ring and heme centre to centre of mass of the isoalloxazine ring, are same in both the cases, i.e. 6.4Å and 17.2Å, respectively (Figure 4.13). In FHP, Tyr190 is in van der Waal contact to Lys84, GLu394 and flavin ring, similarly in docked structure, Phe36 is seen to form van der Waal contact with Thr49 and flavin ring. This is the most possible orientation in which HbN and reductase can participate because all the vital criteria: such as a polar environment, a pre-requisite for electron transfer, which is created by Ser47, Thr49 and Asn50 amino acids, flexible portion, which is provided in the C-D and F-G loop region, to adjust the intruding reductase protein and proximity to the porphyrin ring are fulfilled by this interaction. Another possible direction from which the FAD molecule can approach is near the pre-F region, which exists in loop confirmation but it consists of hydrophobic amino acid such as Gly74, Ala75, Met77 and Val 80. Therefore, it cannot be the site for electron transfer. The validity of the docked structure was verified by mutating the amino acids, Thr (49) and Asn (50), present in the CD loop (interface region), to Trp and Ile, respectively (Figure 4.14). The reduction in the electron transfer efficiency in the mutant could be due to the steric hindrance, provided by the indole ring of Trp and apolar, long side chain of Ile to the flow of electrons between FAD and heme domain. Additionally, Trp must have also disrupted the H-bond triad with the porphyrin ring and the FAD moiety, which the Thr residue forms, similar to the triad made by Glu394, porphyrin ring and FAD moiety in the *E. coli*'s flavohemoglobin (Figure 4.15). NOD activity of the TN-WI mutant was comparable to that of the wild type HbN, signifying that CD loop is not

important for the NOD activity and the movement of helices required for opening and closing of the tunnels were intact, giving uninterrupted NO scavenging.

Thus, detailed biochemical experiments have revealed that HbN has a tendency to interact with oxidoreductases, specially ferredoxin-NADP reductases. HbN also shows small degree of structural flexibility while selecting the reductase because electron transfer takes place in the reductases of different structure, although their efficiency varies. Our studies have also conferred a novel role to the pre-A region that it controls the transfer of electrons between HbN and reductase.



Chapter 5

Genetic regulation of glbN gene in Mycobacterium tuberculosis

5.1 Introduction.....	82-84
5.2 Results.....	85-90
5.2.1 In silico analysis of the upstream nucleotide sequence of the <i>glbN</i> gene.....	85
5.2.2 Cloning and expression of WhiB 1 protein.....	85-86
5.2.3 WhiB1 exist in two distinct oligomeric state.....	86
5.2.4 WhiB1 interacts with the <i>glbN</i> promoter.....	86
5.2.5 Autophosphorylation of WhiB1 and its effect on DNA binding.....	86-88
5.2.6 NO abrogates the interaction of WhiB1 with the <i>glbN</i> promoter.....	88
5.2.7 Dnase I footprinting analysis of the promoter element.....	88-90
5.3 Discussion.....	91-94

5.1 Introduction

Mycobacterium tuberculosis, a highly successful pathogen, is an obligate aerobe and ranks second in causing death from an infectious disease worldwide, after the human immunodeficiency virus (HIV) (Global health report 2012). Majority of infected individuals are asymptomatic, because *M. tuberculosis* can dwell inside the macrophage of an infected individual for long time, in a non-replicative, dormant state. However, in one of the ten infected individuals, when the immune response weakens, the pathogen gets reactivated and cause disease. This infection, adaptation and resurrection of the pathogen require highly precise, controlled and complex genetic programmes. The stay of *M. tuberculosis* inside the macrophage is not smooth, as it encounters the hostile response of the host's immunological machinery, such as reactive oxygen species (ROS), reactive nitrogen species (RNS), hypoxia etc. ROS damages the proteins, nucleic acid, cell membrane or other cellular components. Similarly, macrophages also employ the inducible NO synthase (iNOS) to secrete NO, as a defence molecule, which combines with the cellular oxygen to form harmful reactive intermediates, such as nitroxyl (HNO), peroxynitrate (ONOO⁻) (Chan, 2001; MacMicking *et al.*, 1997). Alternatively, NO can also be formed by disproportionation reaction under acidic condition or by reduction of nitrite. NO is harmful for the cell because even below 100nM concentration, it can inactivates sensitive metalloenzymes such as aconitase of Krebs cycle (Stevanin *et al.*, 2002), 6-phosphogluconate dehydratase of Entner-Doudoroff pathway, terminal oxidases etc, which are extremely crucial for the functioning of the cell (Gardner *et al.*, 1998a; Gardner *et al.*, 1997). Thus, *M. tuberculosis* comes across myriad of environmental conditions, mostly unfavourable, during its various stages of life.

M. tuberculosis tackles the menace of RNI stress by up regulating the expression of *glbN* gene, encoding for truncated haemoglobin, HbN. NO scavenging role of HbN in native as well as in surrogate hosts is confirmed through rounds of experiments. Detailed biochemical and structural studies on HbN have been performed, but its regulational study is still untouched. Very few reports are available regarding the factors responsible for its transcription. Pawaria *et al.* have observed that HbN only express during the stationary phase of the *M. tuberculosis* (Pawaria *et al.*, 2008), however, its expression is also seen to be up regulated during the NO stress. To get

further insight into the physiological relevance of the HbN, in context to *M. tuberculosis*, better understanding of its genetic regulation is required.

Bioinformatics analysis of upstream promoter region of HbN unravelled the presence of two putative FNR binding sites. This is quite surprising because *M. tuberculosis* lacks FNR protein. FNR and other Fe-S cluster containing transcriptional regulators, such as SoxR, NsrR etc are missing in mycobacteria. These regulators exploit the ability of their Fe-S cluster to bind with the gaseous ligands, which helps them to behave as a sensor molecule, to relay the signal downstream. *M. tuberculosis* contains WhiB proteins that are generally categorized as FNR family of proteins. WhiB protein was first discovered in an actinobacteria, *Streptomyces coelicolor*, as a factor crucial for sporulation because *S. coelicolor whiB* mutants formed white spores, instead of grey spores, indicating its putative role in regulation of sporulation (Davis and Chater, 1992). Till now, seven types of WhiB proteins (WhiB1-7) have been reported in *M. tuberculosis* (Cole *et al.*, 1998; Soliveri *et al.*, 2000). Although WhiB proteins do not share much sequence similarity among them, they do contain a conserved CXXC motif, with the exception of WhiB5, which has a CXXXXC motif (Gomez and Bishai, 2000). Several WhiB proteins are found to be involved in various physiological functions. WhiB2 which gets downregulated during late stationary phase is found to be responsible for mycobacterial cell division and septum formation (Gomez and Bishai, 2000). WhiB3 is involved in regulating the gene responsible for the synthesis of lipids, such as polyacyltrehaloses (PAT), Diacyl trehaloses (DAT), etc which are important for virulence (Singh *et al.*, 2009). Further, it also acts as a sensor of NO and O₂ and behaves as a transcriptional regulator. Apo-WhiB3 is found to have greater affinity for the promoter regions of *pks2* and *pks3* in comparison to holo-WhiB3 (Singh *et al.*, 2007). WhiB4 is reported as a protein disulphide reductase (Chawla *et al.*, 2012), whereas, WhiB6 responds to general stress that *M. tuberculosis* face. WhiB7 is involved in synthesis of proteins requires for neutralizing the antibiotics because *whiB7* null mutants of *M. tuberculosis* and streptomyces were hypersensitive to antibiotics (Fu and Shinnick, 2007; Geiman *et al.*, 2006).

WhiB1 is also a member of WhiB family of proteins, containing [4Fe-4S]²⁺ cluster. The [4Fe-4S]²⁺ cluster of WhiB1 is relatively oxygen insensitive than the other WhiB family members. Upon exposure to oxygen, the [4Fe-4S]²⁺ cluster get converted to [2Fe-2S]²⁺ or get completely destroyed. The [4Fe-4S]²⁺ cluster of holo WhiB1

protein shows high reactivity to the eight NO molecules to form dinuclear dinitrosyl-iron thiol complex or octa-nitrosylated species (Crack *et al.*, 2011). Apo-WhiB1 and NO-treated holo-WhiB1 (but not holo WhiB1) is shown to bind the *PwhiB1* (*whiB1* promoter region) to repress its own transcription, thus auto regulating itself (Smith *et al.*, 2010). WhiB1 is found to act as protein disulphide reductase. Looking into its ability to bind DNA and its sensitivity towards NO, makes it a probable candidate for the transcriptional regulator of HbN.

The present study has been undertaken to understand the molecular mechanism of genetic regulation of *glbN* gene in the context of its NO scavenging function. Here, we have demonstrated for the first time that NO sensitive WhiB1 of *M. tuberculosis* plays a vital in controlling the expression of *glbN* gene in response to NO. Interaction of WhiB1 with *glbN* gene promoter has been validated by gel shift assays and exact sequence of binding was identified using DnasI footprinting assay. Based on the experimental results, a working model for the genetic regulation of HbN expression has been presented that may shed light on the control of *glbN* gene expression in response to NO and redox environment of macrophages.

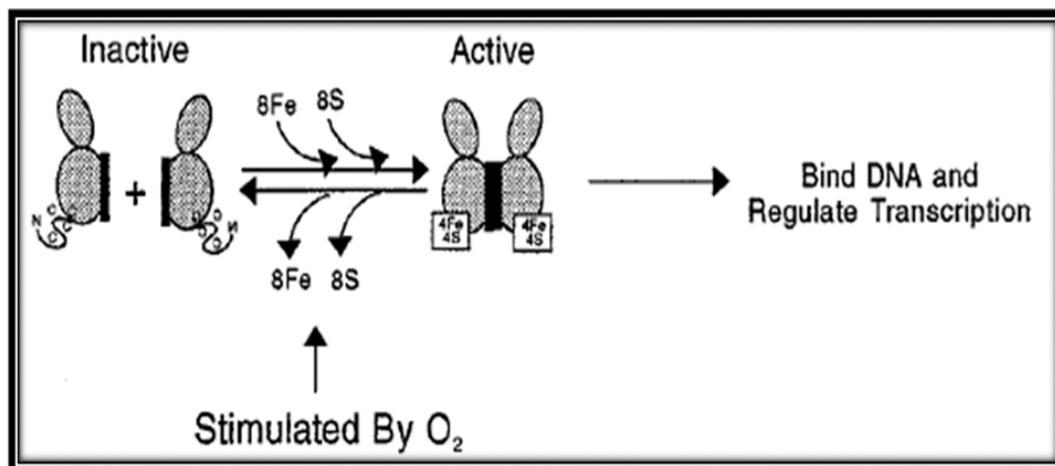


Figure 5.1: Model for the association of the Fe–S cluster with FNR and regulation of FNR activity by oxygen. A model for regulation of FNR activity by the stability of a [4Fe–4S] cluster to oxygen. Inactive refers to the form of FNR that is predominant under aerobic conditions and shows decreased DNA binding activity. Active refers to the form that shows enhanced DNA binding activity and is present predominantly under anaerobic conditions (Lazazzera *et al.*, 1996).

5.2 Results

5.2.1 In silico analysis of the upstream nucleotide sequence of the *glbN* gene

To study the precise regulation of the *glbN* gene, 228bp of nucleotide sequence from the upstream intergenic region of the *glbN* gene were analyzed. *In silico* analysis of the promoter region showed the recognition sequences for two putative sigma factors binding site i.e. SigF (GTTAAG-N₁₇-GGGTAG) and SigE (GGATC-N₂₁-CGTTG), approximately -200bp and -117bp upstream of the ATG start codon. Promoter region analysis also predicted to have two regions, (TTGCG-N₅-ATCTG) and (TTGGC-N₄--ATCAG), approximately -110bp and -90bp upstream of the ATG start codon, having similarity to FNR consensus binding site (TTGAT-N₄-ATCAA). One of the FNR binding site overlaps the sigE consensus sequence (Figure 5.2).

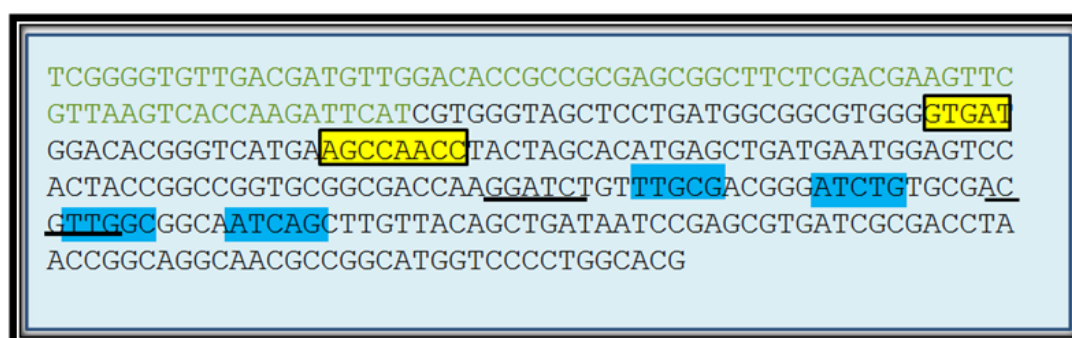


Figure 5.2: Diagrammatic presentation of putative binding sites in the promoter element of *glbN* gene. The putative FNR and SigF binding sites are highlighted in blue and yellow, respectively, whereas SigE binding site is underlined with black.

5.2.2 Cloning and expression of WhiB 1 protein

Although *M. tuberculosis* lacks a conventional FNR global gene regulator, there are some WhiB like proteins that are known to act as a transcriptional regulator in a manner similar to FNR protein. Therefore, here we explored the involvement of [4Fe-4S]²⁺ containing protein WhiB1 protein. The *whiB1* gene was PCR amplified from genomic DNA of *Mycobacterium tuberculosis* Ra using gene specific primers. The forward and reverse primers were designed based on the sequence of the genes which contained *NdeI* and *Xho* sites, respectively. The PCR product of *whiB1* gene was cloned into pBS KS⁺ cloning vector at *SmaI* site. Blue white selection was performed and the plasmid from correct clone was digested with *NdeI* and *Xho* restriction enzymes and cloned into *NdeI* and *Xho* site of pET28c vector. This construct was then transformed into BL21DE3 strain of *E.coli* for over expression. WhiB1 was purified using Ni-NTA

affinity column chromatography and its size was confirmed by comparing its molecular weight with the standard molecular weight marker in the 15% SDS-PAGE gel.

5.2.3 WhiB1 exist in two distinct oligomeric state

Size exclusion chromatography gave two separate peaks corresponding to the molecular weight of approximately 12kDa and 25kDa, respectively. It proved the protein to be present in two separate oligomeric states, i.e. monomeric (9kDa) as well as dimeric (18kDa), where the dimeric form was predominant. Additional mass can be due to the N-terminal histidine tag attached to the protein (Figure 5.3).

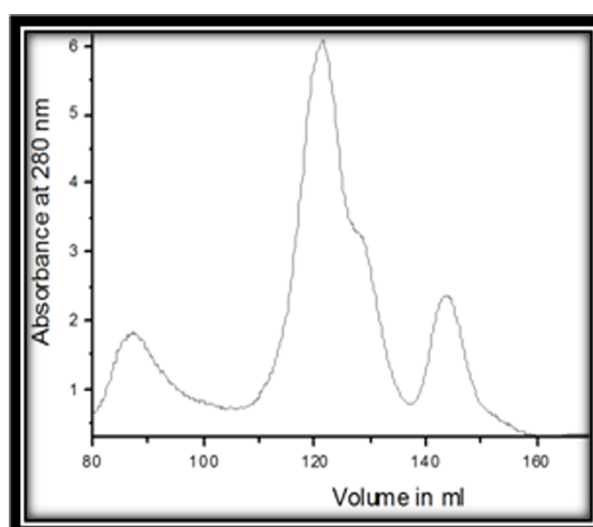


Figure 5.3: Gel filtration profile of the WhiB1 protein.

5.2.4 WhiB1 interacts with the glbN promoter

DNA binding ability of WhiB1 to the *glbN* promoter (*PglbN*) was checked by electrophoretic mobility shift assays (EMSA). 60ng of purified WhiB1 protein was able to bind to the *glbN* promoter, giving a retarded complex of protein and DNA. However, upon increasing the concentration of the protein to 100ng, greater retarded complex of protein and DNA were observed with the band shifting further upwards. Two distinct pattern of DNA binding was observed with the EMSA analysis (Figure 5.4).

5.2.5 Autophosphorylation of WhiB1 and its effect on DNA binding

In silico analysis of WhiB1 protein sequence revealed the presence of two unique phosphorylation binding motif, which has not been reported yet. Therefore, to

validate its ability to get phosphorylated, kinase assay was performed. Surprisingly, WhiB1 was able to get autophosphorylated, which was confirmed by the autoradiograph, where the band corresponds to the molecular weight of the protein. However, phosphorylation had no effect on DNA binding ability of the WhiB1 protein, as phosphorylated protein was also able to bind DNA (Figure 5.5 and 5.6).

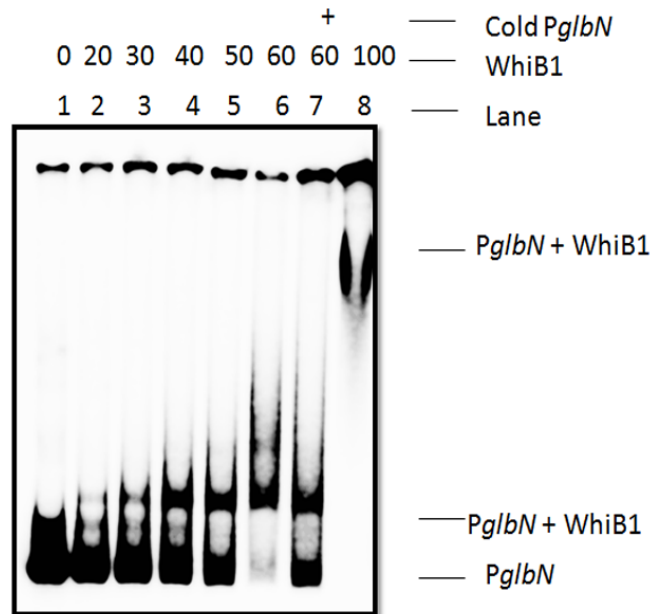


Figure 5.4: WhiB1 binds to *PglbN*. Interaction of WhiB1 with *glnB* promoter (*PglbN*). Lane 1, ³²P-labelled promoter alone; lanes 2–6 and 8, labelled promoter with increasing concentrations of WhiB1 in ng; lane 7, ³²P-labelled promoter with WhiB1 and cold promoter.

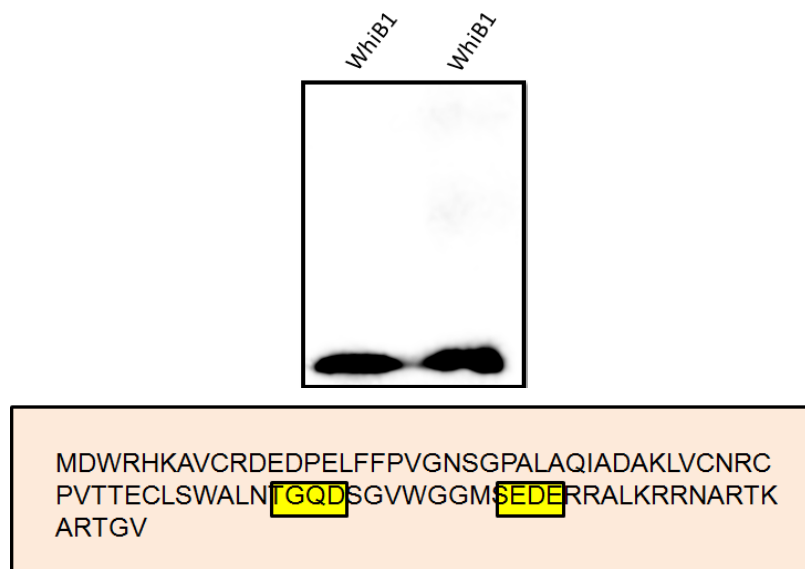


Figure 5.5: WhiB1 gets autophosphorylated. Left side: WhiB1 incubated with ³²P γ labelled ATP in the presence of 5mM Mg²⁺ ion and 10mM tris for 20 mins and then run on SDS-PAGE gel to get the autoradiograph. Both the lanes contain same amount of WhiB1 protein. Right side: Amino acid sequence of the WhiB1 protein where phosphorylation site is highlighted in yellow colour.

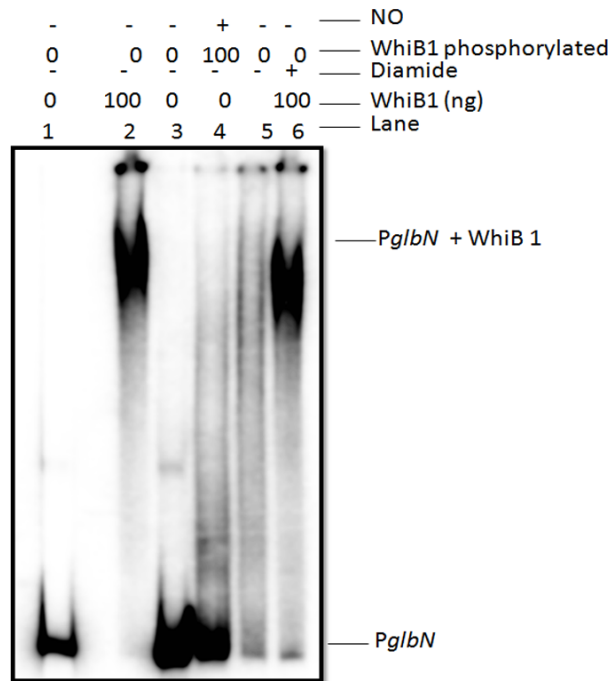


Figure 5.6: Autophosphorylation and oxidation of WhiB1 has no effect on it binding to *PglbN*. Lane 1 and 3 contain ^{32}P -labelled promoter alone; Lane 2 and 4 contain phosphorylated WhiB1 and NO treated phosphorylated WhiB1; Lane 6 contain diamide treated WhiB1.

5.2.6 NO abrogates the interaction of WhiB1 with the *glbN* promoter

WhiB1 protein was unable to bind to *PglbN* in the presence of nitric oxide. WhiB1, which was pre exposed to NO, prior to incubation with the promoter, showed no binding with the promoter element and the band corresponding to protein–DNA complex disappeared. On the other hand, presence of DTT had no effect on the binding of WhiB1 to the promoter. In the presence of DTT, binding pattern of DNA and protein was similar to that of the binding seen in the absence of it. At low concentration of WhiB1 protein (60ng), we got DNA-protein complex of faster mobility as compared to the complex formed at higher concentration of WhiB1 (100ng) (Figure 5.7 and 5.8).

5.2.7 Dnase I footprinting analysis of the promoter element

To delineate the binding sequence of WhiB1 in the promoter region, *in vitro* DnaseI footprinting analysis was done. Footprinting result of WhiB1 and *PglbN* displayed a distinctive Dnase I cleavage pattern characterized by a protective region of 12 nucleotides (-110bp from ATG start codon), located in between the putative sigE binding site and partially overlap with the one of the putative FNR binding site (Figure 5.9).

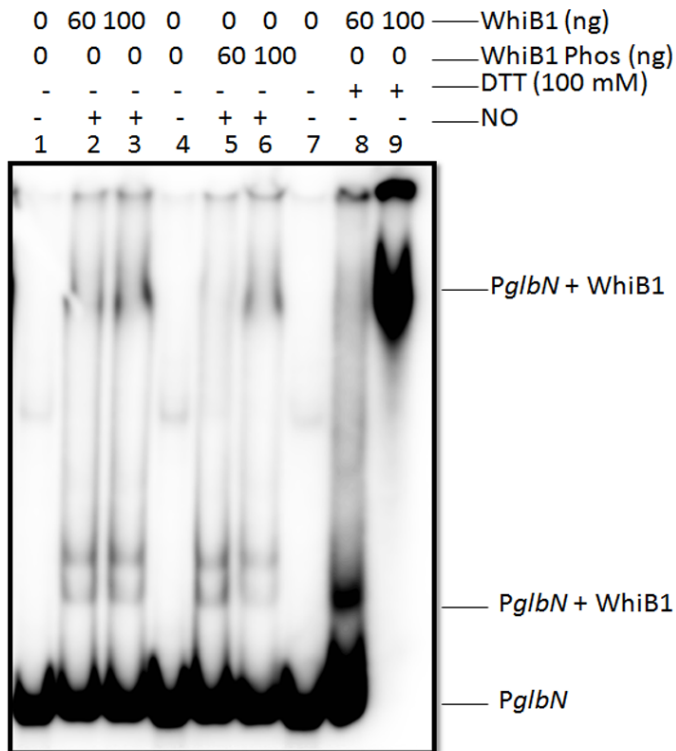


Figure 5.7: NO disrupts the binding of WhiB1, whereas, DTT has no effect. Lane 1, 4 and 7 contain ³²P-labelled promoter alone; Lane 2 and 3 contain NO and increasing concentration of WhiB1 protein; Lane 5 and 6 contain NO and increasing concentration of phosphorylated WhiB1; Lane 8 and 9 contain increasing concentration of whiB1 and DTT.

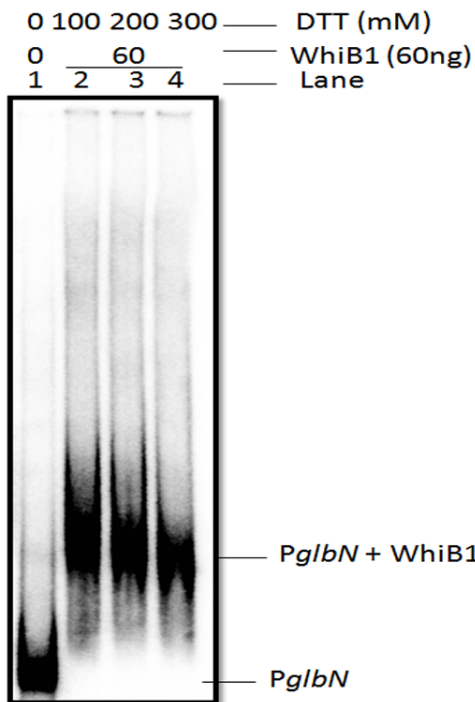


Figure 5.8: DTT has No effect on WhiB1 binding. Lane 1 contain ³²P-labelled promoter alone; Lane contain WhiB1 and increasing concentration of DTT.

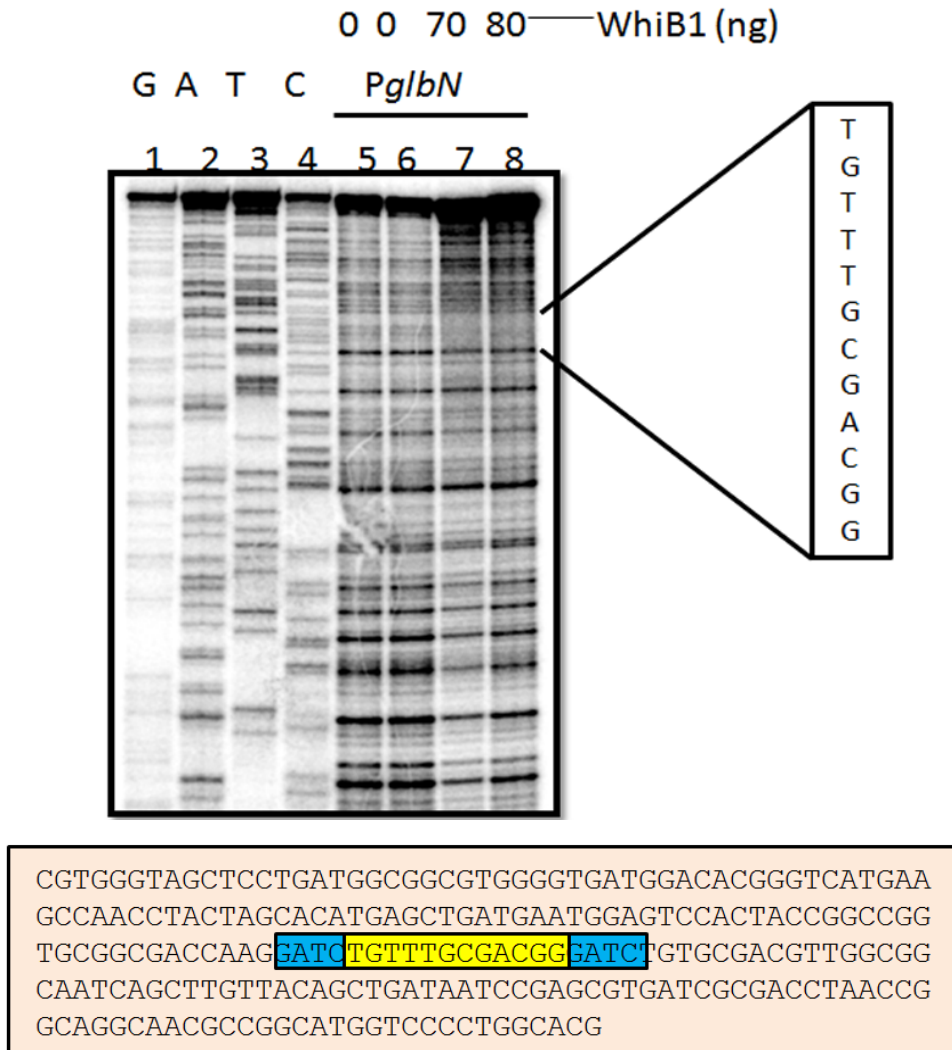


Figure 5.9: Dnase I footprint of WhiB1 at *PglbN*

Lane 1-4 contain G, A, T, C standard ladder; Lane 5-8 shows the increasing concentration of WhiB1, as indicated above each lane, were incubated with *PglbN* before Dnase I digestion. Hypersensitive sites associated with interaction with WhiB1 are indicated in the box. Lane 1-4 contain standard ladder. Lower panel depicts the nucleotide sequence of the upstream region of the *glnN* gene, where the protected region is highlighted in yellow.

5.3 Discussion

Mycobacterium tuberculosis is a facultative intracellular pathogen. Its success depends upon its ability to swiftly adapt to the environmental conditions. The genome of *M. tuberculosis* is the largest of the obligate human pathogens and intracellular bacteria. It encodes approximately 190 regulatory proteins, including 11 two component systems, five unpaired response regulators, two unpaired histidine kinases, 11 protein kinases, 15 sigma factors and over 140 other transcription regulators (Rodrigue *et al.*, 2006). Accumulating evidences suggest that *M. tuberculosis* undergoes co-ordinated gene expression in response to signals associated with infection, survival and growth of the bacteria.

HbN protein is associated with the dormancy of the tubercule. Unlike its other molecular relative globin, HbO, which is expressed throughout the life span of *M. tuberculosis*, HbN is expressed only in the stationary phase of the pathogen. Its ability to neutralize the NO response of the host immunological machinery makes it a special protein. Although many reports on the NO scavenging mechanism of the HbN have been documented, not much study has been done on the genetic regulation of this protein. In this study, for the first time, we report the regulation of *glbN* gene by a FNR type, Fe-S cluster containing protein, known as WhiB1, with respect to nitrosative stress.

The gel shift assays have clearly shown that holo-WhiB1 protein was able to bind the *glbN* promoter whereas NO-treated holo-WhiB1 showed no binding to the promoter. WhiB1 protein binds with the *glbN* promoter to form DNA-protein complexes of two separate mobilities. This can be possible, if the promoter element contains multiple binding sites. At the low concentration the protein binds at single location, however, as the concentration increases, the other available binding sites are also filled and the larger complex of less mobility is formed, forming two separate bands in the gel. This binding is opposite to the binding pattern of WhiB1 to its own promoter, where holo-WhiB1 is unable to bind its own promoter, whereas, NO treated holo-WhiB1 can bind and repress the transcription of *whiB1* gene. Each monomer of WhiB1 contains a $[4\text{Fe-4S}]^{2+}$ cluster, which dimerizes to form a molecule with a stoichiometry of 2 clusters per dimer, which is a DNA binding form. Each $[4\text{Fe-4S}]^{2+}$ cluster reacts with 8 NO molecule to form unusual octa-nitrosylated iron-sulphur which does not bind the

promoter *PglbN*. Size exclusion chromatography has clearly demonstrated that the DNA binding dimeric form is the predominant population present in the purified protein. The formation of octa-nitrosylated species from a [4Fe-4S] species within the protein cavity brings about a rearrangement of the iron positions relative to the cysteine thiols, and hence will drive a protein conformational change to switch the DNA binding properties of WhiB1 protein upon reaction with NO (Figure 5.11). *M. tuberculosis* has exploited the NO as well as DNA binding property of the WhiB1 to function as a transcription regulator. FNR in bacteria is highly susceptible to oxygen, whereas crucial mutation of serine to proline amino acid adjacent to Cys2 in WhiB1 confers it insensitivity to oxygen to a very great extent (Jervis *et al.*, 2009). This can be accounted for the retention of [4Fe-4S] cluster during the experimental procedure in an absence of anaerobic chamber. The large difference in the stability of the protein also hints at the evolution of the WhiB1 for the NO chemistry. Structural aspects that are responsible for the differential binding can be further investigated. The abolishment of DNA-protein binding in the presence of NO further substantiated the fact that Fe-S cluster was intact because NO will only bind to Fe atom of the cluster to form the octa-nitrosylated species, which do not bind to DNA due to its conformational change. Reduction of WhiB1 with DTT or oxidation with diamide had no effect on the DNA binding ability of the protein. For the first time, we are reporting the autophosphorylating ability of the WhiB1, however, its phosphorylation did not affect its binding pattern in comparison to its non phosphorylated form. Phosphorylated WhiB1 was able to bind the promoter DNA, whereas, NO bound phosphorylated WhiB1 was showing no binding, which is similar to the binding pattern of unphosphorylated WhiB1.

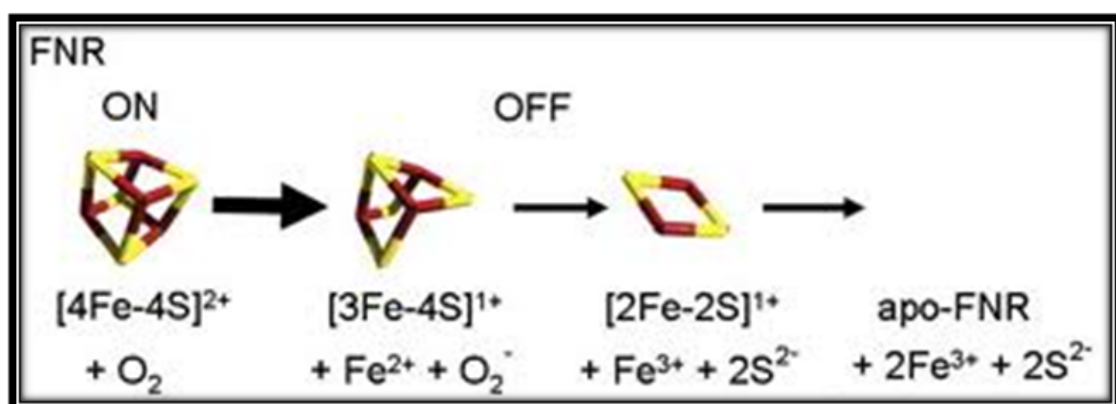


Figure 5.10: Disruption of Fe-S cluster. This graph represents the step wise dissolution of [4Fe-4S]²⁺ cluster to apo-FNR form in the presence of oxygen.

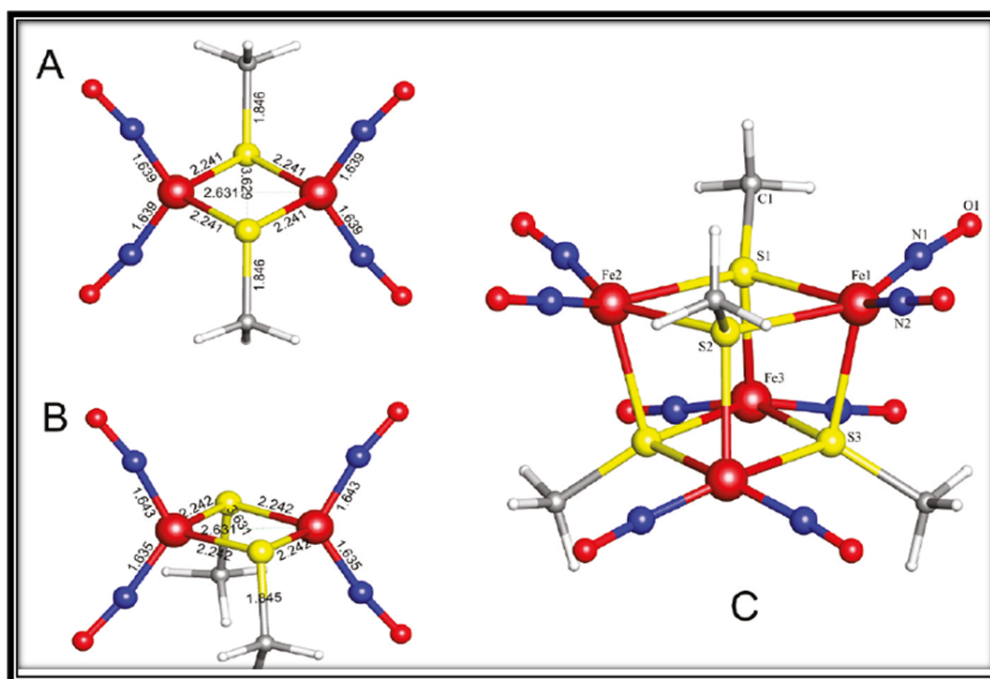


Figure 5.11: Roussin's red ester (RRE) and a proposed novel octa-nitrosyl cluster resulting from nitrosylation of the [4Fe-4S] cluster of Wbl proteins. (A) and (B) represents the cis and trans conformations of RRE, $[\text{Fe}_2(\text{NO})_4(\text{CH}_3\text{S})_2]^0$, with methyl thiolates bridging in between. (C) Represents the energy minimised structure of RRE, which explains the structure of DNIC (dinitrosyl-iron thiol complex), formed by the reaction of $[\text{4Fe-4S}]^{2+}$ cluster with 8 molecules of NO (Crack *et al.*, 2011).

WhiB1 protection assay with the *PglbN* promoter region showed a 12 nucleotide protected region, which overlaps with the putative sigE binding site. This region also coincides with the one of the putative FNR binding site predicted by bioinformatics analysis. It can be explained that WhiB1 might interfere with the sigE binding to the promoter region, which eventually blocks the RNA polymerase binding, thus playing a role in transcriptional repression. This binding also explains the earlier result, where the promoter activity of *glbN* was decreased when FeCl_3 was added to the medium (Pawaria *et al.*). Addition of iron in the medium must have retained the [4Fe-4S] cluster in the WhiB1 protein, which must have allowed the protein to remain bound to the promoter region, thus repressing the transcription.

Thus, the overall mechanism that is evident from this study combined with the previous findings is given in the (Figure 5.12). In the normal condition [4Fe-4S] containing WhiB1 is bound to the *glbN* promoter in a dimeric form. This binding might block the sig E binding which eventually blocks the RNAP binding to the promoter. This results into repression of *glbN* gene. During the NO challenge, the NO binds to the

WhiB1 to form octa-nitrosylated species which does not bind to the *glnB* promoter and transcription of *glnB* occurs. This WhiB1-NO bound form which gets detached from the *PglnB* can bind to the promoter of the *PwhiB1* causing no further synthesis of WhiB1, by repressing its transcription. This reduction in the level of WhiB1 will further upregulate the production of HbN. Thus, the repression of WhiB1 protein synthesis will upregulate the HbN's production in a positive manner.

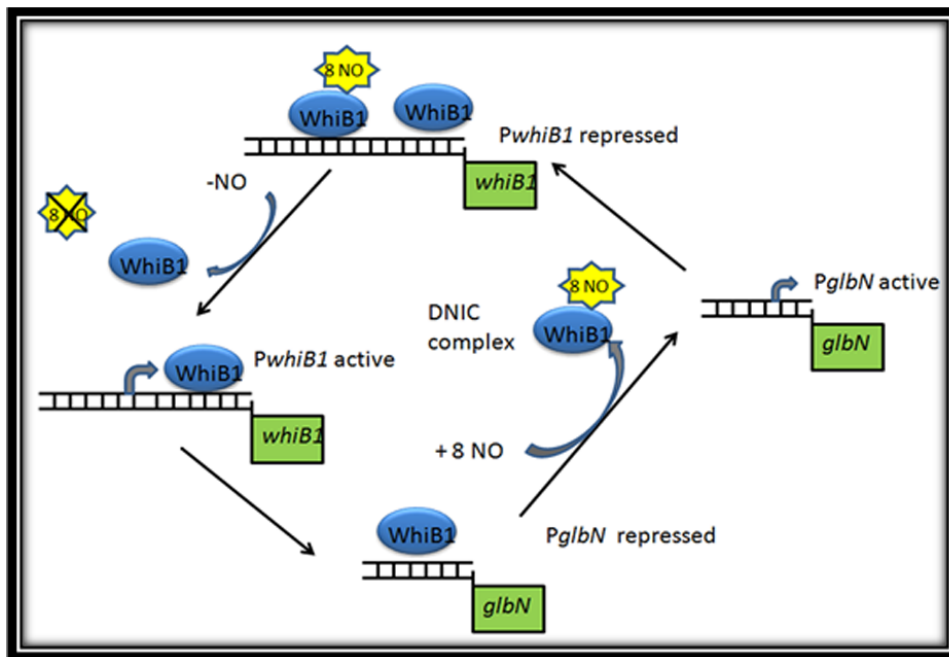
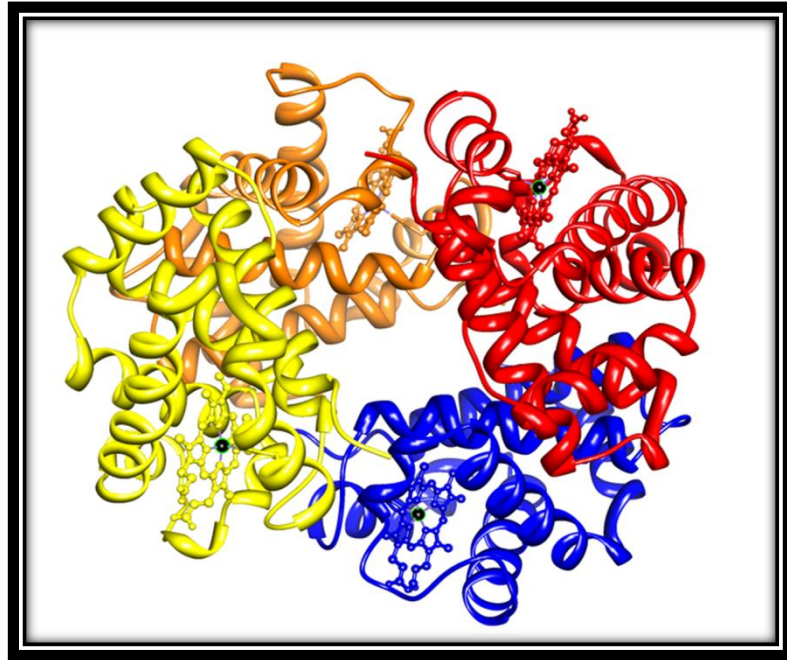


Figure 5.12: Plausible model for the regulation of *glnB* gene. This hypothetical model explains the up and down regulation of *glnB* gene in the context of NO. WhiB1 binds to the *glnB* promoter to repress its transcription. WhiB1 reacts with 8 molecules of NO to form DNIC complex, which gets detached from *glnB* promoter, but binds to *PwhiB1* to repress its transcription. This allows the *glnB* to overexpress. At low levels of NO the DNIC complex is destroyed the WhiB1 loses its affinity for *PwhiB1*, resulting in its expression, which eventually will suppress the transcription of *glnB* gene.

Finally, in this study, we have identified a transcription factor WhiB1 which shows differential binding to *PglnB* in a nitric oxide dependent manner. We have also discovered the phosphorylating ability of WhiB1, which will add new dimension to the understanding of the transcriptional machinery of the pathogen, especially during the latent phase.



Overview

Overview

The exploration of mycobacterial genome sequences, since it was published, has surfaced several novel insights into the biology of this pathogenic organism, leading to the identification of several unidentified genes, including the presence of genes for novel haemoglobins (Cole *et al.*, 1998). Two genes *glbN* and *glbO*, encoding truncated haemoglobin like proteins: namely HbN and HbO respectively, were the first to be discovered in the genome of virulent microorganism *M. tuberculosis*. Subsequently, haemoglobins like proteins were found to be ubiquitous in *Mycobacterial* species. Three distinct types of truncated hemoglobins were found in the mycobacterial genome, belonging to three different groups and having 18% similarity, among them. The opportunistic pathogen, *M. avium*, carries all three types of trHbs, namely HbN, HbO and HbP, belonging to groupI, groupII and groupIII, respectively, whereas, intracellular pathogens, like *M. tuberculosis*, *M. bovis*, *M. marinum* etc carry two types of haemoglobins, HbN and HbO. Interestingly, the obligate intracellular pathogen, *M. leprae*, which has undergone extensive reductive evolution, carries a minimal set of genes required for persistence and pathogenesis, retains only one type of haemoglobin, HbO (Wittenberg *et al.*, 2002). Presence of more than one type of haemoglobin, in one organism, signifies that they must be playing different physiological roles, many of which are yet to be discovered.

Studies on the mycobacterial Hbs have been mainly concentrated on HbN and HbO of *M. tuberculosis*. Physiological studies performed on the *M. bovis*, demonstrated that *glbO* is expressed throughout the growth phase whereas, expression of *glbN* is induced only during the stationary phase, thus, giving invaluable hint about their physiological roles in the microorganism (Mukai *et al.*, 2002; Pathania *et al.*, 2002b). HbO of *M. tuberculosis* has been implicated in the oxygen uptake and transfer process during its aerobic growth stages. HbO has been proved to be beneficial for its host to sustain aerobic metabolism during hypoxic condition, thus facilitating its intracellular survival (Liu *et al.*, 2004; Pathania *et al.*, 2002b). On the other hand, HbN is shown to exhibit distinct nitric oxide dioxygenase activity, which protects *M. tuberculosis* from the poisonous effect of NO, generated by inducible nitric oxide synthase in a copious amount (Ouellet *et al.*, 2002). NO acts on key enzymes such as terminal respiratory oxidases, aconitase etc (Gardner *et al.*, 1997; Stevanin *et al.*, 2002). It has also been

demonstrated that the disruption of the *glnN* gene, encoding HbN, in the *M. bovis* bacillus Calmette-Guérin, caused a dramatic reduction in the NO-consuming activity of the stationary phase cells, resulting in marked NO-induced inhibition of aerobic respiration, relative to the wild type cells (Ouellet *et al.*, 2002). Similarly, HbN also provided growth advantage to its surrogate hosts, such as *E. coli* and *Salmonella typhimurium* during nitric oxide stress condition (Pathania *et al.*, 2002a; Pawaria *et al.*, 2007). However, HbN present in other organisms is found to perform different functions: *Chlamydomonas eugametos* HbN has been implicated in photosynthesis (Couture *et al.*, 1994; Das *et al.*, 1999) whereas, the probable function of *Paramecium caudatum* HbN is to supply O₂ to the mitochondria (Wittenberg *et al.*, 2002). HbN of the cyanobacterium, *Nostoc commune* is a part of a microaerobically functioning electron transfer system (Potts *et al.*, 1992).

Three dimensional structure of *M. tuberculosis* HbN conform well with its functional properties and present a unique structure among the trHb family. It carries two special features: firstly, a pre-A region and secondly, the presence of two orthogonal tunnels, called as long and short tunnels (Milani *et al.*, 2001). Pre-A region is highly flexible in nature and it consists of 12 amino acids. It is an extended N-terminal portion of HbN that protrude from the compact protein core. Tunnels are apolar in nature and connect the outer protein surface to the inner distal heme pocket. It has been proposed that due to the crowded oxygen binding distal site these hydrophobic tunnels facilitate the efficient migration of ligands towards the active site. Simulations studies have suggested that access of O₂ to the heme cavity primarily involves migration through the tunnel short branch (10 Å long, shaped by residues in helices G and H). Binding to the heme then regulates opening of the tunnel long branch (20 Å long, mainly defined by helices B and E) through a ligand-induced conformational change of PheE15 residue, which would act as a gate (Bidon-Chanal *et al.*, 2006; Crespo *et al.*, 2005). This is the working hypothesis of the NOD toxification.

HbN of saprophyte and non pathogenic *M. smegmatis*, lacks the NOD activity in spite of having 80% similarity with *M. tuberculosis* HbN (Lama *et al.*, 2006). This functional deviation goes well with its life style in comparison to the pathogenic species, *M. tuberculosis*. Unlike *M. tuberculosis*, which resides within the macrophages and avascular calcified granulomas and encounters severe hypoxia and nitrosative stress, *M. smegmatis* neither enters epithelial cells nor persists in the professional phagocytes,

although it has been known to cause soft tissue and bone infection in rare cases. A careful comparison of the sequences of HbN from *M. tuberculosis* and *M. smegmatis* revealed a distinct difference in the N-terminal region of the two genes. HbN of *M. smegmatis*, lacks the pre-A region and thus has a compromised NOD activity. Therefore, the role of pre-A region in NOD activity of HbN was discovered. Pre-A deleted *M. tuberculosis* HbN possess 1/3rd the NOD activity of wild HbN (Lama *et al.*, 2009). This result was further confirmed when *M. smegmatis* HbN was shown to regain the ability of NOD to some extent when pre-A motif was added to it. The explanation for this behaviour was only provided by MD simulations. It showed that the deletion of pre-A motif hampered the motion of Phe62 amino acid, causing the long tunnel to remain in closed state for longer duration, thus inhibiting the diffusion of gaseous ligand into the distal heme pocket. This interruption in the gaseous exchange led to compromised NOD activity. However, the exact molecular mechanism behind the pre-A region controlling the opening and closing of Phe62 is not known. It will be interesting to explore the mechanism of signal being relayed from an extended pre-A region to the Phe62 amino acid residue, inside the protein core. Therefore, detailed study is conducted to understand the molecular mechanism of the NOD activity.

Careful observation of the pre-A region revealed that it is highly polar in nature and contains four positively charged amino acids, Arg6, Lys8, Arg9 and Arg10. Therefore, to understand the relevance in protein function, site directed mutagenesis was carried out to mutate all of them to alanine, named as Nter-all, and checked the effect of mutations on the NOD activity. We found that NOD activity of the Nter-all mutant was reduced to 1/3rd of the wild type HbN. Even the individual mutants, with the charged amino acids were individually mutated to alanine, showed compromised NOD activity, indicating that positively charged amino acids are crucial for the catalytic activity of the HbN. All the mutants carrying single or multiple mutations displayed spectral characteristic identical to wild type HbN and formed typical oxyform spectra after oxygen binding, indicating that these HbN mutants are able to interact with oxygen and form stable oxyform. The CO dissociation kinetics of these mutants was checked to evaluate the effect of these mutations on CO binding properties of the mutants. The dissociation constant (K_{on}) value for the wild type HbN was $2.5 \times 10^7 \text{M}^{-1} \text{s}^{-1}$, under our experimental condition, that is slightly higher than the value reported by Couture *et al* ($0.657 \times 10^7 \text{M}^{-1} \text{s}^{-1}$) (Couture *et al.*, 1999). K_{on} values for the pre-A mutants were

comparable to that of wild type, suggesting similar behaviour towards CO dissociation. It is, therefore, likely that these positively charged amino acids of pre-A interact with other amino acids on the surface of the core domain. O₂ binding and CO dissociation studies implied that the mutations had no effect on the short tunnel, which is responsible for the entry of oxygen. It is the NO whose entry is hampered, which eventually affect the NO metabolizing property of HbN. This is highly probable because pre-A is flexible in nature as seen in the crystal structure (pdb: 1IDR), consisting of a short helix and a small loop. Recently, NMR analysis solved the pre-A region as a random coil, which means that it is more flexible than what we have considered it previously (Savard *et al.*, 2011). Thus, it imparts a greater degree of freedom to form salt bridges with the negatively charged amino acids, such as Asp17 and Glu70, present along with the His22 amino acid, on the surface of the protein core. MD simulation experiments have captured the interactions between Arg6 and Asp17 and Arg10 and Glu70. Therefore, it might be possible that charged amino acids on the pre-A region and the triad (Asp17, His22 and Glu70) allow the breakage and formation of non-covalent bonds to modulate the motion of the backbone in an ATP independent manner. This dynamics of the backbone helices leads to the opening and closing of Phe62 amino acid to facilitate the diffusion of NO from the long tunnel, ultimately executing the NOD activity.

Experimental studies were extended further to establish the importance of Phe62 amino acid in NOD function of HbN. Phe62 amino acid was mutated to alanine, Isoleucine, tyrosine and tryptophan by site directed mutagenesis. Mutations were chosen to span a wide range of sizes, varying small size of alanine to bulky indole ring of tryptophan and replacement of planar benzene ring with branched Isoleucine. Phenylalanine was changed to tyrosine because its side chain contains benzene ring with an additional OH group. These amino acids were selected because side chain plays a very important role in chemistry of the protein. Variable side chains will have different interactions with the neighbouring amino acids, leading to differences in motion of the backbone, which in turn may affect the NOD activity. To compare the activities of the mutants, they were cloned, expressed and purified. Absorption spectra of O₂ and CO bound mutant proteins were similar to that of the wild type HbN, indicating that mutants have similar ability to bind these gaseous ligands. This was further confirmed by calculating the p^{50} value for oxygen binding and the measured values for the wild type HbN and mutants were found to be comparable (0.019), suggesting that oxygen binding

properties of the mutants are unaffected. To further validate these results CO dissociation values of the various mutants were assessed and all the proteins were found to have values in comparable range ($2.7 \times 10^7 \text{M}^{-1}\text{s}^{-1}$). K_{on} values clearly demonstrated that Phe62, long tunnel gate mutations have no effect on O_2/CO binding properties of HbN. Even though mutants showed similar O_2 binding properties, distinct differences were documented in their NO metabolizing activity. The NOD activity of Phe62Ile was reduced to around 55% of the activity measured for the wild type, whereas larger reduction was observed in Phe62Trp mutant, around 70%. Surprisingly, did encounter reduction in activity in alanine and tyrosine mutant. NO oxidation profile also depicted the same thing, where similar addition of NO to the oxygenated form of mutants Phe62Ile, Phe62Trp and Phe62Tyr did not change the spectra to the oxidised form immediately and changed slowly after 30-35 mins of exposure, signifying slow oxidation of NO. Phe62Ala mutant also showed activity in between the activity observed for wild type HbN and Phe62trp mutant. Thus, Phe62 amino acid is established as a gatekeeper residue, which plays a key role in mediating the access of NO to the oxygen bound iron through the long tunnel. These findings agree with the dual-path mechanism of ligand entry to the heme pocket.

Another important aspect of the NOD activity of HbN is the reduction of heme iron from Fe^{3+} to Fe^{2+} state. This is because, while catalysing the NO to NO_3^- , HbN gets oxidised from active Fe^{2+} form to inactive Fe^{3+} form, which Fe^{3+} form cannot bind oxygen. To regain its functional form for the next round of NOD activity, HbN has to be reduced back to Fe^{2+} state, with the help of a reductase protein, which it lacks, being a single domain protein. However, inspite of being a single domain protein, the catalytic efficiency of HbN is very similar to that of a two domain flavohemoglobin that carries an integrated reductase domain, which allows efficient recycling of electrons to maintain the globin in Fe^{2+} state. Expression of HbN in heterologous hosts, such as *E. coli*, *Salmonella* etc confer distinct NOD activity to these heterologous hosts implying that HbN is able to utilize electrons donating system of these hosts. Therefore, it is likely that HbN is likely to interact with different redox partners. However, till now, no experimental evidence have been available about the cognate reductase partner of the HbN. Truncated haemoglobin characterised in other organisms, such as, ciliated protozoan *Paramecium caudatum*, the unicellular alga *Chlamydomonas eugemetos* and the eubacteria *Nostoc commune* are all single domain and lack a reductase partner. Till

date, no experimental evidence is present regarding the probable reductase partner. Therefore, detailed characterisation of HbN-reductase interaction was required to present the complete picture of the NOD process.

To check this probability ferredoxin-NADP type reductases were screened from native as well as heterologous hosts and looked for their interactions with HbN. This is because flavohemoglobins from *Erwinia chrysanthemi* (Favey *et al.*, 1995), *Bacillus subtilis*, *Salmonella enterica* serovar typhimurium and *M. tuberculosis* have contain a 29kDa, ferredoxin-NADP type reductase domain attached to their C-terminus region (Bollinger *et al.*, 2001). They are naturally suited for the electron transfer to the heme moiety present inside the globin fold and the basic FAD and NADPH binding domains are conserved throughout the species. Therefore, reductases such as Ferridoxin reductase from *E. coli* and reductase domain of the *E. coli* hmp were cloned. These reductases come under the family of oxidoreductases, therefore other reductases, which comes under this family but do not have ferredoxin-NADP type fold, such as KshB (Rv3571) and trxB (Rv3913) were also cloned.

The interactions of these reductases with HbN were tested by a simple biochemical assay that exploits the inability of oxidised Fe^{3+} HbN to bind with CO (Hayashi *et al.*, 1973). Only Fe^{2+} HbN will bind with CO, giving the soret peak at 420nm. Thus, when the oxidised HbN along with reductase and NADH, as a cofactor were added to buffer flushed with CO in a chamber, the reductase will reduced the HbN and the CO bound to it, was easily monitored by the shift of the soret peak from 406nm to 420nm. This reductase assay showed that HbN was able to interact with *E. coli* ferridoxin reductase and the reductase domain of *E. coli* Hmp, both having the ferredoxin-NADP type fold. On the other hand, KshB and trxB that do not contain ferredoxin –NADP reductase like fold were unable to transfer electrons with much efficiency with trxB being the least efficient one. This proved that ferredoxin type reductase is better evolved to transfer electrons to the heme iron as compared to the reductase, which lacks this fold. This fact was further confirmed by joining the reductase domain to the C-terminal of the HbN to mimic the natural two domain flavohemoglobin. In this scenario, HbN-KshB chimera was not functional, suggesting that they might have interacted in a wrong conformation, which was not favourable for the transfer of electrons (they were functional to some extent when they were not fused to each other). On the other hand, ferredoxin reductase was able to transfer the electrons very

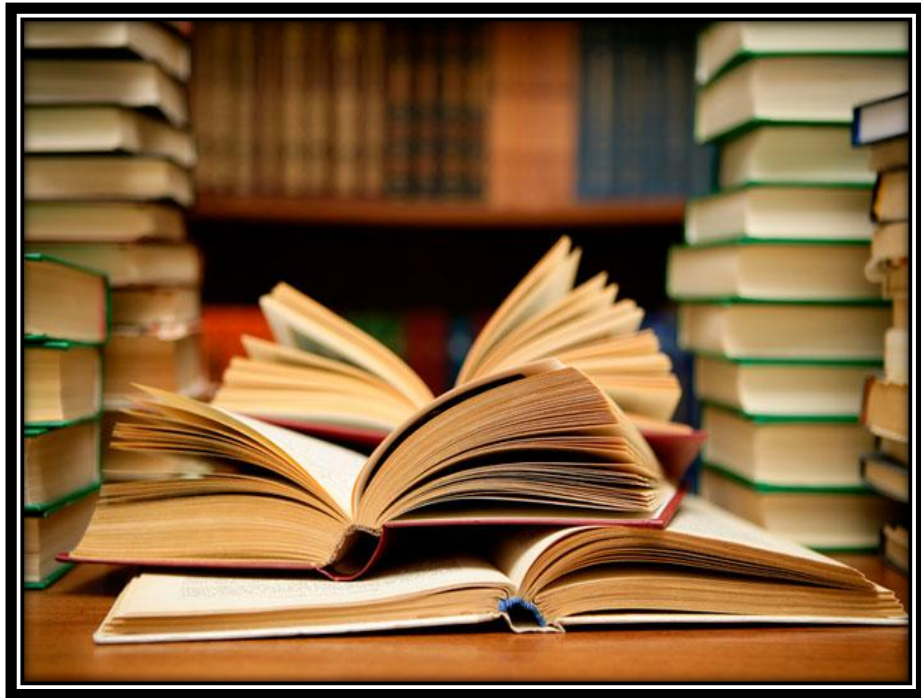
efficiently. Our results also suggest that ferredoxin reductase can replace the less efficient reductase to bring about faster reduction of oxidised heme. This ability of HbN can be very beneficial, as it can form alliance with any reductase to reduce itself, when a better partner is not available during the unfavourable condition and it can easily switch to another partner, when it is available. This might be the common scenario during stress conditions when the resources are very limited. Surprisingly, it was found out that pre-A region is not only crucial for the NOD activity, but also plays a very important role in regulating the interaction of HbN with reductase. HbN lacking the pre-A deleted region was having compromised reduction efficiency in the presence of a reductase. To further investigate the role of the pre-A region we have deleted the pre-A motif from the HbN-ferredoxin chimera, which otherwise showed excellent activity. Deletion of the pre-A region caused diminished transfer of electrons, suggesting its important role. Pre-A motif is highly polar in nature, so to investigate the role of these charged amino acids in Hbn-reductase interaction, they were mutated to neutral amino acid alanine, by site directed mutagenesis. Our results demonstrated that when all the positively charged amino acids were mutated to alanine, the reductase activity diminished, comparable to that of the pre-A deleted HbN. To further pinpoint the importance of each positively charged amino acid, we have created individual mutants, where each of the positive charged amino acid were mutated to alanine. Positively charged residues Arg8, Lys9 and Arg10 were proved to be important for the optimum electron transfer activity whereas, Arg6 showed no effect on this process. Asp17 amino acid, which is hypothesised to interact with Arg6 amino acid, by the MD simulation data (Lama *et al.*, 2009), when mutated to alanine, showed no effect on electron transfer.

To get an insight into the mode of electron movement from redox domain to the heme we attempted to identify the possible interface region of the HbN and reductase complex through docking analysis. In the absence of crystal structure of HbN interacting with reductase protein, we have docked the crystal structure of *E. coli* ferridoxin reductase (pdb:1FDR) onto the crystal structure of HbN (pdb:1IDR), using online GRAMM-X docking server. Out of the many probable solutions, the structure highly favourable for electron transfer was chosen. The docked structure resembles the crystal structure of flavohemoglobin from *E. coli* (pdb:1GVH) and *A. eutropha* (pdb:1CQX), in terms of the alignment of porphyrin ring and FAD moiety and the distance between them (~6.5Å). In FHP, Tyr190 is in van der Waal contact to Lys84, GLu394 and flavin

ring, similarly in docked structure, Phe36 is seen to form van der Waal contact with Thr49 and flavin ring. The accuracy of the docked structure was verified by mutating the amino acids, Thr (49) and Asn (50), present in the CD loop (interface region), to Trp and Ile, respectively. This mutant showed reduced activity, because the bulky indole ring of Trp and apolar side chain of the Ile, might have sterically hindered the electron transfer from FAD molecule to porphyrin ring. The compromised activity, establishes the correct alignment of the globin and the reductase protein. We have also checked the NOD activity of the TN-WI mutant to explore the effect of mutations on it, but the mutant behaved similar to that of the wild type, signifying that CD loop is not essential for the NOD activity and the movement of helices required for opening and closing of the tunnels were intact, giving uninterrupted NO scavenging.

Although the NO scavenging property of HbN was discovered a decade back, no experimental work has been carried out regarding its genetic regulation. It has been established that the expression of HbN gets upregulated during nitrosative stress or the stationary phase of the *M. tuberculosis*. However, till now no transcription factors have been reported to be participating in its transcription. Therefore, to decipher the genetic regulation of *glbN* gene attempts have been made. We have identified, for the first time, that a FNR type, iron sulphur cluster containing protein, known as WhiB1, binds to the promoter element of *glbN* gene (*PglbN*), in a NO dependent manner. Holo-WhiB1 binds to the promoter *PglbN*, whereas, NO treated WhiB1 protein showed no binding to the promoter. We have find out the binding site of WhiB1 by DnaseI protection assay, which revealed it to be coinciding with the putative sigE and FNR binding sites. *In silico* analysis of the protein sequence of WhiB1 have suggested a novel phosphorylation site. Therefore, for the first time, we have discovered and validated the autophosphorylation property of WhiB1 protein, by experimental results. However, phosphorylation of WhiB1 did not influence its binding to the *PglbN*, as it showed similar binding pattern to that of the unphosphorylated protein, suggesting it might be playing some other physiological function. To summarize the overall mechanism of *glbN* regulation that is evident from this study, combined with the previous findings is given in the figure (Figure 5.12). In the normal condition [4Fe-4S] containing WhiB1 is bound to the *glbN* promoter in a dimeric form. This binding might blocks the sig E binding which eventually blocks the RNAP binding to the promoter. This results into repression of *glbN* gene. During the NO challenge, the NO binds to the Whib1 to form octa-

nitrosylated species which does not bind to the *glbN* promoter and transcription of *glbN* occurs. This WhiB1-NO bound form which gets detached from the *PglbN* promoter can bind to the promoter of the *PwhiB1* causing no further synthesis of WhiB1, by repressing its transcription. This reduction in the level of WhiB1 will further upregulate the production of HbN. Thus, the repression of WhiB1 protein synthesis will upregulate the HbN's production in a positive manner.



Bibliography

-
- ✿ **Aono, S., Matsuo, T., Shimon, T., Ohkubo, K., Takasaki, H., and Nakajima, H. (1997).** Single transduction in the transcriptional activator *CooA* containing a heme-based CO sensor: isolation of a dominant positive mutant which is active as the transcriptional activator even in the absence of CO. *Biochem Biophys Res Commun* 240, 783-786.
- ✿ **Ascenzi, P., Bolognesi, M., Milani, M., Guertin, M., and Visca, P. (2007).** Mycobacterial truncated hemoglobins: from genes to functions. *Gene* 398, 42-51.
- ✿ **Bang, I.S., Liu, L., Vazquez-Torres, A., Crouch, M.L., Stamler, J.S., and Fang, F.C. (2006).** Maintenance of nitric oxide and redox homeostasis by the salmonella flavohemoglobin *hmp*. *J Biol Chem* 281, 28039-28047.
- ✿ **Bidon-Chanal, A., Marti, M.A., Crespo, A., Milani, M., Orozco, M., Bolognesi, M., Luque, F.J., and Estrin, D.A. (2006).** Ligand-induced dynamical regulation of NO conversion in *Mycobacterium tuberculosis* truncated hemoglobin-N. *Proteins* 64, 457-464.
- ✿ **Bolli, A., Ciaccio, C., Coletta, M., Nardini, M., Bolognesi, M., Pesce, A., Guertin, M., Visca, P., and Ascenzi, P. (2008).** Ferrous *Campylobacter jejuni* truncated hemoglobin P displays an extremely high reactivity for cyanide - a comparative study. *FEBS J* 275, 633-645.
- ✿ **Bollinger, C.J., Bailey, J.E., and Kallio, P.T. (2001).** Novel hemoglobins to enhance microaerobic growth and substrate utilization in *Escherichia coli*. *Biotechnol Prog* 17, 798-808.
- ✿ **Bolognesi, M., Cannillo, E., Ascenzi, P., Giacometti, G.M., Merli, A., and Brunori, M. (1982).** Reactivity of ferric *Aplysia* and sperm whale myoglobins towards imidazole: X-ray and binding study. *Journal of Molecular Biology* 158, 305-315.
- ✿ **Bonamore, A., Attili, A., Arengi, F., Catacchio, B., Chiancone, E., Morea, V., and Boffi, A. (2007).** A novel chimera: the "truncated hemoglobin-antibiotic monooxygenase" from *Streptomyces avermitilis*. *Gene* 398, 52-61.
- ✿ **Boudko, D., Yu, H.S., Ruiz, M., Hou, S., and Alam, M. (2003).** A time-lapse capillary assay to study aerotaxis in the archaeon *Halobacterium salinarum*. *J Microbiol Methods* 53, 123-126.
-

-
- ✿ **Burmester, T., Ebner, B., Weich, B., and Hankeln, T. (2002).** Cytoglobin: a novel globin type ubiquitously expressed in vertebrate tissues. *Mol Biol Evol* 19, 416-421.
- ✿ **Burmester, T., Weich, B., Reinhardt, S., and Hankeln, T. (2000).** A vertebrate globin expressed in the brain. *Nature* 407, 520-523.
- ✿ **Chan, M.K. (2001).** Recent advances in heme-protein sensors. *Curr Opin Chem Biol* 5, 216-222.
- ✿ **Chawla, M., Parikh, P., Saxena, A., Munshi, M., Mehta, M., Mai, D., Srivastava, A.K., Narasimhulu, K., Redding, K.E., and Vashi, N. (2012).** Mycobacterium tuberculosis WhiB4 regulates oxidative stress response to modulate survival and dissemination in vivo. *Molecular Microbiology*.
- ✿ **Cole, S.T., Brosch, R., Parkhill, J., Garnier, T., Churcher, C., Harris, D., Gordon, S.V., Eiglmeier, K., Gas, S., Barry, C.E., 3rd, et al. (1998).** Deciphering the biology of Mycobacterium tuberculosis from the complete genome sequence. *Nature* 393, 537-544.
- ✿ **Couture, M., Chamberland, H., St-Pierre, B., Lafontaine, J., and Guertin, M. (1994).** Nuclear genes encoding chloroplast hemoglobins in the unicellular green alga Chlamydomonas eugametos. *Mol Gen Genet* 243, 185-197.
- ✿ **Couture, M., Yeh, S.R., Wittenberg, B.A., Wittenberg, J.B., Ouellet, Y., Rousseau, D.L., and Guertin, M. (1999).** A cooperative oxygen-binding hemoglobin from Mycobacterium tuberculosis. *Proc Natl Acad Sci U S A* 96, 11223-11228.
- ✿ **Crack, J.C., Smith, L.J., Stapleton, M.R., Peck, J., Watmough, N.J., Buttner, M.J., Buxton, R.S., Green, J., Oganessian, V.S., and Thomson, A.J. (2011).** Mechanistic Insight into the Nitrosylation of the [4Fe- 4S] Cluster of WhiB-like Proteins. *Journal of the American Chemical Society* 133, 1112.
- ✿ **Crespo, A., Marti, M.A., Kalko, S.G., Morreale, A., Orozco, M., Gelpi, J.L., Luque, F.J., and Estrin, D.A. (2005).** Theoretical study of the truncated hemoglobin HbN: exploring the molecular basis of the NO detoxification mechanism. *J Am Chem Soc* 127, 4433-4444.
- ✿ **Das, T.K., Couture, M., Lee, H.C., Peisach, J., Rousseau, D.L., Wittenberg, B.**
-

- A., Wittenberg, J.B., and Guertin, M. (1999).** Identification of the ligands to the ferric heme of *Chlamydomonas* chloroplast hemoglobin: evidence for ligation of tyrosine-63 (B10) to the heme. *Biochemistry* 38, 15360-15368.
- ✿ **Davis, N.K., and Chater, K.F. (1992).** The *Streptomyces coelicolor* *whiB* gene encodes a small transcription factor-like protein dispensable for growth but essential for sporulation. *Molec Gen Genet* 232, 351-358.
- ✿ **de Sanctis, D., Dewilde, S., Pesce, A., Moens, L., Ascenzi, P., Hankeln, T., Burmester, T., and Bolognesi, M. (2004a).** Crystal structure of cytoglobin: the fourth globin type discovered in man displays heme hexa-coordination. *J Mol Biol* 336, 917-927.
- ✿ **de Sanctis, D., Dewilde, S., Pesce, A., Moens, L., Ascenzi, P., Hankeln, T., Burmester, T., and Bolognesi, M. (2004b).** Mapping protein matrix cavities in human cytoglobin through Xe atom binding. *Biochem Biophys Res Commun* 316, 1217-1221.
- ✿ **Doyle, M.P., and Hoekstra, J.W. (1981).** Oxidation of nitrogen oxides by bound dioxygen in hemoproteins. *J Inorg Biochem* 14, 351-358.
- ✿ **Edmond, J.M., Damm, K.L.V., McDuff, R.E., and Measures, C.I. (1982).** Chemistry of hot springs on the East Pacific Rise and their effluent dispersal. *Nature* 297, 187-191.
- ✿ **Eich, R.F., Li, T., Lemon, D.D., Doherty, D.H., Curry, S.R., Aitken, J.F., Mathews, A.J., Johnson, K.A., Smith, R.D., Phillips, G.N., Jr., et al. (1996).** Mechanism of NO-induced oxidation of myoglobin and hemoglobin. *Biochemistry* 35, 6976-6983.
- ✿ **Elvers, K.T., Wu, G., Gilberthorpe, N.J., Poole, R.K., and Park, S.F. (2004).** Role of an inducible single-domain hemoglobin in mediating resistance to nitric oxide and nitrosative stress in *Campylobacter jejuni* and *Campylobacter coli*. *J Bacteriol* 186, 5332-5341.
- ✿ **Ermler, U., Siddiqui, R.A., Cramm, R., and Friedrich, B. (1995).** Crystal structure of the flavohemoglobin from *Alcaligenes eutrophus* at 1.75 Å resolution. *EMBO J* 14, 6067-6077.
- ✿ **Fabozzi, G., Ascenzi, P., Renzi, S.D., and Visca, P. (2006a).** Truncated hemoglo-

- bin GlbO from *Mycobacterium leprae* alleviates nitric oxide toxicity. *Microb Pathog* 40, 211-220.
- ✿ **Fabozzi, G., Ascenzi, P., Renzi, S.D., and Visca, P. (2006b).** Truncated hemoglobin GlbO from *Mycobacterium leprae* alleviates nitric oxide toxicity. *Microbial Pathogenesis* 40, 211-220.
- ✿ **Favey, S., Labesse, G., Vouille, V., and Boccara, M. (1995).** Flavohaemoglobin HmpX: a new pathogenicity determinant in *Erwinia chrysanthemi* strain 3937. *Microbiology* 141 (Pt 4), 863-871.
- ✿ **Flogel, U., Merx, M.W., Godecke, A., Decking, U.K., and Schrader, J. (2001).** Myoglobin: A scavenger of bioactive NO. *Proc Natl Acad Sci U S A* 98, 735-740.
- ✿ **Freitas, T.A., Hou, S., Dioum, E.M., Saito, J.A., Newhouse, J., Gonzalez, G., Gilles-Gonzalez, M.A., and Alam, M. (2004).** Ancestral hemoglobins in Archaea. *Proc Natl Acad Sci U S A* 101, 6675-6680.
- ✿ **Freitas, T.A.K., Saito, J.A., Hou, S., and Alam, M. (2005).** Globin-coupled sensors, protoglobins, and the last universal common ancestor. *Journal of Inorganic Biochemistry* 99, 23-33.
- ✿ **Frey, A.D., and Kallio, P.T. (2005).** Nitric oxide detoxification--a new era for bacterial globins in biotechnology? *Trends Biotechnol* 23, 69-73.
- ✿ **Fu, L.M., and Shinnick, T.M. (2007).** Genome-wide exploration of the drug action of capreomycin on *Mycobacterium tuberculosis* using Affymetrix oligonucleotide GeneChips. *The Journal of infection* 54, 277.
- ✿ **Gardner, A.M., Martin, L.A., Gardner, P.R., Dou, Y., and Olson, J.S. (2000).** Steady-state and transient kinetics of *Escherichia coli* nitric-oxide dioxygenase (flavo-hemoglobin). The B10 tyrosine hydroxyl is essential for dioxygen binding and catalysis. *J Biol Chem* 275, 12581-12589.
- ✿ **Gardner, P.R. (2005).** Nitric oxide dioxygenase function and mechanism of flavo-hemoglobin, hemoglobin, myoglobin and their associated reductases. *J Inorg Biochem* 99, 247-266.
- ✿ **Gardner, P.R., Costantino, G., and Salzman, A.L. (1998a).** Constitutive and adaptive detoxification of nitric oxide in *Escherichia coli*. Role of nitric-oxide dioxygenase in the protection of aconitase. *J Biol Chem* 273, 26528-26533.

-
- ✿ **Gardner, P.R., Costantino, G., Szabo, C., and Salzman, A.L. (1997).** Nitric oxide sensitivity of the aconitases. *J Biol Chem* 272, 25071-25076.
- ✿ **Gardner, P.R., Gardner, A.M., Martin, L.A., and Salzman, A.L. (1998b).** Nitric oxide dioxygenase: an enzymic function for flavohemoglobin. *Proc Natl Acad Sci U S A* 95, 10378-10383.
- ✿ **Geiman, D.E., Raghunand, T.R., Agarwal, N., and Bishai, W.R. (2006).** Differential gene expression in response to exposure to antimycobacterial agents and other stress conditions among seven *Mycobacterium tuberculosis* whiB-like genes. *Antimicrobial agents and chemotherapy* 50, 2836-2841.
- ✿ **Geuens, E., Brouns, I., Flamez, D., Dewilde, S., Timmermans, J.P., and Moens, L. (2003).** A globin in the nucleus! *J Biol Chem* 278, 30417-30420.
- ✿ **Gilles-Gonzalez, M.A., and Gonzalez, G. (2005).** Heme-based sensors: defining characteristics, recent developments, and regulatory hypotheses. *J Inorg Biochem* 99, 1-22.
- ✿ **Giordano, D., Parrilli, E., Dettai, A., Russo, R., Barbiero, G., Marino, G., Lecointre, G., di Prisco, G., Tutino, L., and Verde, C. (2007).** The truncated hemoglobins in the Antarctic psychrophilic bacterium *Pseudoalteromonas haloplanktis* TAC125. *Gene* 398, 69-77.
- ✿ **Gomez, J.E., and Bishai, W.R. (2000).** whmD is an essential mycobacterial gene required for proper septation and cell division. *Proceedings of the National Academy of Sciences* 97, 8554-8559.
- ✿ **Gong, W., Hao, B., Mansy, S.S., Gonzalez, G., Gilles-Gonzalez, M.A., and Chan, M.K. (1998).** Structure of a biological oxygen sensor: a new mechanism for heme-driven signal transduction. *Proc Natl Acad Sci U S A* 95, 15177-15182.
- ✿ **Gray, B. (1983).** Hemoglobin: Structure, function and evolution by Richard E Dickerson & Irving Geis. pp 176. Benjamin Cummings, Menlo Park, California. 1983. \$29.95 ISBN 0-8053-2411-9. *Biochemical Education* 11, 123-123.
- ✿ **Gupta, S., Pawaria, S., Lu, C., Hade, M.D., Singh, C., Yeh, S.R., and Dikshit, K.L. (2012).** An unconventional hexacoordinated flavohemoglobin from *Mycobacterium tuberculosis*. *J Biol Chem* 287, 16435-16446.
- ✿ **Hankeln, T., Ebner, B., Fuchs, C., Gerlach, F., Haberkamp, M., Laufs, T.L.,**
-

- Roesner, A., Schmidt, M., Weich, B., Wystub, S., et al. (2005).** Neuroglobin and cytoglobin in search of their role in the vertebrate globin family. *J Inorg Biochem* 99, 110-119.
- ✿ **Hardison, R.C. (1996).** A brief history of hemoglobins: plant, animal, protist, and bacteria. *Proc Natl Acad Sci U S A* 93, 5675-5679.
- ✿ **Hardison, R.C. (2001).** New views of evolution and regulation of vertebrate beta-like globin gene clusters from an orphaned gene in marsupials. *Proc Natl Acad Sci U S A* 98, 1327-1329.
- ✿ **Hausladen, A., Gow, A., and Stamler, J.S. (2001).** Flavohemoglobin denitrosylase catalyzes the reaction of a nitroxyl equivalent with molecular oxygen. *Proc Natl Acad Sci U S A* 98, 10108-10112.
- ✿ **Hausladen, A., Gow, A.J., and Stamler, J.S. (1998).** Nitrosative stress: metabolic pathway involving the flavohemoglobin. *Proc Natl Acad Sci U S A* 95, 14100-14105.
- ✿ **Hayashi, A., Suzuki, T., and Shin, M. (1973).** An enzymic reduction system for metmyoglobin and methemoglobin, and its application to functional studies of oxygen carriers. *Biochim Biophys Acta* 310, 309-316.
- ✿ **Herold, S., Fago, A., Weber, R.E., Dewilde, S., and Moens, L. (2004).** Reactivity studies of the Fe(III) and Fe(II)NO forms of human neuroglobin reveal a potential role against oxidative stress. *J Biol Chem* 279, 22841-22847.
- ✿ **Horng, Y.T., Chang, K.C., Chien, C.C., Wei, Y.H., Sun, Y.M., and Soo, P.C. (2010).** Enhanced polyhydroxybutyrate (PHB) production via the coexpressed phaCAB and vgb genes controlled by arabinose PBAD promoter in *Escherichia coli*. *Letters in Applied Microbiology* 50, 158-167.
- ✿ **Hou, S., Larsen, R.W., Boudko, D., Riley, C.W., Karatan, E., Zimmer, M., Ordal, G.W., and Alam, M. (2000).** Myoglobin-like aerotaxis transducers in *Archaea* and *Bacteria*. *Nature* 403, 540-544.
- ✿ **Hultquist, D.E., and Passon, P.G. (1971).** Catalysis of methaemoglobin reduction by erythrocyte cytochrome B5 and cytochrome B5 reductase. *Nat New Biol* 229, 252-254.
- ✿ **Ilari, A., Bonamore, A., Farina, A., Johnson, K.A., and Boffi, A. (2002).** The X-

- ray structure of ferric *Escherichia coli* flavohemoglobin reveals an unexpected geometry of the distal heme pocket. *J Biol Chem* 277, 23725-23732.
- ✿ **Ilari, A., Kjølgaard, P., von Wachenfeldt, C., Catacchio, B., Chiancone, E., and Boffi, A. (2007).** Crystal structure and ligand binding properties of the truncated hemoglobin from *Geobacillus stearothermophilus*. *Arch Biochem Biophys* 457, 85-94.
- ✿ **Iwaasa, H., Takagi, T., and Shikama, K. (1989).** Protozoan myoglobin from *Paramecium caudatum*. Its unusual amino acid sequence. *J Mol Biol* 208, 355-358.
- ✿ **Iyer, L.M., Anantharaman, V., and Aravind, L. (2003).** Ancient conserved domains shared by animal soluble guanylyl cyclases and bacterial signaling proteins. *BMC Genomics* 4, 5.
- ✿ **Jervis, A.J., Crack, J.C., White, G., Artymiuk, P.J., Cheesman, M.R., Thomson, A.J., Le Brun, N.E., and Green, J. (2009).** The O₂ sensitivity of the transcription factor FNR is controlled by Ser24 modulating the kinetics of [4Fe-4S] to [2Fe-2S] conversion. *Proceedings of the National Academy of Sciences* 106, 4659-4664.
- ✿ **Karow, D.S., Pan, D., Tran, R., Pellicena, P., Presley, A., Mathies, R.A., and Marletta, M.A. (2004).** Spectroscopic Characterization of the Soluble Guanylate Cyclase-like Heme Domains from *Vibrio cholerae* and *Thermoanaerobacter tengcongensis*†. *Biochemistry* 43, 10203-10211.
- ✿ **Karplus, P.A., Daniels, M.J., and Herriott, J.R. (1991).** Atomic structure of ferredoxin-NADP⁺ reductase: prototype for a structurally novel flavoenzyme family. *Science* 251, 60-66.
- ✿ **Kaur, R., Pathania, R., Sharma, V., Mande, S.C., and Dikshit, K.L. (2002).** Chimeric *Vitreoscilla* hemoglobin (VHb) carrying a flavoreductase domain relieves nitrosative stress in *Escherichia coli*: new insight into the functional role of VHb. *Appl Environ Microbiol* 68, 152-160.
- ✿ **LaCelle, M., Kumano, M., Kurita, K., Yamane, K., Zuber, P., and Nakano, M.M. (1996).** Oxygen-controlled regulation of the flavohemoglobin gene in *Bacillus subtilis*. *J Bacteriol* 178, 3803-3808.
- ✿ **Lama, A., Pawaria, S., Bidon-Chanal, A., Anand, A., Gelpi, J.L., Arya, S.,**

-
- Marti, M., Estrin, D.A., Luque, F.J., and Dikshit, K.L. (2009).** Role of Pre-A motif in nitric oxide scavenging by truncated hemoglobin, HbN, of *Mycobacterium tuberculosis*. *J Biol Chem* 284, 14457-14468.
- ✿ **Lama, A., Pawaria, S., and Dikshit, K.L. (2006).** Oxygen binding and NO scavenging properties of truncated hemoglobin, HbN, of *Mycobacterium smegmatis*. *FEBS Lett* 580, 4031-4041.
- ✿ **Lazazzera, B.A., Beinert, H., Khoroshilova, N., Kennedy, M.C., and Kiley, P.J. (1996).** DNA binding and dimerization of the Fe-S-containing FNR protein from *Escherichia coli* are regulated by oxygen. *J Biol Chem* 271, 2762-2768.
- ✿ **Liang, Z.X., Jiang, M., Ning, Q., and Hoffman, B.M. (2002).** Dynamic docking and electron transfer between myoglobin and cytochrome b(5). *J Biol Inorg Chem* 7, 580-588.
- ✿ **Liu, C., He, Y., and Chang, Z. (2004).** Truncated hemoglobin o of *Mycobacterium tuberculosis*: the oligomeric state change and the interaction with membrane components. *Biochem Biophys Res Commun* 316, 1163-1172.
- ✿ **MacMicking, J.D., North, R.J., LaCourse, R., Mudgett, J.S., Shah, S.K., and Nathan, C.F. (1997).** Identification of nitric oxide synthase as a protective locus against tuberculosis. *Proc Natl Acad Sci U S A* 94, 5243-5248.
- ✿ **Milani, M., Pesce, A., Nardini, M., Ouellet, H., Ouellet, Y., Dewilde, S., Bocedi, A., Ascenzi, P., Guertin, M., Moens, L., et al. (2005).** Structural bases for heme binding and diatomic ligand recognition in truncated hemoglobins. *J Inorg Biochem* 99, 97-109.
- ✿ **Milani, M., Pesce, A., Ouellet, Y., Ascenzi, P., Guertin, M., and Bolognesi, M. (2001).** *Mycobacterium tuberculosis* hemoglobin N displays a protein tunnel suited for O₂ diffusion to the heme. *EMBO J* 20, 3902-3909.
- ✿ **Milani, M., Pesce, A., Ouellet, Y., Dewilde, S., Friedman, J., Ascenzi, P., Guertin, M., and Bolognesi, M. (2004).** Heme-ligand tunneling in group I truncated hemoglobins. *J Biol Chem* 279, 21520-21525.
- ✿ **Milani, M., Savard, P.Y., Ouellet, H., Ascenzi, P., Guertin, M., and Bolognesi, M. (2003).** A TyrCD1/TrpG8 hydrogen bond network and a TyrB10TyrCD1 covalent link shape the heme distal site of *Mycobacterium tuberculosis* hemoglobin
-

O. Proc Natl Acad Sci U S A 100, 5766-5771.

- ✿ **Minning, D.M., Gow, A.J., Bonaventura, J., Braun, R., Dewhirst, M., Goldberg, D.E., and Stamler, J.S. (1999).** Ascaris haemoglobin is a nitric oxide-activated 'deoxygenase'. *Nature* 401, 497-502.
- ✿ **Mukai, M., Savard, P.Y., Ouellet, H., Guertin, M., and Yeh, S.R. (2002).** Unique ligand-protein interactions in a new truncated hemoglobin from *Mycobacterium tuberculosis*. *Biochemistry* 41, 3897-3905.
- ✿ **Olson, J.S., Mathews, A.J., Rohlfs, R.J., Springer, B.A., Egeberg, K.D., Sligar, S.G., Tame, J., Renaud, J.P., and Nagai, K. (1988).** The role of the distal histidine in myoglobin and haemoglobin. *Nature* 336, 265-266.
- ✿ **Orii, Y., and Webster, D.A. (1986).** Photodissociation of oxygenated cytochrome o(s) (*Vitreoscilla*) and kinetic studies of reassociation. *J Biol Chem* 261, 3544-3547.
- ✿ **Ouellet, H., Juszczak, L., Dantsker, D., Samuni, U., Ouellet, Y.H., Savard, P.Y., Wittenberg, J.B., Wittenberg, B.A., Friedman, J.M., and Guertin, M. (2003).** Reactions of *Mycobacterium tuberculosis* truncated hemoglobin O with ligands reveal a novel ligand-inclusive hydrogen bond network. *Biochemistry* 42, 5764-5774.
- ✿ **Ouellet, H., Ouellet, Y., Richard, C., Labarre, M., Wittenberg, B., Wittenberg, J., and Guertin, M. (2002).** Truncated hemoglobin HbN protects *Mycobacterium bovis* from nitric oxide. *Proc Natl Acad Sci U S A* 99, 5902-5907.
- ✿ **Park, K.W., Kim, K.J., Howard, A.J., Stark, B.C., and Webster, D.A. (2002).** *Vitreoscilla* hemoglobin binds to subunit I of cytochrome bo ubiquinol oxidases. *J Biol Chem* 277, 33334-33337.
- ✿ **Pathania, R., Navani, N.K., Gardner, A.M., Gardner, P.R., and Dikshit, K.L. (2002a).** Nitric oxide scavenging and detoxification by the *Mycobacterium tuberculosis* haemoglobin, HbN in *Escherichia coli*. *Mol Microbiol* 45, 1303-1314.
- ✿ **Pathania, R., Navani, N.K., Rajamohan, G., and Dikshit, K.L. (2002b).** *Mycobacterium tuberculosis* hemoglobin HbO associates with membranes and stimulates cellular respiration of recombinant *Escherichia coli*. *J Biol Chem* 277, 15293-15302.
- ✿ **Pawaria, S., Lama, A., Raje, M., and Dikshit, K.L. (2008).** Responses of *Mycob-*

- acterium tuberculosis* hemoglobin promoters to in vitro and in vivo growth conditions. *Appl Environ Microbiol* 74, 3512-3522.
- ✿ **Pawaria, S., Rajamohan, G., Gambhir, V., Lama, A., Varshney, G.C., and Dikshit, K.L. (2007).** Intracellular growth and survival of *Salmonella enterica* serovar Typhimurium carrying truncated hemoglobins of *Mycobacterium tuberculosis*. *Microb Pathog* 42, 119-128.
- ✿ **Pellicena, P., Karow, D.S., Boon, E.M., Marletta, M.A., and Kuriyan, J. (2004).** Crystal structure of an oxygen-binding heme domain related to soluble guanylate cyclases. *Proceedings of the National Academy of Sciences of the United States of America* 101, 12854-12859.
- ✿ **Perutz, M.F. (1978).** Hemoglobin structure and respiratory transport. *Sci Am* 239, 92-125.
- ✿ **Perutz, M.F. (1989a).** Mechanisms of cooperativity and allosteric regulation in proteins. *Q Rev Biophys* 22, 139-237.
- ✿ **Perutz, M.F. (1989b).** Myoglobin and haemoglobin: role of distal residues in reactions with haem ligands. *Trends Biochem Sci* 14, 42-44.
- ✿ **Pesce, A., Bolognesi, M., Bocedi, A., Ascenzi, P., Dewilde, S., Moens, L., Hankeln, T., and Burmester, T. (2002).** Neuroglobin and cytoglobin. Fresh blood for the vertebrate globin family. *EMBO Rep* 3, 1146-1151.
- ✿ **Pesce, A., Couture, M., Dewilde, S., Guertin, M., Yamauchi, K., Ascenzi, P., Moens, L., and Bolognesi, M. (2000).** A novel two-over-two alpha-helical sandwich fold is characteristic of the truncated hemoglobin family. *EMBO J* 19, 2424-2434.
- ✿ **Pesce, A., Dewilde, S., Nardini, M., Moens, L., Ascenzi, P., Hankeln, T., Burmester, T., and Bolognesi, M. (2003).** Human brain neuroglobin structure reveals a distinct mode of controlling oxygen affinity. *Structure* 11, 1087-1095.
- ✿ **Potts, M., Angeloni, S.V., Ebel, R.E., and Bassam, D. (1992).** Myoglobin in a cyanobacterium. *Science* 256, 1690-1691.
- ✿ **Priscila, G., Fernández, F.J., Absalón, A.E., Suarez, M.D.R., Sainoz, M., Barrios-González, J., and Mejía, A. (2008).** Expression of the Bacterial Hemoglobin Gene from *Vitreoscilla stercoraria* Increases Rifamycin B Production

- in *Amycolatopsis mediterranei*. *Journal of Bioscience and Bioengineering* 106, 493-497.
- ✿ **Ramandeep, Hwang, K.W., Raje, M., Kim, K.J., Stark, B.C., Dikshit, K.L., and Webster, D.A. (2001).** Vitreoscilla hemoglobin. Intracellular localization and binding to membranes. *J Biol Chem* 276, 24781-24789.
- ✿ **Reuss, S., Saaler-Reinhardt, S., Weich, B., Wystub, S., Reuss, M.H., Burmester, T., and Hankeln, T. (2002).** Expression analysis of neuroglobin mRNA in rodent tissues. *Neuroscience* 115, 645-656.
- ✿ **Roberts, G.P., Thorsteinsson, M.V., Kerby, R.L., Lanzilotta, W.N., and Poulos, T. (2001).** CooA: a heme-containing regulatory protein that serves as a specific sensor of both carbon monoxide and redox state. *Prog Nucleic Acid Res Mol Biol* 67, 35-63.
- ✿ **Rodrigue, S., Provvedi, R., Jacques, P.É., Gaudreau, L., and Manganeli, R. (2006).** The σ factors of *Mycobacterium tuberculosis*. *FEMS microbiology reviews* 30, 926-941.
- ✿ **Savard, P.Y., Daigle, R., Morin, S., Sebilo, A., Meindre, F., Lague, P., Guertin, M., and Gagne, S.M. (2011).** Structure and dynamics of *Mycobacterium tuberculosis* truncated hemoglobin N: insights from NMR spectroscopy and molecular dynamics simulations. *Biochemistry* 50, 11121-11130.
- ✿ **Scott, N.L., Falzone, C.J., Vuletich, D.A., Zhao, J., Bryant, D.A., and Lecomte, J.T. (2002).** Truncated hemoglobin from the cyanobacterium *Synechococcus* sp. PCC 7002: evidence for hexacoordination and covalent adduct formation in the ferric recombinant protein. *Biochemistry* 41, 6902-6910.
- ✿ **Shimizu, T., Ohtani, K., Hirakawa, H., Ohshima, K., Yamashita, A., Shiba, T., Ogasawara, N., Hattori, M., Kuhara, S., and Hayashi, H. (2002).** Complete genome sequence of *Clostridium perfringens*, an anaerobic flesh-eater. *Proc Natl Acad Sci U S A* 99, 996-1001.
- ✿ **Singel, D.J., and Stamler, J.S. (2005).** Chemical physiology of blood flow regulation by red blood cells: the role of nitric oxide and S-nitrosohemoglobin. *Annu Rev Physiol* 67, 99-145.
- ✿ **Singh, A., Crossman, D.K., Mai, D., Guidry, L., Voskuil, M.I., Renfrow, M.B.,**

- and Steyn, A.J.C. (2009).** *Mycobacterium tuberculosis* WhiB3 Maintains Redox Homeostasis by Regulating Virulence Lipid Anabolism to Modulate Macrophage Response. *PLoS Pathog* 5, e1000545.
- ✿ **Singh, A., Guidry, L., Narasimhulu, K., Mai, D., Trombley, J., Redding, K.E., Giles, G.I., Lancaster, J.R., and Steyn, A.J. (2007).** *Mycobacterium tuberculosis* WhiB3 responds to O₂ and nitric oxide via its [4Fe-4S] cluster and is essential for nutrient starvation survival. *Proceedings of the National Academy of Sciences* 104, 11562-11567.
- ✿ **Smith, L.J., Stapleton, M.R., Fullstone, G.J., Crack, J.C., Thomson, A.J., Le Brun, N.E., Hunt, D.M., Harvey, E., Adinolfi, S., and Buxton, R.S. (2010).** *Mycobacterium tuberculosis* WhiB1 is an essential DNA-binding protein with a nitric oxide sensitive iron-sulphur cluster. *The Biochemical journal* 432, 417.
- ✿ **Soliveri, J., Gomez, J., Bishai, W., and Chater, K. (2000).** Multiple paralogous genes related to the *Streptomyces coelicolor* developmental regulatory gene whiB are present in *Streptomyces* and other actinomycetes. *Microbiology* 146, 333-343.
- ✿ **Sonveaux, P., Lobysheva, II, Feron, O., and McMahon, T.J. (2007).** Transport and peripheral bioactivities of nitrogen oxides carried by red blood cell hemoglobin: role in oxygen delivery. *Physiology (Bethesda)* 22, 97-112.
- ✿ **Stark, B.C., Dikshit, K.L., and Pagilla, K.R. (2011).** Recent advances in understanding the structure, function, and biotechnological usefulness of the hemoglobin from the bacterium *Vitreoscilla*. *Biotechnol Lett* 33, 1705-1714.
- ✿ **Stevanin, T.M., Poole, R.K., Demoncheaux, E.A., and Read, R.C. (2002).** Flavohemoglobin Hmp protects *Salmonella enterica* serovar typhimurium from nitric oxide-related killing by human macrophages. *Infect Immun* 70, 4399-4405.
- ✿ **Tarricone, C., Galizzi, A., Coda, A., Ascenzi, P., and Bolognesi, M. (1997).** Unusual structure of the oxygen-binding site in the dimeric bacterial hemoglobin from *Vitreoscilla* sp. *Structure* 5, 497-507.
- ✿ **Taylor, B.L., and Zhulin, I.B. (1999).** PAS domains: internal sensors of oxygen, redox potential, and light. *Microbiol Mol Biol Rev* 63, 479-506.
- ✿ **Thorsteinsson, M.V., Bevan, D.R., Potts, M., Dou, Y., Eich, R.F., Hargrove, M.S., Gibson, Q.H., and Olson, J.S. (1999).** A cyanobacterial hemoglobin with

- unusual ligand binding kinetics and stability properties. *Biochemistry* 38, 2117-2126.
- ✿ **Trent, J.T., 3rd, and Hargrove, M.S. (2002).** A ubiquitously expressed human hexacoordinate hemoglobin. *J Biol Chem* 277, 19538-19545.
- ✿ **Truchot, J.P. (1976).** Carbon dioxide combining properties of the blood of the shore crab *Carcinus maenas* (L): carbon dioxide solubility coefficient and carbonic acid dissociation constants. *J Exp Biol* 64, 45-57.
- ✿ **Tsubamoto, Y., Matsuoka, A., Yusa, K., and Shikama, K. (1990).** Protozoan myoglobin from *Paramecium caudatum*. Its autoxidation reaction and hemichrome formation. *Eur J Biochem* 193, 55-59.
- ✿ **Vasudevan, S.G., Armarego, W.L., Shaw, D.C., Lilley, P.E., Dixon, N.E., and Poole, R.K. (1991).** Isolation and nucleotide sequence of the hmp gene that encodes a haemoglobin-like protein in *Escherichia coli* K-12. *Mol Gen Genet* 226, 49-58.
- ✿ **Vinogradov, S.N., Hoogewijs, D., Bailly, X., Arredondo-Peter, R., Gough, J., Dewilde, S., Moens, L., and Vanfleteren, J.R. (2006).** A phylogenomic profile of globins. *BMC Evol Biol* 6, 31.
- ✿ **Visca, P., Fabozzi, G., Petrucca, A., Ciaccio, C., Coletta, M., De Sanctis, G., Bolognesi, M., Milani, M., and Ascenzi, P. (2002).** The truncated hemoglobin from *Mycobacterium leprae*. *Biochem Biophys Res Commun* 294, 1064-1070.
- ✿ **Vuletich, D.A., and Lecomte, J.T. (2006).** A phylogenetic and structural analysis of truncated hemoglobins. *J Mol Evol* 62, 196-210.
- ✿ **Wainwright, L.M., Elvers, K.T., Park, S.F., and Poole, R.K. (2005).** A truncated haemoglobin implicated in oxygen metabolism by the microaerophilic food-borne pathogen *Campylobacter jejuni*. *Microbiology* 151, 4079-4091.
- ✿ **Wainwright, L.M., Wang, Y., Park, S.F., Yeh, S.R., and Poole, R.K. (2006).** Purification and spectroscopic characterization of Ctb, a group III truncated hemoglobin implicated in oxygen metabolism in the food-borne pathogen *Campylobacter jejuni*. *Biochemistry* 45, 6003-6011.
- ✿ **Wakabayashi, S., Matsubara, H., and Webster, D.A. (1986).** Primary sequence of a dimeric bacterial haemoglobin from *Vitreoscilla*. *Nature* 322, 481-483.

- ✿ **Weber, R.E., and Pauptit, E. (1972).** Molecular and functional heterogeneity in myoglobin from the polychaete *Arenicola marina* L. *Arch Biochem Biophys* 148, 322-324.
- ✿ **Webster, D.A. (1988).** Structure and function of bacterial hemoglobin and related proteins. *Adv Inorg Biochem* 7, 245-265.
- ✿ **Wittenberg, J.B. (1992).** Functions of Cytoplasmic Hemoglobins and Myohemerythrin. In *Blood and Tissue Oxygen Carriers*, C. Mangum, ed. (Springer Berlin Heidelberg), pp. 59-85.
- ✿ **Wittenberg, J.B., Bolognesi, M., Wittenberg, B.A., and Guertin, M. (2002).** Truncated hemoglobins: a new family of hemoglobins widely distributed in bacteria, unicellular eukaryotes, and plants. *J Biol Chem* 277, 871-874.
- ✿ **Wittenberg, J.B., and Wittenberg, B.A. (1990).** Mechanisms of cytoplasmic hemoglobin and myoglobin function. *Annu Rev Biophys Biophys Chem* 19, 217-241.
- ✿ **Wittenberg, J.B., and Wittenberg, B.A. (2003).** Myoglobin function reassessed. *J Exp Biol* 206, 2011-2020.
- ✿ **Yang, J., Kloek, A.P., Goldberg, D.E., and Mathews, F.S. (1995).** The structure of *Ascaris* hemoglobin domain I at 2.2 Å resolution: molecular features of oxygen avidity. *Proc Natl Acad Sci U S A* 92, 4224-4228.
- ✿ **Yeh, S.R., Couture, M., Ouellet, Y., Guertin, M., and Rousseau, D.L. (2000).** A cooperative oxygen binding hemoglobin from *Mycobacterium tuberculosis*. Stabilization of heme ligands by a distal tyrosine residue. *J Biol Chem* 275, 1679-1684.
- ✿ **Zhulin, I.B., Taylor, B.L., and Dixon, R. (1997).** PAS domain S-boxes in Archaea, Bacteria and sensors for oxygen and redox. *Trends Biochem Sci* 22, 331-333.

List of Publications

- ✿ Anand, A., Duk, B., **Singh, S.**, Akbas, M., Webster, D., Stark, B., and Dikshit, K. (2010). Redox-mediated interactions of VHb (Vitreoscilla haemoglobin) with OxyR: novel regulation of VHb biosynthesis under oxidative stress. *Biochem J* 426, 271-280.

 - ✿ Oliveira, A., **Singh, S.**, Bidon-Chanal, A., Forti, F., Martí, M.A., Boechi, L., Estrin, D.A., Dikshit, K.L., and Luque, F.J. (2012). Role of PheE15 Gate in Ligand Entry and Nitric Oxide Detoxification Function of *Mycobacterium tuberculosis* Truncated Hemoglobin N. *PLoS One* 7, e49291
-

Role of PheE15 Gate in Ligand Entry and Nitric Oxide Detoxification Function of *Mycobacterium tuberculosis* Truncated Hemoglobin N

Ana Oliveira¹*, Sandeep Singh²*, Axel Bidon-Chanal¹, Flavio Forti¹, Marcelo A. Martí³, Leonardo Boechi³, Dario A. Estrin³, Kanak L. Dikshit^{2*}, F. Javier Luque^{1*}

1 Department of Physical Chemistry and Institute of Biomedicine (IBUB), Faculty of Pharmacy, University of Barcelona - Recinte Torribera, Santa Coloma de Gramenet, Spain, **2** CSIR-Institute of Microbial Technology, Chandigarh, India, **3** Departamento de Química Inorgánica, Analítica y Química Física/Instituto de Química Física de los Materiales, Medio Ambiente y Energía (INQUIMAE), Facultad de Ciencias Exactas y Naturales, Universidad de Buenos Aires, Buenos Aires, Argentina

Abstract

The truncated hemoglobin N, HbN, of *Mycobacterium tuberculosis* is endowed with a potent nitric oxide dioxygenase (NOD) activity that allows it to relieve nitrosative stress and enhance *in vivo* survival of its host. Despite its small size, the protein matrix of HbN hosts a two-branched tunnel, consisting of orthogonal short and long channels, that connects the heme active site to the protein surface. A novel dual-path mechanism has been suggested to drive migration of O₂ and NO to the distal heme cavity. While oxygen migrates mainly by the short path, a ligand-induced conformational change regulates opening of the long tunnel branch for NO, via a phenylalanine (PheE15) residue that acts as a gate. Site-directed mutagenesis and molecular simulations have been used to examine the gating role played by PheE15 in modulating the NOD function of HbN. Mutants carrying replacement of PheE15 with alanine, isoleucine, tyrosine and tryptophan have similar O₂/CO association kinetics, but display significant reduction in their NOD function. Molecular simulations substantiated that mutation at the PheE15 gate confers significant changes in the long tunnel, and therefore may affect the migration of ligands. These results support the pivotal role of PheE15 gate in modulating the diffusion of NO via the long tunnel branch in the oxygenated protein, and hence the NOD function of HbN.

Citation: Oliveira A, Singh S, Bidon-Chanal A, Forti F, Martí MA, et al. (2012) Role of PheE15 Gate in Ligand Entry and Nitric Oxide Detoxification Function of *Mycobacterium tuberculosis* Truncated Hemoglobin N. PLoS ONE 7(11): e49291. doi:10.1371/journal.pone.0049291

Editor: Paolo Carloni, German Research School for Simulation Science, Germany

Received: August 5, 2012; **Accepted:** October 8, 2012; **Published:** November 8, 2012

Copyright: © 2012 Oliveira et al. This is an open-access article distributed under the terms of the Creative Commons Attribution License, which permits unrestricted use, distribution, and reproduction in any medium, provided the original author and source are credited.

Funding: The authors thank the Department of Biotechnology for providing research fellowship to SS, the Spanish Ministerio de Innovación y Ciencia (SAF2011-27642), Generalitat de Catalunya (2009SGR298), Xarxa de Recerca en Química Teòrica i Computacional (XRQTC), University of Buenos Aires (X074) and CONICET (PIP 2508) for financial support, and the Barcelona Supercomputation Center for computational resources. The funders had no role in study design, data collection and analysis, decision to publish, or preparation of the manuscript.

Competing Interests: The authors have declared that no competing interests exist.

* E-mail: kanak@imtech.res.in (KLD); flluque@ub.edu (FJL)

† These authors contributed equally to this work.

Introduction

Mycobacterium tuberculosis (*Mtb*) poses a serious threat to the public health worldwide, infecting nearly one third of the global population. The remarkable adaptability of tubercle bacillus to cope with hazardous level of reactive nitrogen/oxygen species within the intracellular environment contributes to its pathogenicity. An enhanced level of nitric oxide (NO) and reactive nitrogen species produced within activated macrophages during infection act as a vital part of host defense, limit the intracellular survival of *Mtb*, and contributes in restricting the bacteria to latency. Nevertheless, *Mtb* has evolved efficient resistance mechanisms by which toxic effects of NO and nitrosative stress can be evaded. One of the unique defense mechanisms by which *Mtb* protects itself from the toxicity of NO relies on the oxygenated form of truncated hemoglobin N (HbN), which catalyzes the rapid oxidation of NO to harmless nitrate [1–3]. Compared to horse heart myoglobin, the nitric oxide dioxygenase (NOD) reaction catalyzed by *Mtb* HbN is ~15-fold faster, suggesting that it may be crucial in relieving nitrosative stress [4].

Despite having single domain architecture, the NO-scavenging ability of *Mtb* HbN is comparable to flavoHbs that are integrated with a reductase domain and known to have a high NOD activity. It is thus important to understand what structural and dynamical features contribute to the efficiency of its enhanced NO-scavenging function, and therefore ensure survival of the bacillus under nitrosative stress. X-ray crystallographic studies revealed that *Mtb* HbN hosts a protein matrix tunnel composed by two orthogonal branches [5,6]. In addition, computational simulations performed by some of the authors suggested that *Mtb* HbN has evolved a novel dual-path mechanism to drive migration of O₂ and NO to the distal heme cavity [7,8]. According to such a mechanism (Fig. 1), access of O₂ to the heme cavity primarily involves migration through the tunnel short branch (~10 Å long, shaped by residues in helices G and H). Binding to the heme then regulates opening of the tunnel long branch (~20 Å long, mainly defined by helices B and E) through a ligand-induced conformational change of PheE15 residue, which would act as a gate. It has been recently shown that the opening of PheE15 in the oxygenated protein is also affected by the N-terminal Pre-A motif [9].

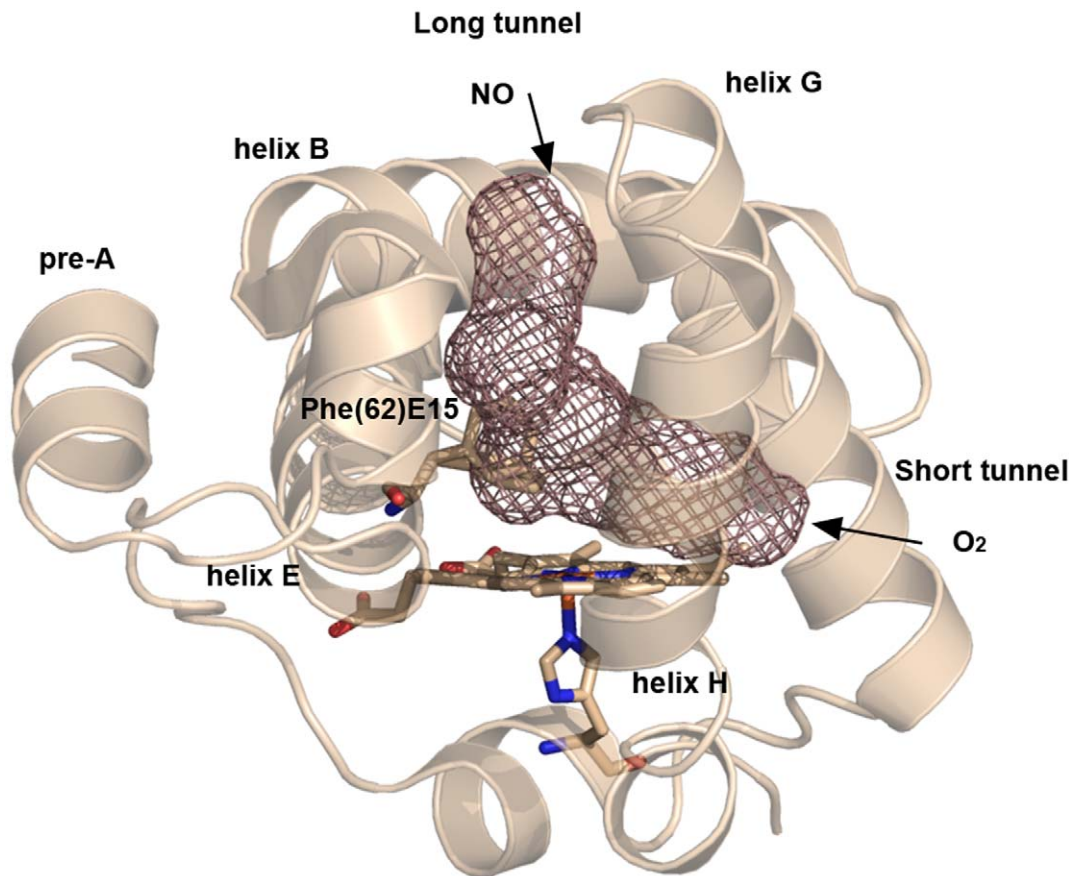


Figure 1. Representation of the long and short branches of the tunnel system. The graphical display is based on the X-ray crystallographic structure of *Mtb* HbN (PDB entry 1IDR), and the access routes of O₂ and NO in the dual-path ligand-modulated mechanism proposed for this protein are indicated. The gating residue PheE15 (residue 62) is shown in the two conformations found in the X-ray structure as sticks.
doi:10.1371/journal.pone.0049291.g001

Since the NOD function of HbN depends on the diffusion of NO to the O₂-bound heme through the long tunnel branch, the PheE15 gate emerges as a fundamental residue in determining the overall efficiency of the NO scavenging. Accordingly, the NOD function of HbN must result from a balanced tuning of the opening/closing events of the gate. Moreover, the functional implication of PheE15 in assisting the NOD activity is supported by the preservation of this residue in mycobacterial HbNs, while it is replaced by other residues in truncated hemoglobins O and P [10,11]. However, to the best of our knowledge, no experimental data have yet been reported to examine the gating role of PheE15 and its influence on the NOD activity conducted by *Mtb* HbN. In this context, this study has been undertaken to probe the role of PheE15 in protein function. To this end, several PheE15 gate mutants have been tested experimentally for their NOD function. In addition, molecular dynamics (MD) simulations have been performed to analyze the structural changes in the topology of long tunnel and the alterations in the protein dynamics, paying attention to the ligand migration properties through the tunnel. Our results confirm the critical role played by E15 in ligand migration along the long channel.

Materials and Methods

Strains, Plasmids and Culture Conditions

Escherichia coli strains, JM109 and BL21DE3 were used for the cloning and expression of recombinant genes. Bacterial cultures

were grown in Luria-Bertani (LB) or Terrific Broth (containing 24 g of Yeast Extract, 12 g of Bacto-Tryptone, 12.54 g of K₂HPO₄, 2.31 g of KH₂PO₄) medium at 37°C at 180 r.p.m. When required, ampicillin and kanamycin (Sigma) were added at a concentration of 100 and 30 µg/ml, respectively. Plasmids, pBluescript (Stratagene) and pET28C (Novagen) were used for cloning and expression of recombinant genes as described earlier [3,12]. The oligonucleotides were custom synthesized by Integrated DNA Technologies Inc. NO (98.5%) was obtained from Sigma Aldrich and saturated NO was prepared as mentioned previously [13]. Heme content of the cell was measured as noted in previous studies [13].

Site-directed Mutagenesis and Construction of PheE15 Gate Mutants of HbN

Recombinant plasmid pPRN [3] was used as a source of HbN gene for the site directed mutagenesis. PheE15 mutants to Ala, Tyr, Ile or Trp were generated using a PCR approach. PCR amplified genes were cloned at NdeI-BamHI site of pET28c and expressed under T7 promoter as described previously [3]. Recombinant HbN and its mutant proteins were purified from the cell lysate of *E. coli* using metal affinity chromatography following standard procedures. Authenticity of mutants was confirmed after nucleotide sequencing.

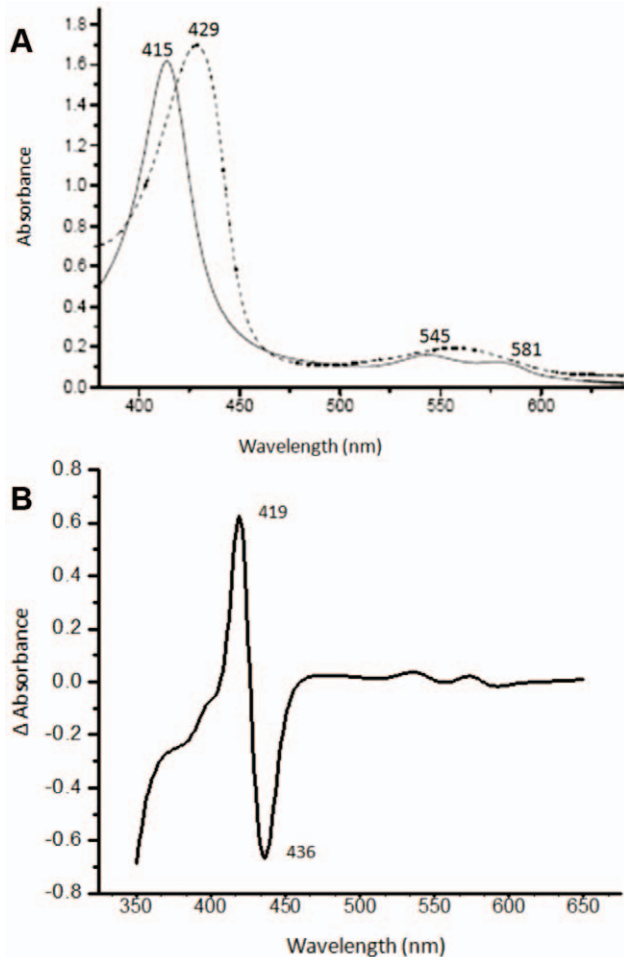


Figure 2. Spectral properties of PheE15Ala mutant of HbN. (A) Optical absorption spectra of oxygenated (solid line) and sodium dithionite reduced species of mutant HbN, recorded in 50 mM Tris.Cl (pH 7.5). (B) CO-difference spectrum of PheE15Ala mutant of HbN. Spectral profile of other PheE15 gate mutants (PheE15Tyr, PheE15Trp and PheE15Trp) appeared similar and matched with the wild type spectrum reported earlier [1].
doi:10.1371/journal.pone.0049291.g002

Measurements of Heme Content and NOD Activity

Total heme content was determined following the procedure described earlier [14]. Heme concentration was calculated from the absorption difference at 556 and 539 nm for the sodium dithionite-reduced and ferricyanide-oxidized sample. NOD activity of cells or purified protein was monitored polarographically as described previously [3,15]. NO consumption buffer assay contained 60 mM K_2HPO_4 , 33 mM KH_2PO_4 , 7.6 mM $(NH_4)_2SO_4$, 1.7 mM sodium citrate, 10 mM glucose and 200 μ g/ml chloramphenicol. NO uptake rate of O_2 -bound HbN and its mutants was measured from the slope of curving traces recorded in the presence of specified concentration of NO following established protocols [3,15].

Measurement of Ligand Binding

O_2 and CO binding was checked from the absorption spectra of O_2 - and CO-bound species [9]. CO difference spectra were recorded between 350 to 600 nm after bubbling CO into the protein sample cuvette and recording the difference spectra against sodium-dithionite reduced protein. Oxygen equilibrium

Table 1. Oxygen binding and CO association kinetics of PheE15 gate mutants of HbN of *M. tuberculosis*.

Protein	$p^{50}(O_2)^a$	$k_{on}(CO)^b$
Wild type	0.019	2.5×10^7
PheE15Ala	0.021	3.0×10^7
PheE15Ile	0.016	2.3×10^7
PheE15Tyr	0.013	2.0×10^7
PheE15Trp	0.023	1.8×10^7

^aIn units of mm Hg.

^b $M^{-1}s^{-1}$. Values derived from three independent measurements, each consisting of multiple shots (>50) and averaged out by the program to give the final value. The standard deviation is in the range 0.3–0.5 ($\times 10^7$).

doi:10.1371/journal.pone.0049291.t001

curves of HbN mutants were checked following the published procedure [16] to check their p^{50} value. The association rate for CO binding to HbN mutants was determined by flash photolysis. A concentrated stock solution of deoxyHbN was diluted anaerobically ($\sim 100 \mu$ M) into a cuvette (1 mm path length) containing CO (1 mM). The fully liganded sample of ferrous HbN was photodissociated by 0.3 μ s excitation pulse from a dye laser. The bimolecular rebinding time courses were collected as described elsewhere [17]. A minimum of five traces were collected and averaged for each experiment.

NO-oxidation by an Oxygenated Adduct of HbN and its Mutants

Wild type and mutant proteins were fully oxygenated by exposing the deoxygenated protein samples to air and checking their absorption spectra, which gave a specific Soret peak at 415 and two peaks, α and β , at 570 and 540 nm, very similar to oxy form of hemoglobin. With a gas tight Hamilton syringe, NO (5 μ M) was sequentially added to the oxygenated protein (40 μ M), and absorption spectra were recorded after each addition to follow the conversion into the oxidized form. The NO-induced oxidation of mutants was compared with the profile determined for the wild type protein.

Molecular dynamics simulations

The dynamical behaviour of the oxygenated form of HbN mutants was examined by means of extended MD simulations and compared to the results reported in previous studies for the wild type protein [7,8]. The X-ray structure of wild type *Mtb* HbN (PDB entry 1HDR, chain A, solved at 1.9 \AA resolution) was used as

Table 2. NO-dioxygenase activity of PheE15 gate mutants of HbN.

Protein	NOD activity ^a	% NOD activity
Wild type	27.8 ± 1.3	100
PheE15Ala	15.9 ± 1.4	51.1
PheE15Ile	12.6 ± 0.6	45.3
PheE15Tyr	9.9 ± 0.6	34.5
PheE15Trp	8.6 ± 0.4	30.2

The NOD activity of HbN mutants were determined at fixed concentration of NO (1.8 micromole).

^aThe activity is expressed as nmole NO/heme/ s^{-1} .

doi:10.1371/journal.pone.0049291.t002

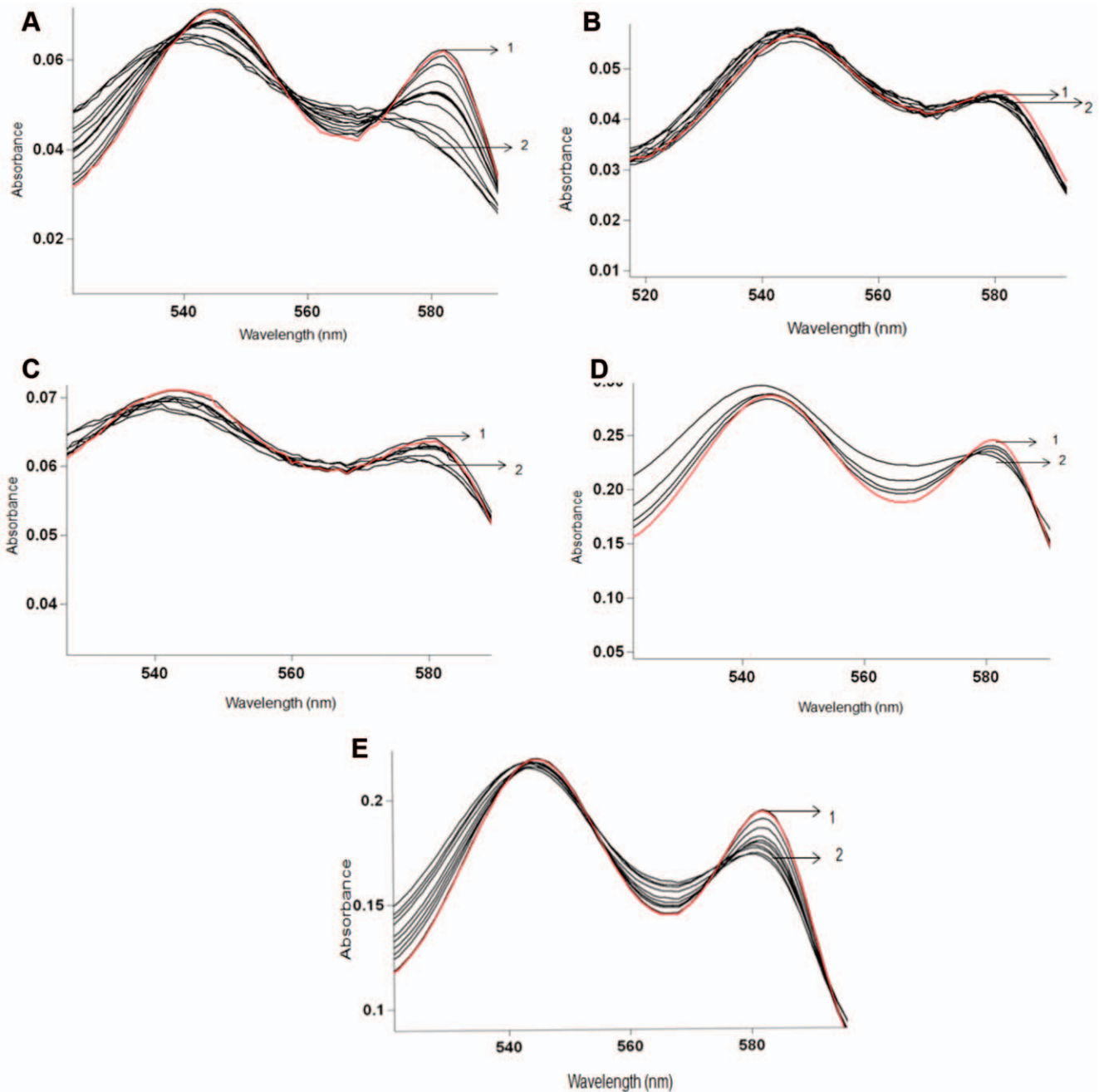


Figure 3. NO oxidation profile of PheE15 gate mutants of HbN. Titration of oxygenated HbN protein (20 μ M) was done by adding 15 μ M NO sequentially and recording spectra after each addition. Wild type HbN displayed fully oxidized spectra after 12 additions (A), whereas mutants PheE15Tyr (B), PheE15Ile (C), PheE15Trp (D) and PheE15Ala (E) displayed very slow oxidation of the protein and could not be fully oxidized even after 20 additions of NO. The first and last additions are labeled as 1 and 2, respectively. doi:10.1371/journal.pone.0049291.g003

starting point for simulations. Mutants were generated by replacing PheE15 by Ala, Ile and Tyr in the X-ray structure of the wild type protein. In all cases simulations were performed using the same protocol adopted in our previous studies [7,8]. Briefly, the enzyme was immersed in a pre-equilibrated octahedral box of TIP3P [18] water molecules. The final systems contained the protein and around 8600 water molecules (*ca.* 28,270 atoms). The system was simulated in the NPT (1 atm.; 298 K) ensemble using SHAKE [19] to keep bonds involving hydrogen atoms at their equilibrium length, periodic boundary conditions, Ewald

sums for treating long range electrostatic interactions [20], and a 1 fs time step for the integration of Newton's equations. All simulations were performed with the parm99SB force field [21] and employing heme parameters developed in previous works [7,8].

MD simulations were performed with the PMEMD module of the AMBER10 program [22]. The geometry of the models was relaxed by energy minimization carried out in three steps where hydrogen atoms, water molecules and finally the whole system were minimized. Equilibration was performed in successive 50 ps

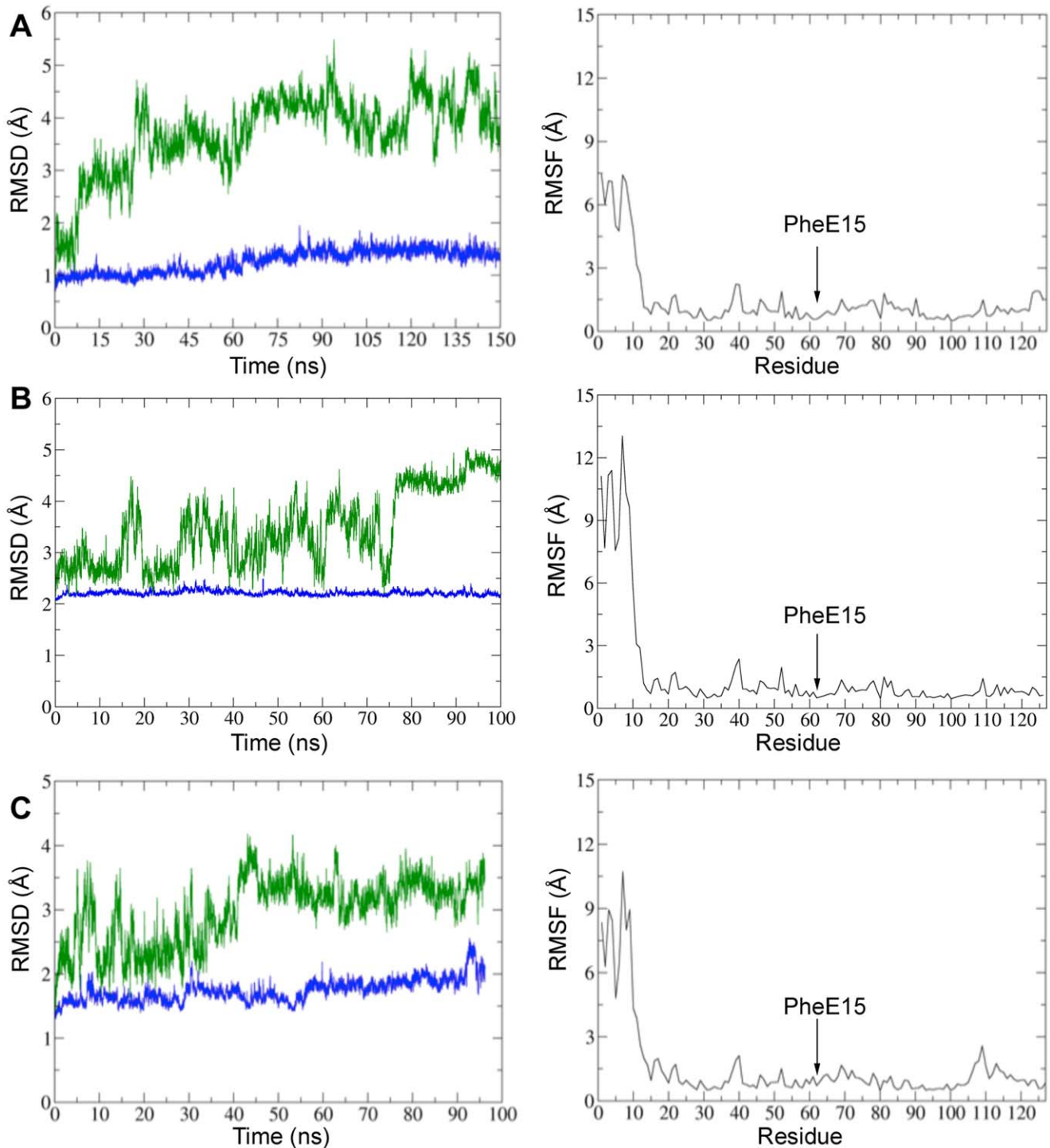


Figure 4. Representation of rmsd and rmsf profiles for PheE15 gate mutants of HbN. (Left) Rmsd (Å) of the protein backbone determined using the X-ray structure (1IDR; subunit A) as reference. The rmsd of the whole protein is shown in green, whereas the rmsd of the residues in the protein core (excluding those in the pre-A segment; residues 1–15) is shown in blue. (Right) Representation of the rmsf (Å) of residues side chains in the protein. The plots correspond to the mutants (A) PheE15Ala, (B) PheE15Ile and (C) PheE15Tyr. The location of the mutated residue Phe(62)E15 is indicated in the plots by an arrow (helix E encompass residues 51–66). doi:10.1371/journal.pone.0049291.g004

runs where the temperature was gradually increased from 100 K to 298 K in four steps at constant volume, followed by an additional step run at constant pressure for 100 ps. Then, a series of 100–150 ns MD simulations (at 298 K and 1 atm) were run.

The analysis of the trajectories was performed using frames collected every 1 ps during the production runs. Furthermore, 75 MD simulations (25 per mutant) were run to explore the pathways for ligand access (free NO in solution) to the heme cavity

Table 3. Global similarity index determined by comparison of the motions of the protein backbone in the oxygenated form of wild type HbN and the PheE15 mutants.

ξ_{AB}	Wild type	PheE15Ala	PheE15Ile	PheE15Tyr
Wild type	0.68	0.65	0.60	0.62
PheE15Ala		0.67	0.63	0.60
PheE15Ile			0.74	0.64
PheE15Tyr				0.78

The comparison is made considering the 10 most relevant essential motions, which encompass 60–75% of the structural variance along the trajectory. doi:10.1371/journal.pone.0049291.t003

in PheE15Tyr, PheE15 Ile and PheE15Ala. To this end, five structures of the protein were taken from the last 25 ns of the trajectories run for the oxygenated mutants. These snapshots were used as starting points for unrestrained simulations run in presence of NO, which was placed at random positions around the protein (5 distinct random positions per protein snapshot). The systems were thermalized following the protocol mentioned above, and MD simulations were run up to 20 ns using the same simulation conditions.

Essential Dynamics

The dynamical behavior of HbN and its mutants was explored by means of essential dynamics [23,24]. Residues 1–15 were excluded as this region is very flexible and would mask the

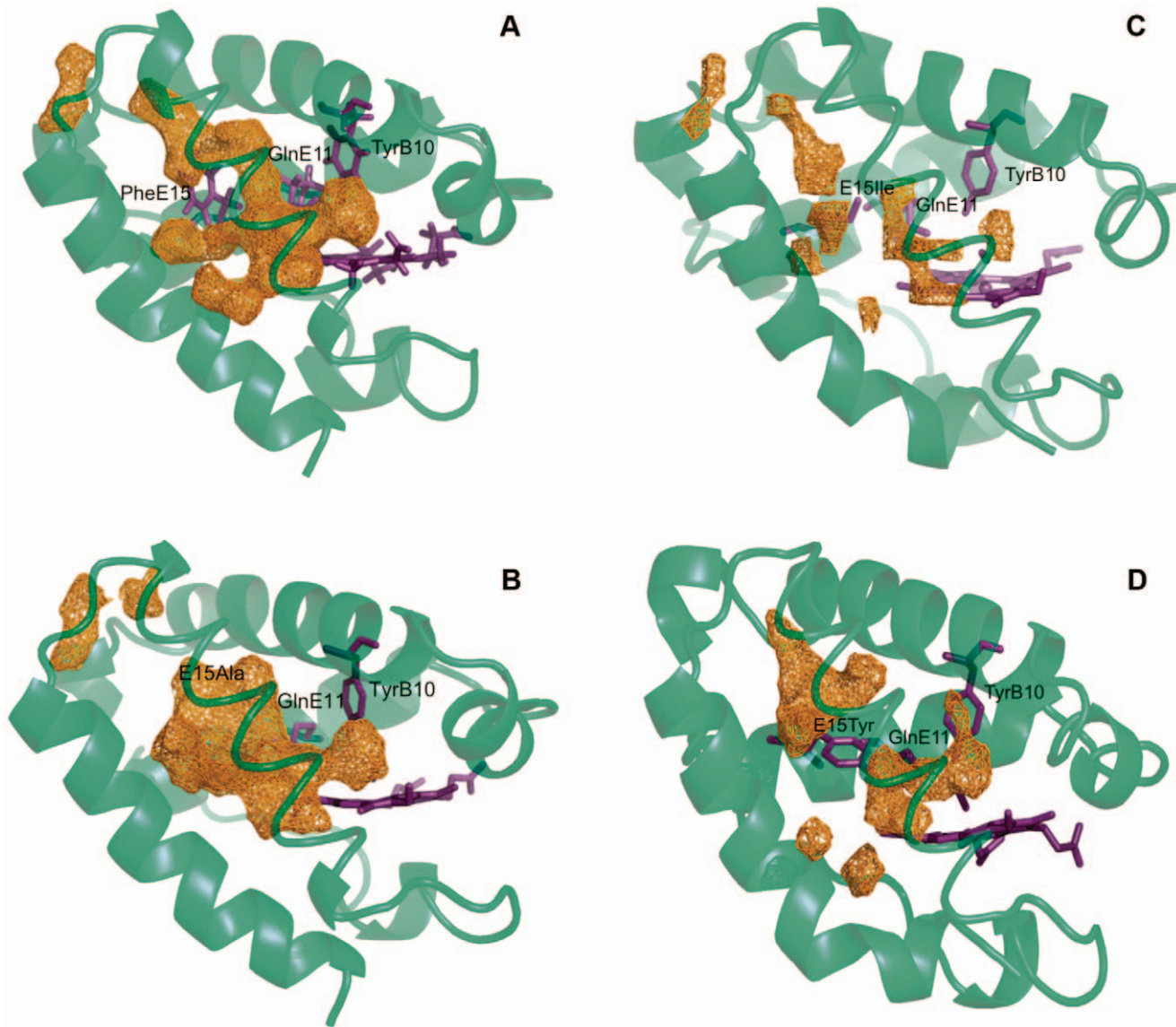


Figure 5. Representation of the accessible volume in wt HbN and its mutants. The accessible volume determined from MDpocket analysis is achieved for a density isocontour of 6.7 in the case of wt protein (A). The use of the same isocontour shows discontinuities in the accessible volume of the tunnel long branch for the different mutants. The disruption is located around the position of the gate in the case of PheE15Ile (C) and PheE15Tyr (D) mutants. For the PheE15Ala species (B) the major disruption involves the region close to the channel entry. Continuous progression of the accessible volume is achieved when the isocontour value is reduced to 5.4 for PheE15Ile and PheE15Tyr, and to 3.4 for PheE15Ala. In the plots the protein backbone corresponds to the energy-minimized structure obtained by averaging the snapshots sampled in the last 0.1 ns for each trajectory. doi:10.1371/journal.pone.0049291.g005

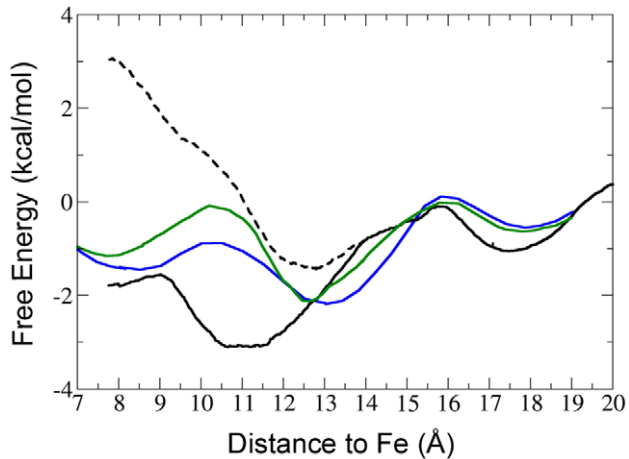


Figure 6. Free energy profile determined for NO migration along the long tunnel branch. MSMD calculations were performed to determine the energetics of ligand migration through the tunnel long branch for Phe15Ile (green) and Phe15Tyr (blue). The profiles are compared with those determined for ligand migration in both *open* (solid line) and *closed* (dashed line) states of oxygenated wt HbN. The free energy is given in kcal/mol, and the distance of the ligand from the heme iron is given in angstroms. For the sake of clarity, error bars are not displayed.
doi:10.1371/journal.pone.0049291.g006

essential motions of the protein core. The backbone atoms were used to superpose the structures sampled in order to derive the essential motions. To this end, for each trajectory the positional covariance matrix of the backbone atoms was built up and diagonalized. The eigenvectors define the type of essential motions of the backbone, and the eigenvalues determine how much of the positional variance in the trajectory is explained by each eigenvector.

Ligand Migration Profiles

The effect of PheE15 mutation on the migration of ligands was examined using two techniques. The preferred docking sites and migration pathways were identified using MDpocket [25]. Then, the migration free energy profiles were obtained using Multiple Steered Molecular Dynamics (MSMD) [26].

MDpocket is a pocket detection program that uses a fast geometrical algorithm based on a Voronoi tessellation centered on the atoms and the associated alpha spheres, which are clustered and filtered giving origin to pockets and channels [27]. These pockets are then used to identify docking sites and migration paths along the protein matrix. Analyses were performed using 10000 snapshots taken equally spread over the last 50 ns of the trajectories. The minimum and maximum alpha sphere radius was 2.8 Å and 5.5 Å, respectively. The identified cavities were superposed in time and space and a density map was generated from this superposition. Stable cavities are identified as high-density 3D isocontours, while low-density isocontours denote transient or nearly non-existent cavities in the MD simulation.

MSMD simulations were run to evaluate the free energy profiles of ligand migration through the tunnels using Jarzynski's equality [26], which estimates the free energy from an ensemble of irreversible works along the same reaction coordinate. A steering potential forces the motion of the probe with constant velocity along the reaction coordinate. The reaction coordinate was the iron-ligand distance, the force constant was $200 \text{ kcal mol}^{-1} \text{ Å}^{-1}$ and the pulling velocity 0.025 Å ps^{-1} . The free energy profile of

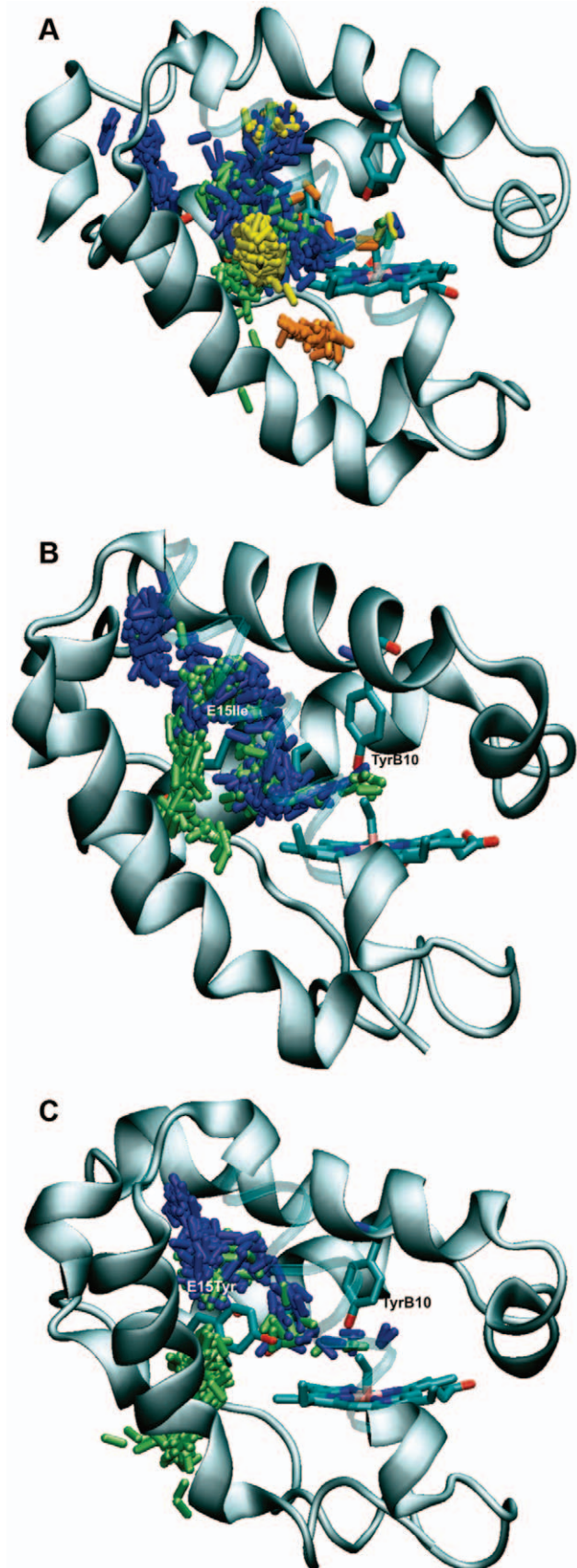


Figure 7. Representative trajectories followed by free NO ligand through the protein matrix. MD simulation of free NO located at random positions from the protein were followed to investigate the pathways leading to the heme cavity for oxygenated forms of (A) PheE15Ala, (B) PheE15Ile and (C) PheE15Tyr. The distinct pathways are indicating by showing the position of NO (represented as sticks) along the trajectory using different colors: long branch (blue), short branch (brown), EH (green), and other (yellow). Note that helix G is displayed as highly transparent cartoon for the sake of clarity. doi:10.1371/journal.pone.0049291.g007

ligand migration along a tunnel was obtained following the computational scheme reported in previous studies [8]. At least twenty SMD simulations were run pushing the ligand through the tunnel from the solvent towards the iron. The starting snapshot for each SMD was taken from the final structure of an equilibrated MD simulation with the ligand placed at a fixed distance from the iron. Typically those distances are chosen from the preferred docking sites found in MDpocket analysis in conjunction with short MD simulations run to examine the motion of the free diatomic ligand along the tunnel.

Results and Discussion

Four gate mutants, where PheE15 in wild type (wt) HbN was replaced by Ala (PheE15Ala), Ile (PheE15Ile), Tyr (PheE15Tyr) and Trp (PheE15Trp), were created by site-directed mutagenesis. Mutations were chosen to span a wide range of sizes, varying from the small methyl group in Ala to the large indole ring in Trp, the replacement of the planar benzene by the branched chain of Ile, and the conservative mutation of PheE15 by Tyr. It was expected that the distinct chemical nature of the side chains would translate into differences in the ligand migration through the long tunnel, which in turn should lead to differences in the NOD activity measured for the mutants. Thus, in the absence of relevant structural alterations in the tunnel due to the mutations at position E15, which might be relevant for the bulky Trp, it was expected that replacement of PheE15 to Ala should open permanently the long tunnel, whereas mutation to Trp should occlude the access of ligands. Likewise, the branched side chain of Ile was expected to limit the accessibility of diatomic ligands through the tunnel. Finally, the conservative PheE15Tyr mutation was *a priori* expected to have little effect on the migration properties.

Effect of Mutations at PheE15 Gate of HbN on O₂/CO Binding

Absorption spectra of O₂ and CO bound forms of mutants were indistinguishable from that of wt HbN (Fig. 2), suggesting that all these mutants bind O₂. The ability to bind O₂ was further assessed by measuring the p^{50} values (Table 1). For the wt protein, the p^{50} value was 0.019 (mm Hg), which compares well with previous data [1]. When the PheE15 gate mutants were compared with wt HbN, no significant difference in their p^{50} profile was observed suggesting that the O₂ binding properties of mutants are not impaired. To substantiate these results, the rate of CO association was also determined to characterize the kinetics of ligand association (Table 1). The k_{on} value determined for the wt protein ($2.5 \times 10^7 \text{ M}^{-1} \text{ s}^{-1}$) is slightly larger than the value reported by Couture *et al.* ($0.657 \times 10^7 \text{ M}^{-1} \text{ s}^{-1}$) [1]. Nevertheless, all the mutants displayed CO association rates comparable to that of wt HbN, indicating that mutation at PheE15 residue does not affect the O₂/CO binding properties of HbN.

Table 4. Analysis of the migration pathways followed by a free NO in a simulation box containing the solvated proteins PheE15Ala, PheE15Ile and PheE15Tyr.

Mutant	Effective path ^a	Long branch ^b	Short branch ^c	EH ^d	Other
PheE15Ala	18 (72.4%)	5	3	7	3
PheE15Ile	21 (85.7%)	15	0	6	0
PheE15Tyr	17 (70.0%)	12	0	5	0

25 independent MD simulations were examined for each mutant in order to determine the migration route followed by NO to reach the heme cavity.

^aFraction of trajectories where the ligand was able to reach the heme cavity in the simulation time. The distinct pathways are displayed in Figure 7 using different colors: long branch (blue), short branch (brown), EH (green), and other (yellow).

^bDefined primarily by helices B and E.

^cDefined primarily by helices G and H.

^dThis pathway is defined by residues located in helices E and H.

doi:10.1371/journal.pone.0049291.t004

Mutations at PheE15 Gate of HbN Alter its NOD Activity

Even though mutants exhibit very similar O₂ binding properties, relevant differences were observed in their NO metabolizing activities (Table 2). The NOD activity of PheE15Ile was reduced to around 55% of the activity measured for the wt enzyme, whereas a larger reduction (around 70%) in NOD activity was observed for the PheE15Trp mutant. Unexpectedly, mutation of PheE15 to Tyr also yielded a significant reduction (around 65%) in the NOD activity, suggesting that the apparently conservative replacement of benzene by phenol has a drastic influence on the ligand migration properties of the mutant. Finally, the PheE15Ala mutant also exhibited a significant reduction (around 49%) in the NOD activity.

Oxidation of NO by Oxygen Adduct of PheE15 Gate Mutants of HbN

The NO oxidation profile of wt HbN and its mutants was determined by titrating the oxy forms of protein with NO in a time course manner (Fig. 3). The addition of NO (5 μM) resulted in the appearance of a partially oxidized spectrum of HbN and repeated addition of NO solution to this sample resulted in a fully oxidized spectrum shifting Soret peak of oxyHbN from 415 to 405 nm. In contrast, similar additions of NO to the oxygenated form of mutants PheE15Trp, PheE15Ile and PheE15Tyr did not change the spectra to the oxidized form immediately and changed slowly after 30–35 min of exposure, indicating very slow NO oxidation. Finally, NO oxidation by PheE15Ala mutant displayed a spectral profile similar to PheE15Ile and PheE15Tyr, which is intermediate between those observed for the wt protein and the PheE15Trp mutant.

MD Simulations

The preceding data indicate that the different PheE15 mutations do not affect the binding of O₂ to the heme. However, since the mutants exhibit a distinctive reduction in the NOD activity, the PheE15 residue has to play a key role in mediating the access of NO to the oxygenated protein. On the basis of these findings, MD simulations were run with a twofold purpose: to examine the structural integrity of the overall protein fold, and to identify local changes in the long branch tunnel that might affect the ligand migration. To this end, a series of 100–150 ns MD simulations were run for the heme-bound O₂ forms of PheE15Ala, PheE15Ile and PheE15Tyr mutants, and the results were

compared with those obtained for the wt protein. This simulation time has been shown suitable to describe the conformational transitions of PheE15 in our previous studies for the wt HbN [7–9]. Choice of the simulation time, however, was also dictated by consistency in the analysis of the structural and dynamical properties of the simulated systems, either related to the overall features of the protein backbone or to the ligand migration through the protein matrix. Such a convergence was achieved for all the simulated systems but for the PheE15Trp mutant (see below).

For the particular case of the PheE15Tyr mutant, two MD simulations differing in the starting orientation of TyrE15 were run. Thus, on the basis of the conformational preferences found for PheE15 in both the X-ray structure [5] and previous MD studies [7,8], the phenol ring was oriented in the closed or open conformations, which prevent or facilitate ligand migration through the tunnel, respectively. When TyrE15 was in the closed orientation, the side chain remained stable, and no transitions between open and closed states were found along the whole trajectory (Fig. S1). There was only a conformational change leading to the transient formation of a hydrogen bond between the hydroxyl group of TyrE15 and the carbonyl group of Ile115. When the MD simulation started from the open conformation, the side chain of TyrE15 suddenly changed to the closed conformation after the first 12 ns and then remained stable until the end of the trajectory (Fig. S1), even though few attempts to form transient hydrogen-bond interactions with Ile115 can be observed. Since the two simulations exhibited the same behavior, hereafter discussion of PheE15Tyr mutant will be limited to the trajectory starting from the closed conformation.

Finally, the MD simulation run for the PheE15→Trp mutant was extended up to 200 ns. However, the results will not be presented here as the analysis of the trajectory points out that the structural changes induced by the mutation both in the tunnel and in the global protein structure are still not fully converged. It seems that a proper description of the structural rearrangements triggered by this mutation would require longer simulations, making it necessary to be cautious for not overinterpreting the structural changes due to the PheE15→Trp mutation, which cannot be easily accommodated in the tunnel (see Fig. S2 for details).

Structural Analysis

For all the simulations, inspection of both the time evolution of the potential energy (Fig. S3) and the rmsd (Fig. 4; see also Fig. S4) determined for the backbone atoms of the protein core (excluding the first 15 residues) supports the integrity of the simulated proteins. Thus, the rmsd of the protein core (ranging from 1.2 to 2.1 Å for the different mutants) remains very stable after the first few nanoseconds. In contrast, a much larger rmsd profile showing notable fluctuations along the trajectory is obtained when the whole protein backbone is included in the analysis. This finding indicates that the pre-A segment is very flexible in all the mutants and can adopt a large number of conformational states, as noted in the formation of distinct structural arrangements for residues 1–15 (data not shown). Therefore, the mutation does not alter the large conformational flexibility found for the pre-A segment in the wt HbN [9,28].

The geometrical arrangement of residues TyrB10 and GlnE11 in the distal cavity is a structural feature of particular relevance, as it has been proposed that opening of the gate is modulated by the oxygen-sensing properties of the TyrB10-GlnE11 pair [8,29]. In the oxygenated wt HbN these residues form a network of hydrogen bonds, where the hydroxyl group

of TyrB10 is hydrogen-bonded to the heme-bound O₂, and also accepts a hydrogen bond from the side chain of GlnE11. Due to these interactions, the GlnE11 side chain lies closer to the benzene ring of PheE15 than in the deoxygenated protein, and the enhanced steric clash favors opening of the PheE15 gate upon O₂ binding. Accordingly, it might be argued that disruption of the hydrogen bonds formed by TyrB10 and GlnE11 could explain the reduction in NOD activity of the mutants. However, the analysis of the trajectories completely rules out this possibility (Fig. S5). Thus, in all the mutants the hydroxyl group of TyrB10 is hydrogen-bonded to the heme-bound O₂ (average distances about 2.85 Å), and the side chain amide nitrogen of GlnE11 is hydrogen-bonded to the TyrB10 hydroxyl group (average distances about 3.0 Å). These interactions reproduce the hydrogen bonds found in the X-ray structure, as the corresponding distances (averaged for subunits A and B) are 3.15 and 2.95 Å. Therefore, the hydrogen-bond network found in wt HbN is not affected by the PheE15 mutations, and hence one should expect that the steric pressure exerted by GlnE11 is retained in the mutated proteins.

Dynamical Analysis of the Protein Backbone

Binding of O₂ to the heme also changes the dynamical motion of the protein backbone [7,8]. Thus, essential dynamics analysis of oxygenated HbN reveals that the major motions in the deoxygenated protein affect helices C, G and H, while the largest contribution to protein flexibility comes from helices B and E in the oxygenated protein. Since helices B and E define the walls of the tunnel long branch, the increased motion of these helices should facilitate the transition between open and closed states of the gate, thus influencing the ligand migration through the tunnel. This dynamical alteration agrees with the large scale conformational change observed experimentally upon binding of NO to the ferric form of wt HbN [30], and with the occurrence of distinct conformational relaxation processes found in the kinetics of CO recombination to the protein encapsulated in gels [31].

In order to investigate whether mutation of the PheE15 gate influences the dynamics of the protein backbone and eventually affects the migration of NO in the oxygenated protein, we determined the essential dynamics of the mutants and compared them with the wt protein. Diagonalization of the positional covariance matrix for the backbone atoms points out that few motions account for a significant fraction of the protein dynamics. Nearly 50% and 70% of the backbone conformational flexibility is accounted for by the first 4 and 10 principal components (Table S1). The two first essential motions, which mainly involves motions of helices B, E and H, loop F and the hinge region around helix C, account for 22–37% of the structural variance in the backbone of the mutants, in agreement with the value (36%) determined for wt HbN.

The similarity between the structural fluctuations of the protein backbone in wt HbN and its mutants was measured by means of the similarity index ζ_{AB} (see Text S1), which takes into account the nature of the essential motions and their contribution to the structural variance of the protein [32]. When the 10 most relevant motions are considered, the similarity index varies in the range 0.60–0.65, which is slightly lower than the self-similarities obtained for wt HbN and mutants (Table 3). These results point out that mutations preserve to a large extent the dynamical behavior of the protein. For the sake of comparison, the similarity indexes determined for the 10 most essential motions between wt HbN and the mutants TyrB10Phe and GlnE11Ala only amount to 0.47 and 0.38, respectively [27], indicating that the hydrogen-bond

network formed by the TyrB10-GlnE11 pair has a larger impact on the protein dynamics than mutation of PheE15.

Ligand Migration

Since the preceding results did not reveal significant changes neither in the hydrogen-bond network of TyrB10-GlnE11 pair nor in the dynamical behavior of the protein skeleton, the reduction in NOD activity determined for PheE15 mutants might reflect a reduced accessibility of ligands for migrating through the long tunnel. To corroborate this hypothesis, we determined the shape of internal tunnels by using MDpocket, which provides a grid that encloses the protein, where each grid point is assigned an occupancy value that denotes the accessibility of the volume associated to that point [23].

For the wt HbN the tunnel long branch appears as a continuous cavity leading from the protein surface to the heme cavity, as noted by the continuous progression of the accessible volume isocontour shown in Fig. 5. In contrast, the representation of the same isocontour for the mutants reveals a discontinuous channel, even in the case of the mutation to Ala.

For mutants PheE15Ile and PheE15Tyr, such a disruption affects the region that surrounds the mutated residue, suggesting that ligand migration through the tunnel long branch is impeded by the steric hindrance imposed by the side chains of the mutated residues (Fig. 5C,D). This is confirmed by the free energy profiles determined by MSMD calculations for these mutants, where the limiting step for ligand migration is associated to surpassing the gate (Fig. 6). In fact, the free energy profiles are intermediate between those obtained for the wt HbN with the PheE15 gate in either closed or open conformational states. Compared to the wt protein in the open state, mutation of the gate slightly destabilizes the minimum located at around 11 Å (i.e., the docking site before the gate), and increases the barrier required to pass above the side chain of the mutated residue in order to access the heme cavity. Therefore, a small diatomic ligand such as NO is expected to be trapped effectively at the highly hydrophobic entrance of the long branch, thus enhancing the local concentration, but access to the heme cavity is mainly limited by the hindrance due to the side chain of the mutated gate.

In contrast with the preceding findings, the isocontour is continuous around the mutated gate in the PheE15Ala mutant, as expected from the small side chain of Ala. However, compared to the wt protein (Fig. 5A), there is a significant occlusion at the entrance of the channel (Fig. 5B), which stems from a slight readjustment of helices B and G that reduces the width of the channel entry by 0.4–0.6 Å (as measured from distances between C α atoms of residues located at the helical ends). Accordingly, the probability of the ligand to be trapped at the entrance of the tunnel long branch is lower compared to wt HbN. In turn, this finding raises the question about the existence of alternative pathways that can justify the remaining NOD activity (around 51% compared to wt protein) retained by PheE15Ala mutant. To this end, we examined the trajectory followed by a free NO in a water box containing the PheE15Ala mutant and determined the routes leading to the heme cavity in 25 independent MD simulations. The results (see Table 4) showed that 18 out of 25 trajectories were successful in allowing the ligand (NO) to achieve the heme cavity within the simulation time. Nevertheless, only 5 trajectories showed that NO migrates via the tunnel long branch, and in 7 simulations the entry pathway involved the EH tunnel (defined by residues in helices E and H) reported by Daigle et al. [33]. Remarkably, in 3 trajectories NO was able to reach the heme cavity through the short branch, and in other 3 trajectories NO accessed the heme cavity via a distinct channel (see Fig. 7A). Thus,

even though the reduction in NOD activity can be related to the occlusion of ligand access at the beginning of the tunnel long branch, this effect is counterbalanced by the existence of three alternative entry pathways, which arise from slight structural alterations in the protein skeleton. This finding reveals the delicate structural balance imposed by the PheE15 gate, which not only regulates ligand migration, but also contributes to avoid the collapse of helices B and E, thus preserving the structural integrity and ligand accessibility along the tunnel long branch.

For the sake of completeness, this analysis was also performed for PheE15Ile and PheE15Tyr mutants. For these mutants the access routes leading to the heme cavity were significantly different. Thus, the trajectories primarily involved migration through the tunnel long branch (Table 4), which should be considered the main pathway for ligand migration in the oxygenated protein. In this pathway, the ligand remained docked in a region before the gate for significant periods of time (as noted in the high density of NO molecules located before the mutated gate residue; see Fig. 7B,C) until it was able to surpass the barrier due to the side chain of Ile/Tyr and access the heme cavity. There were some attempts to get the heme cavity through the short tunnel, but they were unsuccessful. Finally, only in very few cases the ligand entered the protein through the tunnel EH, leading to the docking site located before the mutated gate residue. Therefore, these findings are in contrast with previous modeling studies where the short tunnel was reported to be the main route for NO diffusion [34]. Furthermore, present results indicate that the main route in PheE15Ile and PheE15Tyr is the tunnel long branch, which supports the role of the tunnel long branch in the dual-path migration mechanism [7,8] and particularly the functional relevance of the PheE15 gate.

Conclusion

The experimental data collected for the mutants indicate that the PheE15 mutation does not affect the binding of O₂ to the heme, as noted in the similar absorption spectra of O₂ and CO bound forms, as well as in the similar p^{50} and k_m values determined for both wt and mutated proteins. These findings suggest that the PheE15 mutation has little impact on the tunnel short branch, which is proposed to be the main pathway for migration of O₂ to the heme cavity. However, since the mutants exhibit a distinctive reduction in the NOD activity, PheE15 residue has to play a key role in mediating the access of NO to the oxygenated protein. In agreement with the dual-path migration mechanism [7,8], the main pathway for NO migration is the tunnel long branch. This finding points out the delicate structural balance imposed by the PheE15 gate, which not only regulates ligand migration, but also contributes to avoid the collapse of helices B and E, thus preserving the ligand accessibility along the tunnel long branch. Overall, the results presented herein demonstrate the pivotal role of PheE15 in modulating the NOD function of Mtb HbN, thus confirming the suggestion by Milani and coworkers [5] about the gating role of PheE15 in HbN.

Supporting Information

Figure S1 Representation of the conformational orientation of the TyrE15 side chain in the two trajectories run for the PheE15Tyr mutant. Time (ns) evolution of the dihedral angle H-C α -C β -C δ (degrees) of TyrE15 in the simulation started by placing the phenol ring in (top) open and (bottom) closed conformations, following the two main orientations found for the side chain of PheE15 gate in wild type HbN [7,8]. (TIF)

Figure S2 Representation of structural changes for the PheE15Trp mutant. (Top) Superposition of the backbone of the snapshots sampled at 40 (green) and 180 (orange) ns along the trajectory run for the PheE15Trp mutant. The plot shows the drastic change in the orientation of the Trp side chain, the displacement of the heme, and the structural rearrangement of several helices. For the sake of clarity, helix G is shown as ribbon. (Bottom) Time (ns) evolution of the dihedral angle (degrees) that determines the orientation of the indole ring of Trp. (TIF)

Figure S3 Representation of the potential energy for simulated systems. Time (ns) evolution of the potential energy ($\times 10^3$; kcal/mol) for the simulations of the oxygenated PheE15 mutants. Top: (left) PheE15Ala; (right) PheE15Ile. Bottom: PheE15Tyr in the simulation started by placing the Tyr side chain in (left) closed and (right) open conformations. (TIF)

Figure S4 Representation of rmsd and rmsf profiles for PheE15Tyr gate mutant of HbN (trajectory started from open conformation). (Left) Rmsd (\AA) of the protein backbone determined using the X-ray structure (1HDR; subunit A) as reference. The rmsd of the whole protein is shown in green, and the rmsd of the residues in the protein core (excluding the pre-A segment; residues 1–15) is shown in blue. (Right) Representation of the rmsf (\AA) of residues in the protein. The plots correspond to the trajectory run started by placing the side chain of TyrE15 in the open conformation. (TIF)

Figure S5 Representation of hydrogen-bond distances for the TyrB10-GlnE11. Time (ns) evolution of distances (\AA) from the TyrB10 hydroxyl oxygen to the heme-bound O_2 and from the GlnE11 side chain amide nitrogen to the TyrB10 hydroxyl oxygen are shown in blue and green, respectively. Top: (left) PheE15Ala; (right) PheE15Ile. Bottom: PheE15Tyr in the simulation started by placing the Tyr side chain in (left) closed and (right) open conformations. (TIF)

Table S1 Structural variance (%) of the protein backbone. The contribution of the first essential motions to the structural variance is indicated for the mutated forms of HbN. The cumulative value is given in parenthesis. (DOCX)

Text S1 Global similarity between two sets of essential eigenvectors. (DOCX)

Acknowledgments

We would like to thank Dr. S. Kundu, University of Delhi, South Campus, Delhi, India for helping in ligand binding studies on HbN mutants.

Author Contributions

Conceived and designed the experiments: DAE KLD FJL. Performed the experiments: AO SS ABC FF LB MAM. Analyzed the data: ABC MAM DAE KLD FJL. Wrote the paper: DAE KLD FJL.

References

- Couture M, Yeh SR, Wittenberg BA, Wittenberg JB, Ouellet Y, et al. (1999) A cooperative oxygen-binding hemoglobin from *Mycobacterium tuberculosis*. Proc Natl Acad Sci USA 96: 11223–11228.
- Ouellet H, Ouellet Y, Richard C, Labarre M, Wittenberg BA, et al. (2002) Truncated hemoglobin HbN protects *Mycobacterium bovis* from nitric oxide. Proc Natl Acad Sci USA 99: 5902–5907.
- Pathania R, Navani NK, Gardner AM, Gardner PR, Dikshit KL (2002) Nitric oxide scavenging and detoxification by the *Mycobacterium tuberculosis* haemoglobin, HbN in *Escherichia coli*. Mol Microbiol 45: 1303–1314.
- Pawaria S, Lama A, Raje M, Dikshit KL (2008) Responses of *Mycobacterium tuberculosis* hemoglobin promoters in vitro and in vivo growth conditions. Appl Environ Microbiol 74: 3512–3522.
- Milani M, Pesce A, Ouellet Y, Ascenzi P, Guertin M, et al. (2001) *Mycobacterium tuberculosis* hemoglobin N displays a protein tunnel suited for O_2 diffusion to the heme. EMBO J 20: 3902–3909.
- Milani M, Pesce A, Ouellet Y, Dewilde S, Friedman J, et al. (2004) Heme-ligand tunneling in Group I truncated hemoglobins. J Biol Chem 279: 21520–21525.
- Crespo A, Marti MA, Kalko SG, Morreale A, Orozco M, et al. (2005) Theoretical study of the truncated hemoglobin HbN: Exploring the molecular basis of the NO detoxification mechanism. J Am Chem Soc 127: 4433–4444.
- Bidon-Chanal A, Marti MA, Crespo A, Milani M, Orozco M, et al. (2006) Ligand-induced dynamical regulation of NO conversion in *Mycobacterium tuberculosis* truncated hemoglobin-N. Proteins 64: 457–464.
- Lama A, Pawaria S, Bidon-Chanal A, Anand A, Gelpi JL, et al. (2009) Role of Pre-A motif in nitric oxide scavenging by truncated hemoglobin, HbN, of *Mycobacterium tuberculosis*. J Biol Chem 284: 14457–14468.
- Milani M, Pesce A, Nardini M, Ouellet H, Ouellet Y, et al. (2005) Structural bases for heme binding and diatomic ligand recognition in truncated hemoglobins. J Inorg Biochem 99: 97–109.
- Ascenzi P, Bolognesi M, Milani M, Guertin M, Visca P (2007) Mycobacterial truncated hemoglobins: From genes to functions. Gene 398: 42–51.
- Lama A, Pawaria S, Dikshit KL (2006) Oxygen binding and NO scavenging properties of truncated hemoglobin, HbN, of *Mycobacterium smegmatis*. FEBS Lett 580: 4031–4041.
- Kaur R, Pathania R, Sharma V, Mande SC, Dikshit KL (2002) Chimeric vitreoscilla hemoglobin (VHb) carrying a flavoreductase domain relieves nitrosative stress in *Escherichia coli*: New insight into the functional role of VHb. Appl Environ Microbiol 68: 152–160.
- Appleby CA (1978) Purification of *Rhizobium* cytochromes P-450. Methods Enzymol 52: 157–166.
- Gardner PR (1998) Nitric oxide dioxygenase: an enzymic function for flavoglobin. Proc Natl Acad Sci USA 95: 10378–10383.
- Giardina B, Amiconi G (1981) Measurement of binding of gaseous and nongaseous ligands to hemoglobins by conventional spectrophotometric procedures. Methods Enzymol 76: 417–427.
- Rohlfs RJ, Mathews AJ, Carver TE, Olson JS, Springer BA, et al. (1990) The effects of amino acid substitution at position E7 (residue 64) on the kinetics of ligand binding to sperm whale myoglobin. J Biol Chem 265: 3168–3176.
- Jorgensen WL, Chandrasekhar J, Madura JD, Impey RW, Klein ML (1983) Comparison of simple potential functions for simulating liquid water. J Chem Phys 79: 926–935.
- Ryckaert JP, Ciccotti G, Berendsen HJC (1977) Numerical integration of the cartesian equations of motion of a system with constraints: Molecular Dynamics of *n*-alkanes. J Comput Phys 23: 327–341.
- Darden T, York D, Pedersen L (1993) Particle mesh Ewald: An $N \log(N)$ method for Ewald sums in large systems. J Chem Phys 98: 10089–10092.
- Hornak V, Abel R, Okur A, Strockbine B, Roitberg A, et al. (2006) Comparison of multiple Amber force fields and development of improved protein backbone parameters. Proteins 65: 712–725.
- Case DA, Darden TA, Cheatham TE III, Simmerling CL, Wang J, et al. AMBER, version 10, University of California, San Francisco, CA, 2008.
- García A (1992) Large-amplitude nonlinear motions in proteins. Phys Rev Lett 68: 2696–2699.
- Amadei A, Linssen AB, Berendsen HJC (1993) Essential dynamics of proteins. Proteins 17: 412–425.
- Schmidtke P, Bidon-Chanal A, Luque FJ, Barril X (2011) MDpocket: open-source cavity detection and characterization on molecular dynamics trajectories. Bioinformatics 27: 3276–3285.
- Jarzynski C (1977) Non equilibrium equality for free energy differences. Phys Rev Lett 78: 2690–2693.
- Le Guilloux V, Schmidtke P, Tuffery P (2009) Fpocket: an open source platform for ligand pocket detection. BMC Bioinformatics 10: 168.
- Savard PY, Daigle R, Morin S, Sebilo A, Meindre F, et al. (2011) Structure and dynamics of *Mycobacterium tuberculosis* truncated hemoglobin N: insights from NMR spectroscopy and molecular dynamics simulations. Biochemistry 50: 11121–11130.
- Bidon-Chanal A, Marti MA, Estrin DA, Luque FJ (2007) Dynamical regulation of ligand migration by a gate-opening molecular switch in truncated hemoglobin-N from *Mycobacterium tuberculosis*. J Am Chem Soc 129: 6782–6788.
- Mukai M, Ouellet Y, Guertin M, Yeh SR (2004) NO binding induced conformational changes in a truncated hemoglobin from *Mycobacterium tuberculosis*. Biochemistry 43: 2764–2770.
- Dantsker D, Samuni U, Ouellet Y, Wittenberg BA, Wittenberg JB, et al. (2004) Viscosity-dependent relaxation significantly modulates the kinetics of CO

- recombination in the truncated hemoglobin TrHbN from *Mycobacterium tuberculosis*. *J Biol Chem* 279: 38844–38853.
32. Perez A, Blas JR, Rueda M, Lopez-Bes JM, de la Cruz X, et al. (2005) Exploring the essential dynamics of B-DNA. *J Chem Theory Comput* 1: 790–800.
 33. Daigle R, Guertin M, Lagüe P (2009) Structural characterization of the tunnels of *Mycobacterium tuberculosis* truncated hemoglobin N from molecular dynamics simulations. *Proteins* 75: 735–747.
 34. Daigle R, Rousseau JA, Guertin M, Lagüe P (2009) Theoretical investigations of nitric oxide channeling in *Mycobacterium tuberculosis* truncated hemoglobin N. *Biophys J* 97: 2967–2977.

Redox-mediated interactions of VHb (*Vitreoscilla* haemoglobin) with OxyR: novel regulation of VHb biosynthesis under oxidative stress

Arvind ANAND*¹, Brian T. DUK†¹, Sandeep SINGH*, Meltem Y. AKBAS‡, Dale A. WEBSTER†, Benjamin C. STARK† and Kanak L. DIKSHIT*²

*Institute of Microbial Technology, Sector 39 A, Chandigarh 160036, India, †Division of Biology, Department of Biological, Chemical and Physical Sciences, Illinois Institute of Technology, Chicago, IL 60616, U.S.A., and ‡Gebze Institute of Technology, 41400 Gebze Kocaeli, Turkey

The bacterial haemoglobin from *Vitreoscilla*, VHb, displays several unusual properties that are unique among the globin family. When the gene encoding VHb, *vgb*, is expressed from its natural promoter in either *Vitreoscilla* or *Escherichia coli*, the level of VHb increases more than 50-fold under hypoxic conditions and decreases significantly during oxidative stress, suggesting similar functioning of the *vgb* promoter in both organisms. In the present study we show that expression of VHb in *E. coli* induced the antioxidant genes *katG* (catalase–peroxidase G) and *sodA* (superoxide dismutase A) and conferred significant protection from oxidative stress. In contrast, when *vgb* was expressed in an *oxyR* mutant of *E. coli*, VHb levels increased and the strain showed high sensitivity to oxidative stress without induction of antioxidant genes; this indicates the involvement of the oxidative stress regulator OxyR in mediating the protective effect of VHb under oxidative stress. A putative OxyR-binding site was identified within the *vgb* promoter and a gel-shift assay confirmed

its interaction with oxidized OxyR, an interaction which was disrupted by the reduced form of the transcriptional activator Fnr (fumarate and nitrate reductase). This suggested that the redox state of OxyR and Fnr modulates their interaction with the *vgb* promoter. VHb associated with reduced OxyR in two-hybrid screen experiments and *in vitro*, converting it into an oxidized state in the presence of NADH, a condition where VHb is known to generate H₂O₂. These observations unveil a novel mechanism by which VHb may transmit signals to OxyR to autoregulate its own biosynthesis, simultaneously activating oxidative stress functions. The activation of OxyR via VHb, reported in the present paper for the first time, suggests the involvement of VHb in transcriptional control of many other genes as well.

Key words: bacterial haemoglobin, oxidative stress, OxyR, protein–protein interaction, *Vitreoscilla* haemoglobin (VHb), *Vitreoscilla*.

INTRODUCTION

Haemoglobins present within the microbial world have challenged the common perception that haemoglobins and myoglobins are mainly tailored for oxygen storage and transfer functions. In the last decade a great deal of structural and functional diversity among microbial haemoglobins has been discovered [1–3]. The haemoglobin from the bacterium *Vitreoscilla* [4], VHb, the first haemoglobin discovered in a prokaryote, displays a classic globin fold but has unusual structures in both proximal and distal haem pockets [5,6]. It has been proposed that its unique structural organization and ability to remain in different conformational states may allow it to perform multiple functions. Of the currently known globins, VHb is especially useful for engineering the energy metabolism of various heterologous hosts [7–9] and represents a versatile tool for a variety of biotechnological applications [2,9]. Proteomic and microarray analyses of recombinant *Escherichia coli* expressing VHb have indicated that the presence of VHb in *E. coli* significantly affects the expression of hundreds of genes, including up- and down-regulation of genes involved in energy metabolism, central intermediary metabolism and cellular processes [10,11]. However, the molecular mechanism by which VHb is able to exert such diverse effects on its host metabolism is currently unknown.

VHb exists predominantly as a homodimer [5,12] and binds oxygen reversibly with an oxygen association rate constant similar to eukaryotic haemoglobins; its rate of oxygen dissociation, however, is unusually high [12,13]. Under hypoxic conditions the level of VHb increases more than 50-fold in *Vitreoscilla* and in recombinant *E. coli* expressing VHb under control of its native promoter [14,15]. This led to the proposal that one of its functions is to facilitate oxygen flux to the respiratory apparatus of its host under oxygen-limiting conditions [12,15,16]. This is supported by the observations that VHb remains localized and concentrated near the periphery of the cytosolic face of the cell membrane in both *Vitreoscilla* and *E. coli* [17], improves the oxygen uptake of its host [18] and specifically interacts with cytochrome *o* [17,19] and phospholipids of cell membranes [20].

VHb displays structural characteristics for lipid attachment that are similar to flavohaemoglobins and it exhibits a relatively high propensity towards phospholipid binding *in vitro* [20]. It has been noted that when VHb binds lipids there is a several fold decrease in its oxygen affinity, and a commitment increase in oxygen release, compared with lipid-free VHb [20]; this might allow VHb to deliver oxygen directly to the respiratory apparatus of cells for efficient utilization. These lipid-binding effects suggest that interaction of VHb with other molecules may mediate VHb function in diverse ways. Correspondingly, VHb has been shown to stimulate oxygenase activity [21–23], serve as an alternate

Abbreviations used: ArcA, aerobic respiration control A; Crp, catabolic repressor protein; Fnr, fumarate and nitrate reductase; Kat, catalase–peroxidase; LB, Luria–Bertani; metVHb, *Vitreoscilla* methaemoglobin; ROS, reactive oxygen species; RT, reverse transcription; Sod, superoxide dismutase; *vgb*, gene encoding *Vitreoscilla* haemoglobin; VHb, *Vitreoscilla* haemoglobin.

¹ These authors contributed equally to this work.

² To whom correspondence should be addressed (email kanak@imtech.res.in).

terminal oxidase [24], modulate the redox status of cells [25] and be involved in nitric oxide detoxification [26,27] and protection from oxidative stress [28,29].

Regardless of how many processes Vhb may affect, its expression probably increases the amount of oxygen within the cell. This is presumably related to its interaction with the terminal respiratory oxidase [17,24] and may explain the improved growth and bioproductivity of a variety of heterologous hosts engineered to express Vhb [7,9]. High oxygen concentrations in a cell are known to result in generation of ROS (reactive oxygen species) and potentially lethal damage to membranes and DNA [30,31]. On the other hand, in several cases the presence of Vhb provides the ability to cope better with oxidative stress by altering the status of antioxidant enzymes. For example, Vhb-expressing *Enterobacter aeruginosa* cells have been found to have elevated levels of catalase activity and become more tolerant to oxidative stress [28], Vhb-bearing *Streptomyces lividans* cells exhibit significant up-regulation of *kataA* (catalase-peroxidase A) and *sodF* (superoxide dismutase F), two antioxidant enzymes [32], and Vhb expressed in the plant *Arabidopsis endogenesis* has been correlated with higher levels of antioxidants, such as ascorbate, and higher tolerance to photoxidative damage [33].

The involvement of Vhb in the antioxidant systems of heterologous cells might be a common phenomenon that can be correlated with the observation that the biosynthesis of catalase in *Vitreoscilla* increases when there is an increase in Vhb level [34]. How Vhb maintains the fine balance between sustaining the beneficial level of oxygen within the cell, necessary for shifting the cellular physiology to the energetically more efficient aerobic state, and keeping checks on detrimental levels of ROS in the cell is currently unknown. Also we do not know how Vhb modulates expression of antioxidant systems in diverse host cells. Studies on Vhb in its native host, *Vitreoscilla*, have been hampered due to the unavailability of a suitable and stable gene transfer system. Although transformation of *Vitreoscilla* with *E. coli* plasmid vectors was successfully attempted [35], the recombinants were found to be unstable after subsequent transfer. Therefore the present study was undertaken to understand the molecular mechanism of Vhb function(s) in the context of oxidative stress management using *E. coli* as a model system. As *vgb* (the gene encoding Vhb) is expressed efficiently in *E. coli*, through its natural promoter, and the transcriptional response of the *vgb* promoter to oxygen availability in *E. coli* and *Vitreoscilla* is similar [14,15], an insight into the function of Vhb in *E. coli* can be extended to its native host *Vitreoscilla* and possibly to other heterologous hosts as well.

EXPERIMENTAL

Bacterial strains, plasmids and culture conditions

The *Vitreoscilla* C1 strain, described previously [4,14], was utilized for monitoring the effect of oxidative stress on *vgb* transcription and Vhb biosynthesis in its native host. *E. coli* strains JM109 and BL21 DE3 were used for routine cloning and expression of recombinant proteins. *E. coli* AB1157 and its *sodA*-negative derivative PN132 [36] were a gift from Professor James Imlay (School of Molecular and Cellular Biology, University of Illinois at Urbana Champaign, IL, U.S.A) and *E. coli* NC4963 and its *oxyR*-negative strain NC4112 were a gift from Professor Herb Schellhorn (Department of Biology, McMaster University, Hamilton, Ontario, Canada); the strain NC4112 displays enhanced sensitivity towards H₂O₂ and other oxidants [37]. The recombinant plasmid pUC8:16, was used as a source of Vhb and has been described previously [38]. Details of the bacterial

strains, oligonucleotide primers used for PCR amplification for wild-type and mutant genes and the *oxyR* antisense RNA sequence are provided in Supplementary Tables S1 and S2 (available at <http://www.BiochemJ.org/bj/426/bj4260271add.htm>).

E. coli strains were grown in LB (Luria–Bertani) or Terrific broth at 37 °C with shaking at 180 rev./min unless otherwise indicated. When required, ampicillin and kanamycin (Sigma–Aldrich) were added at concentrations of 100 µg/ml and 30 µg/ml respectively. *Vitreoscilla* strain C1 was grown in PYA medium (1% peptone, 1% yeast extract and 0.02% sodium acetate, pH 7.8) at 30 °C with shaking at 180 rev./min [34]. The growth profiles of *E. coli* strains NC4936 and NC4112, carrying either pUC8:16 or pUC19 (New England Biolabs), and the control strains transformed with pUC8:16 or pUC19, were checked at sublethal concentrations of H₂O₂ by monitoring the attenuation at 600 nm and compared with growth without H₂O₂ addition.

RT (reverse transcription)–PCR and protein expression analysis

To monitor the level of *vgb* transcription under oxidative stress, 1% inocula from overnight cultures of *Vitreoscilla* and *E. coli* JM109 bearing plasmid pUC8:16 were added to 20 ml of LB broth and grown to a *D*₆₀₀ of 0.5. At this point, 1 mM H₂O₂ was added and cells were harvested 6 h and 12 h later for *E. coli*, or 10 h and 18 h later for *Vitreoscilla*, and used for RNA isolation [with an RNeasy Mini Kit (Qiagen) and RNase-free DNase I (Qiagen) according to the manufacturer's instructions]. RT–PCR was performed with the One-Step RT–PCR Kit (Stratagene) using *vgb*-specific primers. RT–PCR of 16S rRNA served as the control for analysis of RT–PCR products.

Vhb content was determined by SDS/PAGE (12% gels) of total cell lysates, followed by Western blotting using polyclonal anti-Vhb antibodies [17] and densitometric analysis of the Vhb band with Alphaimager 3300 (Alpha Innotech), or by using CO-difference spectra of whole cells [38]. The fraction of total Vhb that was bound to haem was determined by measuring the amount of Vhb protein through densitometric analysis (which measures both holo and apo forms of Vhb) and comparing it with the Vhb content determined by CO-difference spectral analysis (which measures only the haem-bound form of Vhb). These measurements indicated that 80–85% of Vhb is associated with haem and thus may be in the functional state.

Cloning and expression of genes encoding OxyR, Fnr and their redox-sensitive mutants

oxyR and *fnr* were cloned from the genome of *E. coli* by PCR amplification using primers designed on the basis of their respective sequences. The OxyR-C199S mutant has been described previously and carries a serine residue at position 199 resulting in a mutant OxyR that remains trapped in a reduced form [39]. Fnr-D154A, reported previously [40], is a mutated form of Fnr where Asp-154 has been replaced by an alanine residue and remains oxidized. These two mutants were generated by site-directed mutagenesis using the PCR-based overlap extension method as described previously [41]. Amplified gene sequences were authenticated by nucleotide sequencing, cloned into expression vector pET28c (Novagen) and then expressed in *E. coli* strain BL21 DE3 as His₆-tagged proteins. Recombinant OxyR, Fnr and their mutants were isolated and purified from cell extracts using metal-affinity columns (Qiagen) according to the manufacturer's instructions.

Gel-shift assays and competitive binding of transcriptional activators with *vgb* promoter

The 250 bp *vgb* promoter fragment (−150 to +100 of *vgb*) was end-labelled with [γ - 32 P]ATP using T4 polynucleotide kinase (New England Biolabs). The labelled promoter (3.8 pM) was then incubated with 0.2–0.5 μ M purified wild-type or mutant OxyR protein at 20 °C for 20 min in buffer A [25 mM Tris/HCl, pH 7.5, 50 mM KCl, 5 mM MgCl₂ and 5% (v/v) glycerol] containing 5 μ g/ml herring sperm DNA. Unlabelled promoter was added at a concentration of 8 pM per assay when required for competition with the labelled *vgb* promoter. Samples were analysed for DNA–protein complex formation on TBE (Tris/borate/EDTA)-buffered 6% polyacrylamide gels. After electrophoresis, the gels were transferred on to filter paper (3MM, Whatman) and dried for autoradiography.

For the competitive DNA-binding assay, increasing concentrations of Fnr (0–100 nM) were added to a mixture of labelled *vgb* promoter fragment and oxidized OxyR (0.5 μ M each) that had been pre-incubated in buffer A; this was followed by incubation for an additional 10 min at 25 °C. Conversely, increasing concentrations of OxyR (0–500 nM) were added to a pre-incubated mixture of labelled *vgb* promoter and Fnr (50 nM each) in buffer A followed by further incubation for 10 min at 25 °C. Samples of each reaction mixture were electrophoresed on 6% polyacrylamide gels at 4 °C; the gels were transferred on to filter paper for autoradiography following standard protocols.

OxyR antisense constructs and strains

In order to substantiate the role of OxyR in the regulation of Vhb production, *oxyR* was cloned in the antisense configuration, adjacent to *vgb* in pUC8:16, creating pUC8:16T. Both pUC8:16 and pUC8:16T were transformed into *E. coli* strains AB1157 and PN132 (the latter is deficient in Sod function) to produce strains PN132-(pUC8:16), PN132-(pUC8:16T), AB1157-(pUC8:16) and AB1157-(pUC8:16T) (see Supplementary Table S1). The efficient expression and function of the *oxyR* antisense sequence was indicated by the complete absence of catalase activity in both PN132-(pUC8:16T) and AB1157-(pUC8:16T), in contrast with the presence of considerable catalase activity in the other four strains.

Yeast two-hybrid experiments

Yeast two-hybrid screen experiments were performed using the DupLex Yeast two-hybrid kit (Origene Technologies). *Saccharomyces cerevisiae* strain EGY48 was used as host for the transformation of bait, prey and reporter plasmids and vectors pEG202, pSH18-34 and pJG4-5 were used for cloning the relevant genes (see Supplementary Table S1). Plasmids pUC8:16 and pNKD1 [38] were used as sources of *vgb*. The *E. coli* strain JM109 was used as the host strain for all subcloning and for maintenance of plasmids, and was the source of DNA for *fnr* and *oxyR*. All clones were verified by restriction digestion and agarose gel electrophoresis, as well as by sequencing at the University of Illinois at Chicago Core Facility. All sequences were examined and found to be without error and in the correct reading frame. β -Galactosidase activity was used to quantify each interaction according to the method described previously [42].

Rifampicin resistance assay and exposure to H₂O₂

Rifampicin was dissolved in 50% (v/v) ethanol by heating slightly in a microwave followed by vortexing. Cultures of PN132, PN132-(pUC8:16), PN132-(pUC8:16T), AB1157, AB1157-(pUC8:16)

and AB1157-(pUC8:16T) were grown by inoculating 5 ml of LB, or LB containing ampicillin for plasmid-bearing strains, with isolated colonies and incubating at 37 °C with shaking at 220 rev./min for approx. 19 h, or until 10-fold dilutions yielded a D_{600} of 0.4 (such stationary-phase cultures of AB1157 and one of its Sod-deficient derivatives have been used successfully previously to monitor the sensitivity of these strains to ROS [43]). Then, 150 μ l of each culture was incubated overnight at 37 °C on LB plates containing 100 μ g/ml rifampicin to measure the number of rifampicin-resistant cells. In parallel, 150 μ l of each culture was diluted by a factor of 10⁶ with sterile distilled water and grown on LB plates with or without ampicillin, as appropriate for presence or absence of plasmid, in order to measure total cell numbers. All plates were incubated for 20 h at 37 °C prior to the colonies being counted. The mutation frequency was evaluated by dividing rifampicin resistant cell numbers by the corresponding total cell numbers.

For testing the effects of exposure to H₂O₂, cells were grown as described above (or until 10-fold dilutions yielded an D_{600} of 0.2). A sublethal dose of H₂O₂ (48 μ M) was then added [concentrations of H₂O₂ stocks were determined using a PeroXOquant kit (Pierce)] and cultures were returned for an additional hour to the same shaking and growth conditions. The sublethal dose was employed in order to elicit up-regulation of the Sod and Kat protective enzymes [43]. All cultures were then removed from the incubator and treated with H₂O₂ at a total concentration of 5 mM for 15 min at room temperature (25 °C) with gentle vortexing every 5 min. Finally, cultures were diluted by a factor of 10⁶ with sterile distilled water and grown on LB plates, with or without ampicillin as appropriate for presence or absence of plasmid. All plates were incubated for 20 h at 37 °C and colonies were counted.

Protein–protein interactions

Purified Vhb (5 μ M) was incubated with 5 μ M oxidized OxyR or 5 μ M of the OxyR-C199S reduced mutant protein for 10 min at 25 °C. The Vhb–OxyR complex, along with samples of Vhb and OxyR, were subjected to native PAGE (10% gels) and analysed after Western blotting using anti-Vhb antibodies. OxyR protein was oxidized with 0.5 μ M H₂O₂.

Catalase assay

An in-gel catalase activity assay was performed as described previously [44]. Briefly, cell lysates of control and Vhb-expressing *E. coli* were separated by native PAGE (10% gels) and were then incubated with 0.1% H₂O₂ for 10 min, washed twice with water, and treated with a solution containing 1% FeCl₃ and 1% K₃[Fe(CN)₆]. After that reactions were stopped by washing the gel with water and the presence of catalase was visualized on the gel as an unstained band.

RESULTS

Down-regulation of Vhb biosynthesis in *Vitreoscilla* and *E. coli* under oxidative stress

Biosynthesis of Vhb is regulated similarly, via an oxygen-sensitive promoter, at the transcriptional level in *Vitreoscilla* and *E. coli* [14]; 80–85% of Vhb is associated with haem (as described in the Experimental section) and is therefore in a functional state. To explore the Vhb biosynthesis response to oxidative stress, we first examined the content of Vhb in *Vitreoscilla* and Vhb-expressing *E. coli* in the presence of sublethal concentrations of H₂O₂. CO-difference spectra (results not shown) and densitometry of total protein profiles (Figures 1A

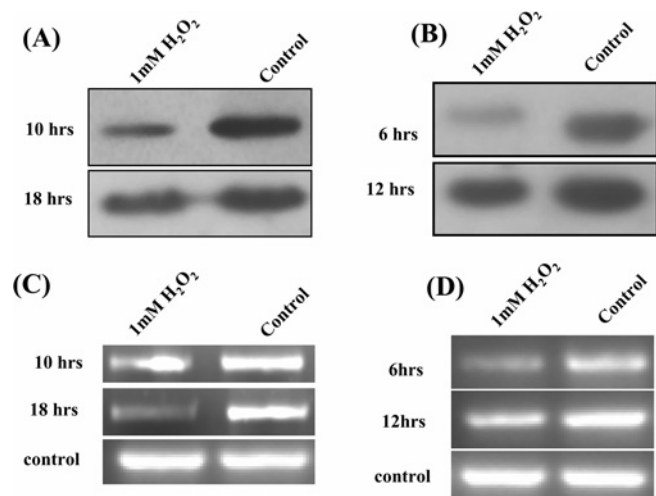


Figure 1 Vhb biosynthesis in *Vitreoscilla* and Vhb-expressing *E. coli* under oxidative stress

Cultures of *Vitreoscilla* and *E. coli*, expressing Vhb, were grown in the presence and absence (Control) of 1 mM H_2O_2 at 37°C with shaking. Cells were withdrawn at the specified times. (A and B) Expression of Vhb in *Vitreoscilla* and *E. coli* respectively in the presence and absence of 1 mM H_2O_2 analysed via SDS/PAGE and Western blotting. (C and D) Transcript levels of *vgb* in *Vitreoscilla* and *E. coli* respectively were determined by RT-PCR in the presence and absence of 1 mM H_2O_2 . 16S rRNA amplification served as the control.

and 1B) of Vhb-expressing cells revealed a 40–50% reduction in Vhb content in both *Vitreoscilla* and *E. coli*. RT-PCR analysis indicated that there was a further substantial reduction in the level of Vhb transcripts in both *Vitreoscilla* and Vhb-expressing *E. coli* (Figures 1C and 1D).

Vhb relieves oxidative stress in an OxyR-dependent manner

We next undertook further studies to gain an insight into the precise mechanism of the Vhb down-regulation under oxidative stress using *E. coli* as a model system due to the availability of well-defined mutant strains. Strains NC4936 (wild-type for *oxyR*) and NC4112 (*oxyR*-negative) were transformed either with pUC8:16, to enable *vgb* expression from its native promoter, or a control plasmid vector pUC19, which does not carry *vgb*. Growth of NC4936, either expressing or not expressing Vhb, was tested in the presence of increasing concentrations of H_2O_2 (Figure 2A). Although Vhb levels decreased under oxidative stress, NC4936 cells expressing Vhb were able to grow better than non-Vhb-expressing counterparts under these conditions, especially in the presence of high concentrations of H_2O_2 (Figures 2A and 2C). Interestingly, the Vhb-expressing *oxyR* mutant (NC4112 Vhb) displayed 2–3-fold higher Vhb levels (Table 1) but significantly slower growth compared with its counterpart not expressing Vhb (Figures 2B and 2C). These results suggest that the Vhb-mediated protection from H_2O_2 -induced oxidative stress relies on the presence of OxyR.

The involvement of OxyR with Vhb-mediated protection against H_2O_2 was confirmed by the experiments shown in Figure 3(A). Cell survival after a 15 min exposure to H_2O_2 was greatly enhanced by the presence of Vhb but the protective effect of Vhb was eliminated by the additional presence of *oxyR* antisense RNA. The same effect was observed for Sod-positive (AB1157) and Sod-negative (PN132) strains, indicating that the protective effect of Vhb is independent of Sod but not of OxyR. A further experiment was performed to assess the extent of damage

Table 1 Effect of *oxyR* absence on the cellular level of Vhb in *E. coli*

The Vhb level was measured as the nmol per g (wet weight) of cells by subtracting the untreated CO-spectra from dithionite-treated CO-spectra [38] from cells sampled at stationary phase (after 19 h); the residual levels detected in untransformed strain AB1157 are presumably *E. coli* flavohaemoprotein and/or cytochrome *bo*. Relative Vhb levels were determined by Western blot analysis in an *oxyR* mutant and compared with wild-type cells sampled at stationary phase (after 14 h). Values are means \pm S.D. for 3–5 independent experiments. n/a, not applicable.

Strain used	Cellular level of Vhb
Effect of <i>oxyR</i> antisense RNA	Vhb level [nmol per g (wet weight) of cells]
<i>E. coli</i> AB1157 (wild-type)	12 \pm 4
<i>E. coli</i> AB1157 (pUC8:16)	190 \pm 32
<i>E. coli</i> AB1157 (pUC8:16T)	774 \pm 217
Effect of <i>oxyR</i> deletion	Relative Vhb expression value (%)
<i>E. coli</i> NC4936 (OxyR wild-type)	n/a
<i>E. coli</i> NC4936 (pUC8:16)	100
<i>E. coli</i> NC4112 (Δ <i>oxyR</i>)	n/a
<i>E. coli</i> NC4112 (pUC8:16)	225 \pm 23

caused by superoxide ions produced during normal aerobic growth in the various *E. coli* strains (Figure 3B). This is measured by assessing the rate of mutation to rifampicin resistance (i.e. the increase in the proportion of rifampicin-resistant cells) [36]. As expected, the rate is negligible in the wild-type strain (AB1157), but high in the SOD-deficient strain (PN132), where the presence of Vhb has a large protective effect. This is probably due to a direct effect of Vhb on superoxide degradation, independent of the Vhb induction of *sodA* expression as described below.

OxyR controls Vhb levels

Further investigation of the connection between Vhb and OxyR included measurement of Vhb levels in *E. coli* strains NC4963 (wild-type for *oxyR*) and NC4112 (*oxyR*-negative) transformed with *vgb*. In stationary-phase cells, the Vhb level of NC4112(*vgb*) was increased 2.2-fold compared with NC4963(*vgb*). Similarly, stationary-phase cells of *E. coli* strain AB1157-(pUC8:16T) (*vgb* plus *oxyR* antisense) had Vhb levels approx. 4-fold that found in AB1157-(pUC8:16) (Table 1). Subsequent re-examination of the upstream control region of *vgb* indicated a site with near-identity to the consensus OxyR-binding motif identified previously by Tartaglia et al. [45]. As shown in Figure 4(A), this putative OxyR-binding site overlaps the Fnr-, Crp- (catabolic repressor protein) and ArcA (aerobic respiration control A)-binding sites identified previously within the *vgb* promoter [46–48]. The possible involvement of OxyR in regulation of Vhb production was then assessed via a gel-shift assay, which provided direct evidence that OxyR, but not a non-specific *E. coli* protein mixture, binds the *vgb* promoter (Figure 4B).

Binding of OxyR with the *vgb* promoter is modulated by its redox state

It is known that OxyR is activated by the formation of an intramolecular disulfide bond and activity of OxyR *in vivo* is determined by the balance between oxidative stress generated by cellular oxidants and the redox environment [39]. The presence of large amounts of Vhb in a cell is expected to result in significant changes in the redox state of cells under specific environmental conditions. Therefore we determined whether the interaction of OxyR with the *vgb* promoter is modulated by its redox state. To test this possibility we utilized the gel-shift assay with

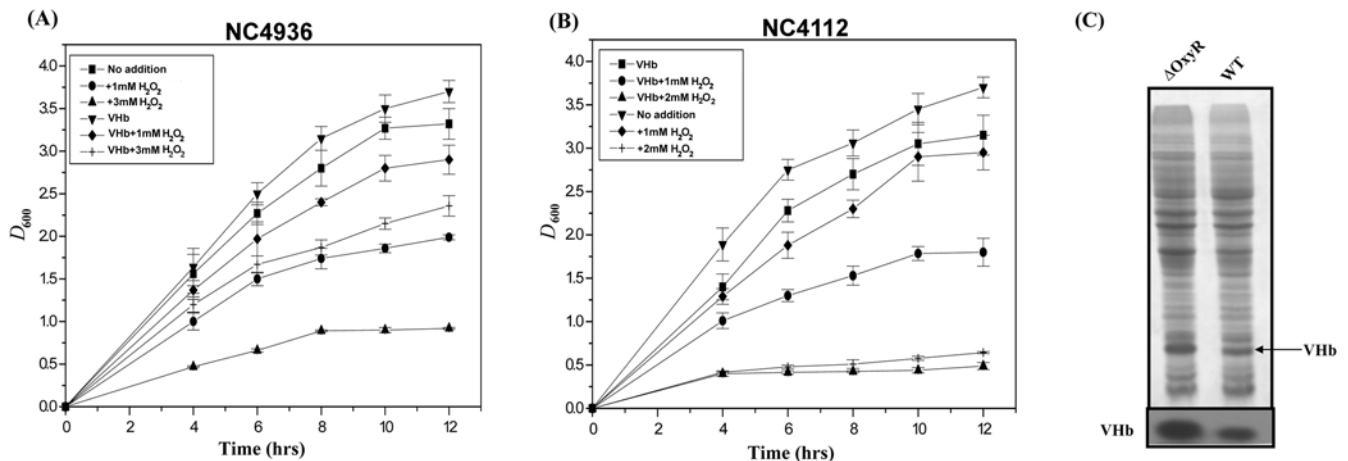


Figure 2 Growth profiles and VHb contents of *E. coli* wild-type and OxyR mutant under oxidative stress with or without VHb expression

(A) Growth trajectories of OxyR wild-type *E. coli* NC4936 transformed with either control (pUC19) plasmid or the VHb-expressing plasmid (VHb) in the presence of 0 mM, 1 mM or 3 mM H_2O_2 . (B) Growth trajectories of OxyR-mutant *E. coli* NC4112 carrying the VHb-expressing pUC8:16 plasmid (VHb) or the non-expressing control pUC19 plasmid in the presence of 0 mM, 1 mM or 2 mM H_2O_2 . (C) Western blot analysis of VHb content in strains NC4112 (Δ OxyR) and NC4936 (WT) bearing the VHb-expressing pUC8:16 and grown in the presence of 1 mM H_2O_2 .

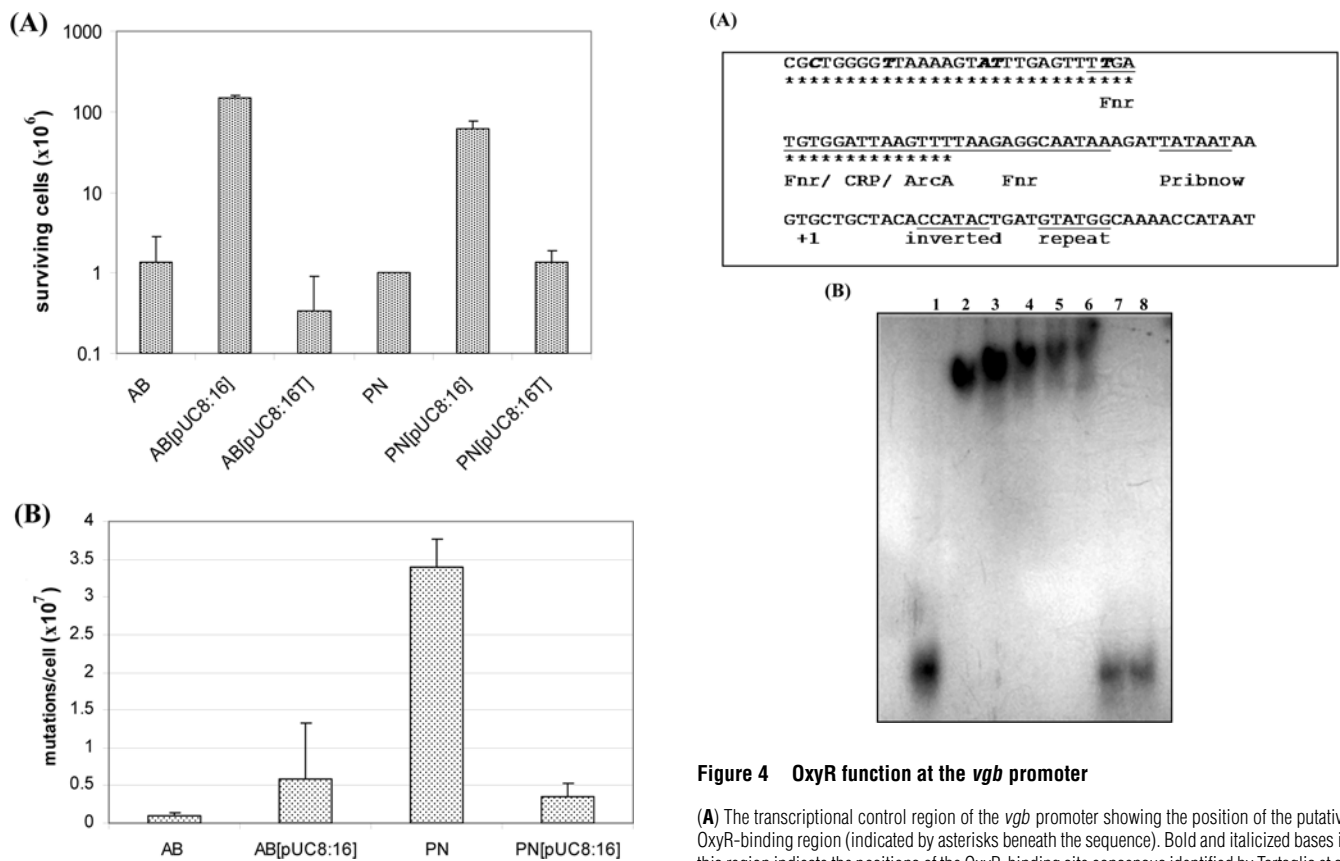


Figure 3 Effect of VHb on survival of Sod-mutant *E. coli* under oxidative stress

(A) Wild-type *E. coli* AB1157 (AB) and its Sod-mutant derivative PN132 (PN) were exposed to 5 mM H_2O_2 for 15 min as described in the Experimental section. Survival of cells was determined by counting colony-forming units. (B) Frequency of mutation to rifampicin resistance in strains AB1157 (AB) and PN132 (PN). Cells were plated on LB medium containing 100 μ g/ml rifampicin in order to count the number of rifampicin-resistant cells and LB medium (plus ampicillin for plasmid bearing strains) to measure total number of cells. pUC8:16, VHb-expressing plasmid. All values are means \pm S.D. for three independent experiments.

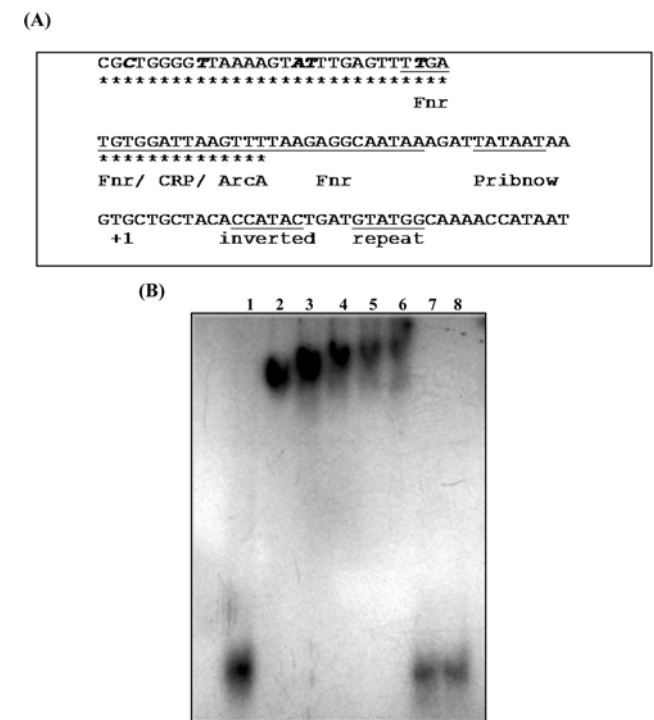


Figure 4 OxyR function at the *vgb* promoter

(A) The transcriptional control region of the *vgb* promoter showing the position of the putative OxyR-binding region (indicated by asterisks beneath the sequence). Bold and italicized bases in this region indicate the positions of the OxyR-binding site consensus identified by Tartaglia et al. [45]. All except the most left-hand C (which is G in the consensus) are identical to the consensus in both identity and position (and there is a G immediately adjacent to the unconserved C). Other motifs, which are putative binding sequences for other regulators are underlined and identified beneath the sequence. (B) Binding of OxyR to the *vgb* promoter region as determined by gel-shift assay. Lane 1, 3.8 pM 32 P-labelled *vgb* promoter; lane 2, labelled promoter and 0.2 μ M OxyR; lane 3, labelled promoter and 0.2 μ M OxyR; lane 4, labelled promoter and 0.3 μ M OxyR; lane 5, labelled promoter and 0.4 μ M OxyR; lane 6, labelled promoter and 0.5 μ M OxyR; lane 7, labelled promoter, 0.5 μ M OxyR and 8 pM unlabelled promoter; and lane 8, labelled promoter and 5 μ g of non-specific protein mixture.

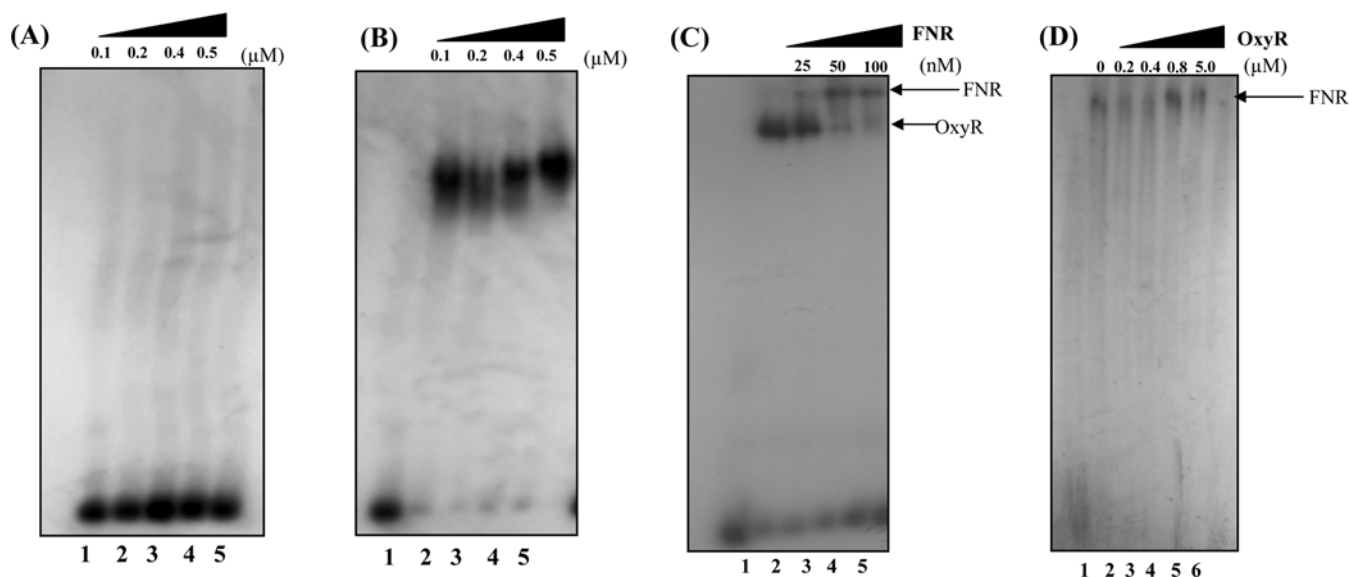


Figure 5 Redox-mediated interactions and competitive binding of OxyR and Fnr with the *vgb* promoter

(A) Interaction of OxyR-C199S (a mutant which is locked in the reduced form) with the *vgb* promoter. Lane 1, 32 P-labelled promoter alone; lanes 2–5, labelled promoter with increasing concentrations of OxyR-C199S (0.1, 0.2, 0.4 and 0.5 μ M). (B) Interaction of oxidized wild-type OxyR with the *vgb* promoter. Lane 1, labelled promoter alone. Lanes 2–5, labelled promoter with increasing concentrations of oxidized OxyR (0.1, 0.2, 0.4 and 0.5 μ M). OxyR was oxidized using 0.5 μ M H_2O_2 . (C) Increasing concentrations of Fnr (0–100 nM) were added to labelled *vgb* promoter that had been pre-incubated with 0.5 μ M oxidized OxyR, followed by incubation for 10 min at 25 $^{\circ}$ C (lanes 2–5). Lane 1 contains promoter alone. (D) Increasing concentrations of OxyR (0–5 μ M) were added to labelled *vgb* promoter that had been pre-incubated with 50 nM Fnr, followed by incubation for 10 min 25 $^{\circ}$ C (lanes 2–5). Lane 1 contains promoter alone.

wild-type OxyR and an OxyR mutant (OxyR-C199S) that does not reversibly form the disulfide bond and thus cannot be activated into the oxidized state. Unlike wild-type OxyR, OxyR-C199S was unable to interact with the *vgb* promoter (Figures 5A and 5B).

VHb interacts directly with OxyR and modifies its redox state

It has been shown previously that VHb is relatively more auto-oxidizable than eukaryotic haemoglobins and the products of its auto-oxidation are metVHb (*Vitreoscilla* methaemoglobin) and H_2O_2 [49]. Therefore it is possible that VHb itself may transmit signals for OxyR activation. To explore this possibility, we tested whether VHb was able to interact directly with OxyR. Initial experiments using a yeast two-hybrid assay showed a strong interaction between VHb and OxyR (Figure 6A). In order to describe the VHb–OxyR interaction in more detail we next performed an experiment where VHb was allowed to interact with fully oxidized OxyR prepared after H_2O_2 exposure and OxyR-C199S, which exists only in the reduced state. Protein–protein interactions of these proteins in equimolar concentrations (5 μ M) were analysed by native PAGE followed by Western blotting using anti-VHb antibodies (Figure 6B). A distinct complex of VHb with OxyR was detected with the reduced state OxyR-C199S but not with the fully oxidized form of OxyR.

The role of VHb in altering the redox state of OxyR was examined further by studying the redox status of OxyR in the presence of VHb and H_2O_2 . The fully reduced form of a His₆-tagged wild-type OxyR was incubated with VHb and NADH, separately or in combination, or with H_2O_2 , and conversion from reduced into oxidized OxyR was monitored by non-reducing SDS/PAGE after Western blotting using anti-His₆ polyclonal antibodies (as it has been described previously [50]) (Figure 6C). In the presence of H_2O_2 , OxyR was rapidly converted into the oxidized state. A similar change in the redox state of OxyR was observed in the presence of VHb and NADH (the condition that generates H_2O_2), whereas no change in OxyR was observed when

it was allowed to interact with either VHb or NADH alone. This change in the redox state of OxyR mediated by VHb and NADH was prevented in the presence of catalase, suggesting that the superoxide ion released by the oxidase activity of VHb may be responsible for OxyR oxidation.

Fnr interrupts interaction of OxyR with the *vgb* promoter

As VHb biosynthesis is positively regulated via Fnr and the *vgb* promoter carries an Fnr-binding site [46,48], which overlaps the putative OxyR site, we tested whether OxyR competes with Fnr for promoter binding. When Fnr and OxyR were allowed to interact individually with the *vgb* promoter, gel-shift assays demonstrated specific binding of both transcriptional regulators (Figures 5C and 5D). A competitive binding assay was then used to assess the interactions of these two transcriptional regulators at the *vgb* promoter. When the *vgb* promoter was allowed to interact initially with OxyR followed by addition of Fnr, gel-shift analysis indicated gradual displacement of OxyR with increasing concentration of Fnr. In contrast, when the *vgb* promoter was allowed to interact initially with Fnr, followed by addition of 200 nM to 5 μ M OxyR, no displacement of Fnr was observed. These results suggested that OxyR interacts with the *vgb* promoter only when Fnr is not operative.

VHb expression induces transcription of genes encoding antioxidant enzymes

As VHb interacts with reduced OxyR and converts it into the oxidized state, which is known to positively regulate the expression of many genes involved in the oxidative stress response [51], we checked the status of several genes that encode antioxidant enzymes (*katE*, *katG* and *sodA*) in *E. coli* over-expressing VHb. Transcript analysis of VHb-expressing cells revealed distinct increases in the expression of *katG* and *sodA*

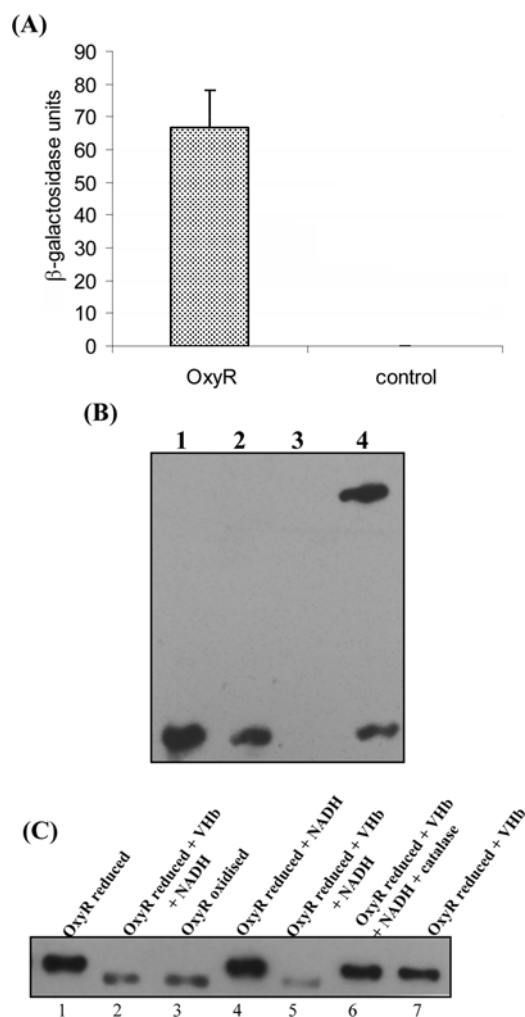


Figure 6 Protein-protein interactions between VHb and OxyR

(A) Two-hybrid screen showing binding between VHb and wild-type *E. coli* OxyR. Values are means \pm S.D. for four independent measurements. Cells bearing the prey vector with a *vgb* insert and bait vector with no insert (Control) were used to check that VHb alone does not result in activation; they have no detectable β -galactosidase activity. (B) VHb associates with reduced OxyR (OxyR-C199S) but not oxidized wild-type OxyR. Lane 1, purified VHb; lane 2, VHb and wild-type OxyR (oxidized with $0.5 \mu\text{M}$ H_2O_2); lane 3, purified OxyR; lane 4, VHb and reduced OxyR (OxyR-C199S). The samples were subjected to native PAGE and anti-VHb antibodies were used to detect the interaction. (C) VHb-mediated redox change in OxyR. Either reduced or oxidized OxyR wild-type protein (at $5 \mu\text{M}$) was incubated with or without VHb ($5 \mu\text{M}$), NADH ($100 \mu\text{M}$) and catalase (328 units) as indicated. The samples were subjected to native PAGE and anti-His₆ antibodies were used to detect the change in redox state.

compared with control cells (Figure 7A). In addition, when lysates of control and VHb-expressing cells were analysed on gels using zymography, a catalase-specific band appeared in cells expressing VHb but not in control cells (Figure 7B). These results substantiate further that there is an increase in the antioxidant activities of VHb-expressing cells.

DISCUSSION

ROS are generated primarily as by-products of intense respiratory activities and aerobic metabolism of cells. VHb-expressing bacteria display enhanced oxygen uptake and have a more oxidized cytoplasm than their non-VHb carrying counterparts [18,25]. In addition, VHb is more auto-oxidizable than eukaryotic haemoglobins and the products of this auto-oxidation are metVHb

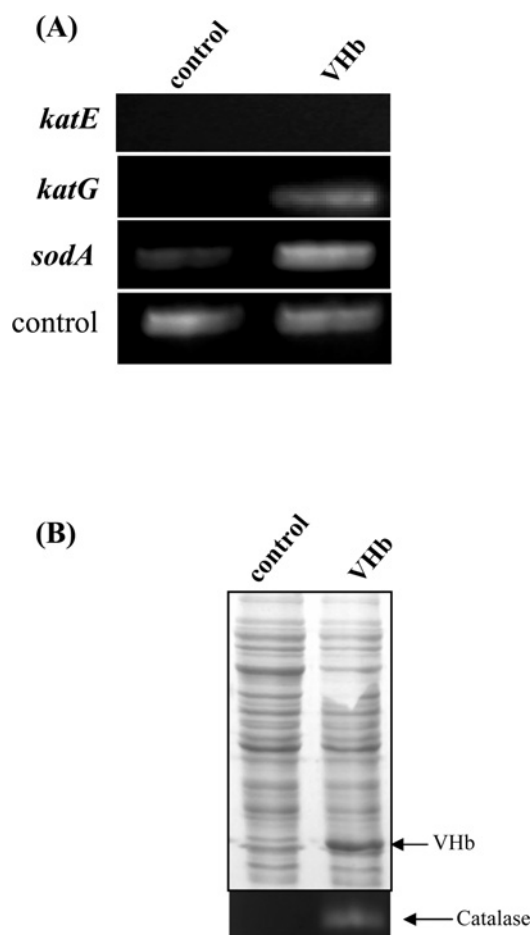


Figure 7 Transcription levels of antioxidant genes in *E. coli* expressing VHb

(A) Transcript level of antioxidant genes in VHb-expressing cells. Levels of genes encoding antioxidant functions in VHb-expressing *E. coli* (*katE*, *katG* and *sodA*) were determined by RT-PCR after exposure to 2 mM H_2O_2 as described in the Experimental section. The 16S rRNA transcript was used as a control. (B) Zymographic analysis of catalase activity in VHb-expressing *E. coli*. Control and VHb-expressing *E. coli* cells were analysed through zymography on native PAGE as described in the Experimental section.

and H_2O_2 [49]. Nevertheless, VHb has been found to provide protection from oxidative stress in several cases, although the mechanism by which it is able to do so has until now been unknown [28,29]. The present study has uncovered key aspects of this mechanism, especially the interaction between VHb and the oxidative stress regulator OxyR, an apparently interconnected regulatory mechanism which involves regulation of VHb biosynthesis and a more general induction of the host cell protective response to the toxicity of ROS.

OxyR is known to be both a positive and negative regulator of transcription, with the potential for acting positively only when oxidized but able to act negatively in either the oxidized or reduced form [51,52]. The levels of both VHb and *vgb* transcription are reduced under oxidative stress in both *Vitreoscilla* and *E. coli*. In the present study we observed distinct increases in VHb content in OxyR-mutant *E. coli* (2–3-fold), or in wild-type *E. coli* expressing *oxyR* antisense RNA (4-fold), suggesting that OxyR is acting as a negative regulator of *vgb* transcription. The *vgb* promoter carries binding sites for the global transcription regulators Fnr, ArcA and Crp, which have been shown to regulate *vgb* transcription in response to oxygen availability; Fnr, in conjunction with Crp,

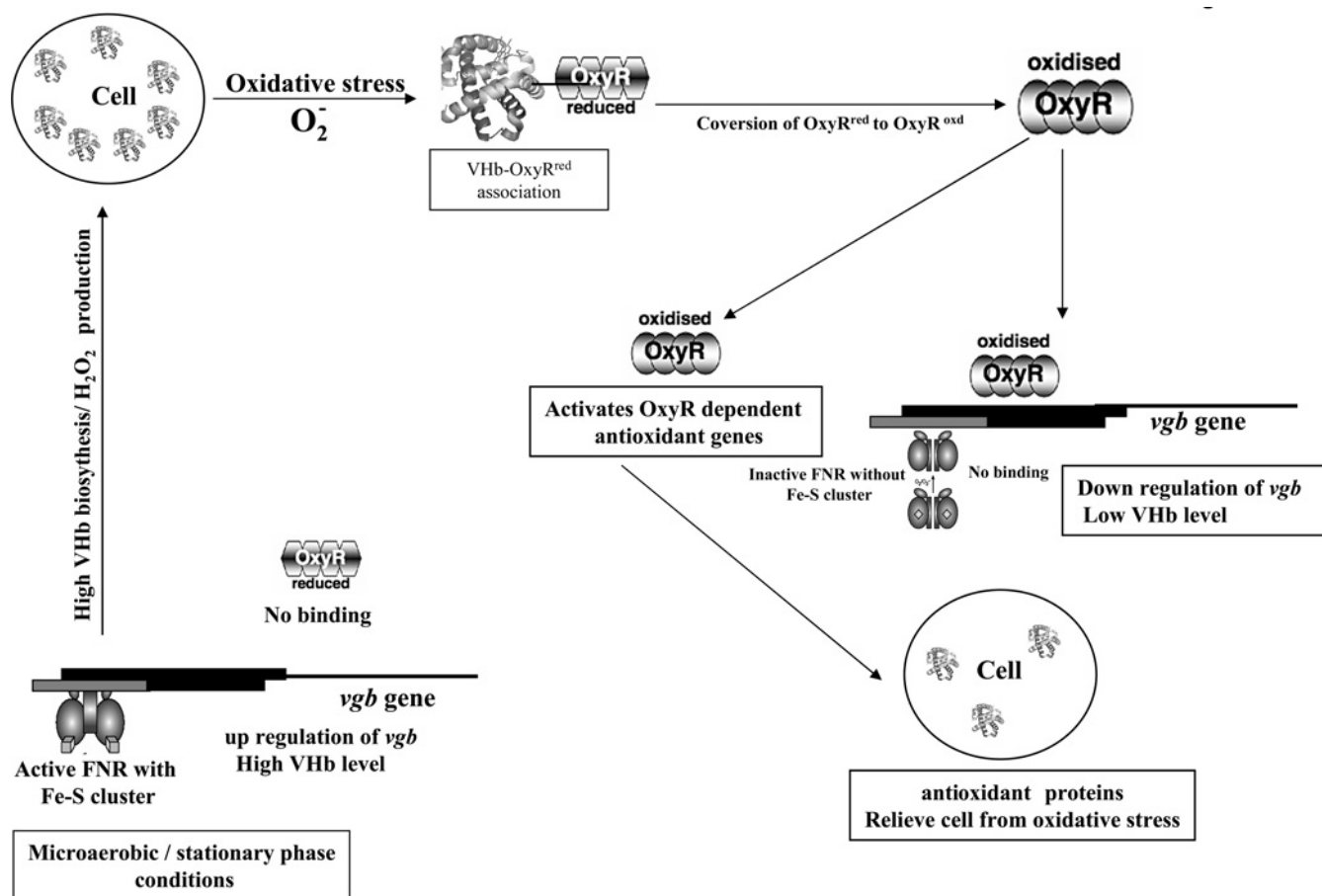


Figure 8 A model for the interactions between VHb and OxyR and their possible functions

The model indicates protein–protein interactions between VHb and OxyR and DNA–protein interactions between the *vgb* promoter and OxyR and Fnr, and how these interactions might be related to the control of VHb biosynthesis and the involvement of VHb in the response to oxidative stress. See the Discussion section for further details.

has been found to up-regulate transcription of VHb several fold under hypoxia [48]. The putative OxyR-binding site within the *vgb* promoter overlaps the Fnr-, ArcA- and Crp-binding sites, suggesting that multiple circuits may work to exert fine-level control of *vgb* expression in response to different oxygen levels and environmental stimuli.

Aerobic metabolism under high aeration may result in significant superoxide stress and is known to activate OxyR, whereas the same conditions inactivate Fnr [31]. Gel-shift assays indicate that OxyR binds with the *vgb* promoter only in its oxidized form and in the absence of Fnr. In the presence of higher VHb levels reactive oxygen within the cell may increase due to higher oxygen levels and respiratory activities and/or the redox status of cell may change. This, in turn, may work to disrupt the association of Fnr with the *vgb* promoter and activate OxyR to alleviate the situation by down-regulating VHb biosynthesis. The 2–4-fold negative control exerted by OxyR on VHb production could serve to allow VHb to reach a level that can provide oxygen availability for maximum benefit without exerting stress on cells owing to production of H₂O₂ (see below) or diversion of cell resources to produce an unnecessary VHb excess. OxyR, however, does not appear to down-regulate *vgb* by dislodging Fnr from the *vgb* promoter, although Fnr appears to dislodge OxyR, presumably when VHb levels need to be increased. This type of regulatory combination of OxyR and Fnr has also been observed

in the case of two *E. coli* superoxide stress responsive genes, *yhiA* and *katG* [53,54].

Despite having a relatively low VHb content under conditions of oxidative stress, VHb-expressing cells displayed significant protection from H₂O₂, demonstrated by enhancement of both growth rates (Figures 2A and 2B) and survival (Figure 3A). The dependence of VHb on OxyR for relieving oxidative stress and the induction of the antioxidant system in the presence of VHb [32,33] suggest a close correlation between VHb and OxyR in controlling this function. VHb associates only with the reduced state of OxyR and is able to convert it into oxidized OxyR *in vitro*, but only in the presence of NADH, conditions under which VHb has been shown to generate H₂O₂ [48]. VHb may then regulate the redox state of OxyR directly by transmitting the H₂O₂ stress signal. This hypothesis is also supported by our observation of the stimulation by VHb of transcription of *E. coli katG*, which is known to be induced by H₂O₂-activated OxyR [54].

The protective effect of VHb found in several heterologous hosts, where VHb is not regulated under its native promoter, might also be due to activation of OxyR by VHb and subsequent induction of the antioxidant genes. Indeed, it has been demonstrated that the expression of VHb activates antioxidant systems in various heterologous hosts, e.g. the *kat* and *sod* genes in *E. aerogenes* [29] and *S. lividans* [32], and the level of ascorbate, a component of the antioxidant system, in *Aradiopsis* [33]. This

mechanism may also be involved in the parallel increases in catalase and Vhb, which occur in *Vitreoscilla* [34].

Up-regulation of *sodA* transcription in Vhb-expressing cells indicates that, in addition to its involvement in the response to H₂O₂, Vhb may aid in protection from the superoxide ion. It has been reported that the *soxRS* regulon, to which *sodA* belongs, is also triggered by H₂O₂ [55]. In addition, the results of the experiment in Figure 3(B), which was performed in a Sod-mutant strain, indicate Vhb has a direct role in protection against superoxide. One possible mechanism for this effect is the reaction of metVhb with superoxide to yield oxygenated Fe²⁺-Vhb [56]. The apparent ability of Vhb to affect the activities of both the *soxRS* and *oxyR* regulons may indicate a broader ability of Vhb to affect, either directly or indirectly, the activities of other transcription factors, as is also suggested by the changes in expression of a large number of genes during Vhb overexpression in different heterologous hosts reported previously [10,11].

Implications of OxyR regulation of Vhb biosynthesis: a proposed model

OxyR is known to process different redox-related signals into distinct transcriptional processes [39]. *vgb* has an oxygen-responsive promoter that is 'crowded' with binding sites for the redox-sensitive transcriptional regulators Fnr, ArcA and Crp, and these sites overlap the OxyR-binding site. This indicates that regulation of *vgb* expression may occur in response to different redox signals, either independently or in co-ordination with each other. On the basis of results in the present study, we propose a mechanism for the regulation of Vhb biosynthesis via OxyR (Figure 8). This mechanism may also provide an insight into the protective effect of Vhb observed under oxidative stress in different hosts, as well as in *Vitreoscilla* itself.

Under hypoxic conditions transcription of *vgb* is up-regulated several fold by Fnr [46], presumably facilitating oxygen availability and enhancing respiratory activity. This, in turn, may generate elevated levels of superoxide due to the ability of Vhb to produce H₂O₂ in the presence of NADH [48]. This may be detrimental to cells, particularly during externally imposed oxidative stress. Accumulation of Vhb within the cell may also lead to close association of Vhb with reduced OxyR so that the superoxide released by Vhb is readily available to activate OxyR, in some way more efficiently or more sensitively than by direct oxidation of OxyR by H₂O₂. A subsequent conformational change due to the change in the redox state of OxyR may disrupt the OxyR-Vhb association and allow OxyR binding to the *vgb* promoter. Simultaneously, the oxidizing conditions created due to the accumulation of Vhb may disrupt the iron-sulfur cluster of Fnr and thus binding with the *vgb* promoter. This would help clear the region on the promoter to allow OxyR binding to down-regulate Vhb production and thus reduce the level of Vhb-generated superoxide. A redox change in OxyR mediated by Vhb may also allow OxyR to activate its regulon and thus provide more widespread protection from the oxidative stress.

Vitreoscilla is an obligate aerobe and may require a sufficient amount of Vhb to sustain its aerobic metabolism under the low oxygen conditions of its natural habitat [4,12]. The down-regulation of Vhb biosynthesis by OxyR may optimize the beneficial effects of Vhb by keeping its levels high enough to provide sufficient oxygen for the cell while acting to minimize the level of Vhb-generated H₂O₂ due to aerobic metabolism. A role for the Vhb-OxyR association in protecting the aerobic metabolism of its native host by inducing antioxidant genes may also be relevant in this respect. Our proposed model also explains

the protective effect of Vhb against oxidative damage observed in several heterologous hosts [28,32,33].

AUTHOR CONTRIBUTION

Arvind Anand and Brian Duk performed the experiments on protein-protein interactions, DNA-protein interactions and the genetic regulation studies of Vhb by OxyR. Sandeep Singh contributed to the experiments on protein-protein interactions of Vhb and OxyR spectral studies. Meltem Akbas performed the analysis of Vhb cellular content in recombinant cells. Benjamin Stark, Dale Webster and Kanak Dikshit conceived the ideas, planned and designed experimental strategies, analysed the data and prepared the manuscript.

ACKNOWLEDGEMENTS

We thank Professor James Imlay and Professor Herb Schellhorn for gifts of bacterial strains. We are grateful for the help with the spectral studies provided by Bela Modi and Dr Sangeeta Patel (Department of Biological, Chemical and Physical sciences, Illinois Institute of Technology, Chicago, IL, U.S.A.).

FUNDING

This work was supported by the National Science Foundation, U.S.A. [grant number OISE-0422555]; and by the Department of Science and Technology, India.

REFERENCES

- Poole, R. K. and Hughes, M. N. (2000) New functions for the ancient globin family: bacterial responses to nitric oxide and nitrosative stress. *Mol. Microbiol.* **36**, 775–783
- Frey, A. D. and Kallio, P. T. (2003) Bacterial hemoglobins and flavohemoglobins: versatile proteins and their impact on microbiology and biotechnology, *FEMS Microbiol. Rev.* **27**, 525–545
- Ascenzi, P., Bolognesi, M., Milani, M., Guertin, M. and Visca, P. (2007) Mycobacterial truncated hemoglobins: from genes to functions. *Gene* **398**, 42–51
- Wakabayasi, S., Matsubara, H. and Webster, D. A. (1986) Primary sequence of a dimeric bacterial hemoglobin from *Vitreoscilla*. *Nature* **322**, 481–483
- Tarricone, C., Galizzi, A., Coda, A., Asenzi, P. and Bolognesi, M. (1997) Unusual structure of the oxygen binding site in the dimeric bacterial hemoglobin from *Vitreoscilla* Sp. *Structure* **5**, 497–507
- Kaur, R., Ahuja, S., Anand, A., Singh, B., Stark, B. C., Webster, D. A. and Dikshit, K. L. (2008) Functional implications of the proximal site hydrogen bonding network in *Vitreoscilla* hemoglobin (Vhb): role of Tyr95 (G5) and Tyr126 (H12). *FEBS Lett.* **15**, 3494–3500
- Khosla, C. and Bailey, J. E. (1988) Heterologous expression of bacterial hemoglobin improves the growth properties of recombinant *E. coli* *Nature* **331**, 633–635
- Holmberg, N., Lilius, G., Bailey, J. E. and Bulow, L. (1997) Transgenic tobacco expressing *Vitreoscilla* hemoglobin exhibits enhanced growth and altered metabolic production. *Nat. Biotechnol.* **15**, 244–247
- Zhang, L., Li, Y., Wang, Z., Xia, Y., Chen, W. and Tang, K. (2007) Recent developments and future prospects of *Vitreoscilla* hemoglobin applications in metabolic engineering. *Biotechnol. Adv.* **25**, 123–136
- Roos, V., Andersson, C. I. J. and Bulow, L. (2004) Gene expression profiling of *Escherichia coli* expressing double *Vitreoscilla* haemoglobin. *J. Biotechnol.* **114**, 107–120
- Isarankura-Na-Ayudhya, C., Panpumthong, P., Tangkosakul, T., Boonpangrak, S. and Prachayasittikul, V. (2008) Shedding light on the role of *Vitreoscilla* hemoglobin on cellular catabolic regulation by proteomic analysis. *Int. J. Biol. Sci.* **4**, 71–80
- Webster, D. A. (1988) Structure and function of bacterial hemoglobin and related proteins. *Adv. Inorg. Biochem.* **7**, 245–265
- Orri, Y. and Webster, D. A. (1986) Photodissociation of oxygenated cytochrome *o*(s) (*Vitreoscilla*) and kinetic studies of reassociation. *J. Biol. Chem.* **249**, 4261–4266
- Dikshit, K. L., Spaulding, D., Braun, A. and Webster, D. A. (1989) Oxygen inhibition of globin gene transcription and bacterial hemoglobin production in *Vitreoscilla*. *J. Gen. Microbiol.* **135**, 2601–2609
- Dikshit, K. L., Dikshit, R. P. and Webster, D. A. (1990) Study of *Vitreoscilla* globin (*vgb*) gene expression and promoter activity in *E. coli* through transcription fusion. *Nucleic Acids Res.* **18**, 4149–4155
- Tsai, P. S., Nageli, M. and Bailey, J. E. (2002) Intracellular expression of *Vitreoscilla* hemoglobin modifies microaerobic *Escherichia coli* metabolism through elevated concentration and specific activity of cytochrome *o*. *Biotechnol. Bioeng.* **79**, 558–567
- Ramandeep, D., Hwang, K. W., Raje, M., Kim, K.J., Stark, B.C., Dikshit, K.L. and Webster, D. A. (2001) *Vitreoscilla* hemoglobin: intracellular localization and binding to membranes. *J. Biol. Chem.* **277**, 24781–24789

- 18 Erenler, S. O., Gencer, S., Geckil, H., Stark, B. C. and Webster, D. A. (2004) Cloning and expression of the *Vitreoscilla* hemoglobin gene in *Enterobacter aerogenes*: effect on cell growth and oxygen uptake. *Appl. Biochem. Microbiol.* **40**, 241–248
- 19 Park, K. W., Kim, K. J., Howard, A. J., Stark, B. C. and Webster, D. A. (2002) *Vitreoscilla* hemoglobin binds to subunit I of cytochrome *bo* ubiquinol oxidases. *J. Biol. Chem.* **277**, 33334–33337
- 20 Rinaldi, A. C., Bonamore, A., Maccone, A., Boffi, A., Bozzi, A. and Di Giulio, A. (2006) Interaction of *Vitreoscilla* hemoglobin with membrane lipids. *Biochemistry* **45**, 4069–4076
- 21 Fish, P. A., Webster, D. A. and Stark, B. C. (2001) *Vitreoscilla* hemoglobin enhances the first step in 2,4-dinitrotoluene degradation *in vitro* and at low aeration *in vivo*. *J. Mol. Catal. B. Enzym.* **9**, 75–82
- 22 Lin, J. M., Stark, B. C. and Webster, D. A. (2003) Effects of *Vitreoscilla* hemoglobin on the 2,4-dinitrotoluene (DNT) dioxygenase activity of *Burkholderia* and on DNT degradation in two-phase bioreactors. *J. Ind. Microbiol. Biotechnol.* **30**, 362–368
- 23 Lee, S. Y., Stark, B. C. and Webster, D. A. (2004) Structure-function studies of the *Vitreoscilla* hemoglobin D-region. *Biochem. Biophys. Res. Comm.* **316**, 1101–1106
- 24 Dikshit, R. P., Dikshit, K. L., Liu, Y. and Webster, D. A. (1992) The bacterial hemoglobin from *Vitreoscilla* can support the aerobic growth of *E. coli* lacking terminal oxidases. *Arch. Biochem. Biophys.* **293**, 241–245
- 25 Tsai, P. S., Rao, G. and Bailey, J. E. (1995) Improvement of *Escherichia coli* microaerobic oxygen metabolism by *Vitreoscilla* hemoglobin: new insights from NAD(P)H fluorescence and culture redox potential. *Biotechnol. Bioeng.* **47**, 347–354
- 26 Kaur, R., Pathania, R., Sharma, V., Mande, S. and Dikshit, K. L. (2002) Chimeric *Vitreoscilla* hemoglobin (VHb) carrying a flavoreductase domain relieves nitrosative stress in *Escherichia coli*: new insight into the terminal role of VHb. *Appl. Environ. Microbiol.* **68**, 152–160
- 27 Frey, A. D., Farres, J., Bollinger, C. J. T. and Kallio, P. T. (2002) Bacterial hemoglobins and flavohemoglobins for alleviation of nitrosative stress in *Escherichia coli*. *Appl. Environ. Microbiol.* **68**, 4835–4840
- 28 Geckil, H., Gencer, S., Kahraman, H. and Erenler, S. O. (2003) Genetic engineering of *Enterobacter aerogenes* with the *Vitreoscilla* hemoglobin gene: cell growth, survival, and antioxidant enzyme status under oxidative stress. *Res. Microbiol.* **154**, 425–431
- 29 Kvist, M., Ryabova, E. S., Nordlander, E. and Bulow, L. (2007) An investigation of the peroxidase activity of *Vitreoscilla* hemoglobin. *J. Biol. Inorg. Chem.* **12**, 324–334
- 30 Keyer, K. and Imlay, J. A. (1996) Superoxide accelerates DNA damage by elevating free iron levels. *Proc. Natl. Acad. Sci. U.S.A.* **93**, 13635–13640
- 31 Fridovich, I. (1998) Oxygen: the dark side. *Age (Dordr.)* **21**, 77
- 32 Kim, Y. J., Sa, S. O., Chang, Y. K., Hong, S. K. and Hong, Y. S. (2007) Overexpression of *Shinorhizobium meliloti* hemoprotein in *Streptomyces lividans* to enhance secondary metabolite production. *J. Microbiol. Biotechnol.* **12**, 2066–2070
- 33 Wang, Z., Xiao, Y., Chen, W., Tang, K. and Zhang, L. (2009) Functional expression of *Vitreoscilla* hemoglobin (VHb) in *Arabidopsis* relieves submergence, nitrosative, photo-oxidative stress and enhances antioxidants metabolism. *Plant Sci.* **176**, 66–77
- 34 Abrams, J. J. and Webster, D. A. (1990) Purification, partial characterization, and possible role of catalase in the bacterium *Vitreoscilla*. *Arch. Biochem. Biophys.* **279**, 54–59
- 35 Navani, N. K., Joshi, M. A. and Dikshit, K. L. (1996) Genetic transformation of *Vitreoscilla* sp. *Gene* **177**, 265–266
- 36 Benov, L. and Fridovich, I. (1995) A superoxide dismutase mimic protects *sodA sodB Escherichia coli* against aerobic heating and stationary-phase death. *Arch. Biochem. Biophys.* **322**, 291–294
- 37 Mukhopadhyay, S. and Schellhorn, H. E. (1994) Identification and characterization of hydrogen peroxide-sensitive mutants of *Escherichia coli*: genes that require OxyR for expression. *J. Bacteriol.* **176**, 2300–2307
- 38 Dikshit, K. L. and Webster, D. A. (1988) Cloning, characterization and expression of the bacterial globin gene from *Vitreoscilla* in *Escherichia coli*. *Gene* **70**, 377–386
- 39 Zheng, M., Aslund, F. and Storz, G. (1998) Activation of the OxyR transcription factor by reversible disulfide bond formation. *Science* **279**, 1718–1721
- 40 Lazizzera, B. A., Beinert, H., Khoroshilova, N., Kennedy, M. C. and Kiley, P. J. (1996) DNA binding and dimerization of the Fe–S-containing FNR protein from *Escherichia coli* are regulated by oxygen. *J. Biol. Chem.* **271**, 2762–2768
- 41 Verma, S., Patel, S., Kaur, R., Stark, B. C., Dikshit, K. L. and Webster, D. A. (2005) Mutational study of the bacterial hemoglobin distal heme pocket. *Biochem. Biophys. Res. Commun.* **326**, 290–297
- 42 Miller, J. H. (1972) Experiments in Molecular Genetics, pp. 352–355, Cold Spring Harbor Laboratory Press, Cold Spring Harbor
- 43 Imlay, J. A. and Linn, S. (1987) Mutagenesis and stress responses induced in *Escherichia coli* by hydrogen peroxide. *J. Bacteriol.* **169**, 2967–2976
- 44 Woodbury, W., Spencer, A. K. and Stahman, M. A. (1971) An improved procedure using ferricyanide for detecting catalase isozymes. *Anal. Biochem.* **44**, 301–305
- 45 Tartaglia, A. L., Gimeno, C. J., Storz, G. and Ames, B. N. (1992) Multidegenerate DNA recognition by the OxyR transcriptional regulator. *J. Biol. Chem.* **267**, 2038–2045
- 46 Khosla, C. and Bailey, J. E. (1989) Characterization of the oxygen-dependent promoter of the *Vitreoscilla* hemoglobin gene in *Escherichia coli*. *J. Bacteriol.* **171**, 5995–6004
- 47 Yang, J. G., Webster, D. A. and Stark, B. C. (2005) ArcA works with Fnr as a positive regulator of *Vitreoscilla* (bacterial) hemoglobin gene expression in *Escherichia coli*. *Microbiol. Res.* **160**, 405–415
- 48 Joshi, M. and Dikshit, K. L. (1994) Oxygen dependent regulation of *Vitreoscilla* globin gene: evidence for positive regulation by FNR. *Biochem. Biophys. Res. Comm.* **202**, 535–542
- 49 Webster, D. A. (1975) The formation of hydrogen peroxide during the oxidation of reduced nicotinamide adenine dinucleotide by cytochrome *o* from *Vitreoscilla*. *J. Biol. Chem.* **250**, 4955–4958
- 50 Tao, K. (1999) *In vivo* oxidation-reduction kinetics of OxyR, the transcriptional activator for an oxidative stress-inducible regulon in *Escherichia coli*. *FEBS Lett.* **457**, 90–92
- 51 Zheng, M. and Storz, G. (2000) Redox sensing by prokaryotic transcription factors. *Biochem. Pharmacol.* **59**, 1–6
- 52 Storz, G., Tartaglia, L. A. and Ames, B. N. (1990) Transcriptional regulator of oxidative stress-inducible genes: direct activation by oxidation. *Science* **248**, 189–194
- 53 Partridge, J. A., Poole, R. K. and Green, J. (2007) The *Escherichia coli* *yhjA* gene, encoding a predicted cytochrome *c* peroxidase, is regulated by FNR and OxyR. *Microbiology* **153**, 1499–1507
- 54 Constantinidou, C. M., Hobman, J. L., Griffith, L., Patel, M. D., Penn, C. W., Cole, J. A. and Overton, T. W. (2006) A reassessment of the FNR regulon and transcriptomic analysis of the effects of nitrate, nitrite, NarXL, and NarQP as *Escherichia coli* K12 adapts from aerobic to anaerobic growth. *J. Biol. Chem.* **281**, 4802–4815
- 55 Manchado, M., Michan, C. and Pueyo, C. (2000) Hydrogen peroxide activates the SoxRS regulon *in vivo*. *J. Bacteriol.* **182**, 6842–6844
- 56 Orii, Y. and Webster, D. A. (1977) Oxygenated cytochrome *o* (*Vitreoscilla*) formed by treating oxidized cytochrome with superoxide anion. *Plant Cell Physiol.* **18**, 521–526

Received 10 September 2009/17 December 2009; accepted 22 December 2009
Published as BJ Immediate Publication 22 December 2009, doi:10.1042/BJ20091417

SUPPLEMENTARY ONLINE DATA

Redox-mediated interactions of VHb (*Vitreoscilla* haemoglobin) with OxyR: novel regulation of VHb biosynthesis under oxidative stress

Arvind ANAND*¹, Brian T. DUK†¹, Sandeep SINGH*, Meltem Y. AKBAS‡, Dale A. WEBSTER†, Benjamin C. STARK† and Kanak L. DIKSHIT*²

*Institute of Microbial Technology, Sector 39 A, Chandigarh 160036, India, †Division of Biology, Department of Biological, Chemical and Physical Sciences, Illinois Institute of Technology, Chicago, IL 60616, U.S.A., and ‡Gebze Institute of Technology, 41400 Gebze Kocaeli, Turkey

Table S1 Plasmids and strains used in the present work

Plasmid or strain	Description and source
EGY48	<i>S. cerevisiae</i> strain; Origene Technologies
pSH18-34	Origene Technologies
pEG202	Bait vector; Origene Technologies
pJG4-5	Target vector; Origene Technologies
EG202oxyR	oxyR cloned into plasmid pEG202; present work
pJG4-5vgb	vgb cloned into plasmid pJG4-5; present work
AB1157	<i>E. coli</i> wild-type for Sod; [27]
AB1157-(pUC8:16)	AB1157 transformed with pUC8:16; present work
AB1157-(pUC8:16T)	AB1157 transformed with pUC8:16T; present work
PN132	Sod-negative derivative of AB1157; [27]
PN132-(pUC8:16)	PN132 transformed with pUC8:16; present work
PN132-(pUC8:16T)	PN132 transformed with pUC8:16T; present work
pUC8:16	vgb expression vector; [38]
pUC8:16T	pUC8:16 plus oxyR in the antisense orientation; present work
NC4963	<i>E. coli</i> wild-type; [37]
NC4112	oxyR-negative mutant of nc4963; [37]

Table S2 Primers used for cloning and mutation of *E. coli* Fnr and OxyR

Protein	Primers
<i>E. coli</i> FNR	5'-GATCCACATATGATCCCGAAAAGCGAATTATAC-3' and 5'-GAGCGGATCCTCAGGCAACGTTACGCGTATGACCA-3'
Fnr-D154A mutant	5'-AATCAAAGCGCTCAGGACATGA-3' and 5'-CATGTCCTGACCGCCTTTGATT-3'
<i>E. coli</i> OxyR	5'-GATACATATGAATATTCGTGATCTTGAGT-3' and 5'-GATAGGATCCTTAGACCGCCTGTTTAACT-3'
OxyR-C199S mutant	5'-CTGGAGCATGCTCACTTTGCGCGA-3' and 5'-CTGACGCGCAATGAGTGACCATCTTCC-3'

Received 10 September 2009/17 December 2009; accepted 22 December 2009
Published as BJ Immediate Publication 22 December 2009, doi:10.1042/BJ20091417

¹ These authors contributed equally to this work.

² To whom correspondence should be addressed (email kanak@imtech.res.in).

